UNIVERSITY OF SOUTHAMPTON

FACULTY OF MEDICINE

Cancer Sciences Unit

Regulation of RNA Translation by Phenethyl Isothiocyanate

by

Alison Marie Yeomans (née Donlevy)

M.Res, B.Sc (Hons)

Thesis for the degree of Doctor of Philosophy

September 2013

UNIVERSITY OF SOUTHAMPTON

ABSTRACT

FACULTY OF MEDICINE

Cancer Sciences Unit

Thesis for the degree of Doctor of Philosophy

REGULATION OF RNA TRANSLATION BY PHENETHYL ISOTHIOCYANATE

By Alison Marie Yeomans (née Donlevy)

Phenethyl isothiocyanate (PEITC) is a dietary phytochemical that has received considerable interest for its potential chemopreventive/therapeutic anti-cancer activity. PEITC inhibits cancer cell proliferation and/or survival *in vitro*, suppresses angiogenesis and decreases tumour growth *in vivo* with little toxicity. However, the mechanisms by which PEITC exerts its anti-cancer effects are not known. The goal of this project was to investigate the hypothesis that anti-cancer effects of PEITC may involve inhibition of mRNA translation.

Effects of PEITC on global mRNA translation were first studied in human MCF7 breast cancer cells using both polysome profiling and ^{35}S-metabolic labelling experiments. PEITC caused a dose- and time-dependent inhibition of mRNA translation, which was partially reversed following removal of PEITC. Inhibition of mRNA translation was associated with decreased expression of HIF1α and VEGF, two proteins that are key for pro-angiogenic responses of malignant cells, in both normoxic and hypoxic conditions, at least in part via effects on translation of *HIF1A* and *VEGF* mRNAs. Although PEITC has previously been shown to inhibit signalling via the mTORC1 pathway, further analysis demonstrated that PEITC also caused a rapid increase in phosphorylation of eIF2α at Ser51 which can result in inhibition of initiation of mRNA translation. Increased eIF2α phosphorylation was important for PEITC-mediated inhibition of mRNA translation since mouse embryo fibroblasts expressing non-phosphorylatable eIF2α were relatively resistant to PEITC-induced inhibition of mRNA translation compared to control cells. In addition, PEITC caused the accumulation of stress granules, which have previously been associated with translationally stalled mRNAs.

To extend these results to a more clinically relevant setting, further studies were performed using cells isolated from the blood of patients with chronic lymphocytic leukaemia (CLL), the most common leukaemia in the Western world. Signalling via the B-cell receptor (BCR) is known to play a major role in the development and progression of CLL, and studies first investigated how BCR stimulation altered mRNA translation in primary CLL cells. Stimulation of surface IgM (sIgM) resulted in significant, but variable, increases in mRNA translation. Overall, increases in mRNA translation were higher in samples that were considered as sIgM responsive (based on previous analysis of anti-IgM-induced intracellular Ca^{2+} mobilisation) compared to non-responsive samples, and in samples stimulated with anti-IgM compared to anti-IgD. Anti-IgM also increased expression of *MYC* and *MCL1*, two key targets for CLL proliferation and survival, via increased transcription and mRNA translation. PEITC inhibited both basal and anti-IgM-induced RNA translation, whereas ibrutinib and tamatinib, inhibitors of the BCR-associated signalling kinase BTK and SYK, predominantly inhibited anti-IgM-induced mRNA translation. PEITC, ibrutinib and tamatinib also decreased translation of *MYC* and *MCL1* RNAs in anti-IgM treated cells. Similar to MCF7 cells, PEITC caused a rapid increase in eIF2α phosphorylation in CLL cells. Overall, these results are consistent with the hypothesis that inhibition of mRNA translation by PEITC may contribute to its anti-cancer effects. In particular, the work has revealed the eIF2α pathway as a novel target for PEITC and uncovered new links between translation and BCR signalling in human leukaemia. Inhibition of mRNA translation, in response to PEITC or novel kinase inhibitors may play an important role in the therapeutic effects of these agents.

Table of Contents

List of Figures

List of Tables

Publications Arising from this Thesis

The publications arising from this thesis are listed below and can be found in the appendix.

Cavell, B. E., S. S. Syed Alwi, A. Donlevy and G. Packham (2011). "Anti-angiogenic effects of dietary isothiocyanates: mechanisms of action and implications for human health." Biochem Pharmacol **81**(3): 327-336.

Cavell, B. E., S. S. Syed Alwi, A. M. Donlevy, C. G. Proud and G. Packham (2012). "Natural Product-Derived Antitumor Compound Phenethyl Isothiocyanate Inhibits mTORC1 Activity via TSC2." J Nat Prod **75**(6): 1051-1057.

Syed Alwi, S. S., B. E. Cavell, A. Donlevy and G. Packham (2012). "Differential induction of apoptosis in human breast cancer cell lines by phenethyl isothiocyanate, a glutathione depleting agent." Cell Stress Chaperones **17**(5): 529-538.

DECLARATION OF AUTHORSHIP

I, Alison Marie Yeomans,

declare that the thesis entitled

REGULATION OF RNA TRANSLATION BY PHENETHYL ISOTHIOCYANATE

and the work presented in the thesis are both my own, and have been generated by me as the result of my own original research. I confirm that:

- this work was done wholly or mainly while in candidature for a research degree at this University;
- where any part of this thesis has previously been submitted for a degree or any other qualification at this University or any other institution, this has been clearly stated;
- where I have consulted the published work of others, this is always clearly attributed;
- where I have quoted from the work of others, the source is always given. With the exception of such quotations, this thesis is entirely my own work;
- I have acknowledged all main sources of help;
- where the thesis is based on work done by myself jointly with others, I have made clear exactly what was done by others and what I have contributed myself;
- ~~none of this work has been published before submission~~, or [delete as appropriate] parts of this work have been published as: [please list references]

Signed: ……..

Date:…….

Acknowledgements

Firstly, I would like to thank my supervisor Professor Graham Packham for his support and guidance throughout my PhD as well as giving me the opportunity to carry out this research in his laboratory. I would also like to thank my second supervisor Doctor Mark Coldwell for allowing me to become part of his group as well as his help and expertise. A proportion of the work in this thesis would not have been possible to carry out without the use of the polysome profiling equipment that Professor Chris Proud (University of Southampton) kindly allowed me to use, so I am thankful for his collaboration.

In addition I would also like to thank Professor Randal Kaufman (University of Michigan Medical Centre, USA) for providing non-phosphorylatable eIF2α MEFs along with wild type MEFs.

Furthermore I am also grateful to members of both the Graham Packham Lab and Mark Coldwell's Lab (both past and present) along with everyone in the CLL group for their support and encouragement throughout my PhD. I would like to thank my friends and family for their support over the past four years. I would especially like to thank my husband, Chris, for his patience as well as his engineering ability that enabled me to install new hardware to make polysome profiling more sensitive.

This PhD was funded by the Gerald Kerkut Charitable Trust, so a final thank you to the Gerald Kerkut trust for funding this research.

Abbreviations

2-AP	2-Aminopurine
2-ME	2-methoxyestradiol
2-OG	2-oxyglutarate
4E-BP1	eIF4E-Binding Protein -1
AIF	Apoptosis Inducing Factor
Akt	Protein Kinase B
ARE	Antioxidant Response Element
BCR	B Cell Receptor
BLAST	Basic Local Alignment Searching Tool
BLNK	B cell linker protein
BSA	Bovine Serum Albumin
BTK	Burton's Tyrosine Kinase
BTKi	Burton's Tyrosine Kinase Inhibitor
$C_{H/L}$	Constant gene for heavy (H) or light (L) chain
CD(19)	Cluster of Differentiation (19)
Cdk	Cyclin dependent kinase
CHX	Cycloheximide
CLL	Chronic Lymphocytic Leukaemia
D_H	Diversity gene for heavy chain
DAG	Diacylglycerol
DAPI	4′,6-Diamidino-2-phenyindole
DMEM	Dulbecco's Modified Eagle Medium
DMSO	Dimethyl sulfoxide
DTT	Dithiothreitol
eEF	eukaryotic Elongation Factor
eIF	eukaryotic Initiation Factor
ELISA	Enzyme Linked Immuno-Sorbent Assay
eRF	eukaryotic Release Factor
ERK	Extracellular signalling Regulated Kinase
FRET	fluorescence resonance energy transfer

GAA	Glacial Acetic Acid
GCN2	General Control Non-depressible kinase -2
GEF	Guanine nucleotide Exchange Factor
HIF	Hypoxic Inducible Factor
HRI	Heme Regulated Inhibitor kinase
HUVEC	Human Umbilical cord Vein Endothelial Cells
IC Beads	Isotype Control Beads
Ig(M/D)	Immunoglobulin (M/D)
IL-10	Interleukin -10
IP3	Inositol trisphosphate
IRES	Internal Ribosome Entry Site
ITAF	IRES Transactivating Factor
ITAM	Immunoreceptor Tyrosine base Activation Motif
ITC	Isothiocyanate
$J_{H/L}$	Joining gene for heavy (H) or light (L) chain
Keap1	Kelch like ECH associated protein -1
M-CLL	Mutated-Chronic Lymphocytic Leukaemia
MEF	Mouse Embryonic Fibroblast
miRNA	micro-RNA
MMP	Matrix Metalloproteinase
mRNA	messenger RNA
mTORC1/2	mammalian Target of Rapamycin Complex 1/2
NF-κB	Nuclear Factor – kappa B
Nrf2	Nuclear factor E2 Related Factor 2
ODDD	Oxygen Dependent Degradation Domain
p70S6K	p70S6 Kinase
PARP	Poly ADP-Ribose Polymerase
PBMC	Peripheral Blood Mononuclear Cells
PBS	Phosphate Buffered Saline
PEITC	Phenethyl Isothiocyanate
PERK	PKR-like Endoplasmic Reticulum Kinase
PHD	Prolyl Dependent Hydroxylase Domain
PI3K	Phosphatidyl inositol 3 Kinase

PIC	Pre-Initiation Complex
PIP3	Phosphoinositol-3,4,5-triphosphate
PKC	Protein Kinase C
PKR	Protein Kinase R
PLCγ	Phospholipase C γ
PPT	Polypyrimidine Tract
PTB	Polypyrimidine Tract Binding protein
qPCR	quantitative Polymerase Chain Reaction
RACE	Rapid Amplification of cDNA Ends
RAG	Recombination Activating Genes
RISC	RNA Induced Silencing Complex
ROS	Reactive Oxygen Species
RPMI	Roswell Park Memorial Institute media
RSS	Recombination Signal Sequence
SDS	Sodium Dodecyl Sulfate
SFN	Sulforaphane
SH2	Src Homology -2 (domain)
sIgM	surface Immunoglobulin M
siRNA	small interfering RNA
SOD	superoxide dismutase
SYK	Spleen Tyrosine Kinase
SYKi	Spleen Tyrosine Kinase Inhibitor
T_{Reg}	Regulatory T cell
TAD	Transactivating Domain
TBS-T	Tris-Buffered Saline-Tween
TC	Ternary Complex
TCA	Trichloroacetic Acid
TFIIH	Transcription Factor for RNA polymerse II H
TG	Thapsigargin
TGFβ	Transforming Growth Factor β
T_H	T Helper Cell
TIA-1	T cell Internal Antigen -1
TIMP	Tissue Inhibitors of MMP (matrix metalloproteinase)

U-CLL	Unmutated - Chronic Lymphocytic Leukaemia
uORF	upstream Open Reading Frame
UT	Untreated
UTR	Untranslated Region
$V_{H/L}$	Variable gene for heavy (H) or light (L) chain
VEGF	Vascular Endothelial Growth Factor
VHL	Von Hippel Lindau
XIAP	X-linked Inhibitor of Apoptosis Protein
ZAP70	Zeta Associated Protein -70

Chapter One

Introduction

1. Introduction

1. 1. Overview

The overall goal of the experiments described in this thesis was to investigate the potential regulation of mRNA translation by phenethyl isothiocyanate (PEITC), a naturally occurring compound with both chemopreventive and anti-cancer properties. Studies were performed in established cancer cell lines as well as primary samples derived from patients with chronic lymphocytic leukaemia (CLL), a common malignancy where PEITC is being considered as a potential therapeutic agent. The introduction will therefore provide the key background to the three main elements of the project; (i) the anti-cancer properties of PEITC, (ii) regulation of mRNA translation and (iii) CLL.

1. 2. Phenethyl Isothiocyanate

Isothiocyanates (ITCs) are a group of compounds with the general formula R-NCS (Figure 1-1). Some ITCs are naturally occurring and consumed as part of everyday diets. For example watercress is a rich source of PEITC, while mustard is a rich source of Allyl-ITC and broccoli is a rich source of sulforaphane (Zhang, 2004) (Figure 1-1). In plants, ITCs are stored as inactive glucosinolate precursors, with gluconasturtiin the precursor for PEITC (Figure 1-2). Following disruption of the plant tissue by cutting and mastication the glucosinolate precursors are converted into ITCs by thioglucosidase enzymes, known as myrosinase (Ji and Morris, 2003) (Figure 1-2). Myrosinase is present within the plant cell in a different cellular compartment, therefore conversion of glucosinolates into ITCs only occurs following cellular damage (Figure 1-2). The presence of high levels of ITCs in diets rich in plants such as cabbage and broccoli may account for the reduced risk of cancer associated with diets rich in these cruciferous vegetables. Non-natural ITCs have

also be synthesised, especially in an attempt to improve the anti-cancer properties of this class of simple chemical compounds.

ITCs are generally reactive compounds due to the central carbon being highly electrophilic, in contrast, glucosinolates are inactive precursors (Zhang, 2004). The electrophilicity of ITCs is thought to underlie much of their biological effects. ITCs can react via reversible thiocarbamoylation or irreversible alkylation reactions, binding ITCs to thiol groups (especially within cysteine) and amino groups (lysine) respectively (Mi et al., 2011). At physiological pH the thiocarbamoylation reaction is preferentially used as this occurs 1000 times faster than alkylation (Mi et al., 2011). Thiocarbamoylation can alter biological activity of target proteins as cysteine residues are often present in catalytic sites, which may significantly alter enzymatic activity, redox status and signalling pathways (Koritzinsky et al., 2006; Mi et al., 2011). The electrophilic nature of the central carbon atom enables nucleophilic targets, such as low pKa cysteines to bind via a thiocarbamoylation reaction (Figure 1-3). This occurs as the thiol group will be converted to a thiolate ion, enabling nucleophilic attack on the highly electrophilic central atom. This will ultimately break one of the N=C double bonds, so that the nitrogen will attack a hydrogen resulting in thiol-ITC conjugate (Figure 1-3). The electrophilic nature of the ITC is modulated by the nature of the side chain (R) group (Figure 1-1). The reaction of ITCs is also influenced by the effects of the R-group on steric hindrance and lipophilicity (Zhang, 2004).

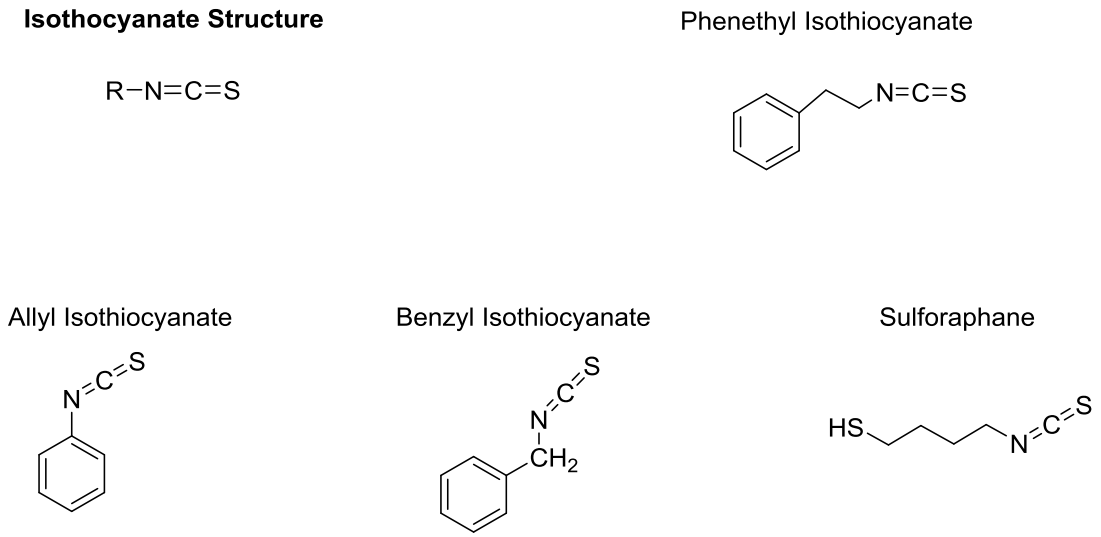

Figure 1-1: Structure of Isothiocyanates

Isothiocyanates have different chemical properties depending on their side chains (R). Illustrated is the general isothiocyanate structure as well as phenethyl isothiocyanate and other common isothiocyanates. Illustration prepared in ChemBioDraw Ultra version 13.0.

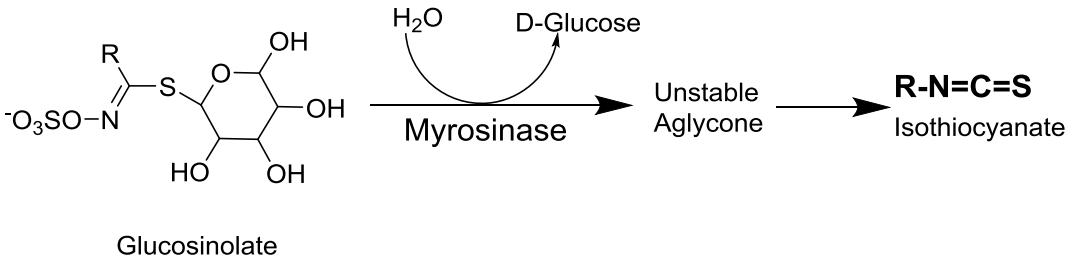

Figure 1-2: Glucosinolate-Myrosinase Reaction

Upon plant cellular damage myrosinase is released and comes into contact with the glucosinolate precursors, resulting in the release of D-glucose and following structural rearrangement isothiocyanates are produced in neutral pH, adapted from (Fahey et al., 2001; Kong et al., 2012). Illustration prepared in ChemBioDraw Ultra version 13.0.

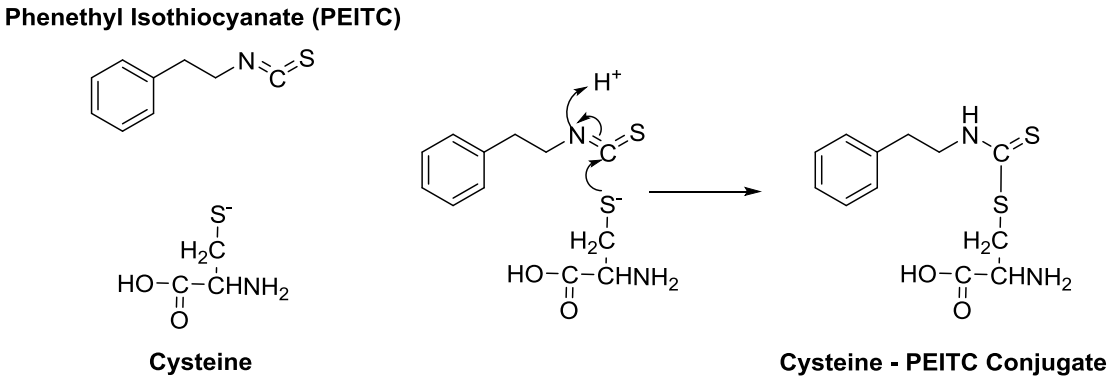

Figure 1-3: PEITC Thiocarbamoylation Reaction.

The N=C=S electrophilic group of PEITC reacts at physiological pH with thiol groups generating a thiocarbamate. Illustration prepared in ChemBioDraw Ultra version 13.0.

The most abundant thiol containing peptide within the cell is glutathione, the major anti-oxidant. PEITC, and other ITCs, freely diffuse across the plasma membrane and into the intracellular environment where PEITC forms a glutathione conjugate that is exported from the cells via efflux pumps on the plasma membrane. In the extracellular environment this conjugate dissociates into free ITC and glutathione, the free ITC can diffuse once again into the cell and bind to more thiol groups (Figure 1-4). This cycle depletes the cell of glutathione and results in the accumulation of PEITC in the cell up to milli-molar concentrations, or up to 100 times the concentration of the extracellular environment (Zhang et al., 2006). After depletion of glutathione, PEITC can then interact with other thiol containing proteins, which may provide a mechanism for decreased proliferation and growth. The interaction with glutathione occurs before PEITC binds to proteins, as analysed using radiolabelled ^{14}C-PEITC (Mi et al., 2011; Mi et al., 2007). Within 30 minutes 80% of radiolabelled PEITC was conjugated to glutathione, whereas following 4 hours of incubation with ^{14}C-PEITC 90% of all cellular PEITC was conjugated to proteins (Mi et al., 2011; Mi et al., 2007). Interestingly the binding of PEITC to proteins appears to be relatively selective perhaps due to steric or electrochemical influences of amino acid residues surrounding the target thiol group. To date about 30 proteins have been shown to conjugate with PEITC (Mi et al., 2011). Proteins known to conjugate with PEITC include actin, tubulin as well as to two ribosomal proteins; 40S ribosomal protein S21 and 60S acidic ribosomal protein P2 (Mi et al., 2011). These ribosomal proteins are important for translation as S21 is present on the surface of the 40S ribosome (Torok et al., 1999), while P2 is important for the activation of the elongation factors (Bargis-Surgey et al., 1999). Binding of PEITC to these ribosomal proteins may provide a mechanism for altered translation in response to PEITC treatment.

One main mechanism for the biological effects of PEITC is mediated by reactive oxygen species (ROS) as a consequence of glutathione depletion due to the thiocarbamyolation reaction of PEITC with glutathione (Figure 1-5). ROS production occurs as a result of metabolic activity and under normal physiological conditions the ROS production is counterbalanced by anti-oxidant activity. A modest increase in ROS is believed to have a proliferative advantage whereas excessive ROS production will result in cellular damage (Hu et al., 2005). Malignant cells

often have elevated ROS (superoxide, O_2^-) levels compared to their non-malignant counterparts. For example ovarian cancer cells have elevated ROS compared to normal ovarian cells and leukaemia patients have lymphocytes with elevated ROS compared to the levels present in lymphocytes from a healthy volunteer (Hileman et al., 2004; Hu et al., 2005). Addition of PEITC has a selective detrimental effect on cancerous cells because they are dependent on their antioxidant system for survival and PEITC depletes the cellular levels of glutathione, the major antioxidant.

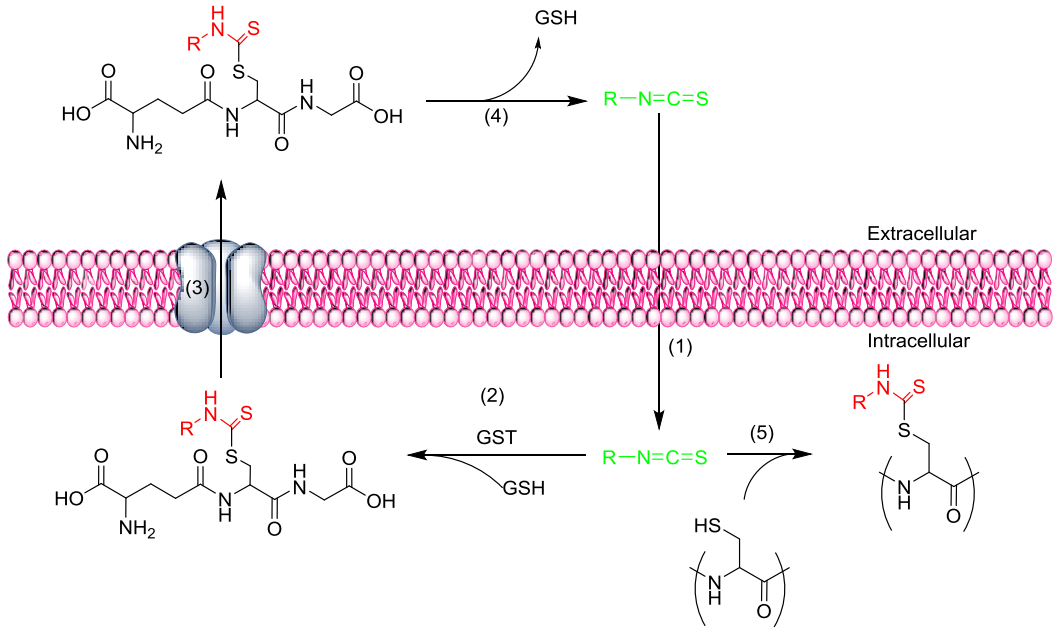

Figure 1-4: Intracellular Accumulation of ITCs

ITCs (in green) diffuse across the plasma membrane (1) and once in the intracellular environment bind to thiol groups in glutathione (GSH),via the action of glutathione-S-transferase (GST) (2). The GSH-ITC conjugate is removed from the cell via efflux pumps (3) (with the ITC group shown in red). The GSH-ITC conjugate dissociates (4) in the extracellular environment releasing free ITC (green) to continue the cycle 1-4 until intracellular GSH levels are depleted, ITCs will then bind via thiol groups to other proteins (5) via protein thiocarbamoylation. Adapted from (Cavell et al., 2011). Illustration prepared in ChemBioDraw Ultra version 13.0.

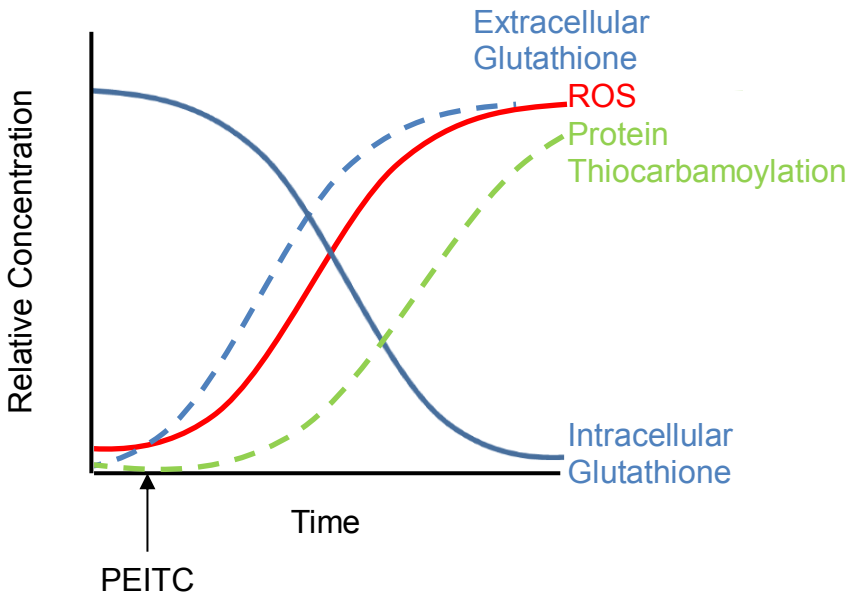

Figure 1-5: Effect of PEITC on Reactive Oxygen Species and Glutathione Levels

Schematic representation of the effect of PEITC on ROS, glutathione and thiocarbamylation conjugate levels. Following PEITC treatment ROS levels will increase as a consequence of increased thiocarbamoylation, ultimately resulting in decreased glutathione levels.

A secondary mechanism for the biological effect of PEITC is mediated via direct interaction of PEITC with proteins. A known biological effect of PEITC treatment is increased activity of the transcription factor Nrf2 (nuclear factor E2 related factor 2) that results in enhanced expression of phase II detoxifying enzymes (Dinkova-Kostova et al., 2002; Hong et al., 2005). Increased Nrf2 activity following treatment with ITCs occurred due to inhibition of the Nrf2 binding protein, Keap-1 (Kelch like ECH associated protein -1). Keap-1 binds and sequesters Nrf2 in the cytoplasm as the complex is anchored to the actin cytoskeleton (Dinkova-Kostova et al., 2002). Activation of Nrf2 results in release of Nrf2 from Keap-1 allowing migration into the nucleus, where heterodimeric interactions with other transcription factors occurs and Nrf2 will bind to the antioxidant response element (ARE) upstream of the promoter, leading to enhanced expression of phase II detoxifying enzymes (Dinkova-Kostova et al., 2002). Keap-1 has also been shown to inhibit Nrf2 activity by enhancement of Nrf2 ubiquitination and degradation. Keap-1 has 27 Cys residues that are available to react with electrophiles and have been shown to be modified by ITCs (Hong et al., 2005). The effect of ITCs on cancer progression are reviewed by Cavell et al (Cavell et al., 2011), with details provided in sections 1. 2. 1. - 1. 2. 6. , inclusive and summarised in Figure 1-6 and Table 1-1.

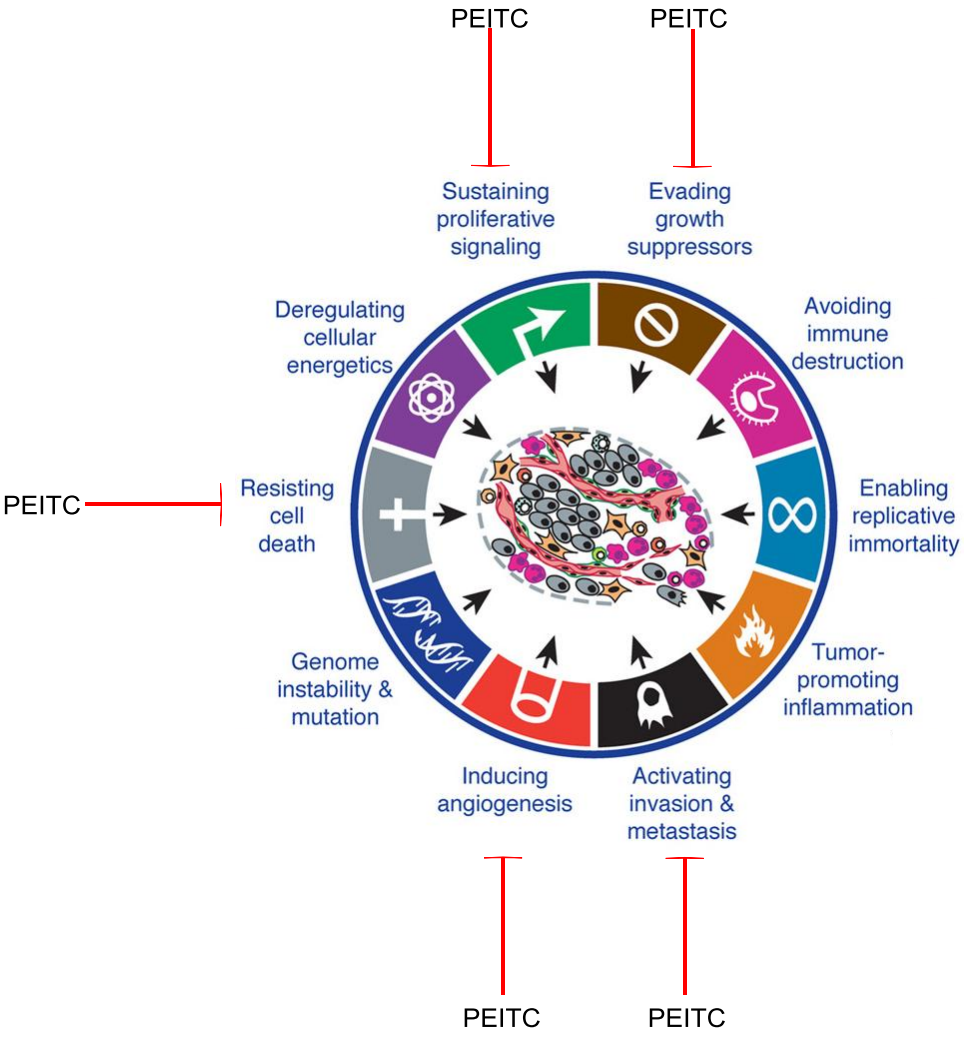

Figure 1-6: Effect of PEITC on Cancer Progression

PEITC has previously been shown to inhibit five hallmarks of cancer progression. Diagram adapted from (Hanahan and Weinberg, 2011)

1. 2. 1. PEITC as a Chemopreventive Agent

PEITC is thought to be a chemopreventative compound and is currently being investigated to determine whether PEITC can prevent lung cancer in smokers (ClinicalTrials.gov NCT00691132). NNK, a nicotine-derived nitrosamine is believed to be involved in the development of carcinogen induced lung cancer. Rats treated with NNK in combination with a diet rich in PEITC developed significantly fewer lung tumours than control diet NNK treated rats (Chung et al., 1992). Pre-treatment of PEITC can also prevent tumour development in mice (Chung et al., 1992; Gross and Kinzy, 2007). The inhibition of carcinogen induced carcinogenesis by ITCs is believed to occur due to the inhibition of phase I cytochrome P450 enzymes, the induction of phase II detoxifying enzymes and the expression of anti-oxidant genes such as glutathione-S-transferase, NAD(P)H:quinone oxidoreductase, UDP-glucurosyl transferase and thioreductase, all of which are mediated by the transcription factor Nrf2 (Wang et al., 2009), see section 1. 2.

The chemopreventive activity of PEITC is currently being investigated in a phase II clinical trial. This trial consists of a short one month trial where participants smoke only deuterated NNK cigarettes provided and during week two they will be given PEITC orally four times daily and in week four placebo will be given orally four times daily. A longer trial will also be carried out where participants are given PEITC or placebo twice daily for 12 months. Smokers will be randomized in this trial and samples will be analysed at baseline and completion of the study, which will analyse metabolism of NNK, PEITC uptake (analysed by the method described by Chung et al 1992), cell proliferation (by Ki67 immunohistochemistry) and markers of apoptosis will be analysed including caspase 3 (ClinicalTrials.gov NCT00691132).

1. 2. 2. Anti-Cancer Activity of PEITC

PEITC is believed to not only be a chemopreventive compound but may also possess direct anti-cancer activity, these effects have been seen in established cancer cells where carcinogens are no longer involved in the effect of PEITC on these cells. PEITC is currently in a phase I clinical trial to investigate the effect of PEITC on oral cells with mutant p53 (ClinicalTrials.gov NCT01790204). The tumour suppressor protein, p53, has many functions including regulation of the cell cycle. Mutations within p53 are believed to be a marker of malignant cells and can occur following DNA damage, for example from NNK in cigarettes. Mutant p53 is known to inhibit wild type p53 transcriptional activity resulting in decreased tumour suppressor expression (Goh et al., 2011). The gain of function effect of mutant p53 promotes invasion, migration, angiogenesis, survival, proliferation and tissue remodelling, resulting in the development of carcinomas, sarcomas and lymphomas (Muller and Vousden, 2013). This phase I clinical trial aims to investigate the effect of PEITC on cell survival of p53 mutant cells. Oral cells will be collected from smokers as these participants are likely to have measurable levels of mutant p53 cells, due to the presence of the carcinogens in cigarettes. Participants will be given watercress juice, made from 55g of watercress, with the hypothesis that the ITCs in the juice will deplete p53 mutant cells. (ClinicalTrials.gov NCT01790204).

It is known that PEITC has anti-cancer activity but the mechanisms are still being investigated. The traditional hallmarks of cancer include sustained proliferation, evading growth suppression, enhanced invasion and metastasis, replicative immortality, increased angiogenesis and resisting cell death (Hanahan and Weinberg, 2000), with emerging hallmarks including avoidance of immune destruction, tumour promoting inflammation, genome instability and deregulation of cellular energetics (Figure 1-6) (Hanahan and Weinberg, 2011). Research into the anti-cancer activity of PEITC has demonstrated that PEITC can inhibit five out of six of the traditional hallmarks of cancer, with little known regarding the effect of PEITC on replicative immortality. The mechanisms behind these anti-cancer actions are very complex and not fully understood. Possible mechanisms for inhibition of

proliferation and survival could be due to cellular stress, via enhanced ROS levels or via direct interaction with cellular proteins.

1. 2. 3. Effect of PEITC on Proliferation

PEITC inhibits the proliferation of many different cancer types, including prostate cancer, breast cancer cells as well as oncogene transformed cell lines grown as xenografts in immunocompromised animals (Khor et al., 2006). The IC_{50} for growth inhibition of MCF7 (breast cancer) cells was approximately 11µM (Wang et al., 2009). Progression through the cell cycle is mediated via activation of cyclin dependent kinases (Cdk) associated with their corresponding cyclins. Entry into mitosis (M phase) is regulated by Cdk1 and the associated cyclin B; activation of Cdk1 occurs via phosphorylation on Thr^{161}, while phosphorylation of Thr^{14} and Thr^{15} results in inhibition of Cdk1 (Xiao et al., 2004). Dual specificity phosphatases, Cdc25B and Cdc25C, can remove the inhibitory phosphate groups to promote Cdk1 activation (Xiao et al., 2004). In PC3 cells PEITC had no effect on cyclin B and Cdc25B levels as determined by immunoblotting. Whereas Cdk1 and Cdc25C protein levels were decreased in response to PEITC treatment and the inactive form of Cdk1 (Cdk1 Thr^{15}) accumulated with PEITC treatment (Xiao et al., 2004). The decrease in both Cdk1 and Cdc25C in response to PEITC treatment was prevented by the addition of the proteasome inhibitor, lactacystin, prior to and during PEITC treatment. The G_2-M block by PEITC was also attenuated in the presence of lactacystin (Xiao et al., 2004). This indicated that PEITC inhibited cell proliferation in a proteasome dependent manner via the degradation of Cdk1 that induced a cell cycle block.

1. 2. 4. Effect of PEITC on Tumour Metastasis

Once cells have specialised and differentiated they are generally maintained in the organ or tissue that they are specialised for and do not spread into different

tissues. In cancer cells there appears to be a reversal of the differentiated state and the cells can act more like a pluripotent cell enabling invasion and metastasis to occur. Metastasis is the process where tumour cells migrate away from the primary tumour site and will develop in secondary locations, often transported in the blood or lymphatic vessels. These tumour cells are therefore able to move around the body and generate tumours in other locations by invasion into other tissues. Metastasis is a complex process that alters adhesion, invasion and migration properties of the cell and is now an area of intense research. Cancer associated death is often due to metastasis, therefore prevention of metastasis may prolong the life expectancy of many cancer patients. In order for a solid tumour to metastasise the extracellular matrix needs to be degraded at the site of the primary tumour and at the site of invasion. Degradation of the extracellular matrix is carried out by matrix metalloproteinases (MMPs), with MMP-2 and MMP-9 known to degrade type IV collagen, the major component in the basement membrane (Hwang and Lee, 2006). Metastasis is a highly regulated process with MMPs released as a pro-MMP that require proteolytic conversion into the active MMP. Membrane type 1 MMP (MT1-MMP) is known to promote migration, invasion and proliferation by activating pro-MMP-2 to MMP-2 (Hwang and Lee, 2006). While tissue inhibitors of MMPs (TIMPs) are known to inhibit active MMP. Treatment with PEITC has been shown to significantly inhibit cell adhesion and invasion, using transwell assays, as well as inhibit migration, analysed by scratch wound assays in hepatocellular carcinoma and non-small cell lung cancer cells (Hwang and Lee, 2006; Wu et al., 2010). Protein and mRNA expression levels of MMP-2 were significantly decreased in PEITC treated cells (Hwang and Lee, 2006; Wu et al., 2010). MT1-MMP levels were also significantly reduced indicating a severe block in active MMP-2 levels, while TIMP-1 levels were unaltered (Hwang and Lee, 2006). These data indicated that treatment with PEITC decreased metastasis by inhibiting invasion and migration. A possible mechanism for this may be due to the prevention of matrix degradation due to decreased levels of active MMP-2, while the inhibitory TIMP levels were maintained.

1. 2. 5. Effect of PEITC on Angiogenesis

Tumour development often results in areas being insufficiently supplied with oxygen due to the rapid development of the tumour without development of adequate blood vessels. When cells are greater than 200µm from a blood vessel they will not receive oxygen by diffusion therefore these cells are in hypoxic (low oxygen) conditions. Hypoxic conditions stimulate blood vessel development, known as angiogenesis. Angiogenesis is important for malignant development as well as non-malignant development, such as wound healing and growth (Weidemann and Johnson, 2008). Insufficient blood supply can lead to many physiological complications including stroke, heart attack and neurological problems, due to inadequate oxygen supply and removal of waste products (Carmeliet and Jain, 2000; Hanahan and Weinberg, 2011).

Hypoxic conditions lead to the stabilisation of the transcription factor HIF (hypoxia inducible factor) involved in promoting the expression of pro-angiogenic molecules such as VEGF (vascular endothelial growth factor) (Carmeliet and Jain, 2000; Weidemann and Johnson, 2008). HIF is a heterodimeric transcription factor consisting of the constitutively expressed HIF-1β and hypoxia inducible HIF-1α subunit (Figure 1-7). HIF-1α is stabilised in hypoxic conditions, therefore regulated by oxygen levels (Weidemann and Johnson, 2008). In normoxic conditions HIF-1α is rapidly hydroxylated by the oxygen sensing prolyl dependent hydroxylase (PHD) enzymes on prolines 402 and 564 in the oxygen dependent degradation domain (ODDD) of HIF-1α (Figure 1-7) (Weidemann and Johnson, 2008). PHD enzymes are known as oxygen sensing because the hydroxylation of HIF-1α requires oxygen and Fe(II). PHD enzymes hydroxylate HIF-1α while converting 2-oxyglutarate (2-OG) to succinate and carbon dioxide (Dann and Bruick, 2005). PHD enzymes bind Fe(II), 2-OG, HIF-1α and oxygen. The initial step is an electron transfer from Fe(II) to oxygen generating an oxygen free radical (Dann and Bruick, 2005). The oxygen free radical attacks 2-OG, causing decarboxylation generating succinate and carbon dioxide (Dann and Bruick, 2005). In this process the oxygen molecule is split so that one atom is used to produce succinate while the other atom attacks Fe(III) forming Fe(IV)-oxo (Dann and Bruick, 2005). The reactive Fe(IV)-oxo removes a hydrogen

from HIF-1α to generate Fe(III)-hydroxide and a free radical on HIF-1α, this free radical then attacks Fe(IV)-hydroxide causing oxidisation to Fe(II) and hydroxylation of HIF-1α (Dann and Bruick, 2005). PHD enzymes are inactivated in hypoxia due to oxygen being a requirement for the initiation of enzyme activity (Dann and Bruick, 2005; Pouyssegur and Mechta-Grigoriou, 2006).

In normoxic conditions these hydroxyl groups on the ODDD of HIF-1α are recognised by the von Hippel Lindau (VHL) protein, which is part of an E3 ubiquitin ligase that targets HIF-1α to the proteasome for degradation (Figure 1-7) (Weidemann and Johnson, 2008). Whereas in hypoxic conditions PHD enzymes are inactive therefore the VHL protein cannot bind HIF-1α. Resulting in the stabilisation of HIF-1α, which then binds to HIF-1β and translocates into the nucleus. Once in the nucleus the HIF heterodimer will bind to the promoter region of target genes, recognised by the DNA binding domain of HIF-1α/β, enhancing transcription and eventually protein production of pro-angiogenic molecules (Weidemann and Johnson, 2008).

VEGF is fundamental in promoting angiogenesis and the expression of VEGF has been shown to be promoted in hypoxic conditions. HIF has been shown to promote the production of VEGF in hypoxic conditions and has also been shown to promote VEGF expression in HIF-overexpression assays in normoxic conditions, indicating that VEGF is a target of HIF (Forsythe et al., 1996). *VEGF* mRNA is also stabilised in hypoxic conditions, due to the interaction of *VEGF* mRNA with HuR, an RNA binding protein (Levy et al., 1998). HuR binding to *VEGF* mRNA in hypoxic conditions stabilised *VEGF* mRNA even in the presence of actinomycin D, a potent inhibitor of transcription (Levy et al., 1998). The stabilisation of *VEGF* mRNA therefore may indicate that translational regulation of VEGF is also important in the hypoxic-induction of VEGF.

Enhanced VEGF production as a result of HIF-1α stabilisation in hypoxic conditions stimulates vasodilation, capillary permeability as well as detachment of endothelial cells from the basement membrane to enable new blood vessels to form from the existing vasculature (Ruel et al., 2004). Tumour vasculature differs from non-malignant vasculature as a consequence of the rapid rate of growth and development. Tumour vessels are uneven in diameter and often leaky at inter-

endothelial junctions resulting in cycling oxygen levels in the tumour which promotes further angiogenesis (Carmeliet and Jain, 2000; Dewhirst, 2009). Therapeutically targeting angiogenesis to inhibit tumour development has mainly focused on VEGF signalling, with five therapies currently available for renal cell carcinoma, a highly vascular tumour. The response to these therapies is poor and is likely due to tumours becoming VEGF independent (Rini and Atkins, 2009).

PEITC, as well as other ITCs, has been demonstrated to inhibit angiogenesis by decreasing HUVEC (human umbilical vein endothelial cell) viability and migration as well as the ability to form capillary-like structures (Xiao and Singh, 2007). The mechanism for decreased angiogenesis by PEITC is likely to not solely target the VEGF signalling pathway as other therapies specifically targeting VEGF lead to resistance (Rini and Atkins, 2009). It has been shown that PEITC inhibits HIF-1α transcriptional activity as well as decreasing HIF-1α protein expression (Wang et al., 2009). PEITC decreased HIF-1α protein expression in hypoxic conditions in a proteasome independent manner and did not alter *HIF-1A* mRNA levels (Wang et al., 2009). This data suggested that PEITC may inhibit angiogenesis via inhibition of *HIF-1A* mRNA translation.

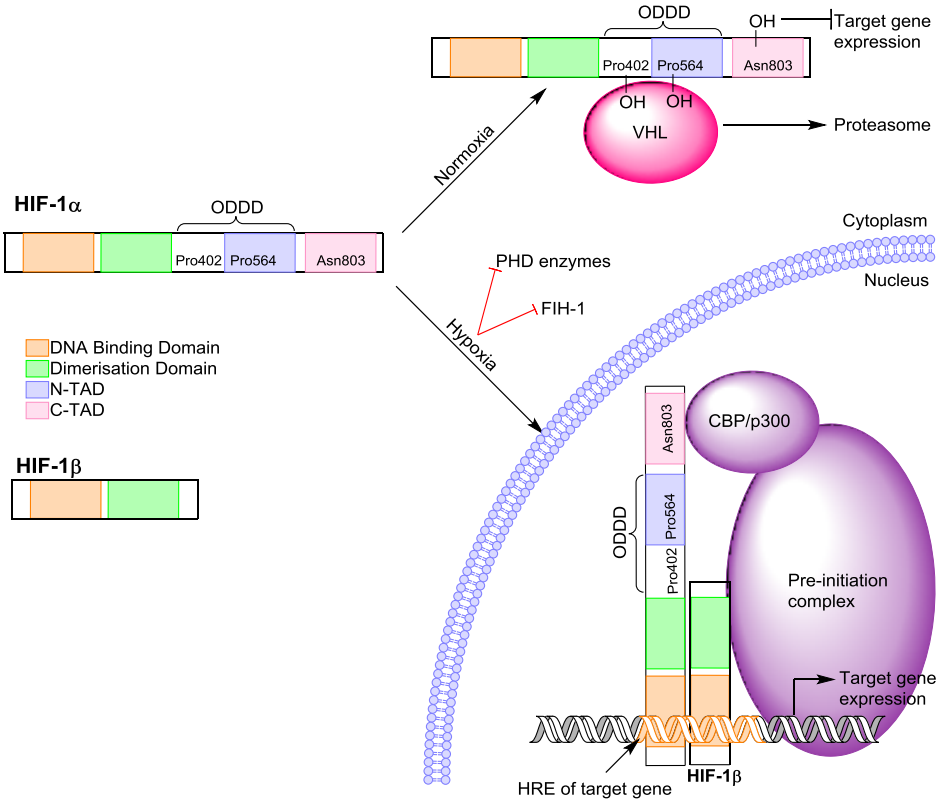

Figure 1-7: Regulation and Function of HIF-1α

The oxygen dependent HIF-1α subunit of HIF is a multi-domain protein consisting of a DNA binding domain that binds to the hypoxic response element (HRE) in the promoter region of target genes. A dimerization domain to enable HIF-1α and HIF-1β to interact. As well as an oxygen dependent degradation domain (ODDD), this contains proline residues at positions 402 and 564 that become hydroxylated by the prolyl hydroxylase domain (PHD) enzymes in normoxic conditions, to enhance degradation of HIF-1α. The hydroxyl groups are then recognised by the von hippel lindau (VHL) protein that will target HIF-1α to the proteasome for degradation. Finally HIF-1α also contains two transactivating domains (TADs) at the N and C terminal. These TADs are involved in the interaction of HIF-1α to the pre-initiation complex (PIC) to enhance transcription of target genes via the co-activators CBP/p300. During normoxic conditions HIF-1α is degraded due to active PHD enzymes. Factor inhibiting HIF (FIH-1) is also active in normoxic conditions resulting in the hydroxylation of Asn803 in the C-TAD preventing the interaction with CBP/p300, thereby inhibiting transcription. While in hypoxic conditions FIH-1 and PHD enzymes are inactivate resulting in the stabilisation and activation of HIF-1α. Illustration prepared in ChemBioDraw Ultra version 13.0.

1. 2. 6. Effect of PEITC on Apoptosis

Apoptosis, or programmed cell death, is vitally important to ensure eradication of non-functional, damaged or aged cells. Many cancers occur due to defects in the apoptotic pathway, with promoting apoptosis an attractive therapeutic target. PEITC has been shown to enhance apoptosis in many different cancer cells (Huong le et al., 2011; Satyan et al., 2006; Syed Alwi et al., 2012; Tang and Zhang, 2005; Xiao et al., 2004). A similar concentration of PEITC that inhibited proliferation (10µM) was required to inhibit the survival of PC3 prostate cancer cells (Xiao et al., 2004). Treatment with PEITC for 24 hours resulted in the accumulation of PC3 cells in the G_2-M phase of the cell cycle as well as an accumulation of cells in the subG_0-G_1 phase (Xiao et al., 2004). The PEITC-induced accumulation of cells in the sub G_0-G_1 phase can be prevented by the addition of anti-oxidants (Syed Alwi et al., 2012). PEITC also significantly increased the levels of cytoplasmic histone bound DNA fragments and PARP (Poly ADP-Ribose Polymerase) cleavage (Xiao et al., 2004). Apoptosis can occur via the activation of the caspase cascade, via intrinsic (Figure 1-8) or extrinsic regulation (Figure 1-9).

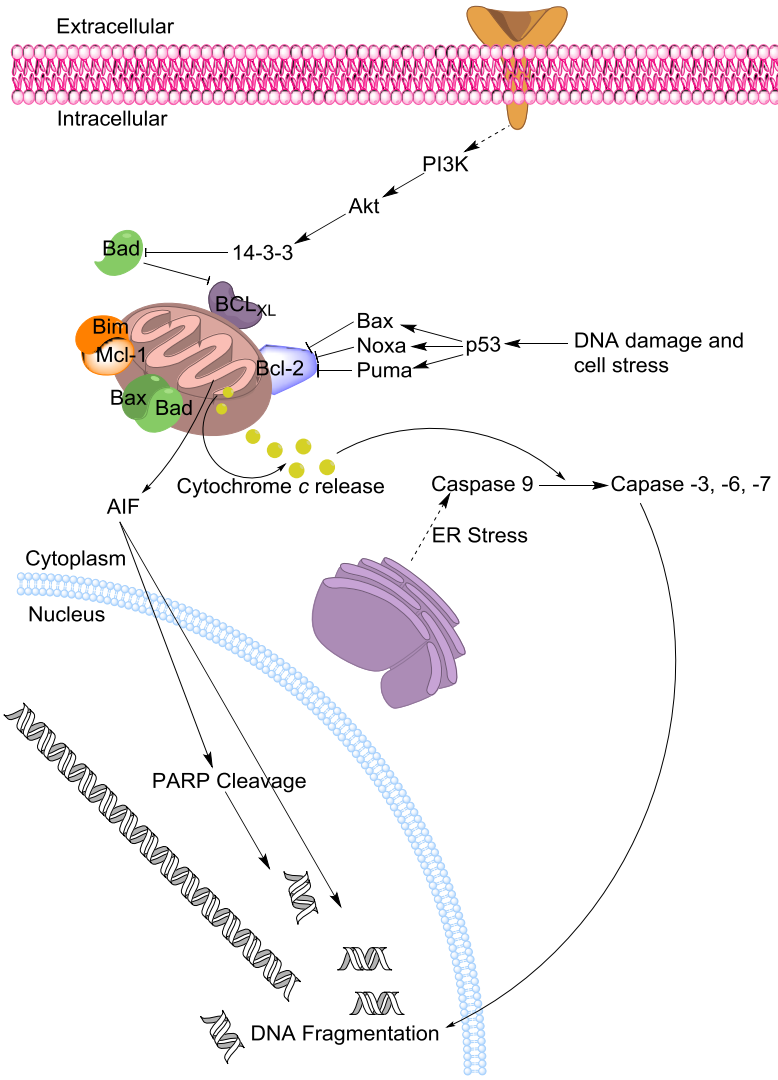

Figure 1-8: Intrinsic Regulation of Apoptosis

Apoptosis is regulated by many different pathways to control cytochrome *c* release from the mitochondria as reviewed by Fogg et al (Fogg et al., 2011). The pro-apoptotic molecule Bax in the heterodimer with Bad will induce cytochrome *c* release from the mitochondria, whereas in a heterodimeric complex with the anti-apoptotic molecule Bcl-2 will prevent the release of cytochrome *c*. Bim is also a pro-apoptotic molecule. Initiation of apoptosis occurs with release of anti-apoptotic molecules Bcl-2 and Bcl_{XL}. Cytochrome *c* release will initiate the caspase cascade firstly by the cleavage of pro-caspase 9 to caspase 9 activating the downstream cleavage and production of caspase -3, -6 and -7. The caspase cascade can also be initiated via ER stress and ultimately results in DNA fragmentation. DNA fragmentation is also initiated by the apoptosis inducing factor (AIF). Illustration prepared in ChemBioDraw Ultra version 13.0.

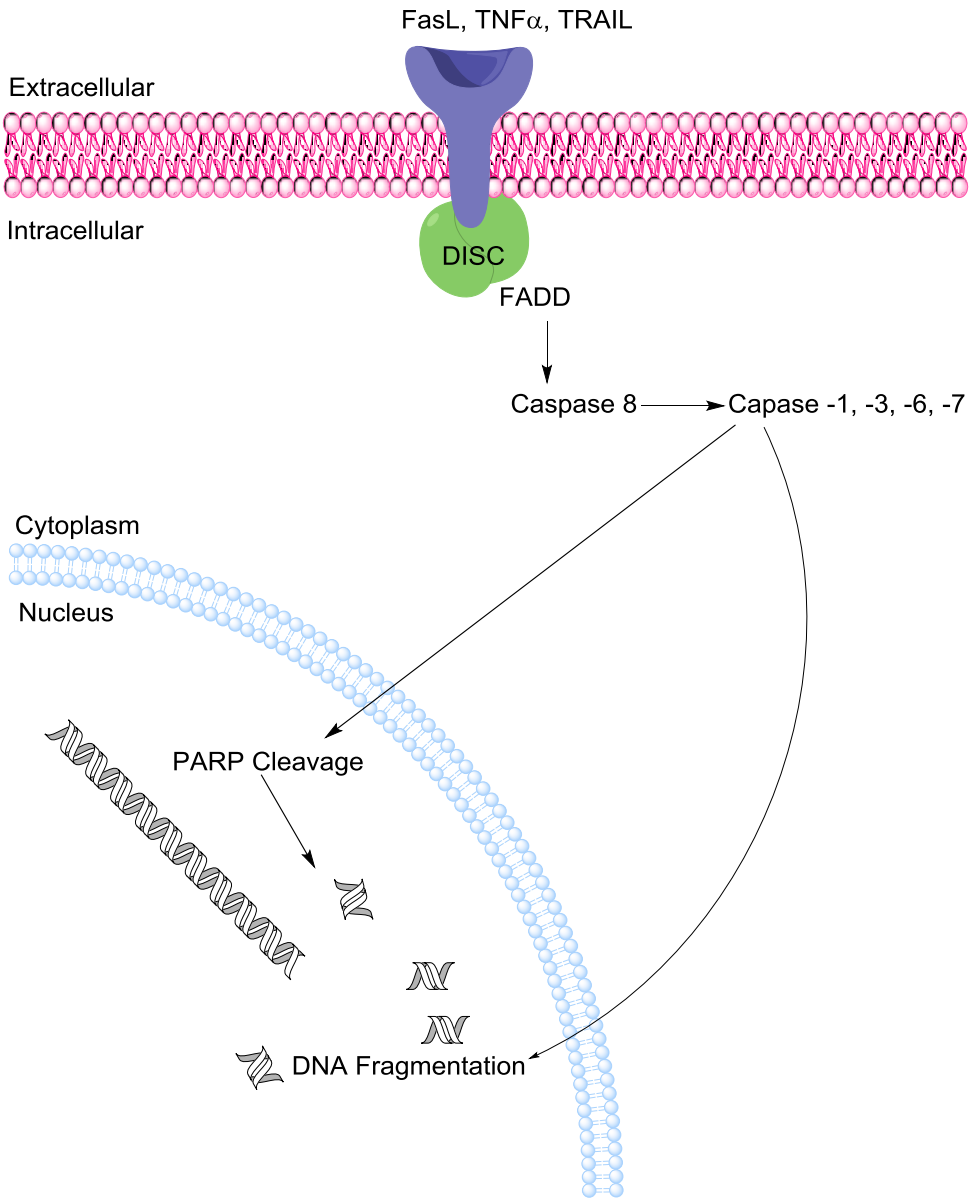

Figure 1-9: Extrinsic Regulation of Apoptosis

Induction of apoptosis via extracellular stimulation occurs via the FasL, TNF-α or TRAIL receptors (Circu and Aw, 2012). The activation of these receptors results in the formation of the death-inducing signalling complex (DISC). This results in the recruitment and activation of a death domain kinase like FADD (Fas associated death domain kinase) that activates caspase-8 resulting in the activation of downstream caspases and ultimately DNA fragmentation leading to cell death (Circu and Aw, 2012). Illustration prepared in ChemBioDraw Ultra version 13.0.

During intrinsic induced apoptosis, the pro-apoptotic protein, Bax, when activated releases cytochrome *c* from the mitochondria, leading to caspase cleavage and activation ultimately resulting in apoptosis (Figure 1-8). The anti-apoptotic proteins, Bcl-2 and Bcl_{XL}, are often up-regulated in cancer and inhibit the activation of Bax and the release of cytochrome *c*. Bcl-2 and Bcl_{XL} protein levels were significantly reduced in response to PEITC treatment, resulting in activation of the apoptosis pathway (Satyan et al., 2006). Apoptosis was induced by PEITC via the caspase cascade (Huong le et al., 2011; Syed Alwi et al., 2012; Tang and Zhang, 2005) and treatment with z-VAD (a caspase inhibitor) counteracted PEITC-induced apoptosis (Huong le et al., 2011).

Table 1-1: Summary of the Biological Effect of PEITC

PEITC has many biological effects and listed in the table below are some of the biological effects with references describing in detail the action of PEITC.

Biological Response	Effect	Reference
Regulation of P450 enzymes	ITCs down regulate P450 enzymes required for carcinogens	(Konsue and Ioannides, 2010; Wang et al., 2009)
Induction of antioxidant gene expression	ITCs increase Nrf2 activity which enhances antioxidant gene expression	(Hong et al., 2005)
Cell Cycle Arrest	ITCs inhibit progression through the cell cycle with accumulation in G_1, S, G_2/M	(Xiao et al., 2004)
Induction of Apoptosis	ITCs induce apoptosis in an intrinsic and extrinsic manner	(Huong le et al., 2011; Satyan et al., 2006; Syed Alwi et al., 2012; Tang and Zhang, 2005; Xiao et al., 2004)
Inhibition of Metastasis	ITCs inhibit cell adhesion, invasion and migration	(Hwang and Lee, 2006)
Inhibition of Proliferation	ITCs inhibit proliferation in many cancer cell lines, including MCF7 and PC3, breast and prostate cancer cell lines respectively	(Wang et al., 2009; Xiao et al., 2004)
Inhibition of Angiogenesis	Angiogenesis has been shown to be inhibited *in vivo* and *ex vivo*	(Wang et al., 2009; Xiao and Singh, 2007)

1. 3. Regulation of Translation

A possible mechanism for the anti-cancer activity of PEITC may be due to the modulation of mRNA translation. Many of the signalling pathways that are deregulated in cancer progression have implications on the regulation of translation, with mRNA translation believed to be a good target for anti-cancer therapies (Mamane et al., 2006). The first indication that PEITC may inhibit translation was discovered in prostate cancer cells (Hu et al., 2007). PEITC increased the total level of eukaryotic initiation factor 4E-binding protein 1 (4E-BP1) as well as decreased the phosphorylation status of 4E-BP1 (Hu et al., 2007). This suggested that less eukaryotic initiation factor 4E (eIF4E) was available to bind to the 5'cap of mRNA to initiate translation (see section 1. 3. 2. and 1. 3. 7. 1.). This was verified using 7-methyl-GTP sepharose pull down assays as well as luciferase assays to determine the translational activity of cells following treatment with PEITC (Hu et al., 2007).

The effect of PEITC on specific mRNA translation was first analysed in a study investigating the effect of PEITC on angiogenesis (Wang et al., 2009). It was shown that PEITC significantly decreased HIF-1α protein levels in a proteasome independent manner while mRNA levels were maintained (Wang et al., 2009). It was also confirmed that PEITC decreased the phosphorylation status of 4E-BP1 (Hu et al., 2007; Wang et al., 2009), which leads to inhibition of translation initiation, see section 1. 3. 2. The phosphorylation status of 4E-BP-1 from peripheral blood mononuclear cells (PBMCs) isolated from healthy volunteers has also been shown to have decreased after ingestion of 100g watercress, with a maximum inhibition seen two to three hours after ingestion (Syed Alwi et al., 2010). Since then investigations into the modification of pathways that regulate translation have started to be analysed (Cavell et al., 2012) although further investigation is still required.

1. 3. 1. Overview of Translation

Gene expression is fundamental in biology with protein production regulated at transcription and translation, with translation known to play a major role in protein production. (Schwanhausser et al., 2011). Translation of mRNA into proteins is a highly regulated process that can occur in a cap-dependent or cap-independent manner. Translation is regulated at initiation (in both cap-dependent and cap-independent translation), elongation (of the growing polypeptide) and at termination of translation. Translation can be regulated due to modifications (phosphorylation) of eukaryotic initiation factors (eIFs), eukaryotic elongation factors (eEFs) and eukaryotic release factors (eRFs). .

Translation, has been reviewed by Sonnenberg and Hinnebusch (Sonenberg and Hinnebusch, 2009), and is known to occur on ribosomes, large complexes of proteins and ribosomal RNA (rRNA) that recognise mRNA and initiate translation at the start codon, most commonly AUG. The ribosome then moves in the 5' to 3' direction and 'decodes' the triplet codon message into protein. The mRNA encodes the amino acid sequence in codons, which are three nucleotides in length, that are recognised by the ribosome and the tRNA molecules containing the complimentary anti-codon and the amino acid associated with that anti-codon (Figure 1-10). The ribosome covalently couples the amino acids releasing them from the tRNA as the ribosome moves along the mRNA. The polypeptide chain will grow out of the ribosome where co-translational modifications such as folding and glycosylation may occur. When the ribosome reaches a stop codon (UAA, UAG or UGA) this results in the termination of protein synthesis. At termination the polypeptide chain is released from the ribosome and post-translational modifications can occur. The ribosome will dissociate from the mRNA and the ribosomal subunits are free to start a new round of translation.

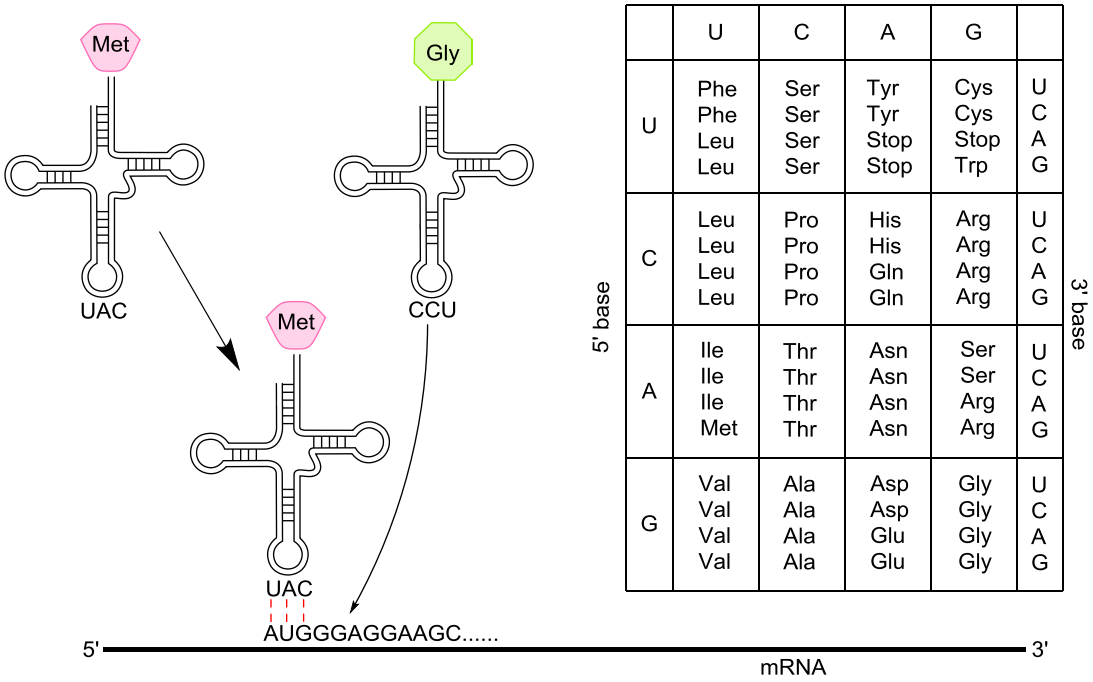

Middle base

5' base	U	C	A	G	3' base
U	Phe Phe Leu Leu	Ser Ser Ser Ser	Tyr Tyr Stop Stop	Cys Cys Stop Trp	U C A G
C	Leu Leu Leu Leu	Pro Pro Pro Pro	His His Gln Gln	Arg Arg Arg Arg	U C A G
A	Ile Ile Ile Met	Thr Thr Thr Thr	Asn Asn Asn Asn	Ser Ser Arg Arg	U C A G
G	Val Val Val Val	Ala Ala Ala Ala	Asp Asp Glu Glu	Gly Gly Gly Gly	U C A G

Figure 1-10: Decoding the Triplet Code Using tRNAs

Translation of mRNA into protein requires correct decoding of the mRNA sequence. The mRNA encodes the amino acid sequence of the protein in triplets known as codons. These codons bind to their anti-codons on tRNA molecules, which are loaded with the amino acid corresponding to that codon-anti-codon pair, as illustrated in the table. Illustration prepared in ChemBioDraw Ultra version 13.0.

1. 3. 2. Cap-Dependent Translation

Cap-dependent translation is the most common method of initiating translation, although cap-independent translation is important in enabling the cell to alter translation in response to cellular stress and is commonly used by viruses; cap-independent translation is detailed in section 1. 3. 3.

Cap-dependent translation is initiated by eIFs binding to the 5'cap of the mRNA. The 5'cap consists of a guanine base in the unconventional 5' to 5' orientation that is methylated generating the 5'-m^7G cap. The 5'cap is recognised by the eIF4F complex consisting of three eIFs; eIF4E, eIF4G and eIF4A (Figure 1-11). eIF4E is the cap binding protein which also interacts with eIF4G, a scaffold protein, while eIF4A, a helicase, unwinds the mRNA to enable translation to occur (Sonenberg and Hinnebusch, 2009). The scaffold protein eIF4G also interacts with the poly(A) binding protein (PABP) that is bound to the 3'poly(A) tail of mRNA. This interaction of eIF4G brings the 5'cap and the 3'tail in close proximity to enhance translation (Sonenberg and Hinnebusch, 2009) (Figure 1-11). The structure of eIF4E enables cap-binding as eIF4E consists of a curved β-sheet with 8 anti-parallel strands with the 5'cap binding on the concave side (Mathews et al., 2007; Tomoo et al., 2003). eIF4E also interacts with the nucleotide adjacent to the cap which alters the conformational shape of eIF4E that is enhanced by the presence of eIF4G (Mathews et al., 2007; von Der Haar et al., 2000). The cap binding potential of eIF4E is enhanced in the eIF4F complex because eIF4E in complex has higher affinity for the cap and dissociates from the cap more slowly compared to eIF4E alone (Mathews et al., 2007). eIF4E is also regulated by 4E-BP1, which acts as a competitive inhibitor of eIF4G. 4E-BP1 in the hypo-phosphorylated form competes with eIF4G for eIF4E binding (Mathews et al., 2007), preventing eIF4E binding the 5'cap. Whereas when 4E-BP1 is hyper-phosphorylated by mTORC1 (see section 1. 3. 7. 1.) eIF4E is able to bind to eIF4G enabling cap binding (Figure 1-11).

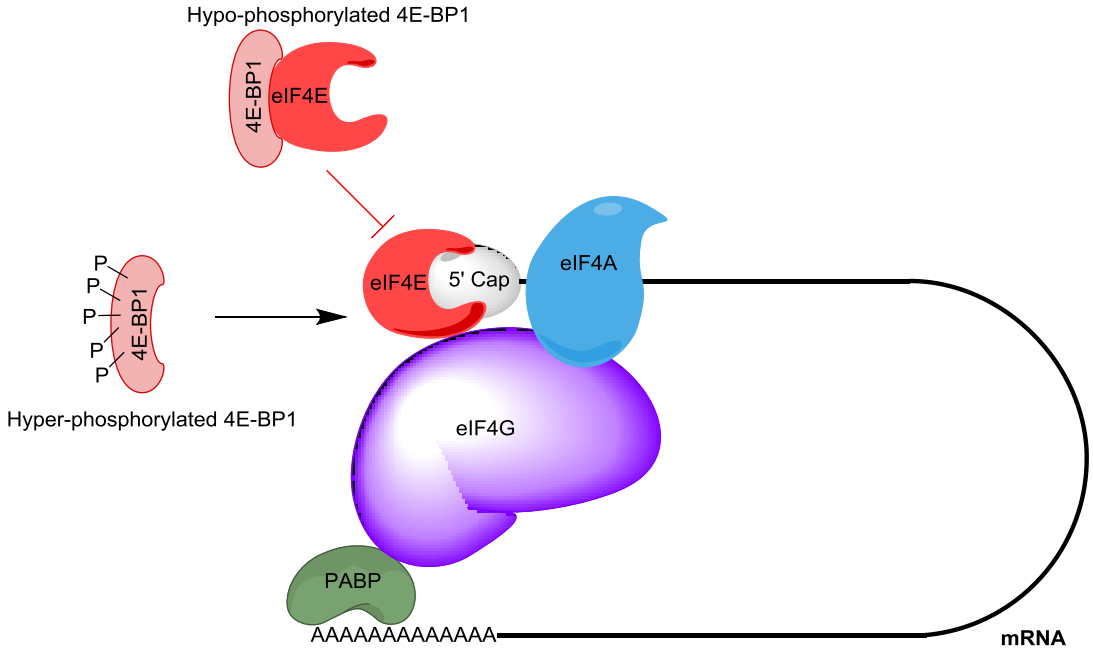

Figure 1-11: eIF4F Complex

Translation is initiated firstly by the formation of the eIF4F complex. The eIF4F complex assembles due to eIF4E binding to the 5'cap on mRNA, while eIF4G and eIF4A are recruited to act as a scaffold protein and helicase, respectively. eIF4G acts as a scaffold protein for many of the eIFs and also binds to poly(A) binding protein (PABP) causing circularisation and stabilisation of the mRNA. eIF4E binding protein 1 (4E-BP1) in the hypo-phosphorylated form prevents eIF4E interacting with eIF4G and eIF4E is prevented from binding to the 5' cap. Hyper-phosphorylation of 4E-BP1 prevents 4E-BP1 binding to eIF4E thus enabling the formation of the eIF4F complex. Illustration prepared in ChemBioDraw Ultra version 13.0.

A key step in initiation of translation is ternary complex (TC) formation (Figure 1-12). The TC consists of eIF2, GTP and methionine loaded initiator tRNA (Met-$tRNA_i$). eIF2 is a heterotrimer consisting of α, β and γ subunits. eIF2γ contains binding sites for GTP and Met-$tRNA_i$, with Met-$tRNA_i$ binding affinity decreased if eIF2 is bound with GDP rather than GTP. eIF2β has binding sites for eIF2γ and RNA although the function of eIF2β is not clear. The critical subunit for eIF2 regulation is eIF2α; eIF2α binds to eIF2γ adjacent to the Met-$tRNA_i$ site and is proposed to be important in tRNA recognition (Mathews et al., 2007). Following a previous round of translation eIF2 is released in the inactive GDP bound form that requires a guanine nucleotide exchange factor (GEF) to catalyse the exchange of GDP to GTP, which is carried out by eIF2B. eIF2B is regulated by the phosphorylation status of eIF2α, with phosphorylation on Ser51 of eIF2α acting as a competitive inhibitor of the GEF activity of eIF2B (Mathews et al., 2007; Williams et al., 2001) (Figure 1-12). eIF2B is also regulated by GSK3β; phosphorylation of eIF2Bε by GSK3β results in decreased activity of eIF2B that can alter TC formation due to the recycling of eIF2α-GTP (Williams et al., 2001).

The interaction of the TC with the 40S subunit of the ribosome, to form the 43S complex, is facilitated by eIF1, eIF1A and eIF3. eIF3 binds directly to the 40S subunit on the solvent surface and interacts with eIF1 which interacts at the interface of the 40S subunit, while eIF1A binds in the A site of the ribosome preventing access of any tRNA molecules (Mathews et al., 2007). eIF2 in the TC is also able to directly interact with the 40S subunit. eIF5 may also be important in the formation of the 43S complex as eIF5 interacts with both eIF3 and eIF2 (Mathews et al., 2007). Recruitment of the 43S complex to the mRNA occurs due to interactions with the eIF4F complex, eIF4B and PABP, generating the 48S complex (Figure 1-13). eIF4B is a co-factor for eIF4A, the helicase in the eIF4F complex (Jaramillo et al., 1991). eIF4B enhances eIF4A helicase activity as well as mRNA affinity (Jaramillo et al., 1991), but eIF4B can be regulated by S6 kinase (Mathews et al., 2007). eIF4G ensures helicase activity occurs following mRNA binding and associates with eIF3 (Figure 1-13).

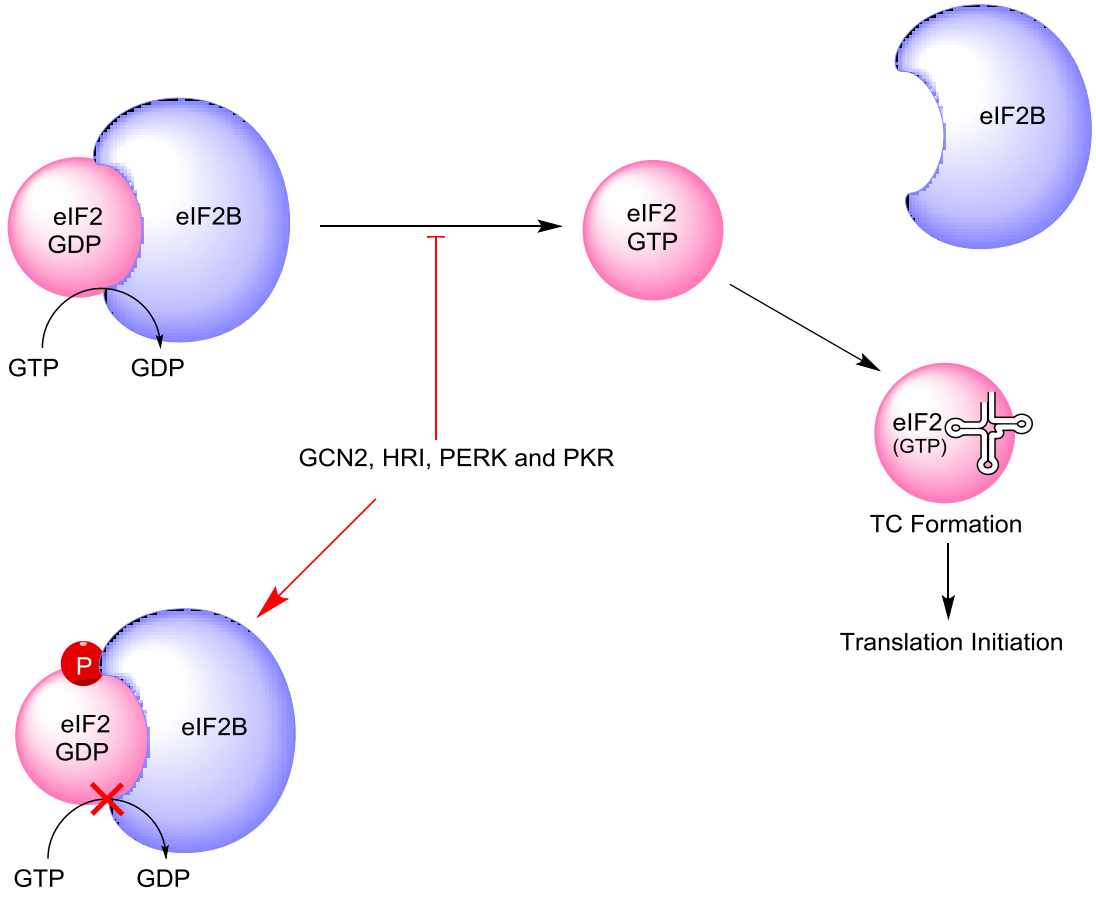

Figure 1-12: Ternary Complex Formation

Formation of the ternary complex (TC) is required for initiation of translation and consists of the eIF2 complex in the GTP form with a initiator Met-loaded tRNA. During translation initiation GTP hydrolysis occurs and eIF2-GDP is released. For subsequent rounds of translation to occur GDP is exchanged for GTP by eIF2B. Negating this GTP exchange are four eIF2α kinases, GCN2, HRI, PERK and PKR. GCN2 (general control non-depressible kinase 2) is activated in response to amino acid deficiency, HRI (Heme regulated inhibitor kinase) is regulated by heme deficiency, PERK, (PKR-like Endoplasmic reticulum (ER) kinase) is activated by oxidative stress and the unfolded protein response in the ER and PKR (protein kinase R) is activated by viral infection (Wek et al., 2006). These four kinases phosphorylate the alpha subunit of eIF2. This phosphorylation event still enables eIF2B to bind to eIF2 but the exchange of GDP for GTP is inhibited, therefore inhibiting TC formation. Illustration prepared in ChemBioDraw Ultra version 13.0.

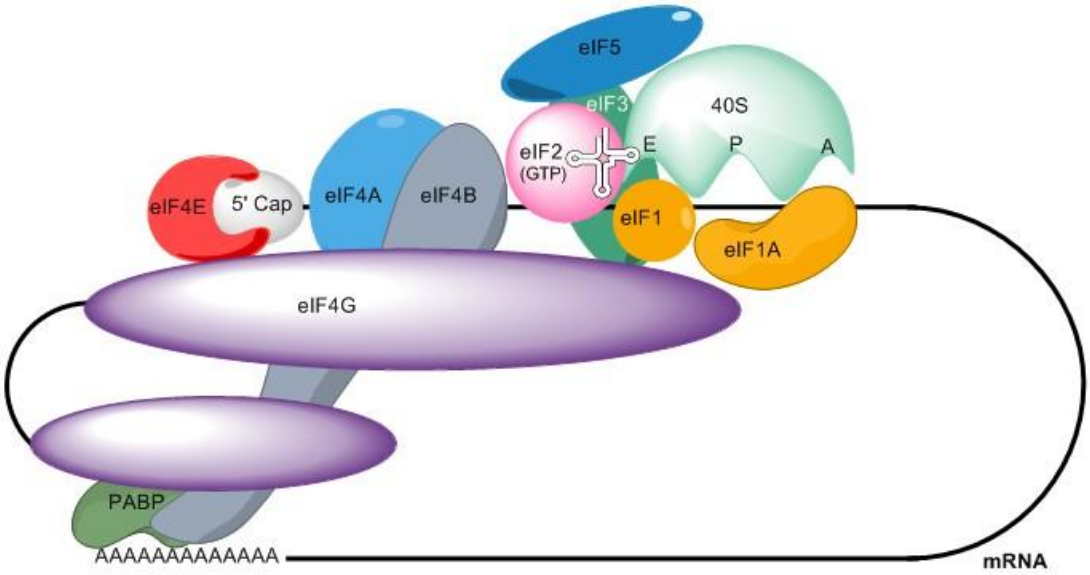

Figure 1-13: 48S Complex

Following assembly of the eIF4F complex other eIFs are recruited to the mRNA, including the TC, eIF1, eIF1A, eIF3 and eIF5. Initiation factors eIF1 and eIF1A play important roles in identifying the correct start codon, while eIF3 and eIF5 are required to interact with the 40S subunit of the ribosome. eIF5 is important for GTP hydrolysis and release of eIF2 once the start codon has been identified. Illustration prepared in ChemBioDraw Ultra version 13.0.

Once the 48S complex has formed the start codon needs to be identified. The initiation factor eIF1 is important in ensuring the correct start codon (most commonly AUG) is identified. eIF1 identifies AUGs as well as destabilises premature and partial base pairing of the codon with the tRNA anticodon (Mathews et al., 2007). The scanning ribosome is maintained in an open conformation by eIF1 and upon AUG recognition a conformational change is induced by eIF1, resulting in the 40S ribosome being in a closed conformation (Mathews et al., 2007). The activity of eIF1 is also altered by nucleotides at positions -3 and +4 of the start codon, ensuring AUG codons only in the correct context are initiated from. AUG codons in a strong context will initiate translation better than AUG codons in a weak context, with the Kozak sequence providing the optimal context (Hinnebusch, 2011). Not all cellular proteins are initiated at an AUG start codon and alternative initiation codons are also used, whether eIF1 is involved in alternative initiation requires further investigation (Touriol et al., 2003) .

The alteration from an open to closed conformation of the scanning ribosome is dependent not only on eIF1 but eIF1A and eIF5 may also play an important role. Once a start codon has been identified the initiation factors eIF1, eIF1A, eIF2 and eIF3 are displaced to enable the 60S ribosomal subunit to bind and form inter-subunit bridges with the 40S ribosome (Figure 1-14). The displacement of the above initiation factors is regulated by the activity of eIF5, a GTPase activating protein specific for eIF2 (Mathews et al., 2007). eIF5 binds to the β and γ subunits of eIF2 and in the presence of the 40S ribosome activates GTPase activity of the γ subunit. The activity of eIF5 is 10^6 fold greater on eIF2-GTP/Met-tRNA$_i$ in the 43S complex compared to the TC alone. eIF1 was also required to dissociate following AUG recognition, for P_i release and irreversible GTP hydrolysis on eIF2 (Algire et al., 2005; Mathews et al., 2007). The hydrolysis of eIF2-GTP does not immediately promote displacement of eIF2-GDP from the ribosome, instead the release of initiation factors is mediated by eIF5B. eIF5B-GTP aids 60S subunit joining and eIF5B-GTP hydrolysis occurs to mediate release of eIF5B, which is crucial to make the A site of the 80S ribosome accessible. It is thought that eIF1A plays an important role in mediating eIF5B-GTP hydrolysis (Mathews et al., 2007; Sonenberg and Hinnebusch, 2009).

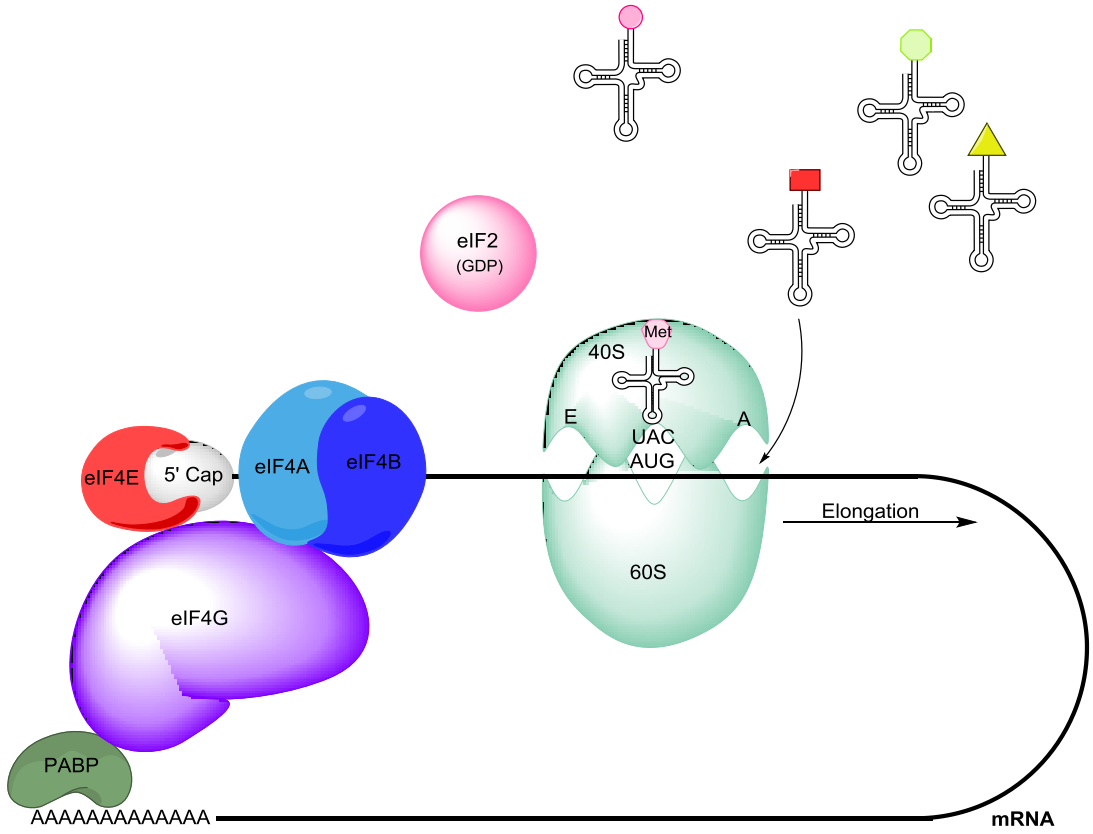

Figure 1-14: 80S Formation

Once the start AUG codon has been identified the 60S subunit is recruited due to the activity of eIF5B. eIF5B triggers the release of eIF1 and eIF1A to enable the 60S subunit access to the 40S subunit, generating the complete 80S ribosome. The 80S ribosome is then ready to accept amino-acyl-tRNA molecules into the A site of the ribosome for elongation to occur. Illustration prepared in ChemBioDraw Ultra version 13.0.

1. 3. 3. Cap-Independent Translation

A small proportion of mRNAs can also be translated in a cap-independent manner which utilise internal ribosome entry sites (IRES). It was first thought that IRES driven translation was specific to viral translation but it has since been shown that cellular IRESes also exist. The first cellular IRES identified regulated the expression of human immunoglobulin heavy chain binding protein, BiP, and since then IRES structures have been identified in *MYC*, *VEGF* and *XIAP* (X-linked inhibitor of Apoptosis Protein) among others, reviewed in (Mathews et al., 2007).

A common feature of an IRES is the presence of a polypyrimidine tract (PPT) in the 5'untranslated region (5'UTR) of the mRNA that is recognised by polypyrimidine tract binding proteins (PTB) to facilitate IRES activity. IRES transactivating factor (ITAFs) have also been demonstrated to be involved in remodelling of the IRES structure enhancing ribosomal recruitment (Mathews et al., 2007; Sonenberg and Hinnebusch, 2009). Cellular IRESes require canonical initiation factors (eIF4F and eIF3) as well as transactiving factors (ITAFs), whereas cricket paralysis virus IRES is capable of initiating translation in the absence of canonical initiation factors are recruits the 80S ribosome directly to the mRNA (Spriggs et al., 2009).

IRES driven translation is important in translation associated with apoptosis as well as under cellular stress. During apoptosis, cap dependent translation is dramatically reduced, due to decreased eIF4E binding to the 5' cap (Bushell et al., 2006) but certain proteins involved in promoting apoptosis still require synthesis. This occurs in the absence of cap-dependent translation and has been shown to be IRES driven (Bushell et al., 2006). During cellular stress eIF2α is often phosphorylated resulting in decreased TC availability and cap-independent translation outcompetes cap-independent translation. For example in hypoxic conditions *VEGF* mRNA stays associated with high molecular weight polysomes (multiple ribosomes on a single mRNA, indicating high levels of translation) and IRES activity was not affected by decreased TC levels (Mathews et al., 2007).

It has recently been suggested that the 5'UTR of *HIF-1A* may contain an IRES, which would enable high translation of *HIF-1A* when global translation rates are reduced in hypoxic conditions. Dicistronic reporter constructs were previously used to demonstrate the ability of the 5'UTR of *HIF-1A* to promote translation in a cap-independent manner (Lang et al., 2002). The construct contained an SV40 promoter region upstream of a stem loop structure followed by *Renilla* luciferase, the 5'UTR of *HIF-1A* and finally firefly luciferase (Lang et al., 2002). The presence of the stem loop structure prevented cap-dependent translation proceeding along the whole construct, therefore prevented the expression of firefly luciferase. In the presence of the 5'UTR of *HIF-1A* firefly luciferase expression occurred, which demonstrated the presence of an IRES within the 5'UTR of *HIF-1A* (Lang et al., 2002). The 5'UTR of *HIF-1A* has been shown to contain a PPT between nucleotides 223-237, which enabled PTB to bind to enhance translation, in a cap-independent manner (Schepens et al., 2005). It has also been demonstrated that the 5'UTR of *HIF-1A* will bind with higher affinity to PTBs in hypoxic conditions compared to normoxic conditions (Schepens et al., 2005).

The presence of an IRES in the 5'UTR of *HIF-1A* is still being disputed, as previously published data suggested that the 5'UTR of many mRNAs believed to contain an IRES may in fact contain cryptic promoters rather than an IRES (Bert et al., 2006). Bert et al demonstrated that the UTRs placed upstream of firefly luciferase and downstream of *Renilla* luciferase in a dicistronic construct required the presence of the SV40 enhancer downstream of firefly luciferase in order to promote firefly luciferase expression, hence concluded that the UTRs were in fact cryptic promoters rather than IRESes (Bert et al., 2006). Further research is required to determine whether the 5'UTR of HIF-1α contains an IRES or a cryptic promoter.

The presence of IRESes in *MYC* and *VEGF* mRNAs have been confirmed via the use of dicistronic plasmids (Huez et al., 1998; Stoneley et al., 1998). The presence of an IRES in *MYC* was confirmed, due to the insertions of hairpin structures inserted upstream of the first *Renilla* luciferase gene preventing read through from renilla luciferase into *MYC*-regulated firefly luciferase from occurring (Stoneley et al., 1998). The presence of the *MYC* IRES was also confirmed using RNase protection assays indicating that the dicistronic construct had not fragmented altering

translational regulation (Stoneley et al., 1998). Interestingly, deletion of the 3' end of the IRES resulted in a gradual decrease in IRES activity, whereas any deletions in viral IRESes results in abolished activity (Stoneley et al., 1998). Therefore the regulation of viral and cellular IRES activity differs and was first identified in the *MYC* IRES (Stoneley et al., 1998).

The investigation into the presence or absence of an IRES in *VEGF* mRNA identified two IRESes (Huez et al., 1998). The two IRESes may enable different regulation of VEGF expression as they are bound by different factors (Huez et al., 1998). It has also recently been identified that regulation of *VEGF* translation is unique; the long, GC-rich 5'UTR is able to form G-quadruplex structures (Morris et al., 2010). The presence of a G-quadruplex usually has an inhibitory effect on translation, but in the regulation of *VEGF* translation the formation of the G-quadruplex was required for IRES activity (Morris et al., 2010).

1. 3. 4. Translation Elongation

Initiation of translation generates the complete 80S ribosome coupled with the initiator Met-tRNAi. To generate the protein, encoded by the mRNA, elongation factors are recruited to ensure ribosome reads and 'decodes' the mRNA correctly. These elongation factors ensure the correct aminoacyl-tRNAs are loaded into the ribosome to generate peptide bond formation between the amino acids. There are two main elongation factors important in this stage of translation; eEF1 (consisting of eEF1A and eEF1Bαβγ) and eEF2. eEF1A-GTP is involved in recruitment of the aminoacyl-tRNA and following correct codon-anticodon interaction initiates a conformational change in the 60S ribosome that leads to the catalysis of GTP hydrolysis (Mathews et al., 2007). eEF1A-GDP is released from the ribosome, leaving the aminoacyl-tRNA in the A site on the ribosome and eEF1Bαβγ exchanges GDP for GTP (Mathews et al., 2007). Following aminoacyl-tRNA binding in the A site of the ribosome, the 60S ribosome catalyses the formation of a peptide bond between the amino acid in the P site and the aminoacyl-tRNA in the A site. After peptide bond formation, eEF2-GTP is recruited which aids translocation of the

peptidyl-tRNA from the P site into the E (exit) site of the ribosome in a GTPase dependent manner; this leads to the A site becoming available for the next aminoacyl-tRNA (Mathews et al., 2007). This process continues with the growing polypeptide moving out of the ribosome through a tunnel at the back of the 60S subunit.

1. 3. 5. Termination of Translation

To complete the synthesis of protein the mRNA encodes a stop codon, either UAA, UAG or UGA, which is not recognised by any tRNA molecules. Stop codons are instead recognised by release factors (RF). eRF1 will recognise all three stop codons and induce the hydrolysis of the ester bond between the last amino acid in the polypeptide chain and the tRNA in the P site of the ribosome (Mathews et al., 2007). This results in release of the protein from the ribosome. eRF3 is then recruited and involved in removal of eRF1 from the ribosome, although the exact mechanisms are unknown (Mathews et al., 2007). The ribosome is then recycled and mRNA released for subsequent rounds of translation to occur, this is believed to be aided by ribosomal recycling factors and IF3 (in bacteria) in a GTPase dependent manner (Mathews et al., 2007).

1. 3. 6. Stress Granules

Translational can also be regulated by mRNA metabolism, which may involve the interaction of micro-RNAs (miRNAs) to specific mRNAs leading to degradation. Although not discussed in this thesis this has been reviewed by Yates et al (Yates et al., 2013).

mRNA metabolism can also be controlled by the presence of cytoplasmic bodies. There have been two cytoplasmic bodies identified that store or degrade mRNA known as stress granules and P (processing) bodies respectively. Stress granules are aggregates of stalled pre-initiation complexes, containing translationally silent

mRNA, the 40S ribosomal subunit and most eIFs. These complexes contain silenced mRNA because the complex lacks the TC (eIF2-GTP/Met-tRNA$_i$) that occurs as a consequence of eIF2α phosphorylation (Chernov et al., 2009; Mathews et al., 2007). Stress granules will sequester mRNA preventing translation, but unlike P bodies, stress granules will not target the mRNA for degradation. Stress granules are believed to be sites of translational repression due to the fact that stress granules contain proteins involved in inhibition of translation, yet they also contain mRNA stabilising molecules, including HuR (an AU-rich element binding protein). Therefore stress granules are sites of mRNA silencing rather than degradation (Mokas et al., 2009). A unique component of stress granules, that is not present in P bodies, is T cell internal antigen-1 (TIA-1) as well as TIAR, which together aid stress granule assembly by promoting aggregation (Chernov et al., 2009; Mathews et al., 2007). Stress granules are sites of storage for silenced mRNAs but these can shuttle to P bodies in sustained stress. P bodies, unlike stress granules, contain 5'-decapping enzymes as well as the 5' exonuclease XRN and therefore are sites for mRNA degradation (Mathews et al., 2007).

Stress granules are believed to enable the cell to adapt to transient cellular stress, whereas prolonged stress, for example by viral infection, will lead to mRNA degradation and apoptosis. The pro-apoptosis mitochondrial apoptosis-inducing factor (AIF) (Figure 1-8) has been shown to inhibit stress granule formation indicating that translational repression in response to apoptosis results in mRNA degradation rather than storage of mRNA molecules (Cande et al., 2004; Mathews et al., 2007). The region of AIF shown to have an inhibitory effect on stress granule formation was linked to redox activity and glutathione oxidative status (Cande et al., 2004). Knock out of AIF enabled arsenite induce stress granules to form, but the addition of glutathione or N-acetylcysteine prevented the formation of stress granules (Cande et al., 2004). Therefore stress granule assembly is linked to the oxidative status of the cell which is modulated by AIF, and links stress granule assembly with apoptosis regulation.

Inhibition of translation via eIF2α phosphorylation has been demonstrated to be important in the formation of stress granules induced by ER stress, heat shock and UV stress (Fournier et al., 2010; Thomas et al., 2011). To add a further level of

complexity stress granules may also promote initiation of translation of certain mRNA molecules, due to the presence of eIF3 in stress granules and uORFs (upstream open reading frames) on mRNA molecules (Kimball et al., 2003; Thomas et al., 2011). This may be important to allow rapid shuttling of mRNAs back to polysomes following removal of the cellular stress.

1. 3. 7. Signalling *Pathways that Regulate Translation*

Translation provides a rapid way for the cell to respond to extracellular and intracellular signalling or cellular stress. Extracellular signals, for example growth factors, will alter translation via the mTORC1 (mammalian target of rapamycin complex 1) pathway altering eIF4E binding to the 5'cap, whereas intracellular stresses alter the phosphorylation status of eIF2α to modulate translation.

1. 3. 7. 1. mTOR Signalling

There are two mTOR complexes; mTORC1 forms a complex with raptor and is sensitive to rapamycin treatment, while mTORC2 forms a complex with rictor and is insensitive to rapamycin (Huang and Manning, 2009). The mTOR complexes are important in the regulation of translation because they integrate the input signals from growth factors and nutrient sensors. If growth factors stimulate the cell to enhance translation rates when there is a deficiency in amino acid availability then mTOR signals to induce protein degradation of endogenous proteins to generate free amino acids for use in translation (Laplante and Sabatini, 2012; Mathews et al., 2007). The regulation of mTORC1 is better understood than the regulation of mTORC2.

Growth factors activate mTORC1 via an upstream signalling cascade involving RAS, PI3K and AKT (Figure 1-15). Following the production of PIP_3 (phosphor-inositol trisphosphate) by PI3K (phosphoinositide 3-kinase) (Figure 1-15) PDK1 (phospholipid dependent kinase 1) is activated. PDK1 phosphorylates and activates

AKT, GSK-3 and S6Ks. AKT phosphorylates TSC2 (tuberous sclerosis complex) a GTPase activating protein (GAP) for the GTPase Rheb (Huang and Manning, 2009; Laplante and Sabatini, 2013). Phosphorylation of TSC2 inhibits the GAP activity of TSC2, resulting in the accumulation of Rheb-GTP. Elevated levels of Rheb-GTP results in increased mTORC1 activity through a predicted GTP dependent manner, although the exact mechanism is unclear. Activated mTORC1 phosphorylates 4E-BP1 and p70S6K (ribosomal protein S6 kinase) (Figure 1-15) (Huang and Manning, 2009; Laplante and Sabatini, 2013). Overexpression of S6K has previously been reported to inhibit the phosphorylation of 4E-BP1 by mTORC1, this has been shown to be due to both substrates competing for the same binding site on mTORC1 (Mathews et al., 2007). The phosphorylation of S6K by mTORC1 is facilitated by eIF3, which acts as a docking site for both (Holz et al., 2005). Only following phosphorylation is S6K released to act on downstream targets (Mathews et al., 2007).

The phosphorylation of 4E-BP1 following mTORC1 activation enhances translation initiation. 4E-BP-1 in the hypo-phosphorylated form sequesters eIF4E thereby preventing interaction with the 5'cap. Following hyper-phosphorylation of 4E-BP1, eIF4E is released enhancing cap-dependent translation. 4E-BP1 has multiple phosphorylation sites and is phosphorylated in a sequential manner. Phosphorylation sites include Thr37, Thr 46, Ser65, Thr70, Ser83, Ser101 and Ser112, with Thr37 and Thr46 required for priming (Heesom et al., 1998; Mathews et al., 2007). Following priming Thr70 is phosphorylated before Ser65 and release of eIF4E, the importance of phosphorylating Ser-83, -101 and -112 is unclear (Mathews et al., 2007).

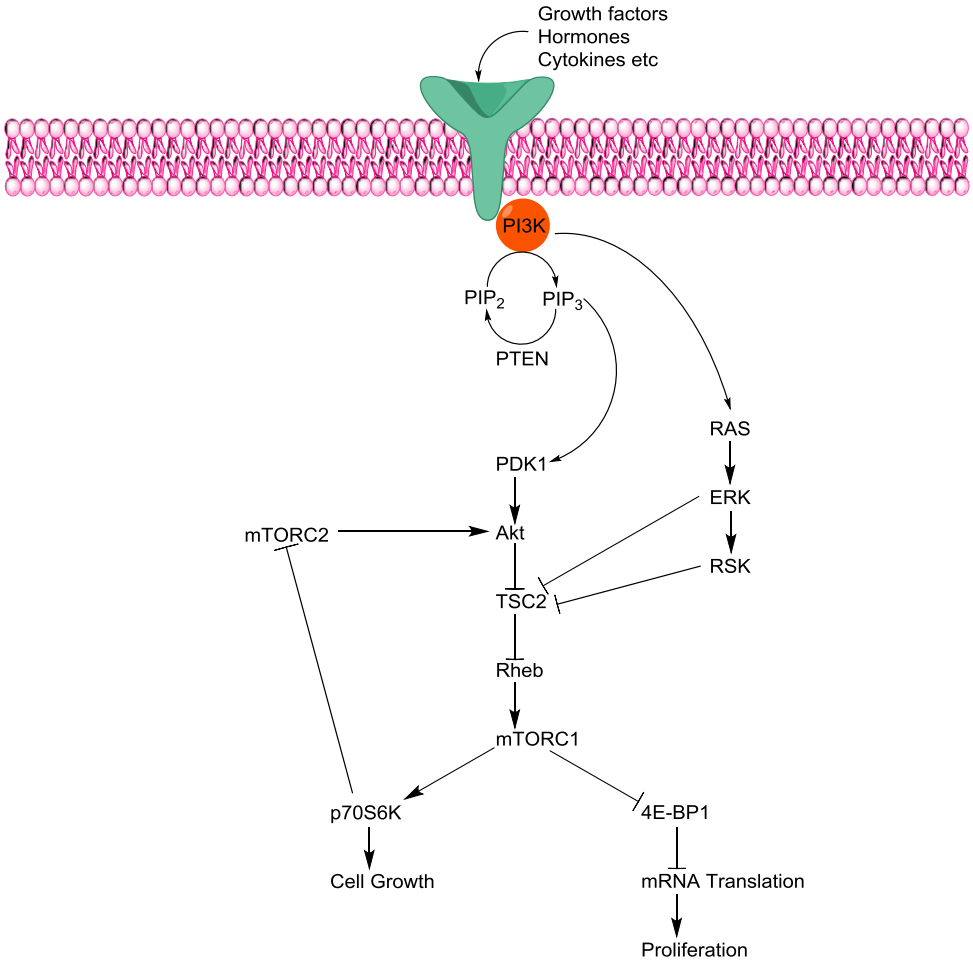

Figure 1-15: mTOR Signalling

Activation of mTORC1 occurs following signalling via extracellular ligands for example growth factors, hormones and cytokines. These extracellular ligands activate phosphatidyl inositol 3 kinase (PI3K) to convert phosphoinositol bisphosphate (PIP_2) to phosphoinositol trisphosphate (PIP_3). Generation of PIP_3 activates phospholipid dependent kinase 1 (PDK1) which phosphorylates and activates Akt. Akt then phosphorylates and deactivates tuberosclerosis complex 2 (TSC2), thus removing the inhibitory effect enabling subsequent downstream activation of mTORC1. mTORC1 is then able to modulate the regulation of translation via 4E-BP1 phosphorylation. Another known target of mTORC1 is p70S6K, which provides a negative feedback to mTORC2. p70S6K will inhibit the action of mTORC2 resulting in decreased activation of Akt thereby decreasing the activation of mTORC1. Ligands may also activate the RAS – ERK pathway to remove the inhibitory action of TSC2 on mTORC1 activation. Illustration prepared in ChemBioDraw Ultra version 13.0.

mTORC1 activity can also be regulated by ERK (extracellular signal-regulated kinase) and RSK (90kD ribosomal S6 protein kinase) as well as mTORC2 (Figure 1-15). mTORC2 has been shown to phosphorylate Akt on Ser 473 upstream of mTORC1. While ERK and RSK both act further downstream and phosphorylate TSC2 inhibiting the GAP activity of TSC2 (Mathews et al., 2007). TCS2 is an important regulator of mTORC1 activity as the TSC2 complex is also phosphorylated on a different site by AMPK (AMP activated protein kinase) (Laplante and Sabatini, 2012). AMPK is activated by energy depletion as determined by the ratio of AMP/ATP with energy depletion resulting in the phosphorylation and activation of TSC2 (Mathews et al., 2007). Activation of TSC2 ultimately decreases translation as Rheb-GTP hydrolysis will occur resulting in decreased mTORC1 activity. This pathway acts to down-modulate mTORC1 activity and is negated by AKT. AKT will decrease AMPK activity resulting in a more complete inhibition of TSC2 activity and greater mTORC1 activity. TSC is also implicated in the regulation of translation during hypoxia. In hypoxic conditions there is an increase in HIF-dependent activation of REDD1 (regulated in development and DNA damage) and REDD2 proteins that act as TSC activators (Laplante and Sabatini, 2012).

1. 3. 7. 2. Ternary Complex Recycling

Intracellular stress regulates translation via a different pathway that will alter the phosphorylation status of eIF2α on Ser51. Phosphorylation of eIF2α can occur following activation of the four eIF2α kinases; GCN2 (general control non-depressible kinase 2), HRI (heme-regulated inhibitor kinase), PERK (PKR-like endoplasmic reticulum (ER) kinase) and PKR (protein kinase R) (Figure 1-12). The phosphorylation of eIF2α will regulate translation initiation as the ternary complex (TC) recycling is inhibited. Recycling of the TC is required because recruitment of the 60S results in GTP hydrolysis and release of eIF2α. For a subsequent TC to form eIF2α-GDP needs to be exchanged for GTP. This exchange is catalysed by eIF2B. But the phosphorylated form of eIF2α acts as a competitive inhibitor of eIF2B (Williams et al., 2001), resulting in a stall in initiation of translation as the TC cannot

be recruited to form a new 43S complex (Figure 1-12). eIF2B is the limiting factor in GTP exchange as eIF2B is expressed at a much lower level (20-30%) than eIF2α (Koumenis et al., 2002; McEwen et al., 2005; van den Beucken et al., 2006). Phosphorylation of eIF2α results in decreased translation in a global manner, although there are a few mRNAs that can still undergo translation due to the presence of uORFs (Wek et al., 2006; Wouters et al., 2005). ATF4 is a transcription factor that is expressed in the presence of eIF2α phosphorylation. ATF4 contains two uORFs, uORF1 is 3 amino acids long and uORF2 is 59 amino acid long and overlaps the main ORF (Somers et al., 2013; Vattem and Wek, 2004). In normal (unstressed) conditions after translation of the first uORF the 40S will interact with a TC and initiate translation from uORF2, preventing the translation from the main ORF (Somers et al., 2013; Vattem and Wek, 2004). Whereas under stress conditions, where eIF2α phosphorylation depletes the pool of TCs, the scanning 40S ribosome may not interact with a TC (due to low TC availability) after expression of the first uORF resulting in the uORF2 not being translated and potentially enabling the 40S ribosome to bind a TC before reaching the main ORF, resulting in initiation of translation from the main ORF and expression of ATF4 (Somers et al., 2013; Vattem and Wek, 2004). In normal conditions where the formation of the 43S complex and initiation of translation occurs rapidly the ribosomes re-initiate at each of the uORFs, which in the case of ATF4 results in the production of an inhibitory element. Under stress conditions, when eIF2α is phosphorylated, the re-initiation of the ribosome is slower due to low TC availability that results in one of the uORFs being ‘skipped’, as ribosome formation is too slow to inititate translation at each uORF. Hence the inhibitory element of ATF4 is not expressed leading to enhanced ATF4 expression (Wek et al., 2006; Wouters et al., 2005). Therefore the phosphorylation of eIF2α enables the cell to respond rapidly to cellular stress by decreasing global translation, with translation of certain mRNAs maintained to allow a dynamic response to intracellular stress to occur.

1. 3. 7. 3. eIF2α Kinases

TC recycling (see section 1. 3. 7. 2.) is regulated by the activation of eIF2α kinases. There are four eIF2α kinases; GCN2, HRI, PERK and PKR that phosphorylate the α-subunit of eIF2. eIF2 consists of α, β and γ subunits as a heterotrimer; the γ-subunit binds GTP, the β-subunit binds tRNA and the α-subunit is involved in regulating the ability of eIF2 to bind to eIF2B and facilitate the exchange of GTP (Mathews et al., 2007). The four eIF2α kinases phosphorylate Ser51 of the mature form of eIF2α. The DNA sequence for mammalian eIF2α places serine at position 52, but due to posttranslational modifications involving the removal of the initiating Met results in serine at position 51 of the mature protein (Mathews et al., 2007). Ser51 is present on the interface of eIF2 that interacts with eIF2B and in the phosphorylated form enhances the interaction of eIF2α with eIF2B and competitively inhibits eIF2B activity (Mathews et al., 2007; Williams et al., 2001).

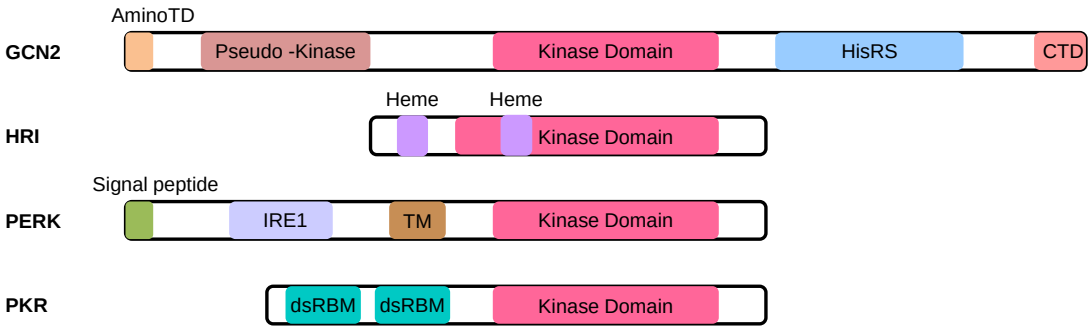

Figure 1-16: eIF2α Kinases

Schematic representation of the domains present in the four eIF2α kinases; GCN2, HRI, PERK and PKR. All four kinases consist of the eIF2α kinase domain and additional domains are present to regulate the activity of the kinase domain following stimulation. GCN2 contains an amino-terminal domain (aminoTD), a pseudo kinase domain, a histidyl-tRNA synthetase related domain (HisRD) and a carboxyl terminal domain (CTD). HRI in addition to the kinase domain contains binding sites for heme. PERK contains a signal peptide sequence to direct PERK to the endoplasmic reticulum, a transmembrane domain (TM) and an IRE1 homology domain. Finally PKR contains the eIF2α kinase domain and two double stranded RNA binding motifs (dsRBMs).

The four eIF2α kinases share 25-37% sequence homology and differ in sequence of the different regulatory domains that enable the kinases to respond to different stimuli (Figure 1-16) (Bertolotti et al., 2000; Chen et al., 1989; Green and Mathews, 1992; Mathews et al., 2007; Qiu et al., 1998). The four kinases are also similar in the mechanism of activation; the regulatory domain removes the inhibitory action resulting in dimerization and autophosphorylation that leads to kinase activation (Bertolotti et al., 2000; Chen et al., 1989; Green and Mathews, 1992; Qiu et al., 1998)

GCN2 is activated in response to amino acid deficiency and specifically binds to uncharged cognate tRNA molecules, which will accumulate when amino acids are sparse (Mathews et al., 2007). The uncharged tRNAs bind to the HisRS (histidyl-tRNA synthetase related domain) and carboxy-terminal domains (CTD) (Figure 1-16). These domains are also important for the interaction of the GCN2 monomer with another GCN2 monomer to form a constitutive dimer (Mathews et al., 2007; Qiu et al., 1998). The HisRS and CTD also interact with the kinase domain in the presence of sufficient amino acids, whereas upon tRNA binding (due to insufficient amino acid availability) the HisRS and CTD are released from the kinase domain resulting in the activation of the kinase (Mathews et al., 2007; Qiu et al., 1998). GCN2 has also been shown to be activated by ultraviolet light (Deng et al., 2002) and in yeast GCN2 is activated in response to rapamycin treatment.

HRI is the main eIF2α kinase in erythroid cells and is activated in heme-deficiency. HRI can additionally be activated by arsenite treatment, heat shock, osmotic shock and nitric oxide (Mathews et al., 2007). HRI is a homodimer formed by intermolecular disulphide bonds (Chen et al., 1989). HRI contains two heme binding sites (Rafie-Kolpin et al., 2000) the first is on the amino-terminal of the kinase while the second heme binding site is present within the kinase domain. In the presence of heme the first heme binding site will interact with the kinase domain and following release of heme (in heme-deficiency) this interaction is disrupted and results in the activation of the kinase domain (Mathews et al., 2007).

PERK not only shares sequence homology with the other eIF2α kinases but also shares homology with the ER responsive IRE1 kinase (Bertolotti et al., 2000; Mathews et al., 2007). The IRE1-like domain in PERK is present in the amino

terminal region of PERK enabling PERK to be inserted into the ER lumen. The kinase domain of PERK is present in the cytosol and the two domains are separated by a transmembrane domain (Figure 1-16), thus allowing the kinase domain access to eIF2α. PERK is activated by ER stress in a similar manner to IRE1 activation (Bertolotti et al., 2000), in that the IRE1 domain of PERK can be replaced with IRE1 and the PERK-kinase domain will be activated (Mathews et al., 2007). In unstressed cells PERK interacts with the ER chaperone BiP; upon ER stress PERK dimerization occurs resulting in the activation of the kinase domain. Dimerization of PERK occurs either via dissociation of BiP from PERK due to an accumulation of unfolded proteins in the ER lumen, which bind BiP, or dimerization occurs due to IRE1 domain oligomerisation (Mathews et al., 2007).

The final eIF2α kinase is PKR that is activated in response to double-stranded RNA (dsRNA), most commonly viral infection. PKR contains the eIF2α kinase domain and two double stranded RNA binding motifs (dsRBMs) (Figure 1-16). The second dsRBM interacts with the kinase domain in the absence of dsRNA. In the presence of dsRNA the dsRBM1 will bind dsRNA in micromolar concentrations, whereas dsRBM2 will only interact with dsRNA weakly and binding is in a co-operative manner with dsRBM1 (Green and Mathews, 1992; Mathews et al., 2007). Following dsRNA binding a conformation change occurs resulting in the activation of the kinase domain. The sequence of the dsRNA bound by PRK is non-specific with each dsRBM requiring a minimum length of 16 base pairs and for activation of PKR the dsRNA needs to be a minimum of 40 base pairs due to two PKR monomers binding to the same dsRNA molecule, hence PKR is only active as a dimer (Mathews et al., 2007).

Each eIF2α kinase has a specific activator but it has also been shown that all four kinases can be activated by nitric oxide as well as PKR being activated by other stresses, including pathogens, nutrients and organelle stress (Nakamura et al., 2010; Tong et al., 2011).

1. 3. 7. 4. Other Pathways

Growth factors are also capable of regulating translation via the mitogen activated protein kinase (MAPK) signalling cascades. Ras (a small GTPase) activated in response to growth factors not only activates PI3K but can also activate the MAPKKK (MAP kinase kinase kinase), Raf (Mathews et al., 2007). Activated Raf phosphorylates and activates MEK1/2 (MAP or ERK kinase), a MAPKK (MAP kinase kinase) (Mathews et al., 2007). ERK (a MAPK (MAP kinase)) is then phosphorylated and activated by MEK1/2. ERK then has multiple substrates including three MK (MAPK activated protein kinases); RSK, MSK, and MNKs 1/2 (MAPK interacting kinases). As mentioned earlier (section 1. 3. 7. 1.), ERK may act upstream of mTORC1 altering translation or activate the downstream MKs to alter translation. MNKs bind to eIF4G localising MNKs to eIF4E, their downstream target (Mathews et al., 2007). Phosphorylation of eIF4E by MNKs does not have a major detrimental effect on translation (Mathews et al., 2007). RSK will phosphorylate ribosomal protein S6 and eIF4B. Hyper-phosphorylation of eIF4B enhances eIF4A helicase activity resulting in increased translation (Mathews et al., 2007).

Other MAPK signalling cascades also influence translation, for example stress signalling results in enhanced JNK and p38 MAPK activity. Translation can also be regulated by calcium signalling, CaMK1 (calmodulin dependent kinase 1) has been shown to phosphorylate eIF4GII in the hinge region of eIF4GII resulting in decreased translation (Mathews et al., 2007).

The activation of AKT also alters translation due to the inhibition of GSK3. GSK3 phosphorylates eIF2Bε on Ser540 and inhibits GEF activity of eIF2B, whereas phosphorylation of eIF2Bε on other phosphorylation sites activates GEF activity (Mathews et al., 2007). This has consequences for TC recycling (see section 1. 3. 7. 2.).

1. 3. 8. Targeting Translation as a Potential Anti-Cancer Therapy

Targeting translation as a potential anti-cancer therapy would be beneficial as overexpression of initiation factors has been linked with tumour progression. Overexpression of eIF4E resulted in malignant transformation of NIH 3T3 cells (Lazaris-Karatzas et al., 1990) and has been shown to increase translation of mRNAs containing highly structured 5'UTRs (Koromilas et al., 1992a), for example MYC. Increased expression of eIF2α has been shown in melanoma's (Rosenwald et al., 2003), while expression of a mutant form of PKR (dominant negative effect) leads to transformation (Koromilas et al., 1992b; Rosenwald, 2004).

Translation is required for progression through the cell cycle, cell survival and adaptation to the environment therefore as translation can modulate many processes it provides a good anti-cancer target. Rapamycin, a specific inhibitor of mTORC1, is a known inhibitor of cap-dependent translation which has recently been shown to promote radiosensitivity in pancreatic cancer cells (Hadjipanayi et al., 2010). This demonstrated the importance of translation as a therapeutic target. Recent data has indicated that PEITC may exert some of its anti-cancer activities via inhibition of translation. PEITC was shown to decrease *HIF-1A* mRNA translation by ^{35}S metabolic labelling experiments without altering *HIF-1A* mRNA levels in breast cancer cells (Cavell et al., 2012). PEITC treatment resulted in decreased phosphorylation of 4E-BP1 as well as decreased p70S6K phosphorylation, indicating decreased mTORC1 activity within 30 minutes of treatment (Cavell et al., 2012). TSC2 knockout mouse embryonic fibroblasts (MEFs) indicated the importance of mTORC1 in this signalling cascade (Figure 1-15). In the presence of PEITC, TSC2 knockout MEFs maintained elevated p70S6K phosphorylation, therefore mTORC1 remained active (Cavell et al., 2012). PEITC has many anti-cancer activities as described earlier and the Cavell et al (2012) paper indicated that decreased translation may be important in decreased angiogenesis in response to PEITC. It would therefore be important to determine whether the effects on translation are gene specific or whether PEITC altered global translation, as this may provide further insight into the mechanism for anti-cancer activity. ITCs have also been shown to inhibit cell viability due to the interaction of PEITC with the cytoskeleton, which is

vital in many cellular processes including proliferation (Martel et al., 2012; Mi et al., 2009). Improper organisation of the actin cytoskeleton has also been linked with regulation of translation (Gross and Kinzy, 2007). The actin cytoskeleton is believed to interact with translational machinery via eEF1A, which is required to deliver the amino-acyl-tRNA to the elongating ribosome (Gross and Kinzy, 2007). eEF1A mutant cells lack actin cables and have reduced protein synthesis (Gross and Kinzy, 2007).

1. 4. Chronic Lymphocytic Leukaemia

1. 4. 1. Clinical Overview

Chronic lymphocytic leukaemia (CLL) is the most common form of leukaemia and over 3,000 people in the UK are diagnosed with CLL each year (Leukaemia and Lymphoma Research, July 2013) accounting for 34% of all diagnosed leukaemias (Cancer Research UK, July 2013), with a similar proportion seen in the United States (Goldin et al., 2010). Patients with CLL often have no symptoms and CLL is detected due to other routine blood tests. Any symptoms associated with CLL are likely due to related illness, due to a deficient immune response as a consequence of CLL. The cause of CLL is not fully understood and there is a chance of genetic inheritance increasing the risk of CLL, although specific inherited genetic alterations have not been determined (Goldin et al., 2010). Leukaemia incidence increases with age and CLL is more common in people over the age of 60; with men more likely to develop CLL than women (Cancer Research UK). CLL progression is determined by the Binet Staging System in the UK, which takes into account the number of swollen lymph nodes as well as white blood cell count. There are three stages of CLL with some patients progressing slowly through the stages and others more rapidly, which may be dependent on the subset of CLL (see section 1. 4. 3.). After diagnosis of CLL, treatment is not always immediately carried out. Instead disease progression is monitored because some patients have very slow disease progression and may require no treatment. If disease progresses therapies such as chemotherapy

and rituximab (monoclonal anti-CD20 antibody) treatment may be offered although despite treatment progressive CLL is fatal. The pathogenesis of the disease is complex with relatively few genetic changes occurring. A recently identified genetic alteration that links to disease progression is the size of the deletion in the short arm of chromosome 13 (13q) (Parker et al., 2011). A 13q deletion resulting in the loss of the miR15a/16-1 cluster has been associated with lymphoproliferation *in vivo* (Parker et al., 2011). The dependence of CLL B cell survival and proliferation (leading to disease progression) has been linked with microenvironment stimulation (Zhang et al., 2012). Microenvironmental influences have a major role in disease behaviour and are therefore an attractive target for therapeutic attack. A key environmental stimulus is the presence of an antigen that will act via the cell surface B-cell receptor (BCR).

1. 4. 2. B Cell Development and the Importance of the B-Cell Receptor

CLL is a B lymphocyte malignancy and B lymphocytes are required to elicit an antibody-directed immune response against infection. Therefore patients with CLL cannot produce an adequate immune response due to the proliferation and accumulation of CLL B-cells. CLL B-cells accumulate as a consequence of defects in the apoptosis pathway as well as enhanced proliferation rates. CLL can also be classified into different subsets (section 1. 4. 3.), these subsets are classified by the origin of the B cell clone that the disease progressed from. In order to understand the difference between the CLL subsets it is important to understand the development of B cells.

1. 4. 2. 1. B-Cell Development

B cells are vital for the antibody-directed immune response and recognise foreign antigens by the B-cell receptor (BCR). The extracellular domain of the BCR

consists of two heavy and two light chain immunoglobulins which together form two antigen binding pockets (Figure 1-17). The development of B cells from the progenitor hemeopoietic stem cell occurs in the fetal liver or adult bone marrow where the early B cell will express µ heavy (H) immunoglobulin chains and surrogate light (L) immunoglobulin chains to form the pre-B cell receptor (LeBien and Tedder, 2008). The next stage of B cell development is to express genuine L chains, which combine with the µ chains to form the extracellular domain of the BCR also known as surface IgM (surface immunoglobulin M (sIgM)), which is essential for B cell survival (LeBien and Tedder, 2008). This cell is now an immature naïve B cell. The immature naïve B cell is then released into the periphery. As this naïve B cell leaves the bone marrow other molecules on its cell surface are expressed including CD19 (cluster of differentiation 19) present on all B cell lineages. CD21 and CD22 are also expressed which are required to inform the B cell of inflammatory responses and B cell survival, respectively (LeBien and Tedder, 2008). The naïve B cell will also express IgD upon exit from the bone marrow (LeBien and Tedder, 2008) (Figure 1-17). The expression of sIgD occurs as a consequence of RNA, rather than DNA, splicing events. The RNA splicing enables the µ locus to be maintained and allows the mature B cell to express both sIgM and sIgD (Wang and Clark, 2003).

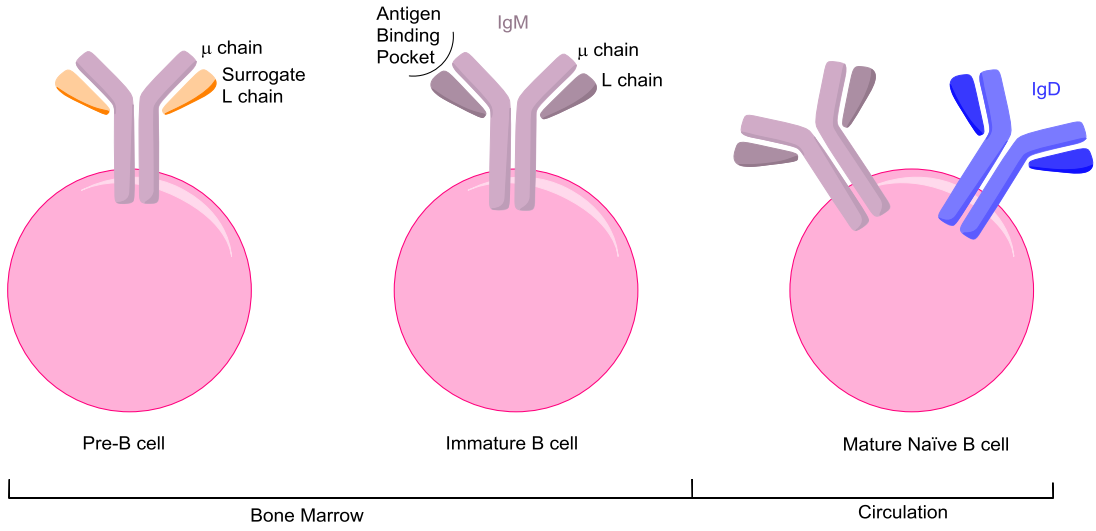

Figure 1-17: B-Cell Development

B cells originate from the bone marrow with the initial production of pre-B cells that contain surface pre-BCRs; composed of the μ heavy chain coupled with a surrogate light chain. These pre-B cells develop into immature naïve B cells due to the production and incorporation of the genuine light chain, generating the mature surface IgM. These immature naïve B cells have not encountered antigen and move out into the peripheral blood to enable further development and differentiation to occur in the presence of antigen. The migration out into the circulation also results in expression of the surface IgD, which has the δ heavy chain. Illustration prepared in ChemBioDraw Ultra version 13.0.

Circulating naïve B cells that are also $CD5^-$ provide innate protection against microbial infection as these cells can recognise and bind bacterial polysaccharides. Cross linking of multiple IgM molecules on a single $CD5^-$ B cell can activate the cell to produce antibodies. But these cells will not differentiate or produce memory B cells therefore these B1 cells will produce low affinity antibodies (IgM) as part of the innate immune response (Alberts, 2002; Wang and Clark, 2003).

Lymphocytes are activated to enable further differentiation, in the lymph nodes or spleen, where lymphocytes will come in close proximity to antigen presenting cells, for example dendritic cells. If the dendritic cell, along with T cell support, presents an antigen complementary to the antigen binding site on the sIgM, downstream activation will occur and the lymphocyte will differentiate and mature. Lymphocytes continuously circulate between the bloodstream and lymphoid organs. Lymphocytes in the circulating blood will pass from the postcapillary venules into lymph nodes due to the presence of specialised endothelial cells (Figure 1-18). These endothelial cells express a counter-receptor that interacts with L-selectin (part of the lectin superfamily class of cell adhesion molecules) on lymphocytes resulting in weak adherence of the lymphocyte to the endothelial cells (Alberts, 2002). Enhancement of this adhesion occurs due to the release of cytokines from the endothelial cells resulting in migration of the lymphocytes between the endothelial cells from the postcapillary venule to the lymph node (Alberts, 2002). The lymphocytes will infiltrate through the lymph node and will accumulate in lymphatic vessels allowing the lymphocyte to pass into other lymph nodes, eventually returning the lymphocyte back to the bloodstream. However, if the lymphocyte interacts with antigen then the lymphocyte is retained in the lymphoid organ to undergo proliferation and differentiation in the germinal centre of the lymph node with the aid of T cell help (Figure 1-18) (see section 1. 4. 2. 2.).

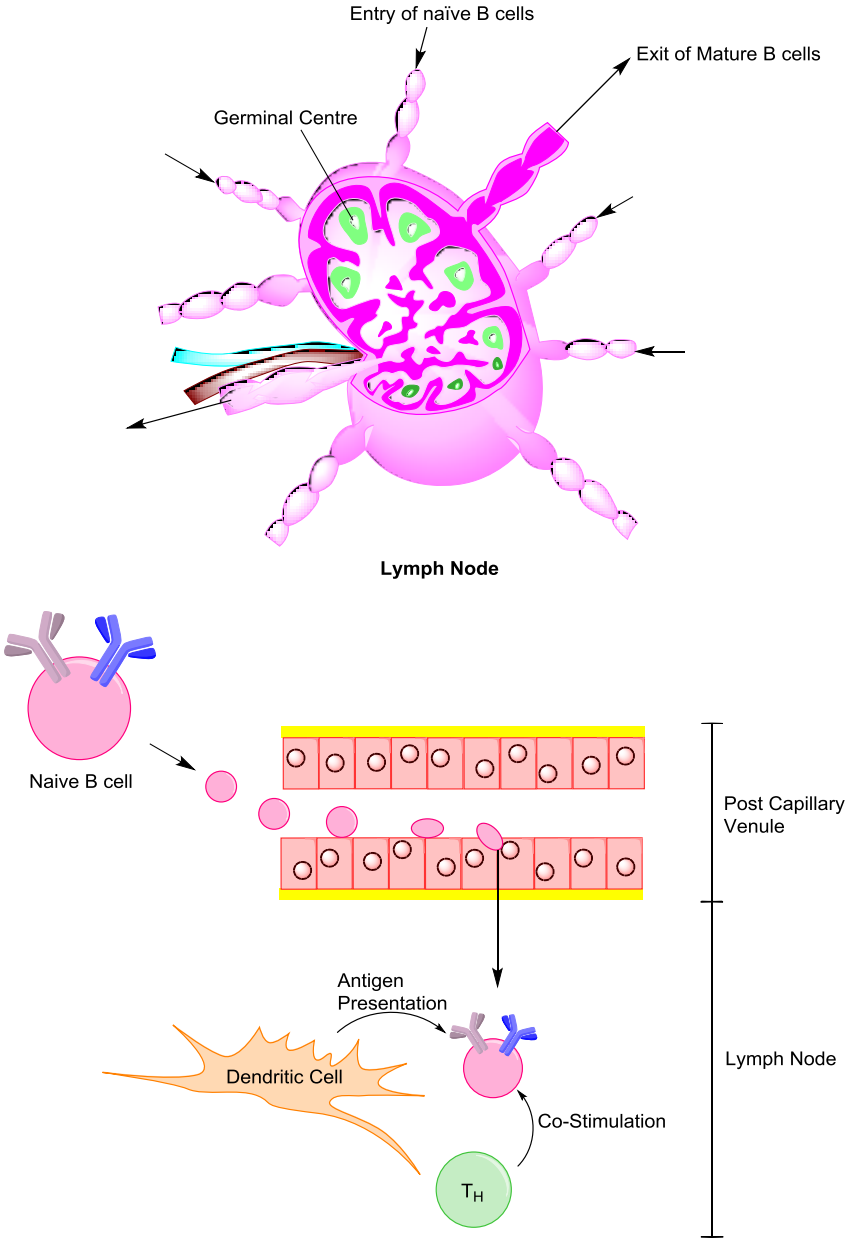

Figure 1-18: Migration of B Cells in the Lymph Node

Lymphocytes migrate from the peripheral blood circulation into lymph nodes due to the presence of specialised endothelial cells present in the postcapillary venule. These endothelial cells will bind to L-selectin on lymphocytes resulting in weak adhesion. Cytokine release from the endothelial cells enhances the adhesion enabling migration of the lymphocyte between the endothelial cells into the lymph node. Antigen presenting cells (follicular dendritic cells), present within the lymph node, will present antigen to the B cell and along with T helper (T_H) cell co-stimulation will lead to proliferation and further differentiation of the B cell. Illustration prepared in ChemBioDraw Ultra version 13.0.

1. 4. 2. 2. Germinal Centre Reaction

The germinal centre contains mainly proliferating B cells, a minority of T cells as well as macrophages and specialised follicular dendritic cells, which have elongated cytoplasmic processes and few lysosomes (Roitt, 1997). Secondary challenge with antigen or immune complexes results in enlargement of the germinal centre and appearance of new germinal centres. Following secondary antigen challenge, primed B lymphocytes are activated by T helper (T_H) cells and dendritic cells resulting in migration into the germinal centre (LeBien and Tedder, 2008; Roitt, 1997). Entry into the germinal centre results in B-lymphocyte differentiation into centroblasts that progress through the cell cycle very rapidly with a cycle time of just six hours. During this rapid proliferation somatic mutations in the Ig genes occur, resulting in altered variable regions on the sIg as well as class switching of the sIg (LeBien and Tedder, 2008; Roitt, 1997) (see section 1. 4. 2. 3.). Centroblasts then differentiate further into the non-dividing centrocytes. Apoptosis of centrocytes occurs readily unless rescued by interaction with an antigen on follicular dendritic cells. The interaction of sIg with antigen results in increased expression of the anti-apoptotic protein, Bcl-2, preventing apoptosis (Roitt, 1997). T_H cells also play an important role in prolonged centrocyte survival, due to interactions of the antigen, T_H cells and the centrocyte. Enhanced apoptosis of centrocytes ensures that only centrocytes expressing high affinity sIg to antigen survive and differentiate. Differentiation of centrocytes into antibody producing cells and memory B cells is dependent on stimulation from follicular dendritic cells and T cells, respectively (Roitt, 1997; Shlomchik and Weisel, 2012) (Figure 1-19). Release of soluble CD23 and IL-1α from dendritic cells stimulates migration of centrocytes into sites of plasma cell activity (e.g. lymph node medulla) whereas CD40 stimulation from T cells will result in expansion of memory B cells (Roitt, 1997; Shlomchik and Weisel, 2012) (see Figure 1-19).

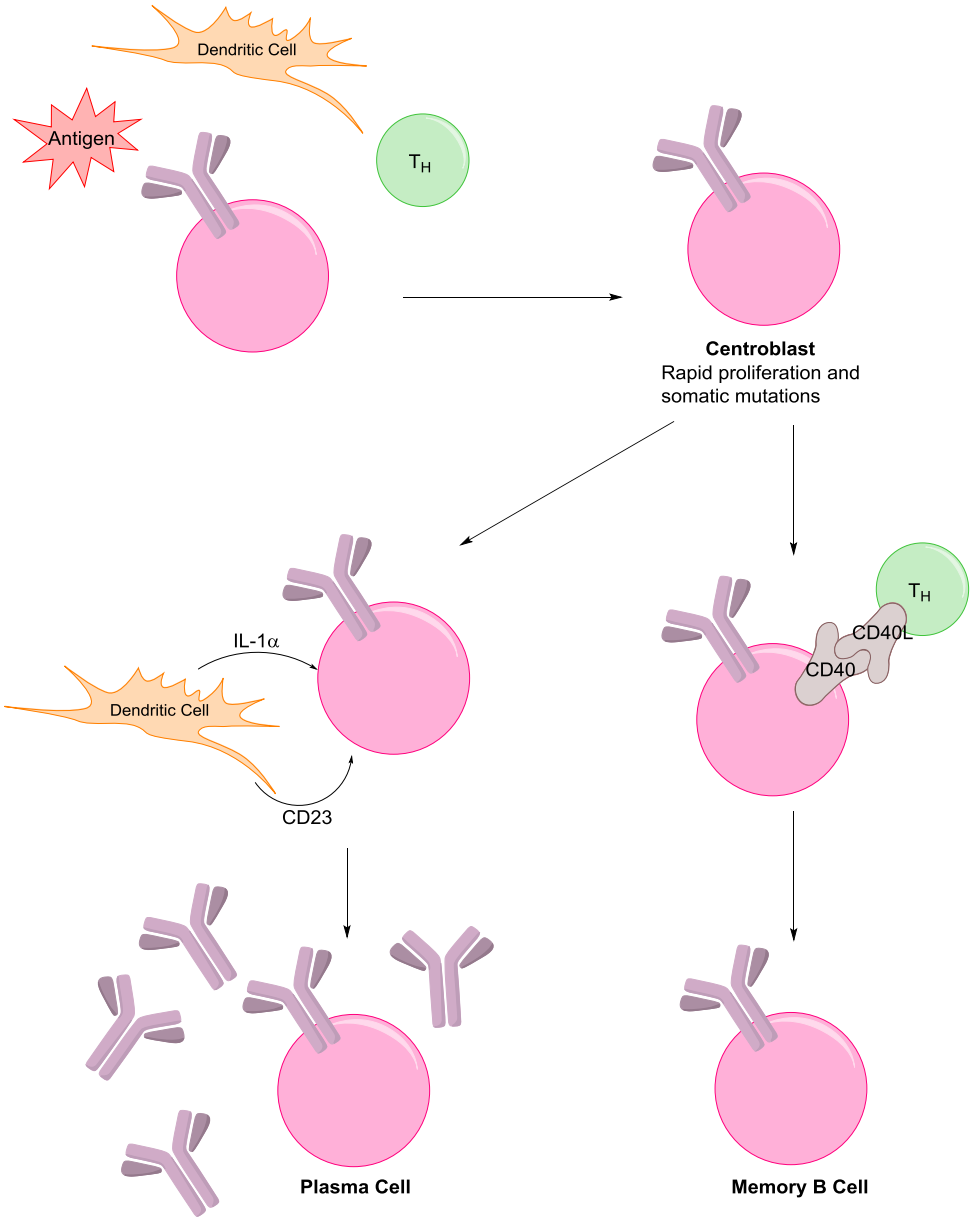

Figure 1-19: Differentiation of the B Cell in the Germinal Centre Reaction

Naïve B cells differentiate due to the presence of antigen. Recognition of antigen on the BCR will enhance survival while co-stimulation by T helper cells (T_H cells) and follicular dendritic cells will enhance proliferation. The centroblast undergoes rapid proliferation as well as somatic mutations to ensure high affinity binding to the antigen. Co-stimulation by follilcular dendritic cells releasing CD23 and IL-1α pushes the centroblast to differentiate into a plasma cell to release soluble antibody. Whereas T_H cell co-stimulation via CD40 directs the centroblast to differentiate into a memory B cell. Illustration prepared in ChemBioDraw Ultra version 13.0.

1. 4. 2. 3. Immunoglobulin Gene Recombination and Class Switching

The variation of sIg seen on B lymphocytes occurs as a consequence of genetic recombination of the Ig genes, which is important for diversity enabling efficient antigen binding. As mentioned previously (section 1. 4. 2. 1.) the sIg consists of a heavy and light chain that together will form an antigen binding pocket (see Figure 1-17). The light chain is encoded in either the κ- or λ- constant (C_L) genes, whereas there are eight different constant (C_H) genes for the heavy chain (μ, δ, ε, α and four γ constant regions) (Berg et al., 2007). The formation of the light chain also requires the incorporation of a variable (V_L) and joining (J_L) gene, while the heavy chains require variable (V_H), diversity (D_H) and joining (J_H) genes as well as the C_H gene. Splicing of the VJ or VDJ genes is required in both the heavy and light chains to ensure high diversity of the sIg. There is greater diversity seen in the heavy chain due to the number of genes involved (Berg et al., 2007).

Recombination of the V(D)J genes occurs due to the presence of Recombination Activating Genes (RAG)-1 and RAG-2 enzymes that nick a single strand of the DNA between the recombination signal sequence (RSS) and the exon (Nishana and Raghavan, 2012). The single strand nick will result in the formation of a hairpin structure that is bound by RAG and modification of the hairpin will result in insertions and deletions occurring at the time of joining the two exons (Nishana and Raghavan, 2012). The RSSs consist of a heptamer (CACAGTG) and an AC rich nonamer (ACAAAAACC) which are separated by a 12 base pair (12RSS) or 23 base pair (23RSS) sequence. The length of the 12RSS and 23RSS is important whereas sequence is not and as a general rule 12RSS recombine with 23RSS (Nishana and Raghavan, 2012).

The J genes provide the residues for the complementary determining region 3 (CDR3) in the hypervariable region of the antigen binding cleft. The CDR3 of the heavy chain can be further diversified due to the action of terminal deoxynucleotidyl transferase, a DNA polymerase that requires no template (Berg et al., 2007). The terminal deoxynucleotidyl transferase will insert additional nucleotides into the sequence between the V_H and D genes. Also the recombined genes can also be

altered by somatic mutation that has been shown to increase binding affinity 1000 fold (Berg et al., 2007).

Diversity of the antigen binding pocket ensures high affinity binding, but B-lymphocytes also undergo class switching that alters the constant region of the Ig without altering the binding specificity. Class switching is carried out by translocation of the VDJ gene to a different C_H gene (Berg et al., 2007). Class switching is important to modulate the downstream effect of the antibody, for example IgM is the first class of antibody produced and can form pentamers, generating 10 binding sites that enables tight antigen binding due to high avidity rather than high affinity (Berg et al., 2007).

1. 4. 2. 4. The B-Cell Receptor

In order for a B lymphocyte to differentiate the cell is activated by antigen and co-stimulated by $CD4^+$ T_H cells. The T_H cells are specific for the same antigen and aid proliferation and differentiation. The antigen will activate the cell by signalling via the BCR. Antigen binding will result in targeting the BCR to membrane rafts resulting in aggregation of antigen bound BCR which promotes downstream signalling (Figure 1-20) (Stevenson and Caligaris-Cappio, 2004; Wang and Clark, 2003). The extracellular domain of the BCR consists of the sIg which spans the plasma membrane and the H chains are non-covalently associated with Igα and Igβ (CD79a and CD79b, respectively) tethering the sIg to the membrane (Gauld et al., 2002; Wang and Clark, 2003). Igα and β contain ITAM (Immunoreceptor Tyrosine base Activation Motifs) that are phosphorylated by SYK and the Src family of receptor tyrosine kinases (Figure 1-20) (Glassford et al., 2003; LeBien and Tedder, 2008; Stevenson and Caligaris-Cappio, 2004). LYN (Src family kinase), bound to the resting BCR, phosphorylates the first ITAM (Wang and Clark, 2003). SYK binds to the phosphorylated ITAM via SYK's SH2 domain (Src Homology 2 domain), resulting in a conformational change of SYK into the active form, and phosphorylates the second ITAM (Wang and Clark, 2003). Following phosphorylation of the ITAMs, BLNK (B cell linker protein) is recruited that can

bind to a non-ITAM tyrosine on Igα via an SH2 domain. Once recruited, SYK phosphorylates BLNK to provide multiple docking sites for downstream targets, including BTK and PLCγ (Figure 1-20) (Kulathu et al., 2008). BTK is also recruited to the BCR complex following activation of PI3K (phosphoinositide-3 kinase). PI3K generates PIP_3 (phosphoinositol-3,4,5-triphosphate) and the production of PIP_3 recruits BTK to the plasma membrane, which facilitates the interaction with BLNK (Figure 1-20) (Glassford et al., 2003). BLNK also provides a docking site for PLCγ, allowing BTK to phosphorylate and activate PLCγ, resulting in the production of inositol trisphosphate (IP_3) and DAG (diacylglycerol) that results in calcium flux and PKC (protein kinase C) activation (Figure 1-20) (Cheung and Kong, 2010; Limon and Fruman, 2012).

Activation of the B cell signalosome (Figure 1-20) (consisting of BLNK, BTK, PI3K and PLCγ) is essential for B cell development and mutations within the *Btk* gene results in X-linked agammaglobulinaemia (XLA), resulting in a lack of mature circulating B cells and immunoglobulins (Glassford et al., 2003; Wang and Clark, 2003). Activation of the B cell signalosome is enhanced by CD19 activation, which lowers the threshold for BCR stimulation to activate the B cell (Figure 1-20) (Gauld et al., 2002). CD19 as well as T cell derived cytokines and Toll-like receptor interaction enhance the activation of PI3K. PI3K activity is important in B cell development as this, along with signalling via the B cell signalosome, increases Akt and mTOR activity, both of which are fundamental in the proliferation of B cells as well as determining whether the B cell should enter the germinal centre reaction (Limon and Fruman, 2012) (see sections 1. 4. 2. 2. and 1. 4. 2. 3.).

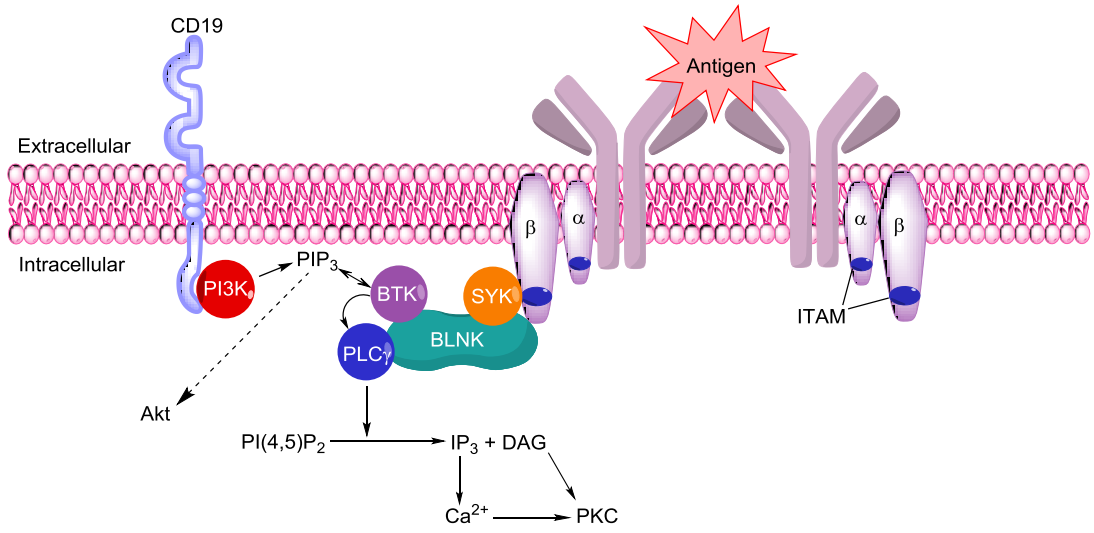

Figure 1-20: B-Cell Receptor Signalling Following Antigen Binding

The extracellular proportion of the BCR consists of a surface Ig, with the intracellular portion of heavy chain non-covalently associated with Igα and Igβ. One Igα/β molecule is associated with each BCR. The Igα/β molecules provide phosphorylation sites following antigen binding in their ITAMs (immunoreceptor tyrosine based activation motifs) that will recruit the downstream kinase SYK (spleen tyrosine kinase) and BLNK. BLNK is phosphorylated by SYK to provide docking sites for BTK (Bruton's tyrosine kinase), a downstream target of SYK, and PLCγ (phospholipase C γ). BTK is also recruited to the plasma membrane by PIP_3 (indicated by the double-headed arrow). Following recruitment downstream signalling cascades are activated ultimately resulting in enhanced intracellular calcium (Ca^{2+}), which acts as a second messenger. Illustration prepared in ChemBioDraw Ultra version 13.0.

1. 4. 3. Two Subsets of CLL

CLL can be classified into two major subsets (Figure 1-21), unmutated and mutated CLL (U- and M-CLL, respectively) depending on mutational status of the variable regions of the H chain of the sIg (Stevenson and Caligaris-Cappio, 2004). U-CLL patients have a worse prognosis compared to M-CLL patients and the diseases also differ in their origins. U-CLL is thought to derive from a naïve B cell that has just left the bone marrow as the B cell expresses CD5 and CD19 but has not undergone antigen affinity maturation in the lymphoid organs (Forconi et al., 2010; Stevenson and Caligaris-Cappio, 2004). M-CLL derives from a memory B cell, these cells have high affinity for antigen and have previously undergone somatic mutation (Forconi et al., 2010; Stevenson and Caligaris-Cappio, 2004). U-CLL B cells also more commonly have high expression of ZAP70 (zeta associated protein 70) which is a receptor associated tyrosine kinase that is mainly expressed in T cells. CLL also have a bias toward the *IGHV* gene used, with 25-30% of U-CLL expressing *IGHV1-69* (Forconi et al., 2010). The *IGHV1-69* gene usage also occurs in 5% of the 'normal' age-matched population, indicating that the sIgM present in CLL is part of the normal repertoire of sIgM (Forconi et al., 2010). As many as 30% of all CLL cases have structurally similar antigen-binding domains suggesting that a common antigen has triggered these cells (Agathangelidis et al., 2012), although the antigen(s) involved in CLL is unknown. To support the idea that a common antigen(s) is involved it has recently been found that cases with different germ-line genes often undergo somatic hypermutation reducing sequence discrepancies (Agathangelidis et al., 2012). At least one IgM produced from the *IGHV1-69* gene has been shown to react with a common pathogen, *Streptococcus pneumoniae* (Forconi et al., 2010). The bias towards this gene usage indicates that there is a shared or common antigen and persistent antigen binding is believed to be involved in disease progression (Forconi et al., 2010).

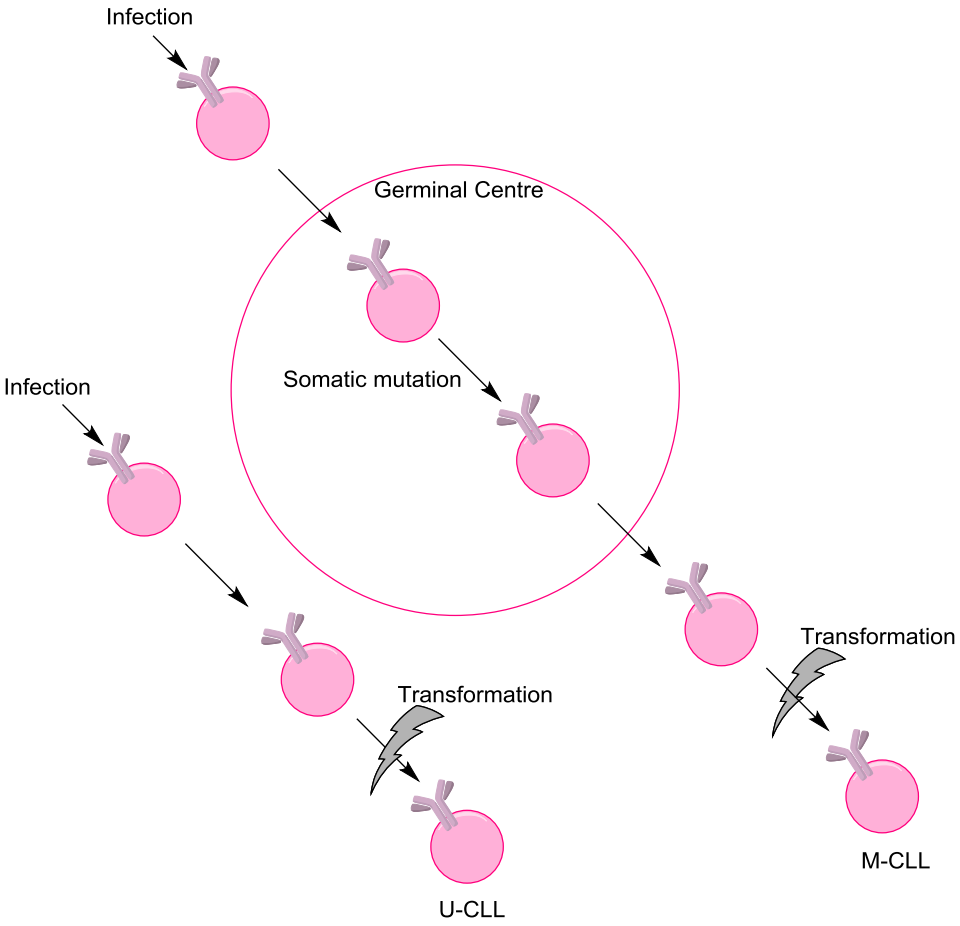

Figure 1-21: Two Subsets of Chronic Lymphocytic Leukaemia

CLL has two major subsets classified as mutated (M-CLL) and unmutated (U-CLL). The initial proliferative drive is believed to occur from a common antigen(s), perhaps associated with infection. M-CLL and U-CLL differ in the B-cell that they were derived from. U-CLL derived from a B cell that had not undergone somatic mutations, whereas M-CLL derived from a B cell that had gone through the germinal centre reaction and undergone somatic mutation, resulting in M-CLL being derived from a more mature B cell. Illustration prepared in ChemBioDraw Ultra version 13.0.

Another classification of CLL is based on signalling. CLL can be sub-classified into ‘responders’ and ‘non-responders’ depending on their signalling capacity in response to surface IgM stimulation. U-CLL cells most commonly respond and signal via the sIgM, while the majority of M-CLL cells are classified as non-responders, although the ability to respond is not perfectly correlated with mutational status (Mockridge et al., 2007). Downstream of the BCR signalosome calcium is released as a second messenger (see section 1. 4. 2. 4.). Responses to BCR stimulation can be monitored by intracellular calcium release and results in this sub-classification of CLL B cells. The percentage of cells that showed an increase in intracellular calcium in each sample was used to classify samples as responders and non-responders (Mockridge et al., 2007). An intracellular calcium release in less than 5% of the cells was classified as a non-responder and a release of equal to or greater than 5% was classified as a responder. This cut off was selected as this was the lowest level of reproducible responses (Mockridge et al., 2007). Another known prognostic marker of CLL is CD38 expression, with high CD38 expression linked with poor prognosis. The ability of a cell to respond to sIgM was also correlated with CD38 expression in U-CLL. U-CLL samples with high CD38 expression were able to respond to sIgM stimulation, while U-CLL samples with lower CD38 expression were classified as non-responders (Mockridge et al., 2007). Whereas CD38 expression had no effect on the signalling capability in M-CLL, generally M-CLL samples had lower CD38 expression compared to U-CLL, but the expression did not correlate with calcium flux (Mockridge et al., 2007). ZAP70 expression did not correlate with the signalling capability of the cell (Mockridge et al., 2007). The signalling capacity of a CLL cell correlated with sIgM expression, with higher expression of sIgM increasing signalling, whereas down-modulation of sIgM decreased signalling (Mockridge et al., 2007).

A CLL cell’s signalling capability following stimulation has important clinical implications with responders having a worse prognosis. The mechanism in which sIgM enhanced proliferation and survival is not fully understood, however the oncoprotein, MYC, is important in proliferation in CLL and the expression of MYC has been shown to be dependent on BCR signalling (Krysov et al., 2012). In all signalling responsive samples (U-CLL and M-CLL) MYC expression was enhanced greater than 2-fold following sIgM stimulation, whereas in non-responsive samples

there was no enhancement of MYC levels (Krysov et al., 2012). sIgD stimulation did not significantly increase MYC protein levels (Krysov et al., 2012) indicating that signalling via sIgM has important implications for proliferation and disease progression. The importance of signalling on disease progression has led to the clinical evaluation of inhibitors of the BCR signalling pathway, including inhibitors targeted against BTK and SYK (NCT01886872 and NCT01499303, respectively, ClinicalTrails.gov).

In general U-CLL samples have elevated sIgM levels and are signalling responsive compared to M-CLL, as summarised in Figure 1-22. The signalling capacity may be a reflection of the cell of origin or previous *in vivo* stimulation. It is important to note that CLL blood samples from a single individual are heterogeneous for the sIgM expression, due to the blood sample providing a 'shadow' of previous events that may modulate sIgM expression (Coelho et al., 2013).

Other markers of poor prognosis patients include CD38 expression and ZAP70 expression, CD38 expression has been linked with signalling capacity of U-CLL cells (as mentioned earlier), whereas ZAP70 expression did not correlate with signalling capacity (Mockridge et al., 2007). ZAP70 expression is strongly associated with unmutated CLL providing another prognostic marker and ZAP70 expression has also been shown to aid migration and survival (Richardson et al., 2006).

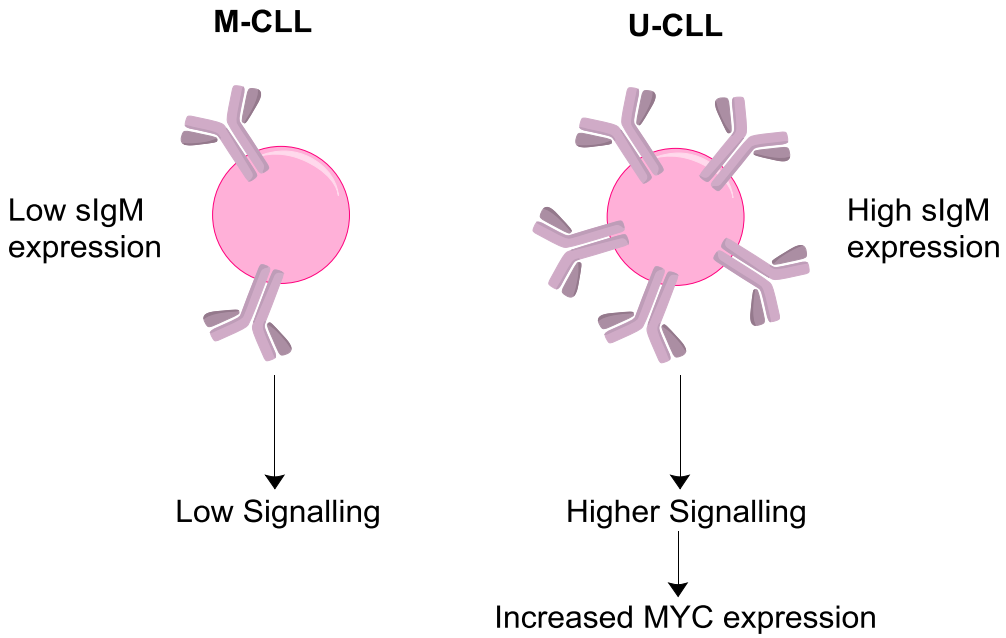

Figure 1-22: Classification of CLL Subsets Based on Signalling Capacity

CLL can be classified by the ability of the cell to signal following sIgM stimulation. Unmutated- CLL (U-CLL), with a poorer prognosis, generally has higher levels of sIgM and increased signalling capability. Mutated - CLL (M-CLL) cells have lower levels of sIgM and have decreased signalling capacity.

1. 4. 4. Signalling Pathways in CLL

1. 4. 4. 1. Apoptosis Pathway

CLL like many cancers develops due to defects in the apoptosis pathway, in particular defects with the BCL-2 family proteins are involved in disrupted apoptosis. CLL cells express high levels of BCL-2 (an anti-apoptotic molecule) that exceeds that of normal peripheral blood lymphocytes. The BCL-2 expression level in CLL is closer to the level expressed in follicular lymphoma; which has the translocation t(14:18) resulting in BCL-2 being regulated by the immunoglobulin promoter and is therefore highly expressed (Packham and Stevenson, 2005), but CLL does not have this translocation. CLL cells do not contain this translocation and it has been shown that the 13q deletion common in CLL (Parker et al., 2011) results in the loss of miR15 and miR16. These microRNAs negate the expression of BCL-2 and loss of 13q subsequently results in elevated BCL-2, seen in CLL (Palamarchuk et al., 2010). The elevated BCL-2 levels in CLL results in higher BCL-2/BAX (pro-apoptotic molecule) ratios (Packham and Stevenson, 2005), thereby preventing BAX from interacting with the mitochondria and releasing cytochrome *c* (Figure 1-8). A decrease in the BCL-2/BAX ratio is associated with increased sensitivity to cytotoxic drugs (Packham and Stevenson, 2005). BCL-2 is not the only pro-survival molecule that is up-regulated in CLL, MCL-1 is also induced in IgM stimulated CLL cells (Petlickovski et al., 2005) and has been linked with poor clinical outcome (Pepper et al., 2008). BIM is the dimerization partner of MCL-1 and is a tumour suppressor in many B cell malignancies, that upon phosphorylation by Extracellular Signal Regulated Kinase (ERK) on Ser^{69} of the extra-long isoform of BIM (BIM_{EL}) results in the release of MCL-1 leading to survival (Paterson et al., 2012). BIM_{EL} phosphorylation occurs within 30 minutes of anti-IgM treatment and results in a dissociation of MCL-1 (Paterson et al., 2012). This phosphorylation and pro-survival response to IgM stimulation also occurs if CLL cells are co-cultured with follicular dendritic cells indicating that the microenvironment is important in enhanced survival rates of CLL cells (Paterson et al., 2012).

1. 4. 4. 2. Signalling Pathways Involved in Proliferation in CLL

The accumulation of CLL cells is not just a result of a defect in the apoptosis pathway but also enhanced proliferation rates. CLL cells circulating in the peripheral blood are virtually all in the G_0-early G_1 phase, indicating that these cells are not actively proliferating. Signal competence is also linked to CD38 expression, a poor prognostic marker of CLL. The two poor prognostic markers, unmutated status and $CD38^+$ expression, could be consistent with increased mitotic rate and the presence of shorter telomeres in U-CLL, indicating that U-CLL cells have undergone more cell divisions compared to M-CLL (Chiorazzi and Ferrarini, 2003; Stevenson and Caligaris-Cappio, 2004). Interestingly when the CLL cells are purified from blood for *in vitro* assays the CLL cells are isolated from T cells and other accessory cells and CLL cells will spontaneously undergo apoptosis, highlighting the importance of the microenvironment for the survival of CLL cells. CLL cells do not proliferate in the peripheral blood but can proliferate in pseudofollicles within the lymph node and bone marrow. CLL cells in these pseuodfollicles express survivin, a member of the inhibitor of apoptosis protein (IAP), promoting survival of these cells (Granziero et al., 2001; Stevenson and Caligaris-Cappio, 2004). There are also many $CD4^+$ T cells in the pseudofollicle that co-express CD40L, indicating activated T cells will be able to interact and promote survival of the CLL cells (Stevenson and Caligaris-Cappio, 2004). Intriguingly, CLL cells in the pseudofollicle express CCL17 and CCL22, two T cell attracting chemokines. Whereas circulating CLL cells do not express CCL17, CCL22 or survivin. In *in vitro* models stimulation of CLL cells with CD40L will enhance RNA levels and secretion of CCL22 and stimulation with IL-4 will result in release of CCL17, therefore all CLL cells retain the ability to respond to proliferation and anti-apoptotic stimuli (Stevenson and Caligaris-Cappio, 2004). But in order to proliferate the CLL cells require activation by T cells as well as other interactions within the psuedofollicle.

1. 4. 4. 3. Importance of the Microenvironment

As described the microenvironment is important to enhance proliferation rates as well as to prevent apoptosis (Mockridge et al., 2007; Paterson et al., 2012; Ramsay and Rodriguez-Justo, 2013; Stevenson and Caligaris-Cappio, 2004). It is thought that the microenvironment may prevent apoptosis and enhance survival and proliferation by the NOTCH signalling pathway that will ultimately lead to the up-regulation of Nuclear Factor- κB (NF-κB) and anti-apoptotic molecules as well as enhancing the expression of MYC (Ramsay and Rodriguez-Justo, 2013). Resistance to apoptosis may also be mediated via CD40 and CD40L (predominately found on T_H cells) (Ramsay and Rodriguez-Justo, 2013). There is also evidence that the stromal cells enhance survival by increasing glutathione levels within the CLL cells.

ROS production occurs as a result of metabolic activity and under normal physiological conditions the ROS production is counterbalanced by anti-oxidant activity. A slight increase in ROS is believed to have a proliferative advantage whereas excessive ROS production will result in cellular damage and it has been shown that malignant lymphocytes have elevated ROS (superoxide, O_2^-) levels compared to their non-malignant counterparts (Hileman et al., 2004). Treatment with 2-methoxyestradiol (2-ME), an anti-cancer agent currently in clinical trials, was shown to enhance ROS levels in leukaemic lymphocytes and decrease activity of the antioxidant, superoxide dismutase (SOD), resulting in cell death (Hileman et al., 2004). Whereas 2-ME only slightly enhanced ROS in the 'normal' lymphocytes therefore the basal elevated ROS levels rendered the leukaemic cells more susceptible to killing (Hileman et al., 2004). PEITC has been shown to work in a similar manner as PEITC increased ROS levels in CLL as a consequence of decreased glutathione levels (Trachootham et al., 2008).

In the absence of stromal cells, CLL cell glutathione levels drop and CLL cells undergo apoptosis (Zhang et al., 2012). The presence of stromal cells prevented apoptosis in CLL cells following oxidative stress (treatment with hydrogen peroxide) as well as cytotoxic drug treatment. The protection provided by stromal cells was a factor that was released into the media and was of low molecular weight, was identified to be cysteine (Zhang et al., 2012). The presence of the stromal cells

ensured that cystine was converted to cysteine, as CLL cells were unable to take up cystine, due to low levels of the cystine transporter on CLL cells (Zhang et al., 2012). The presence of cystine and stromal cells resulted in increased glutathione and free thiol groups within the CLL cell, enhancing survival. The survival protection provided by stromal cells was negated by treatment with PEITC, which decreased free thiol content back down to levels seen in CLL cells cultured alone and decreased cell viability in response to cytotoxic drug treatment (Zhang et al., 2012). This indicated that PEITC prevented stromal protection but it is unclear whether this is the only action of PEITC in CLL cells and requires further investigation.

1. 5. Hypothesis and Aims

1. 5. 1. Hypothesis

The primary hypothesis is that PEITC inhibits mRNA translation, in either a gene specific or global manner. The secondary hypothesis is that BCR stimulation of primary leukaemic cells enhances mRNA translation.

1. 5. 2. Aims

To investigate these hypotheses the main focus of the experiments described in this thesis was to determine how PEITC alters mRNA translation, firstly in a breast cancer cell line, MCF7, before progressing into primary CLL samples. MCF7 cells were selected for study to build on previous analyses of PEITC performed using this cell line (Cavell et al., 2012; Syed Alwi et al., 2012; Syed Alwi et al., 2010) whereas primary CLL samples were selected as a more clinically relevant system to study translational control.

The main aims were to:

- Analyse the effects of PEITC on mRNA translation in MCF7 cells
- Investigate the mechanism for decreased translation in response to PEITC treatment
- Investigate the effects of surface Ig (sIg) stimulation on mRNA translation in primary CLL samples
- Investigate the effect of PEITC as well as novel BCR-targeted kinase inhibitors on sIgM-induced mRNA translation in CLL

Chapter Two

Methods

2. Methods

Cell Culture Techniques

2. 1. Cell Culture Materials

Table 2-1: Materials List for Cell Culture

List of materials used for cell culture and unless otherwise stated chemicals were from Sigma-Aldrich or Thermo Fisher and were of analytical grade.

Reagent	Components
Cell Lines	MCF7 (breast cancer cell line) purchased from American Type Culture Collection (ATCC; Manasses, VA, USA). Mouse embryonic fibroblasts – non-phosphorylatable eIF2α and wild type (kindly provided by Professor Randal Kaufman, University of Michigan Medical Center, USA).
Complete Growth Media	DMEM (Dulbecco's Modified Eagle Medium) (PAA, Somerset, UK) or RPMI (Roswell Park Memorial Institute media)-1640 were supplemented with 10% (v/v) bovine fetal serum (PAA), 2mM L-glutamine (PAA) and 1% (v/v) Penicilin / streptomycin mix (PAA).
Phosphate Buffered Saline (PBS)	140mM NaCl, 2.7mM KCl, 10mM Na_2HPO_4, 1.7mM KH_2PO_4, pH7.4 (adjusted with HCl)
Polysome Cell Lysis Buffer	10mM Tris-HCl (pH7.5), 100mM NaCl, 100mM $MgCl_2$, 10% Triton X-100 and DOC (deoxycholate) (1:1 mix), 1M DTT and 40 units RNasin Ribonuclease Inhibitor (Promega)
RIPA Buffer (5x)	0.75M NaCl, 5% NP40 (v/v), 2.5% DOC (v/v), 0.5% SDS (w/v), 0.25M Tris pH8.0, diluted in 100ml deionised H_2O
All Culture dishes	Greiner, Gloucestershire, UK

2. 1. 1. Primary CLL Samples

The assays carried out in this thesis using primary CLL samples were performed following ethical approval from Southampton and South West Hampshire Research Ethics Committee. Informed consent was provided in accordance with the declaration of Helsinki. Blood was obtained from 15 patients in total with typical CLL who attended hemeatology outpatient clinics at Southampton General Hospital, UK. Peripheral Blood Mononuclear Cells (PBMCs) were isolated by Lymphoprep centrifugation (Axis-Shield Diagnostics), washed and cryopreserved. The isolation of samples was carried out by research technicians in our group. Briefly isolation of PBMCs was carried out by carefully overlaying lymphoprep reagent onto whole (unclotted) blood and centrifuged at 800 g for 20 minutes with the break off. Following centrifugation the PBMCs were present at the interface with the lymphoprep reagent, these were carefully removed and washed in complete RPMI to remove any remaining lymphoprep reagent. The cells were then counted and frozen in freezing media (10% DMSO in fetal calf serum) and stored at -80^{o}C. Clinical details for the patients studied are provided in Table 2-2.

Table 2-2: Clinical Features of CLL Samples

Sample	IGHV Status[1]	CLL (%)[2]	CD38 (%)[3]	ZAP70 (%)[4]	IgM (Ca^{2+}) Response (%)[5]	IgD (Ca^{2+}) Response (%)[6]
348	M	95	4	0	19	53
398	M	97	26	11	2	1.4
414	M	95	1	0	0	62
483	M	90	0	3	5	80
494	M	95	1	19	6	44
505	U	96	14	14	17	34
513	U	99	1	2	NA	NA
526	U	96	3	40	7	16
542	M	93	1	0	2	58
558	M	95	0	4	39	68
561	M	94	2	24	50	63
566	U	96	9	57	7	39
570	M	79	0	3	3	34
583	U	91	1	39	16	23
594	NA	96	7	17	73	73

[1]Mutational status of the IGHV gene; M indicates mutated; U, unmutated and NA, not available. [2]Percentage of CLL ($CD19^+$ $CD5^+$) cells in PMBCs. [3]Percentage of CD38 expression. [4]Percentage of ZAP70 expression. [5]Calcium flux response as a percentage following stimulation with soluble anti-IgM antibody; NA, not available. [6]Percentage of calcium flux response to stimulation with soluble anti-IgD antibody; NA, not available. Characterisation of CLL samples were generated by research technicians.

2. 2. Compounds / Drug Treatment

Table 2-3: Compounds

Compounds used for cell culture experiments

Compound	Company
Phenethyl Isothiocyanate	Sigma-Aldrich, Poole, UK
Dimethyl sulfoxide (DMSO)	Sigma-Aldrich
Rapamycin	Cell Signaling, Hertfordshire, UK
Cycloheximide	Sigma-Aldrich
2-Aminopurine	Sigma-Aldrich
TransFast Reagent	Promega, Southampton, UK.
Interferin	Polyplus-transfection, Southampton, UK

2. 3. Cell Recovery

Cells (MCF7, MEFs or primary CLL samples) were stored in the vapour phase of liquid nitrogen for long term storage, in fetal calf serum containing 10% (v/v) DMSO. Prior to use cells were rapidly thawed and re-suspended in 5ml complete DMEM (MCF7 and MEF cells) or complete RPMI (CLL samples). Cells were then centrifuged at 300 g for 5 minutes at room temperature in a Sorvall Legend RT centrifuge (Kendro, Germany). Media and freezing media was removed by aspiration and cells were re-suspended in fresh complete DMEM/RPMI as required. MCF7 cells and MEFs were cultured for up to 25 passages before new aliquots were recovered. CLL samples were recovered and re-suspended in complete RPMI and incubated at 37^{o}C/5% CO_2 (v/v) for one hour prior to counting and treatment of cells.

2. 4. Oxygen Starvation

MCF7 cells ($3x10^6$) were seeded into 100mm culture dishes in 15ml complete DMEM. The cells were allowed to adhere to the culture dish by incubation at 37°C/10% CO_2 (v/v) for 16 hours for the cells to become 60-70% confluent. The cells were then either incubated at 37°C/10% CO_2 in ambient oxygen levels (20%) (normoxic conditions) for five hours or were placed into the hypoxia chamber (Billups-Rothenberg, Modular Incubator Chamber, California, USA). The hypoxia chamber was filled with 1% O_2 (v/v)/5% CO_2 (v/v) and returned to the 37°C incubator. The cells in the hypoxia chamber were incubated for one hour before the hypoxia chamber was re-gassed with 1% O_2 (v/v)/5% CO_2 (v/v), to ensure that no oxygen had been trapped in any of the plastic ware. The cells were then returned to the 37°C incubator for another four hours to give a total oxygen starvation time of five hours.

2. 5. Luciferase Reporter Assay

MCF7 cells ($1x10^5$) were seeded into 12 well culture plates in 1ml complete DMEM and allowed to adhere at 37°C/10% CO_2 (v/v) for 16 hours. MCF7 cells were transfected with firefly luciferase reporter plasmids alongside a *Renilla* luciferase expression plasmid using Transfast Reagent (Promega, Southampton, UK). Serum free DMEM (200µl) was used to dilute 0.4µg total plasmid DNA and 1.2µl Transfast was added. This transfection mixture was incubated at room temperature for 12 minutes, vortexing every two minutes to enable the Transfast transfection reagent to form a liposome around the plasmid DNA. The plating media was removed from the MCF7 cells and the transfection mixture was added to the cells and incubated at 37°C/10% CO_2 (v/v) for two hours to allow the plasmid DNA to be taken up into the cells. After two hours the transfection mixture was removed and 1ml complete DMEM was added to the cells and were then incubated at 37°C/10% CO_2 (v/v) for a further 16 hours. The transfected cells were treated with 20µM PEITC or equivalent DMSO and incubated in normoxic (20% O_2 (v/v)) or

hypoxic conditions (1% O_2 (v/v)) for two hours. Cell lysates were collected by placing the plates on ice and removing the media before the cells were washed in 1ml ice cold PBS. Passive lysis buffer (400µl) was added directly to the cells and using a cell scraper the cells were collected into microfuge tubes. The samples were then frozen at -20^{o}C to aid cell lysis.

To perform the dual luciferase assay (Promega) the LARII reagent (100µl) was added to a white 96 well plate before 20µl of sample extract was added and mixed by pipetting. The luminescence produced in 10 seconds was detected in the Varioskan Flash plate reader (Thermo Scientific, Essex, UK). Luminescence was produced as firefly luciferase converted luciferin (present in the LARII reagent) into oxyluciferin and light, utilising ATP, oxygen and Mg^{2+} as co-substrates. Stop and Glo reagent (100µl) (Promega) was added to each well and the luminescence was re-measured to detect the activity of *Renilla* luciferase. The Stop and Glo reagent prevents autoluminescence of the *Renilla* substrate, coelenterazine, which in the presence of *Renilla* and oxygen is converted into coelenteramide, carbon dioxide and light, which can then be detected by measuring luminescence.

2. 6. Protein Knock Down using siRNA

Knock down of the kinase, PERK, in MCF7 cells was carried out using siRNA (small interfering RNA) targeted against PERK (EIK2A3K Smart Pool (Dharmacon, Leicestershire, UK)). Reverse transfection was carried out for greater transfection efficiency. Standard transfection protocols require adhesion cells (like MCF7 cells) to be seeded and adhered to the culture dish prior to adding the siRNA, this results in only half of the cells surface area being exposed to the siRNA transfection mixture. To increase the surface area exposed to the siRNA transfection mixture the cells were seeded into culture dishes already containing the siRNA transfection mixture. This enabled the transfection to occur while cells were adhering to the culture dish with the whole surface of the cell exposed to the siRNA transfection mixture. This process of adding the siRNA transfection mixture to the culture dish before the cells were added is known as reverse transfection.

Reverse transfection was carried out using the EIK2A3K Smart Pool (siRNA) (Dharmacon) diluted to 50nM using serum free DMEM. Interferin (PolyPlus, Southampton, UK) was added to the diluted siRNA at a 3:1 ratio (Interferin:siRNA) and incubated at room temperature for 20 minutes with gentle shaking. This enabled the lipid to form a liposome around the siRNA, which provided a delivery system for the siRNA into the cell. The liposome fused with the lipid cell membrane releasing the siRNA into the cytoplasm, the siRNA was then able to bind to its target mRNA and down regulated protein expression of the target mRNA by degradation of the mRNA through the RNA induced silencing complex (RISC). The siRNA binds to RISC and acts as a template; any sequence with exact complementarity binds to the siRNA and is degraded by RISC resulting in significantly less mRNA and ultimately reduced target protein expression. The siRNA – interferin mix was added to 6 well culture dishes before MCF7 cells ($0.2x10^6$) were seeded into the wells in 1ml complete DMEM containing additional fetal calf serum to give a final concentration of 10% serum. Cells were incubated at 37^oC/10% CO_2 (v/v) for 48 hours for optimal transfection prior to any further treatment.

2. 7. VEGF Enzyme Linked Immuno-Sorbent Assay

MCF7 cells (0.2×10^6) were seeded into a 12 well plate in 1ml complete DMEM and incubated for 16 hours at 37^oC/10% CO_2 (v/v) for the cells to adhere to the culture dish. Plating media was aspirated and 500µl fresh complete DMEM was added to the cells. Cells were treated with PEITC or equivalent DMSO and incubated in normoxic or hypoxic (1% O_2) conditions for the experimental times required. Supernatant was collected and the Quantikine Human VEGF Immunoassay (R and D systems, Abingdon, UK) was carried out according to manufacturer's protocol. Briefly, supernatant was added to wells of a 96 well microplate that had been pre-coated with a monoclonal antibody against VEGF (supplied by R and D systems). Any VEGF in the supernatant of the sample would have been immobilised by the antibody. The plate was washed to remove any non-specific binding before an enzyme linked polyclonal anti-VEGF antibody was added.

The substrate solution was added to the wells that in the presence of the enzyme produced a colour change. The colour change was proportional to the amount of VEGF bound to the plate and measured at 540nm, with wavelength correction at 450nm subtracted to remove any alterations due to imperfections in the microplate. A known standard of VEGF (provided by R and D systems) was analysed alongside experimental supernatant collected to quantify the amount of VEGF in pg/ml.

2. 8. Metabolic Labelling and Trichloroacetic Acid Precipitation

MCF7 cells (1 x 10^6) were seeded into 60mm culture dishes in 5ml complete DMEM and incubated at 37°C/10% CO_2 (v/v) for 16 hours prior to treatment with PEITC, Rapamycin or cycloheximide for 30 minutes. Media was removed and replaced with fresh complete DMEM and incubated for one, two or three hours before cell pellets were collected. Two hours prior to cell harvest ^{35}S-TransLabel (MP Biomedical, France) was added to the media on the cells to a final activity of 10µCi/ml (0.37MBq/ml). ^{35}S-TransLabel had a specific activity >37.0TBq/mmol (>1000Ci/mmol) containing (~70%) L-methionine and (~15%) L-cysteine that had been radiolabelled using ^{35}S. After two hours of incorporation media was removed and cell pellets were washed twice in ice cold PBS before scraping the cells in 1ml ice cold PBS. Cell pellets were collected by centrifugation at 4,000rpm (1,520 g) on a bench top centrifuge for three minutes. Cells were then lysed using RIPA buffer and incubated on ice for 15 minutes. RIPA buffer contains DOC, NP40 and SDS that are detergents that lyse the cellular membrane enabling proteins to be extracted. The RIPA buffer was supplemented with protease inhibitors (Sigma) to ensure that proteins were not degraded. After incubation on ice for 15 minutes proteins were isolated from cell debris by centrifugation at 13,000 rpm (16,100 g) on a bench top centrifuge for five minutes. Lysates were stored at -20°C overnight.

CLL B cells were recovered as described previously and after one hour recovery the cells (2 x 10^6) were treated with anti-IgM, anti-IgD or isotype control Dynabeads for a total of 24 hours at 37°C/5% CO_2 (v/v) in the presence of 50µM zVAD (Sigma) a caspase inhibitor. The antibody labelled Dynabeads were kindly prepared by Dr.

Sergey Krysov, University of Southampton. After 23 hours cells were either left untreated, treated with PEITC, equivalent DMSO or 10µg/ml cycloheximide (as a positive control for complete inhibition of translation) for one hour prior to the addition of ^{35}S- TransLabel with a final activity of 10µCi/ml (0.37MBq/ml) and incubated for a further four hours. After four hours cell pellets were collected by centrifugation at 2,000rpm (380 g) for eight minutes at 4^{o}C in a benchtop centrifuge. Media was removed and cells were washed in ice cold PBS and re-pelleted. Cell pellets were snap frozen and stored at -20^{o}C overnight. Cells were lysed by the addition of 50µl H_2O and went through two freeze-thaw cycles. 50µl 10mg/ml L-cysteine and L-methionine was added to the lysed cells and incubated at 37^{o}C for 15 minutes to aid lysis. Samples were centrifuged at 13,000rpm (16,100 g) for five minutes at 4^{o}C on a benchtop centrifuge. Radioactivity of the lysates was determined by scintillation counting as described below.

To determine the amount of translation that had occurred in the incubation period, the activity of the lysates was determined by scintillation counting. Firstly 30µl of lysate was spotted onto filter discs (Whatman, GE Healthcare, Buckinghamshire, UK) and allowed to air dry. Discs were then placed in a beaker containing 10% Trichloroacetic Acid (TCA) and an excess of unlabelled L-methionine (Sigma) and incubated at room temperature for 20 mintues. 10% TCA (v/v) was discarded and 5% TCA (v/v) was added to the samples and heated to boiling point (90^{o}C). The samples were then cooled before discarding the 5% TCA (v/v) and discs were washed in 100% ethanol followed by 100% acetone. Filter discs were placed on foil to air dry completely before being placed in scintillation vials. Samples were covered in scintillation fluid (4ml) (OptiScint 'HiSafe', PerkinElmer) and radioactivity was analysed on a WALLAC 1409 liquid scintillation counter (PerkinElmer) for one minute per sample. For analysis of CLL samples the counts from cycloheximide treated cells were removed from the counts of any other treatment of the cells to remove any variability in background contamination.

2. 9. Polysome Profiling

MCF7 cells or MEFs (2 x 10^6) were seeded into 100mm culture dishes in 15ml complete DMEM and incubated for 16 hours at 37°C/10% CO_2 (v/v) before treatment for the required experimental time. Following treatment, cycloheximide (10µg/ml) was added to 'freeze' the ribosomes to enable profiling to be carried out. Cycloheximide was added for five minutes before cells were placed on ice and media was aspirated. The cells were washed three times in ice cold PBS. Polysome cell lysis buffer was added directly to the cells in the culture dishes and cells were scraped into a DNase/RNase free microfuge tube. The cells were incubated on ice for two minutes to lyse the cells. Centrifugation at 13,000rpm (16,100 g) for five minutes at 4°C was carried out on a bench top centrifuge to separate the cytoplasmic fraction from the nucleic pellet. The cytoplasmic fraction containing the polysomes was snap frozen and stored at -80°C.

CLL B cells (2 x 10^7) were seeded into 24 well plates in 1ml complete RPMI and anti-IgM beads or isotype control beads were added to the cells and incubated for 24 hours at 37°C / 5% CO_2 (v/v) prior to any further treatment. Following treatment, cycloheximide (10µg/ml) was added to 'freeze' the ribosomes to enable profiling to be carried out. Cycloheximide was added for five minutes before cells were collected. Polysome lysates were generated by collecting the cells into a DNase/RNase free microfuge tube and media was removed by centrifugation at 2,000 rpm (380 g) for eight minutes at 4°C to collect a cell pellet. Cells were washed in ice cold PBS and re-centrifuged to remove all PBS from the cell pellet. The cell pellet was lysed with 300µl polysome cell lysis buffer by pipetting and incubated on ice for two minutes. The cytoplasmic fraction was separated from the nucleic pellet by centrifugation as described above and stored at -80°C (for analyses of polysomes see section 2. 15.)

Protein Techniques

2. 10. Materials for Protein Techniques

Table 2-4: Materials List

Reagents used for protein techiques

Reagents	Components
Running Buffer (10x)	250mM Tris-base, 1.9M Glycine, 35mM SDS
Transfer Buffer	200ml 10x running buffer, 500ml 100% ethanol made up to 2 litres with deionised H_2O
Tris-Buffered Saline – Tween (TBS-T)	20mM Tris pH7.6, 137mM NaCl, diluted in 1 litre deionised H_2O plus 1ml Tween-20 (0.1%)
Stripping Buffer	25mM Glycine (pH2.0) and 1% SDS (w/v) diluted to 1 litre using deionised H_2O

2. 11. Antibodies

Table 2-5: Antibodies Used for Immunofluorescence

Antibodies and staining used for fluorescence microscopy

Antibody	Dilution	Company
Goat anti-eIF3η	1:50 0.6% BSA - PBS	Santa cruz, Heidelberg, Germany
Mouse anti-TIA-1	1:100 0.6% BSA - PBS	Abcam, Cambridge, UK
DAPI (4′,6-Diamidino-2-phenyindole)	1µg/µl	Sigma-Aldrich
FITC labelled Rabbit-anti-Goat antibody	1:50 0.6% BSA - PBS	Dako, Cambridgeshire, UK
Alex fluor 594 labelled Donkey-anti-Mouse antibody	1:50 0.6% BSA - PBS	Invitrogen, Paisley, UK

Table 2-6: List of Antibodies Used for Western Blotting

Antibodies used for western blotting, with dilutions.

Antibody	Dilution Factor	Dilution Media	Company
Rabbit Anti-PERK	1:1000	5% BSA-TBS-T	Cell Signaling, Hertfordshire, UK
Rabbit Anti-Phospho-eIF2α (Ser51)	1:1000	5% BSA-TBS-T	Cell Signaling
Rabbit Anti-Total eIF2α	1:1000	5% BSA-TBS-T	Cell Signaling
Mouse Anti-HIF-1α	1:250	5% Milk powder-TBS-T	BD Bioscience, Oxford, UK
Rabbit Anti-β Actin	1:1000	5% Milk powder-TBS-T	Sigma
HRP-Anti Rabbit	1:3000	5% Milk powder-TBS-T	GE Healthcare, Buckinghamshire, UK
HRP-Anti Mouse	1:3000	5% Milk powder-TBS-T	GE Healthcare

2. 12. Immunofluorescence Microscopy and Confocal Microscopy

Prior to plating cells onto glass coverslips the glass coverslips were placed in 12 well plates and were washed with 1ml 100% ethanol. All ethanol was removed by washing three times in PBS. MCF7 cells ($1x10^5$) were then seeded onto the glass coverslips in 2ml complete DMEM. The cells were allowed to adhere to the glass coverslip by incubation at 37°C/10% CO_2 (v/v) for 16 hours. After treatment cells were washed three times with PBS. Cells were then fixed with 4% (w/v) paraformaldehyde / PBS (BDH Laboratory Supplies, Poole, UK). Fixation of cells was essential as fixation immobilises cells by cross-linking molecules within the cell, which enables the cells structure to be preserved. To fix the cells 4% (w/v) paraformaldehyde / PBS was added to the cells and incubated at room temperature for 15 minutes. To enable antibodies access to intracellular compartments the cells were then permeabilised with PBS-Triton X-100 (0.1% (v/v)). Triton-X100 is a non-ionic detergent that permeabilised the cell membrane without disrupting proteins

within the cell, this allowed the structures within the cell to remain intact. The cells were permeabilised by three times five minute washes using PBS-Triton X-100 (0.1% (v/v)) and a final five minute wash in PBS to remove any triton-X100. The cells were then blocked using 3% Bovine Serum Albumin (BSA) (w/v) diluted in complete DMEM, to prevent antibodies binding to non-specific antigens. After removing the blocking solution, primary antibodies were diluted in 0.6% BSA (w/v)–PBS and incubated with the cells for 16 hours at 4^{o}C. Primary antibodies were removed and the cells were washed three times with PBS to remove any non-specifically bound antibody. Fluorescent labelled secondary antibodies were diluted in 0.6% BSA (w/v)–PBS and incubated with the cells for one hour at room temperature in the dark to prevent bleaching of the fluorescent label. After incubating for one hour DAPI (4′,6-Diamidino-2-phenyindole) (Sigma) was added (1µg/µl) and incubated in the dark for 10 minutes. DAPI is a fluorescent nuclear stain that intercalates into double stranded DNA. After incubation with nuclear stain and the secondary antibodies the cells were washed twice in PBS to remove any non-specifically bound antibody/excess DAPI stain. The cells were then washed once in deionised water before mounting the glass coverslips onto microscope slides. The glass coverslips were fixed onto microscope slides using fluorescence mounting media (Dako, Cambridgeshire, UK) and allowed to set for 16 hours at 4^{o}C in the dark. Cells were imaged using the Olympus immunofluorescence microscope and images were captured using the Olympus 1X81 camera (Olympus, Essex, UK). For confocal immunofluorescence microscopy the Leica microscope was used with the LAS AF software.

2. 13. Western Blotting

2. 13. 1. Cell Harvest

After treatment, cells were washed twice with ice cold PBS and scraped in 1ml ice cold PBS before cell pellets were collected by centrifugation at 4,000rpm (1,520 g) on a bench top centrifuge for five minutes. Cells were then lysed using RIPA

buffer and incubated on ice for 15 minutes. The RIPA buffer was supplemented with protease and phosphatase inhibitors (Sigma) to ensure that protein integrity and their phosphorylation status was maintained. After incubation on ice for 15minutes proteins were isolated from cell debris by centrifugation at 13,000 rpm (16,100 g) on a bench top centrifuge for five minutes.

2. 13. 2. Calculating Protein Concentration and Gel Electrophoresis

Protein concentration was determined using the BioRad Protein Assay (BioRad, Hertfordshire, UK). The BioRad protein assay contains coomassie brilliant blue G-250 dye that will bind to proteins, particularly on basic and aromatic amino acid residues, resulting in a colour change from green / red to blue. The colour change is proportional the concentration of protein present and can be measured on a 96 well plate reader by the absorbance of light at a wavelength of 595nm. To carry out protein concentration quantification a standard curve using BSA was used. The BSA standard curve concentrations used were 0, 0.2, 0.4, 0.6, 0.8 and 1µg/µl. 5µl of BSA was added to 250µl BioRad protein assay reagent (1x concentration) in a clear 96 well plate alongside 1µl of each sample in 250µl BioRad protein assay reagent (1x concentration). The colour change was detected on the Varioskan Flash plate reader, at 595nm (ThermoScientific). The protein concentration for each sample was then determined from the standard curve. An equal concentration of each sample was transferred into an eppendorf along with loading dye (Cell Signaling) that contained Dithiothreitol (DTT). The protein samples plus loading dye were heated to 95^{o}C for two minutes to denature proteins and to reduce protein–protein interactions. Boiling reduces protein interactions to enable proteins to migrate through a polyacrylamide gel according to their Stokes radius rather than their conformational shape. To separate proteins polyacrylamide SDS gel electrophoresis was carried out. Polyacrylamide SDS gels were made as described in Molecular Cloning a Laboratory Manual (Sambrook et al., 1989). Separating gels containing 6, 10 or 12% acrylamide were made prior to pouring the stacking gel on top with a 10 or 15 well comb inserted into the stacking gel to generate wells for the protein to be loaded into.

Protein was loaded onto a polyacrylamide gel and electrophoresis was carried out in running buffer (Table 2-4) at 100V for 1 hour. Proteins separate according to their Stokes radius by electrophoresis due to the presence of SDS. SDS, a negatively charged compound, binds to proteins resulting in all proteins being negatively charged therefore enabled proteins to migrate towards the positive electrode. The proteins passed through the polyacrylamide gel according to their Strokes radius such that smaller proteins move more easily through the gel compared to larger proteins, resulting in a resolution of larger proteins at the top of the gel and smaller proteins at the bottom of the gel. An approximation of the size of a protein was determined by running samples alongside a protein ladder. The protein ladder contains multiple proteins of known sizes that have been labelled with dye for visualisation.

Separated proteins were then transferred onto nitrocellulose membrane (Whatman Protran, GE healthcare) by wet transfer in transfer buffer (Table 3) at 100V for 1 hour. Protein transfer required the gel to be sandwiched between nitrocellulose membrane, filter paper and sponges as demonstrated in Figure 2-1. The sandwich was then placed in transfer buffer that enabled an electrical current to be generated that resulted in the proteins moving from the gel towards the nitrocellulose, which was closer to the positive electrode. After 1 hour transfer was stopped to prevent the proteins moving through the nitrocellulose onto the filter paper.

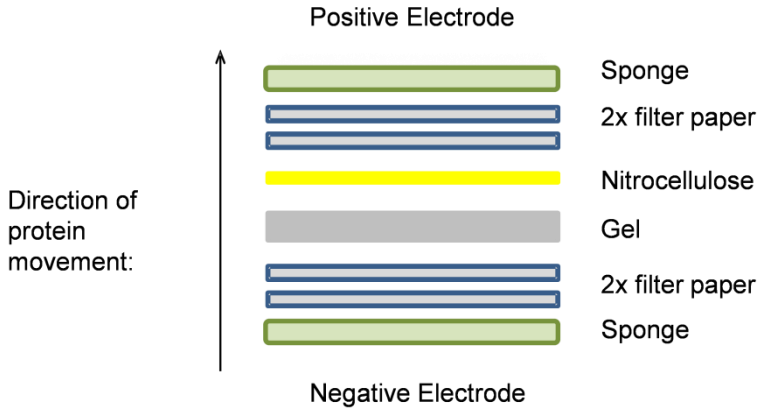

Figure 2-1: Protein Transfer Set Up

Transfer of proteins from the polyacrylamide gel onto nitrocellulose paper was carried out pressing the above components together in the order shown.

2. 13. 3. Antibody Incubation and Visualisation

The membrane was then blocked using 5% (w/v) milk powder–TBS-T and incubated at room temperature for one hour. Primary antibodies were added to the nitrocellulose blot diluted as described in Table 2-6. Nitrocellulose blots were incubated with the primary antibodies for 16 hours at 4^{o}C. Nitrocellulose blots were washed twice (five minutes) with TBS-T before the secondary antibodies were added and diluted as described in Table 2-6 and incubated for one hour at room temperature. After washing twice in TBS-T SuperSignal West Pico Chemiluminescent Substrate (Thermo Scientific) was added as described by the manufacturers protocol. The supersignal reagent contains an enhanced chemiluminescent HRP (horseradish peroxidase) substrate that maintained and enhanced the light emitted from the reaction of luminol in hydrogen peroxide with HRP. The blot was imaged using the UVP ChemiDoc – It Imaging System with the BioChemi HR Camera P/N 97-0155-02, 230V ~ 50Hz (UVP, Cambridge, UK).

2. 13. 4. Stripping and Re-Probing Nitrocellulose Membranes

After probing a nitrocellulose membrane for a phospho-protein the membrane was stripped using stripping buffer (Table 3) to remove the primary and secondary antibodies to allow the total protein to be probed for using anti-total primary antibodies. To strip the primary and secondary antibodies the nitrocellulose was incubated with stripping buffer for three minutes at room temperature prior to washing five times with TBS-T to remove all stripping buffer and also to return the membrane to pH7.6. The nitrocellulose membrane was then blocked in 5% (w/v) milk powder – TBS-T for one hour at room temperature before primary antibodies were added and incubated as previously described.

Molecular Biology Techniques

2. 14. Molecular Biology Materials

Table 2-7: Materials List for Molecular Biology

Reagent	Component
Polysome Gradient Buffer	30mM Tris-HCl (pH7.5), 100mM NaCl, 10mM $MgCl_2$
TAE Buffer (50x)	2M Tris Base, 17.5% (v/v) Glacial Acetic Acid, 100ml 0.5M EDTA (pH8.0), made up to 1 litre with deionised H_2O
0.5M EDTA (pH8.0)	186.1g disodium ethylenediamine tetra acetate dissolved in 1 litre deionised H_2O with the pH adjusted to pH8.0

All RNA techniques were carried out in an RNase free environment. All surfaces, centrifuges and pipettes were treated with RNase Zap (Invitrogen). DNase/RNase free microfuge tubes with used along with filter tips to prevent any degradation of RNA.

2. 15. Polysome Analysis

The cytoplasmic polysome cell lysates stored at -80^{o}C (section 2. 9.) were allowed to thaw on ice before the sample was layered onto a 20-50% continuous sucrose gradient. The 20-50% continuous sucrose gradient was made using 20, 26, 32, 38, 44 and 50% (w/v) sucrose–polysome gradient buffer solutions which were 0.22µm filter sterilised. 1.5ml of each sucrose mixture, starting with the highest percentage to the lowest percentage was layered and snap frozen into a Beckman centrifuge tube. Continuous gradients were formed as the gradients thawed at 4^{o}C

for 16 hours prior to loading the sample on top. After carefully layering the sample on top of the gradient the ribosomes were fractionated by centrifugation at 37,000rpm (234,745 g) in the Beckman Ultra Centrifuge, using the SW41 swing rotor and buckets at 4^{o}C for two and a half hours without braking.

The gradients were then pumped upwards using 60% sucrose containing 0.1mg/ml phenol red (Sigma) for visualisation. To pump the 60% sucrose solution into the bottom of the sucrose gradient a needle was inserted through the gradient so that the 60% sucrose was pumped (using the Gilson Minipuls 3, Mandel) into the bottom of the Beckman centrifuge tube. The pumping of the 60% sucrose displaced the lower density sucrose solutions upwards. The absorbance was continuously recorded at 254nm by the Brandel Optical unit type 11 spectrometer (Teledyne Isco Inc., Lincoln, USA) that enabled ribosome profiles to be generated on the tracer (Teledyne Isco UA-6, UV/ VIS Detector). The absorbance readings were also captured digitally using the Dataq DI-149 acquisition kit with WinDaq software (Dataq Instruments, Cheshire, UK). After passing through the UV spectrometer the samples were fractionated by collecting each fraction for 45s in an RNase free microfuge tube. 30µl 20% (w/v) SDS and 0.25µg/µl carrier tRNA from baker's yeast (Sigma) was added to each fraction to precipitate the mRNA to aid RNA extraction.

2. 16. RNA Extraction from Polysome Fractions

RNA was extracted from the collected fractions by firstly removing all protein by incubating each fraction with 100µg Proteinase K (Promega) for two hours at 37^{o}C. RNA was then extracted using phenol/chloroform (1:1 ratio). Phenol/chloroform was added to the samples and mixed thoroughly (vortex) to create an emulsion. The RNA was separated from any proteins and DNA by centrifugation at 12,000rpm (13,700 g) for 10 minutes at 4^{o}C in a bench top centrifuge. Centrifugation separated proteins into the organic phase while the RNA collected in the aqueous phase. RNA was present in the aqueous phase because negatively charged RNA interacts with polar water in the aqueous phase, whereas RNA did not interact with the organic

phase as the organic phase contained non-polar phenol. Phenol was also involved in denaturing proteins and collecting proteins into the organic phase. Phenol caused proteins to undergo a conformational change so that the hydrophobic (non-polar) amino acids flip out to interact with phenol causing denaturation and sequestration of proteins into the organic phase.

The aqueous phase was removed and placed in a new microfuge tube and the RNA was cleaned up by adding chloroform and centrifuged again to ensure any contaminating DNA and protein was removed from the RNA. The aqueous phase was transferred into a new microfuge tube, isopropanol was added and to aid the precipitation of the RNA the sample was chilled to -20^{o}C for 16 hours. RNA was pelleted by centrifugation at 12,000rpm (13,700 g) for 30 minutes at 4^{o}C and all isopropanol was removed. The RNA pellet was washed in 80% (v/v) ethanol and samples were centrifuged again at 12,000rpm (13,700 g) for 30 minutes at 4^{o}C. All ethanol was removed and RNA pellets were allowed to air dry on the bench for about 10 minutes. RNA was re-dissolved in 30µl RNase-free H_2O before quantified on the NanoDrop (ThermoScientific).

2. 17. First Strand Complementary DNA Synthesis

Complementary DNA was synthesised from the RNA collected using 1µg of RNA diluted in RNase-free H_2O to a total volume of 14µl. 1µl of oligo-dT was added to the samples and heated to 70^{o}C for five minutes to enable the oligo-dT primer to bind to the polyA tail. The mixture was cooled to 4^{o}C before the cDNA synthesis master mix (5µl MMLV Buffer (Promega), 1.25µl 10mM dNTPs, 0.625µl RNasin ribonuclease inhibitor (Promega), 1µl MMLV polymerase (Promega), 2.125µl H_2O) was added. The mixture was heated to 42^{o}C for 60 minutes to generate cDNA and the mixture was then heated to 95^{o}C to inactivate the enzyme before chilling to 4^{o}C as described in Figure 2-2. The cDNA was diluted into a total of 100µl with nuclease-free H_2O and stored at -20^{o}C.

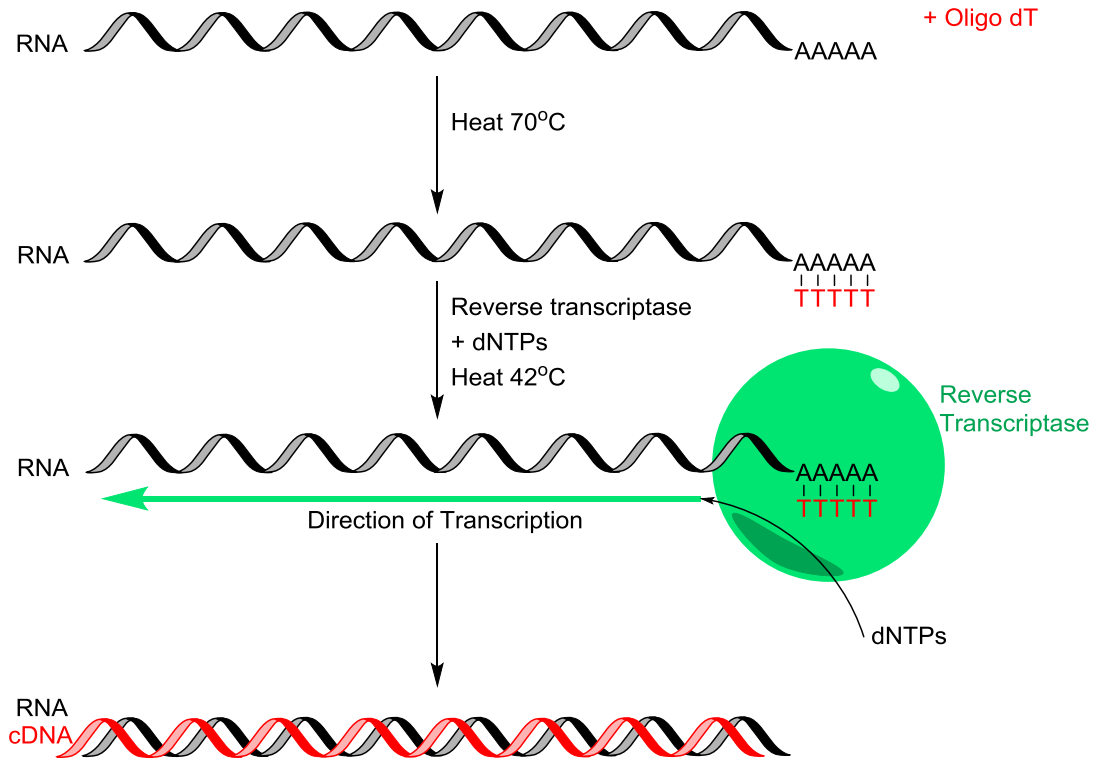

Figure 2-2: First Strand cDNA Synthesis

DNA complementary to mRNA was generated initially by binding the oligo dT primer to the polyA tail, heating to 70°C ensured non-specific binding. Addition of reverse transcriptase and dNTP's enabled DNA to be synthesised that was complementary to the mRNA sequence, heating to 42°C was required for optimal reverse transcriptase activity. The resulting product was heated to 95°C to inactive the enzyme. Illustration prepared in ChemBioDraw Ultra version 13.0.

2. 18. Quantitative Polymerase Chain Reaction

Quantitative polymerase chain reaction (qPCR) was carried out using TaqMan primers (Applied Bioscience, Paisley, UK). TaqMan qPCR was used as the primers and probes, specific for the gene of interest, provided accurate quantification of the cDNA present. The TaqMan primers contained forward and reverse primers for the gene of interest along with a probe that contained a fluorophore and a quencher. In the initial step of the PCR the cDNA was denatured by heating to 95^{o}C, this allowed the primers and the probe access to the cDNA, the temperature was reduced to 60^{o}C for annealing and extension of the primer. Extension of the primer in the 5'-3' direction resulted in the polymerase meeting the 5'end of the probe (Figure 2-3) and the polymerase degraded the probe in order to continue to extend the primer. The degradation of the probe resulted in the fluorophore moving away from the quencher, resulting in fluorescence (Figure 2-3). While the fluorophore and quencher were attached to the probe, no fluorescence was detected because fluorescence resonance energy transfer (FRET) occurred. FRET is the energy transfer between two molecules; the fluorophore becomes excited at a particular wavelength resulting in production of light at a different wavelength, this is normally seen as fluorescence. However in close proximity to a quencher the fluorescence wavelength emitted is absorbed by the quencher, which will produce a different wavelength. This absorbance of fluorescence by the quencher is known as FRET. Therefore only when the probe was degraded by amplification of the target gene was fluorescence detected. As the primers and the probe were specific for the gene of interest the fluorescence produced was directly proportional to the concentration of the cDNA present.

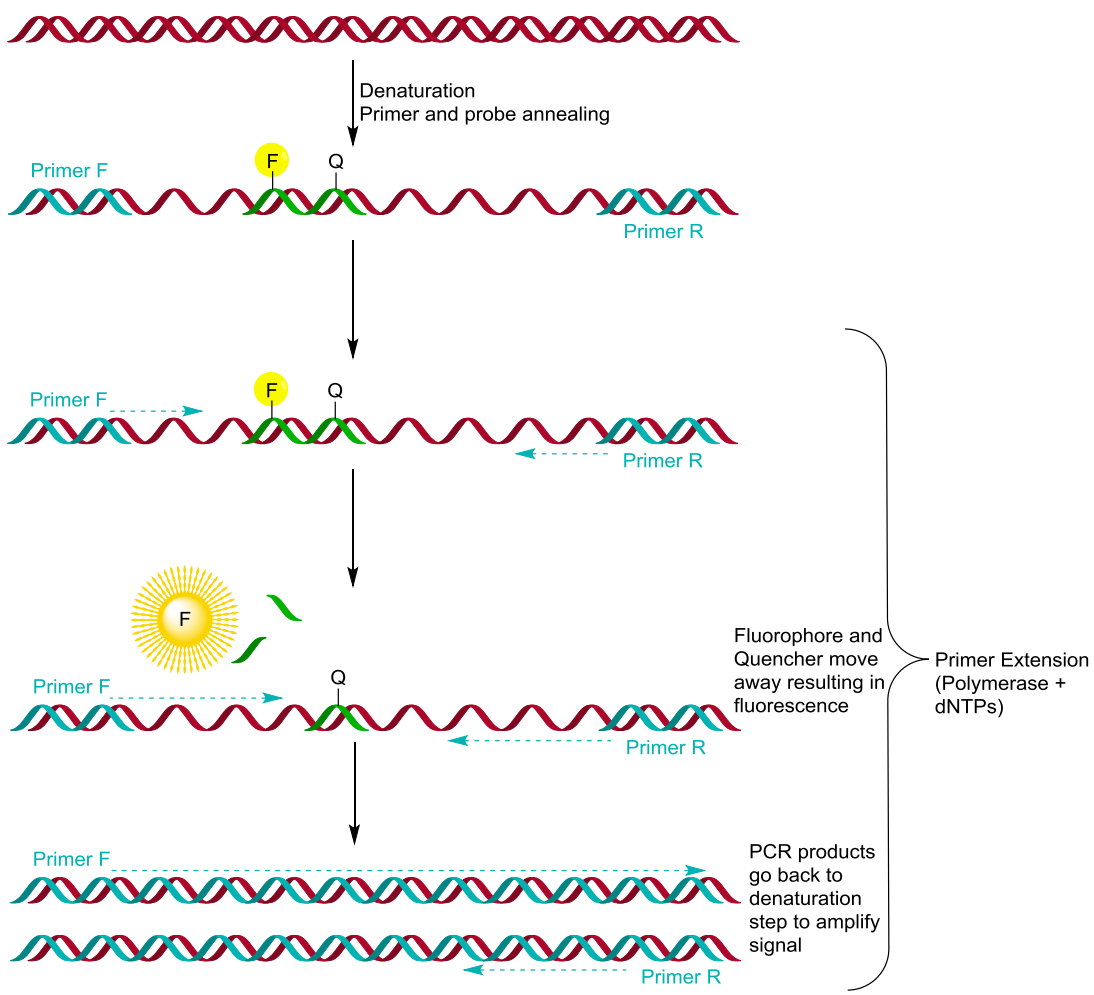

Figure 2-3: TaqMan Quantitative PCR Method

Schematic representation of qPCR using TaqMan primer and probes, where F indicates the fluorophore and Q represents the quencher. Illustration prepared in ChemBioDraw Ultra version 13.0.

The qPCR reaction used 5µl of cDNA, 1µl TaqMan primer/probe and 10µl TaqMan Universal mix (containing polymerase and dNTP's) in a 96 well plate. Once all reagents were added the plate had a clear lid applied and was briefly centrifuged to collect the reaction mixture at the bottom of the wells to ensure equal contact to the heating element in the qPCR thermo cycler (7500 Real-Time PCR System, Applied BioSystems). Each sample was carried out in duplicate alongside a standard curve that was also carried out in duplicate. A standard curve was carried out for each gene of interest and the standard curve was generated from total cDNA from untreated MCF7 cells. Once the total cDNA had been synthesised the concentration was quantified on the NanoDrop (ThermoScientific) and serial dilutions were carried out to generate a standard curve of the following concentrations; 10, 5, 1, 0.5, 0.1ng/µl. The qPCR reaction thermo-cycling and fluorescence detection was carried out in the Applied BioSystems Real-Time PCR thermocycler machine. The Applied BioSystems software (version 2.01) produced Ct values, which are the cycle threshold values; the Ct value was the number of cycles of the PCR that the sample had to go through before the fluorescence produced was above background. Therefore the higher the Ct value the more PCR reactions occurred indicating that the gene of interest was of low abundance, on the other hand low Ct values indicated high cDNA abundance. Once the Ct values for each sample had been collected a standard curve was drawn that correlated the Ct value with a known DNA concentration. By using the standard curve the Ct values were used to calculate the average cDNA concentration present in each sample. Statistical Analysis was carried out using Prism 6 software.

2. 19. Rapid Amplification of cDNA Ends (RACE)

Amplification of the untranslated regions was carried out using the SMARTer RACE DNA Amplification kit (Clonetech, France). The protocol was carried out according to manufacturer's protocol; briefly first strand DNA synthesis was carried out using the provided primers, which allow the untranslated regions to be amplified, by following the protocol this generated RACE ready cDNA (Figure 2-4).

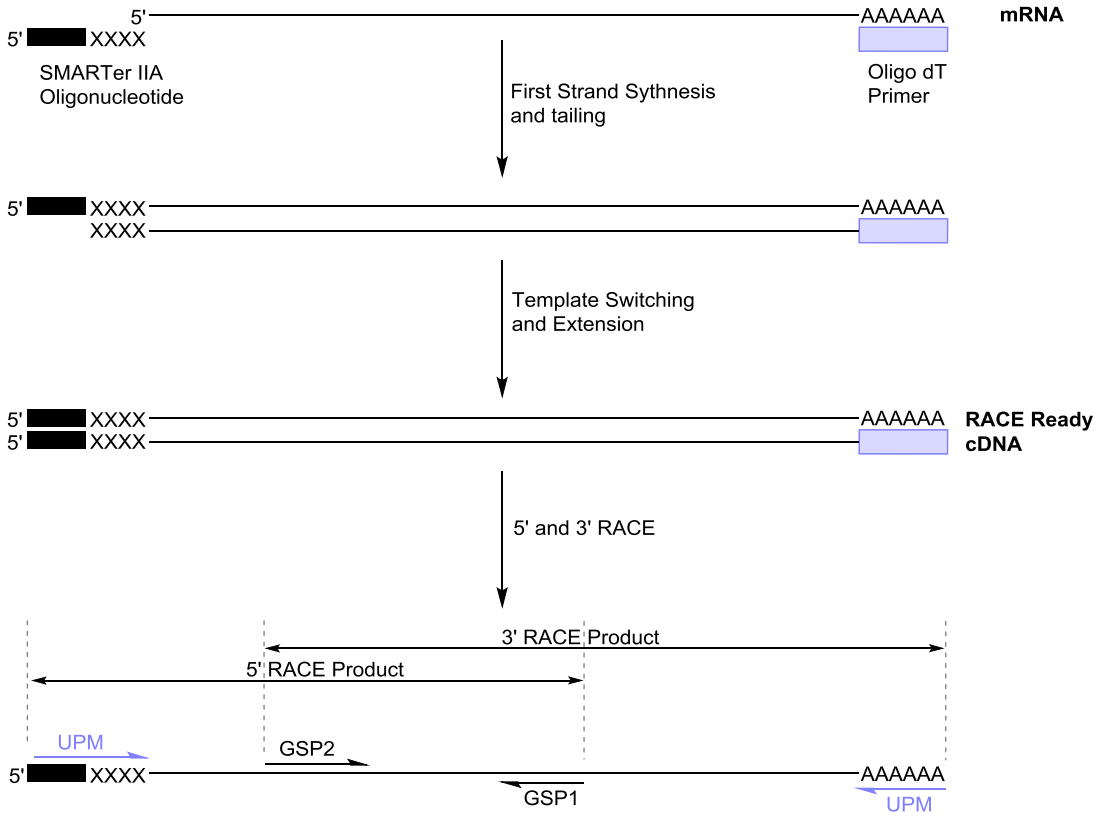

Figure 2-4: Rapid Amplication of cDNA Ends (RACE) Protocol

Polyadenylated mRNA was used as the starting material to generate RACE ready cDNA. cDNA was generated by reverse transcription using the supplied SMARTer II A oligonucleotide primer and the supplied oligo dT primer. The SMARTer II A oligonucleotide primer extended the mRNA at the 5'end to ensure the full length 5'UTR was included in the RACE protocol. The newly synthesised strand also required the addition of the extension before RACE ready cDNA was generated. 5'and 3'RACE was then carried out on the product, using supplied universal primer mix (UPM), which annealled to the 5' and 3' extensions, and gene specific primers 1 and 2 (GSP-1, -2). Illustration prepared in ChemBioDraw Ultra version 13.0.

Gene specific primers were designed for *HIF-1A* that met the SMARTer RACE DNA Amplification kit criteria. The primers were designed using the primer BLAST (Basic Local Alignment Searching Tool) internet search and two primers were designed for both the 3'- and the 5'RACE. The primer sequences are in Table 2-8 and the position of binding onto HIF-1α is illustrated in Figure 2-5.

Table 2-8: Primer Sequences

Primer Name	Sequence (5'-3')	Technical Data
HIF 5'RACE 1787R	TGGCTTTGGCGTTTCAGCGGTG GGT	Length = 25 T_m = 80.8°C GC = 60%
HIF 5'RACE 1615R	GCGGCTGGGGCCAGCAAAGTT AAAGCA	Length = 27 T_m = 80.6°C GC = 59.2%
HIF 3'RACE 2618F	ACAGCAGCCAGACGATCATGC AGCT	Length = 25 T_m = 75.7°C GC = 56%
HIF 3'RACE 2397F	CGGACAGCCTCACCAAACAGA GCAGG	Length = 26 T_m = 77.6°C GC = 61.5%

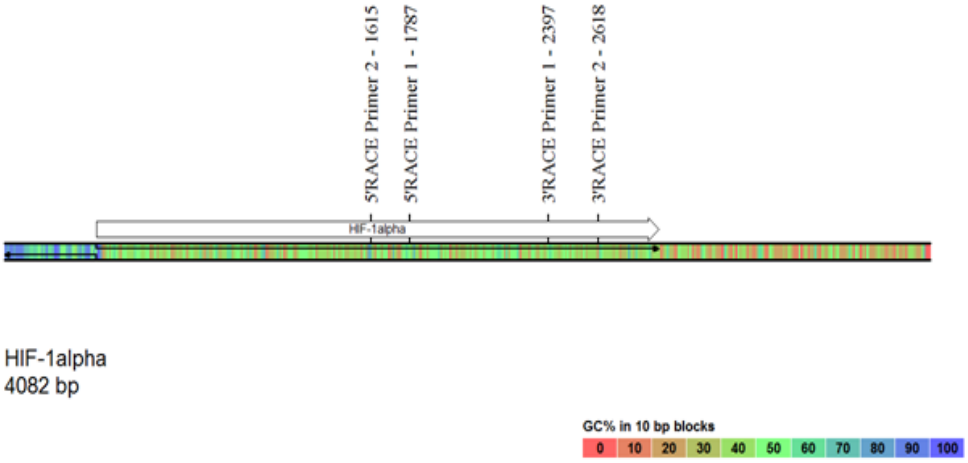

Figure 2-5: Primer Binding Sites on *HIF-1A*

RACE primer binding sites on the *HIF-1A* sequence, diagram produced using pDRAW32.

5'RACE was carried out on RACE ready cDNA from MCF7 cells previously incubated in normoxic or hypoxic conditions for five hours. The 5'RACE PCR used the HIF 5'RACE 1787R primer with the universal primer mix provided in the kit, this HIF-1α primer was used as this would produce the longest sequence that could be verified as being HIF-1α by nested PCR.

The 5'RACE PCR was carried out using the touchdown PCR approach with the following thermal cycling conditions:

Initial denaturation 98°C for 30 seconds

- 98°C for 10 seconds
- 72°C for 1 minute

5 cycles

- 98°C for 10 seconds
- 70°C for 30 seconds
- 72°C for 1 minute

5 cycles

- 98°C for 10 seconds
- 68°C for 30 seconds
- 72°C for 1 minute

25 cycles

72°C for 10 minutes

10°C Hold

This touch down approach initially used a high annealing temperature to enrich for HIF-1α specifically, then to multiply the enriched product a lower annealing temperature was used to ensure high product yield.

2. 20. Agarose Gel Electrophoresis

To visualise DNA products from PCR reactions 10µl of the PCR product was loaded onto a 0.8% (w/v) agarose gel (0.8g agarose (Sigma), 100ml (1x) TAE Buffer, 5µl Safeview (NBS Biologicals, Cambridgeshire, UK)). The gel was placed in a tank filled with (1x) TAE buffer and an electrical current was passed through the buffer so that the DNA would run to the positive electrode separating DNA molecules according to their length. The agarose gel electrophoresis was carried out at 120V for 45 minutes. DNA bands were visualised by placing the gel in UV (UVP Gel Doc-it, Cambridge, UK), the DNA was visualised as Safeview intercalated into the DNA and luminesced in the presence of UV.

2. 21. Ligation of PCR Products into Plasmids

PCR products were cleaned up using the NucleoSpin Extract II kit (Macherey-Nagel Leicestershire, UK) according to manufacturer's protocol. T4 DNA ligase (Promega) was used to ligate PCR product into plasmids, according to manufacturer's protocol. The ligated products were then transformed into JM109 *E.coli* cells. Bacterial cells were thawed on ice and 2µl of ligation products were added to the bacterial cells. Cells were incubated on ice for 20 minutes before heat shock at 42^{o}C for 30 seconds was carried out, the bacterial cells were returned immediately to ice for a further teo minutes. Heat shock was important to enable the plasmid to enter the bacterial cell. The cells were allowed to grow for one hour at 37^{o}C by adding 150µl LB media. LB-ampicillin plates were also pre-warmed to 37^{o}C. After growth for one hour the bacterial cells were plated onto the LB-ampicillin plates and incubated at 37^{o}C for 16 hours. Bacterial cell colonies were selected and were picked using a pipette tip and were grown in 3ml LB-ampicillin media for 16 hours. Plasmid DNA was extracted from the bacterial cells using the Qiagen Spin Mini-Prep kit (Qiagen, Sussex, UK). This kit used SDS to lyse open the bacterial cell wall under alkaline conditions. This resulted in the denaturation and release of proteins, chromosomal DNA and plasmid DNA. An optimal time for

lysis was used (five minutes) to ensure release of plasmid DNA but not chromosomal DNA. The supplied wash buffers were then used to increase the salt concentration; as high salt denatures chromosomal DNA and proteins but not plasmid DNA. The plasmid DNA was then isolated from the remaining cell debris using the supplied spin columns that contained a membrane that only binds DNA in high salt concentrations. Plasmids were eluted from the membrane in low salt conditions (50µl 5mM TRIS/HCl pH 8.5 elution buffer).

2. 22. Restriction Digest

To confirm cloning products were the gene of interest restriction enzyme digestion was carried out. Promega restriction enzymes were used to digest 2µl plasmid DNA, according to manufacturer's protocol. The digestion was incubated at 37^{o}C for 90 minutes to ensure complete digestion. Products were visualised by agarose gel electrophoresis.

2. 23. DNA Sequencing

Plasmid DNA was sequenced by MWG Biotech Ltd (Covent Garden, London, UK) using the Value Read sequencing service. Sequences were aligned with those in the National Centre for Biotechnology Information Genbank database using the BLAST site (http://www.ncbi.nlm.nih.gov/blast/).

Chapter Three

Results – Effect of PEITC on mRNA Translation

3. Effect of PEITC on mRNA Translation

3. 1. Introduction

PEITC is known to have many anti-cancer activities although the mechanisms involved have not been fully elucidated. PEITC has previously been shown to inhibit angiogenesis, which is important for tumour development (Hanahan and Weinberg, 2011; Xiao and Singh, 2007). Decreased HIF-1α protein expression in response to PEITC treatment could inhibit angiogenesis and our group has shown that PEITC may inhibit mRNA translation to down regulate HIF-1α protein expression (Wang et al., 2009). The effects of PEITC on mRNA translation have been analysed before, but only limited research has been carried out to date. Hu et al showed that PEITC inhibited proliferation of colorectal cancer cells as well as increased the expression of 4E-BP1 (Hu et al., 2007). PEITC treatment prevented the phosphorylation of 4E-BP1 (Hu et al., 2007) therefore these data indicated that PEITC decreased cap-dependent translation. Wang et al showed that PEITC induced apoptosis in breast cancer cells and decreased the expression and activity of HIF-1α independently of changes in *HIF-1A* mRNA expression (Wang et al., 2009). Cavell et al showed that PEITC inhibited *HIF-1A* mRNA translation and the mTORC1 complex may be involved in the regulation of mRNA translation by PEITC (Cavell et al., 2012). However investigation is still required to determine whether PEITC specifically inhibits mRNA translation of only certain mRNA molecules or whether all mRNA translation is altered.

3. 2. Hypothesis and Aims

3. 2. 1. Hypothesis

PEITC will decrease translation of *HIF-1A* mRNA as well as decreasing translation in a global manner.

3. 2. 2. Aims

The aim of this chapter was to determine the effect PEITC had on translation in a global manner as well on specific mRNA molecules. Investigation into the effect of PEITC on translation in hypoxic conditions was also be carried out to provide further insight into the possible mechanisms utilised by PEITC to inhibit one hallmark of cancer progression, angiogenesis. These aims were investigated by:

- Analysing polysome profiles of MCF7 cells treated with PEITC
- Metabolic labelling experiments to verify PEITC-induced changes in polysome profiles
- Determining the levels of expressed HIF-1α and VEGF in response to PEITC treatment
- Determining whether PEITC altered translation of *HIF-1A* and *VEGF* mRNA
- Analysing the sequence of the 5'untranslated region of *HIF-1A* to determine whether there are any alterations in this region to enable translation of *HIF-1A* in hypoxic conditions and whether PEITC modulated them.

3. 3. Results

3. 3. 1. Analysing the Effect of PEITC by Metabolic Labelling

Experiments were performed using ^{35}S-Met/Cys incorporation to confirm that PEITC inhibited mRNA translation (Cavell et al., 2012). The control compound cycloheximide (CHX) was used as a positive control for inhibition of translation as CHX 'freezes' the ribosomes on the mRNA inhibiting translation. Treatment of MCF7 cells with PEITC (20µM) for 30 minutes significantly decreased metabolic labelling (Figure 3-1). Metabolic labelling of cells treated with PEITC was significantly reduced to 11% of the labelling in cells treated with DMSO. The extent of inhibition of translation was essentially identical to that induced by CHX (Figure 3-1). The remaining 11% residual ^{35}S may have occurred due to non-specific labelling or trapping in the equipment.

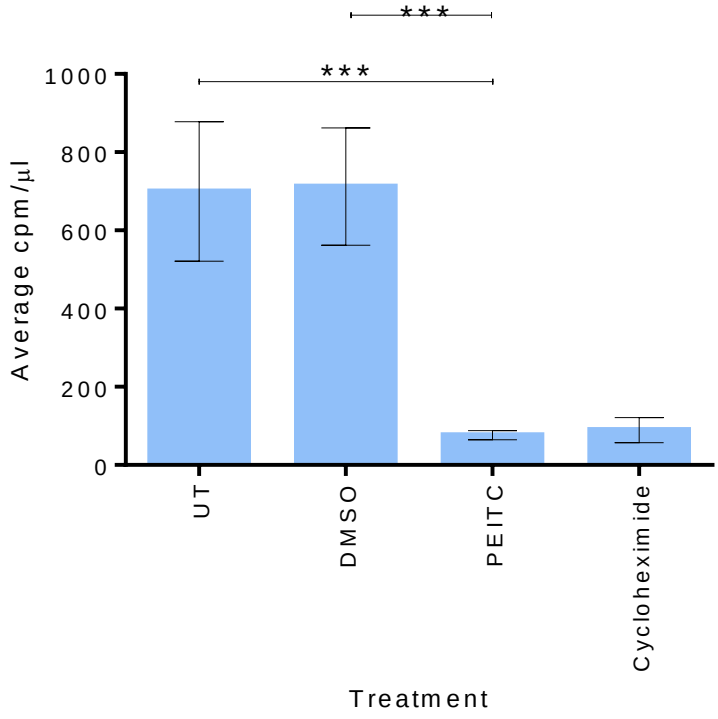

Figure 3-1: ^{35}S Incorporation in Response to PEITC

MCF7 cells were treated with 20µM PEITC, cycloheximide (10µg/ml), equivalent DMSO or untreated (UT) for three hours. Two hours prior to the end of the incubation time ^{35}S-TransLabel was added at a final activity of 10µCi/ml and incubated for two hours before collecting cell pellets. Translation was determined by TCA precipitation of proteins and ^{35}S incorporation was determined by scintillation counting. Bars represent the average incorporation and error bars represent the standard deviation from the mean, n=3. Statistically significant changes are indicated, ***≤0.005, one-way ANOVA, GraphPad Prism 6.

3. 3. 2. Effect of PEITC on mRNA Translation in MCF7 Cells

To investigate the effects of PEITC on mRNA translation, I initially focused on analysis of polysome profiles. In these analyses, cell lysates were prepared and placed on top of 20-50% continuous sucrose gradients. During ultracentrifugation different mRNA fractions separated according to density which was largely dependent on the number of ribosomes bound to the mRNA (Figure 3-2). Polysome profiling was selected as an alternative to ^{35}S-metabolic labelling as polysome profiling provides a more detailed view of any changes in translation and can be used to analyse both global and mRNA specific effects.

An illustrative polysome profile from MCF7 cells is shown in Figure 3-2. The densest fractions contain polysome associated RNAs which are considered to be actively translated since these RNAs are associated with multiple ribosomes. The 'shoulder' seen to the right of each peak represents the next 40S ribosomal subunit becoming associated with the mRNA before the full ribosome assembles (see section 1. 3. 2. for assembly of the complete ribosome). The sub-complexes of the complete ribosome can only be differentiated from each other when different density gradient conditions are employed. The less dense fractions comprise RNAs associated with individual components of the ribosome, the 40 and 60S subunits, followed by the 80S monosome. The polysome peaks increased with amplitude (on the y axis of the profile, measuring the absorbance of RNA at 254nm), indicating the number of mRNA molecules associated with multiple ribosomes increased.

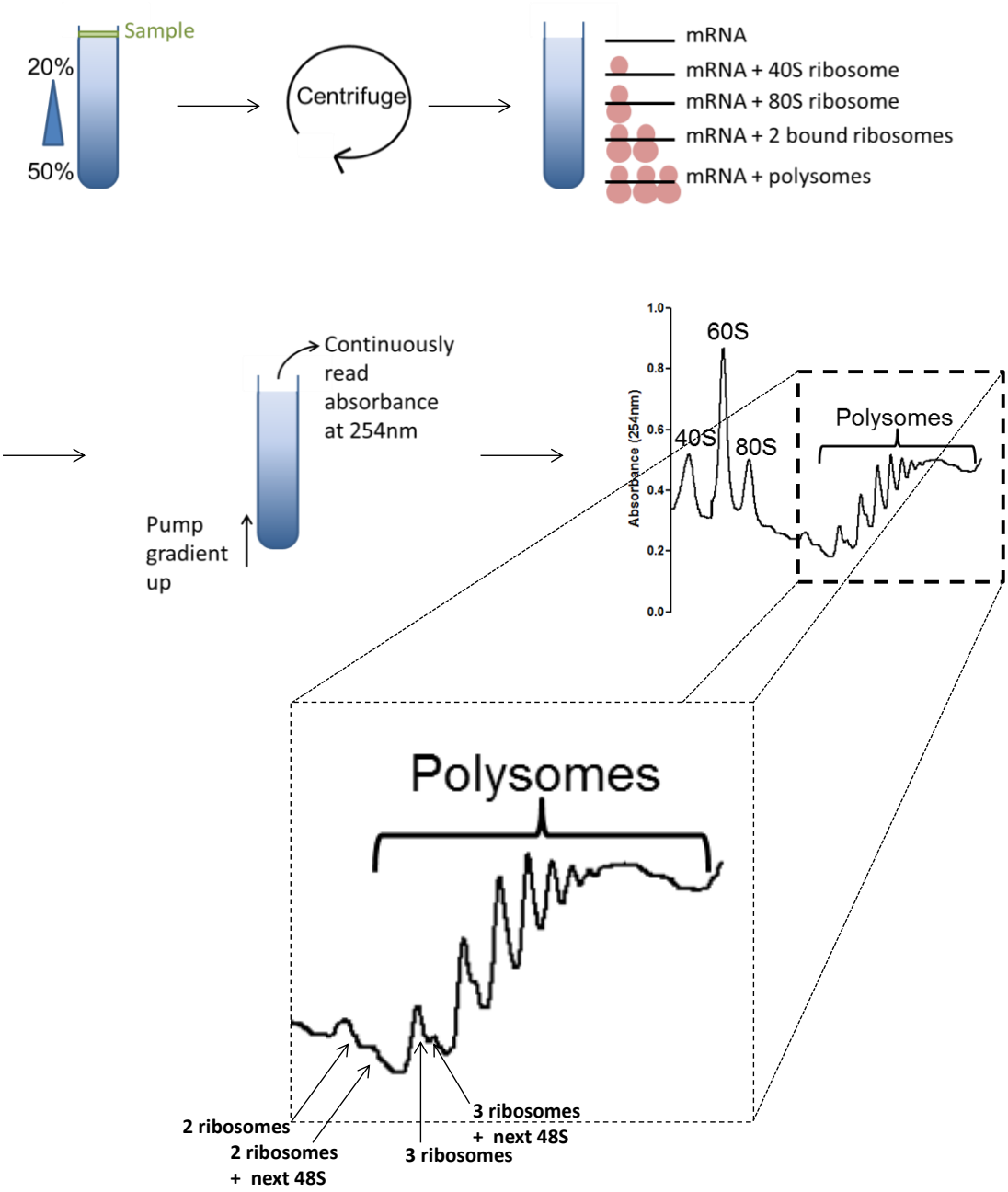

Figure 3-2: Polysome Profiling

Schematic representation of polysome profiling indicating how the mRNA molecules separate according to the density along the sucrose gradient. The peaks associated with each sub-complex form due to the number of partial or full ribosomes bound to the mRNA, with mRNA molecules bound by multiple ribosome, known as polysomes. Polysomes migrate to the higher percentage sucrose during centrifugation. The profile shown is from untreated MCF7 cells.

To analyse the effect of PEITC on mRNA translation MCF7 cells were treated with PEITC, DMSO (solvent control) or were left untreated for one hour. A concentration of 20µM PEITC was selected because PEITC at this concentration is known to have *in vitro* anti-cancer activity (Cavell et al., 2012) as well as be achievable *in vivo* (Cheung and Kong, 2010) . At 20µM PEITC has been shown to induce apoptosis as well as inhibit mTORC1 signalling, analysed by Annexin V/propidium iodide flow cytometry and immunoblottting, respectively (Cavell et al., 2012; Wang et al., 2009). Untreated MCF7 cells yielded typical polysome profiles for cells with active mRNA translation with relatively large numbers of polysomes (Figure 3-3). The polysome profile was not altered by DMSO. By contrast, PEITC treatment resulted in an almost complete loss of polysome peaks and an accumulation in the 80S peak (Figure 3-3). In untreated samples the percentage of total mRNA located in lower density fractions, monosomes or below, was 77% (Figure 3-3). Whereas after treatment with PEITC the percentage of mRNA located in the lower density fractions was 99.6% (Figure 3-3). The results demonstrated that PEITC caused a profound inhibition of global mRNA translation. The accumulation in the 80S peak indicated that translation was stalled at initiation of translation rather than a loss in the available pool of cytoplasmic mRNA. A loss in cytoplasmic mRNA would result in an accumulation in the 80S peak without loss of the polysome peaks (Gross and Kinzy, 2007), which was not seen with PEITC treatment. The accumulation in the 80S peak indicated that the ribosome had not progressed into elongation because progression would enable the start codon on the mRNA to be available for a second ribosome to form and polysome peaks would be formed, which were not seen.

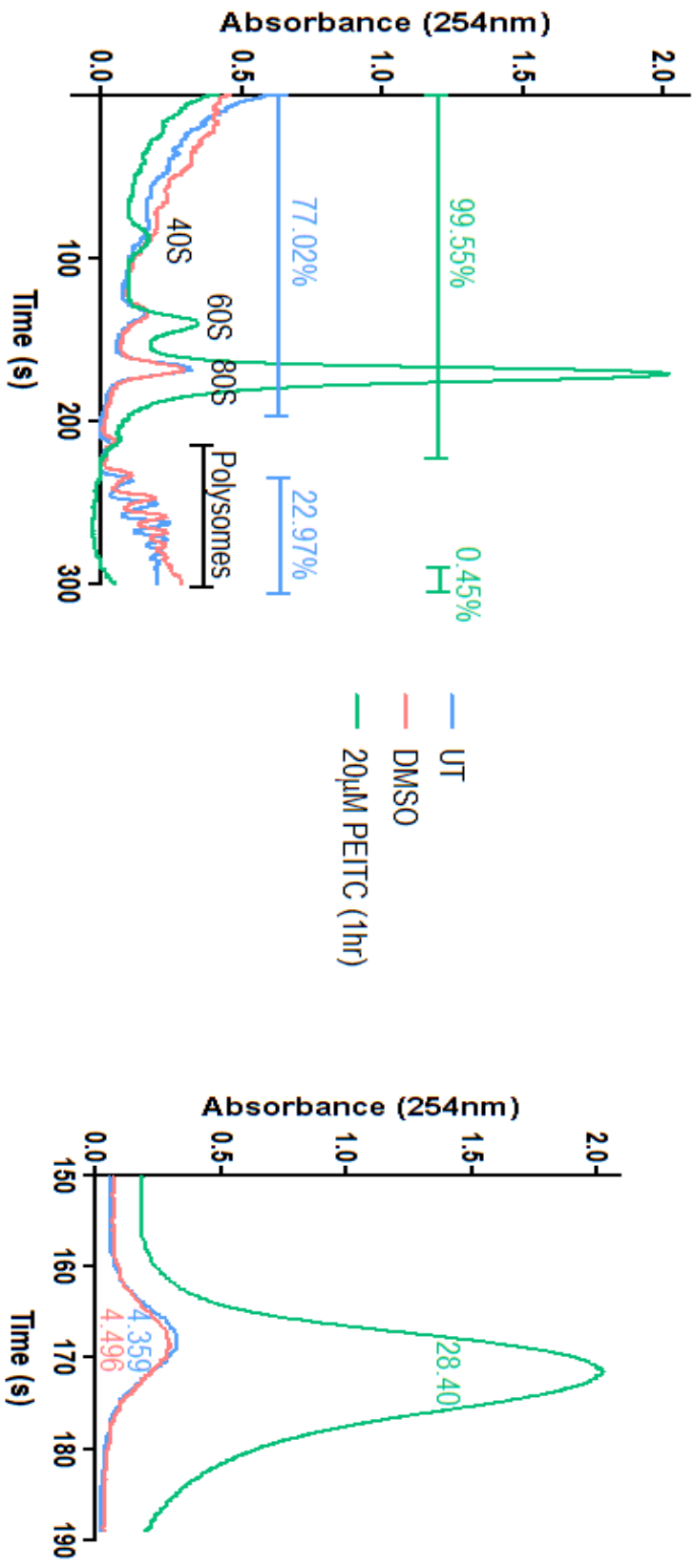

Figure 3-3: Polysome Profiles of MCF7 Cells Following Treatment with PEITC

MCF7 cells were untreated, treated with 20μM PEITC or equivalent DMSO for one hour prior to polysome profiling. (A) Complete polysome profiles with the 40S, 60S, 80S and polysome peaks identified. Percentages represent the area under the curve (prism). (B) Quantification of the area under the 80S peak, representative of three independent experiments.

3. 3. 3. Kinetics and Concentration Dependency of PEITC-Induced mRNA Translation Inhibition

Further experiments were performed to characterise the effect of PEITC on mRNA translation in more detail. MCF7 cells were treated with PEITC (20 µM) for various times (5 to 30 minutes) before polysome profiling to determine the kinetics of inhibition of mRNA translation. The accumulation of mRNA in the 80S peak occurred rapidly. Within five minutes of treatment with 20µM PEITC there was a slight decrease in the height of the polysome peaks and a marked reduction after 10 minutes. By 15, 20 and 30 minutes the polysome peaks were undetectable, similar to that seen after one hour (Figure 3-4 and Figure 3-3). The decrease in polysome amplitude was not merely a consequence of changing the axis range. After treatment with PEITC for 10 minutes the scale of the 80S peak is 0.4, whereas the scale of the 80S peak following PEITC treatment for 30 minutes was 1.5. In order to determine whether the polysome peaks were still present but undetectable due to a larger scale the y-axis was split in two and re-scaled so that the scale would be similar to DMSO treated cells (Figure 3-5). This analysis confirmed that the amplitude of the polysome peaks decreased after PEITC treatment when compared to the DMSO solvent control (Figure 3-5). This decrease in the amplitude along with an increase in the 80S amplitude indicated a block in initiation of translation that occurred rapidly within 10 minutes of treatment. Therefore PEITC rapidly inhibited translation in a time course too rapid to be due to changes in transcription.

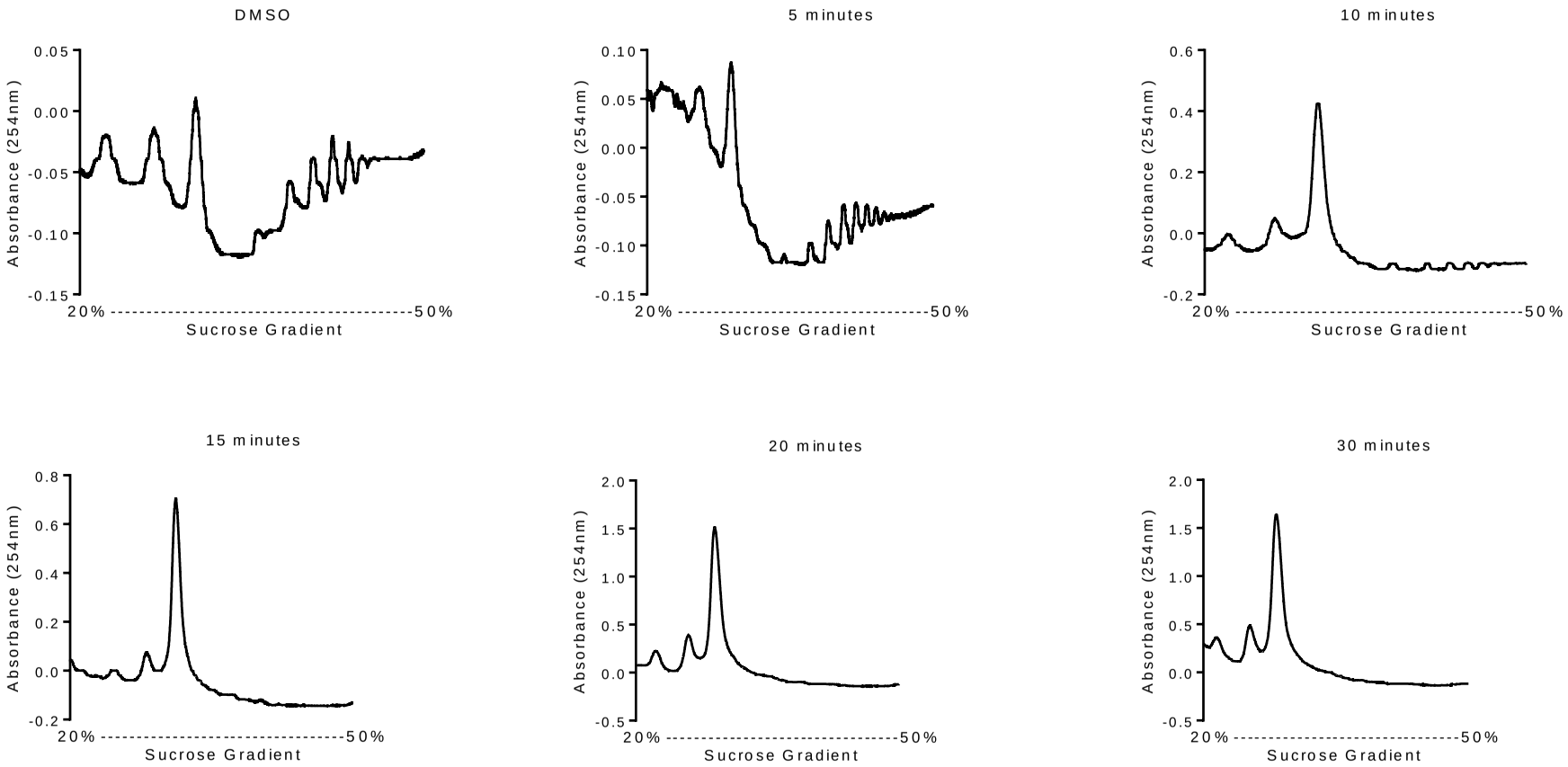

Figure 3-4: Polysome Profiles of MCF7 Cells Treated with PEITC for Differing Times

MCF7 cells were treated with 20μM PEITC, or equivalent DMSO for the indicated times prior to polysome profiling. Data presented are representative of three independent experiments.

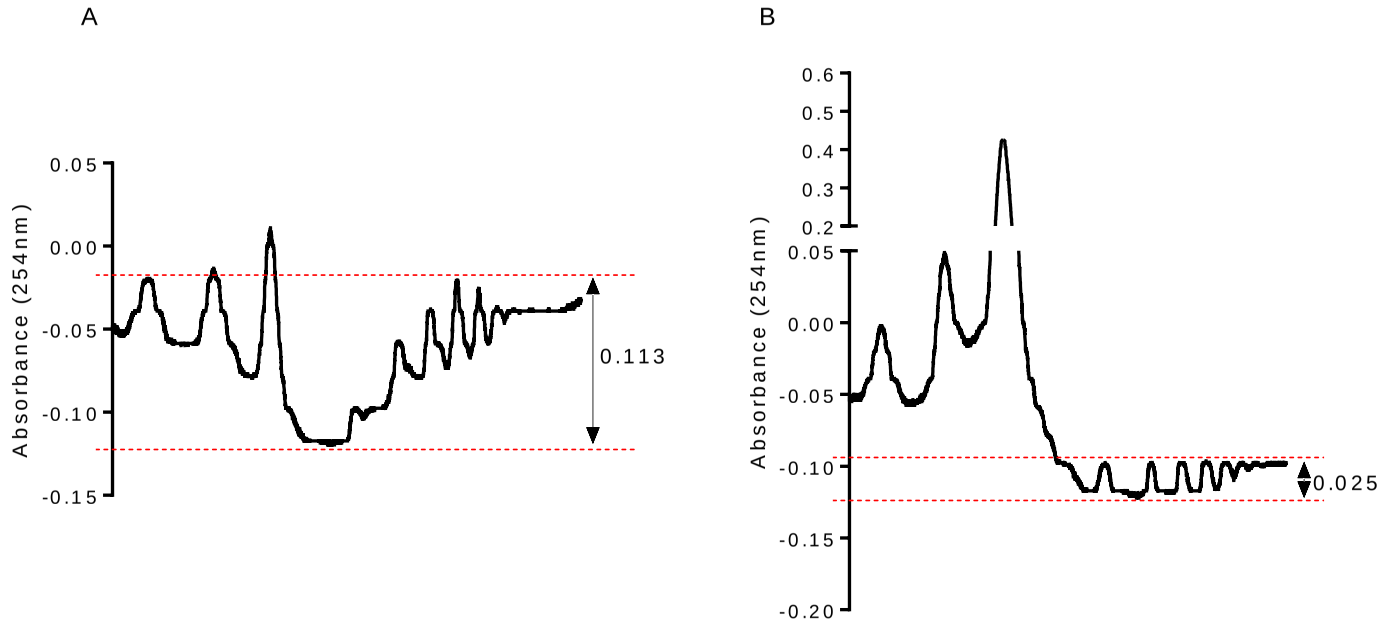

Figure 3-5: Comparison of Polysome Peak Amplitude in Response to PEITC Treatment

MCF7 cells were treated with the solvent control, DMSO, (A) or 20µM PEITC (B) for 10 minutes prior to polysome profiling. A multiple scale axis for absorbance was used for PEITC treated cells (B) for the polysome peaks to be compared to DMSO (A) on the same scale. Red dotted lines indicate the top and bottom of the polysome peak, from baseline to maximal and the amplitude change is indicated.

Concentration response experiments were also performed to determine the active concentration range for inhibition of mRNA translation induced by PEITC. A fixed time point of 30 minutes was selected for these experiments to enable any inhibition to be visualised by polysome profiling (Figure 3-6). The inhibitory effects of PEITC on mRNA translation were concentration dependent. Inhibition of mRNA translation was observed with 7.5μM PEITC, with maximal effects seen following treatment with 15μM PEITC, due to the almost complete loss of polysome peaks (Figure 3-6). These concentrations are in agreement with recently published data following *HIF-1A* mRNA translation by ^{35}S metabolic labelling experiments (Cavell et al., 2012). Therefore PEITC caused a rapid and concentration dependent inhibition of global mRNA translation.

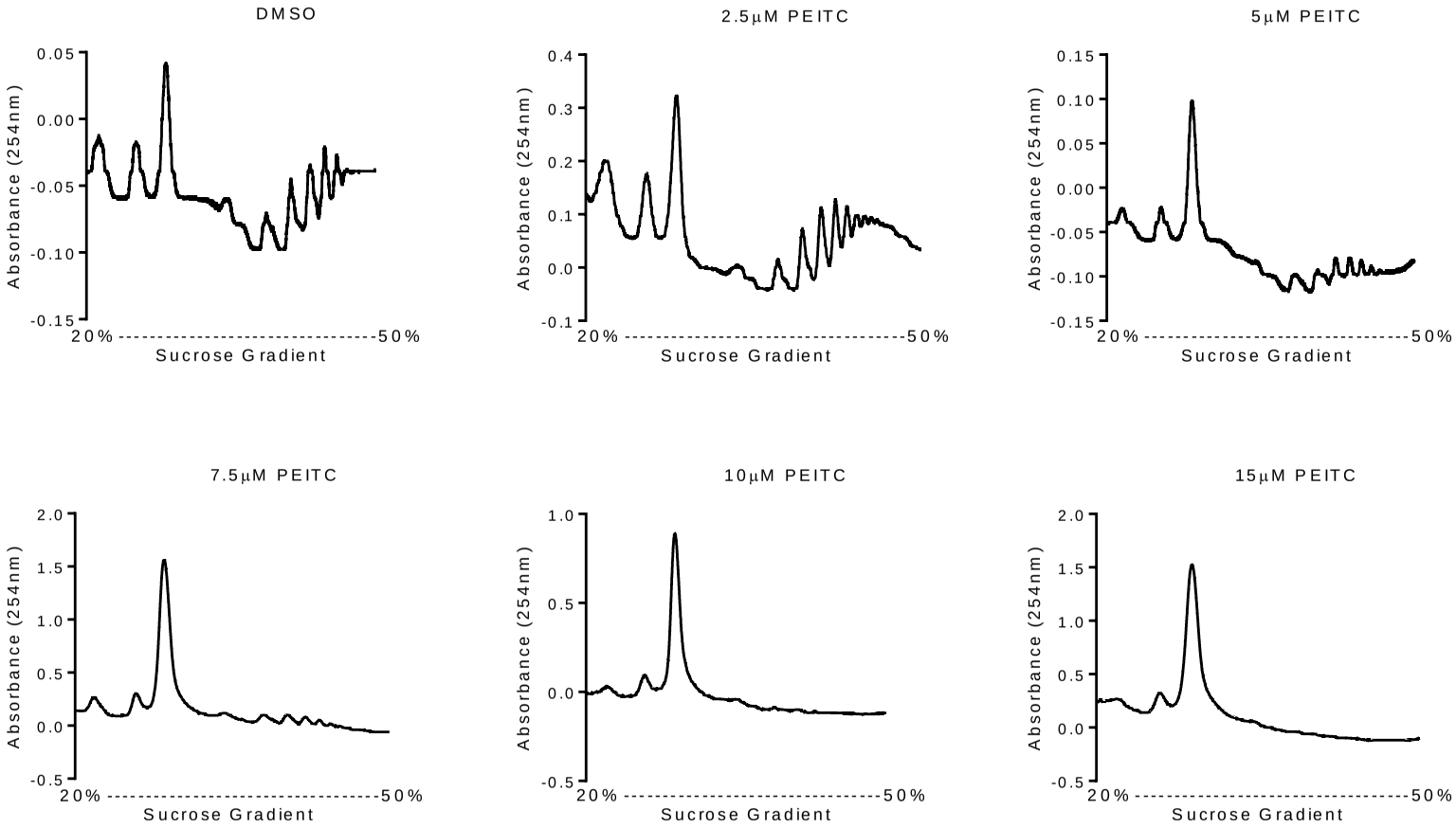

Figure 3-6: Concentration-Dependent Changes to Polysome Profiles in Response to PEITC Treatment

MCF7 cells were treated with 2.5, 5, 7.5, 10 or 15µM PEITC or equivalent DMSO (to the highest concentration) for 30 minutes prior to polysome profiling. Data presented are representative of three independent experiments.

3. 3. 4. Reversibility of PEITC-Induced Inhibition of mRNA Translation

Wash-out experiments were performed to determine if the translational inhibitory effects of PEITC were reversible. Cells were treated with PEITC (20µM), or equivalent DMSO for 30 minutes prior to polysome profiling or cells were treated with PEITC (20µM) for 30 minutes, washed with fresh complete DMEM and incubated in the absence of PEITC for a further one, two or three hours. Cells that were exposed to PEITC had a large accumulation in the 80S peak and almost no polysome peaks, compared to cells just treated with DMSO (Figure 3-7). In contrast, after three hours recovery there was partial recovery of polysome peaks. Therefore the effect of PEITC on mRNA translation was at least partially reversible following removal of the compound, which may be dependent on the ability of the cells to efflux PEITC into the extracellular environment (Figure 1-4).

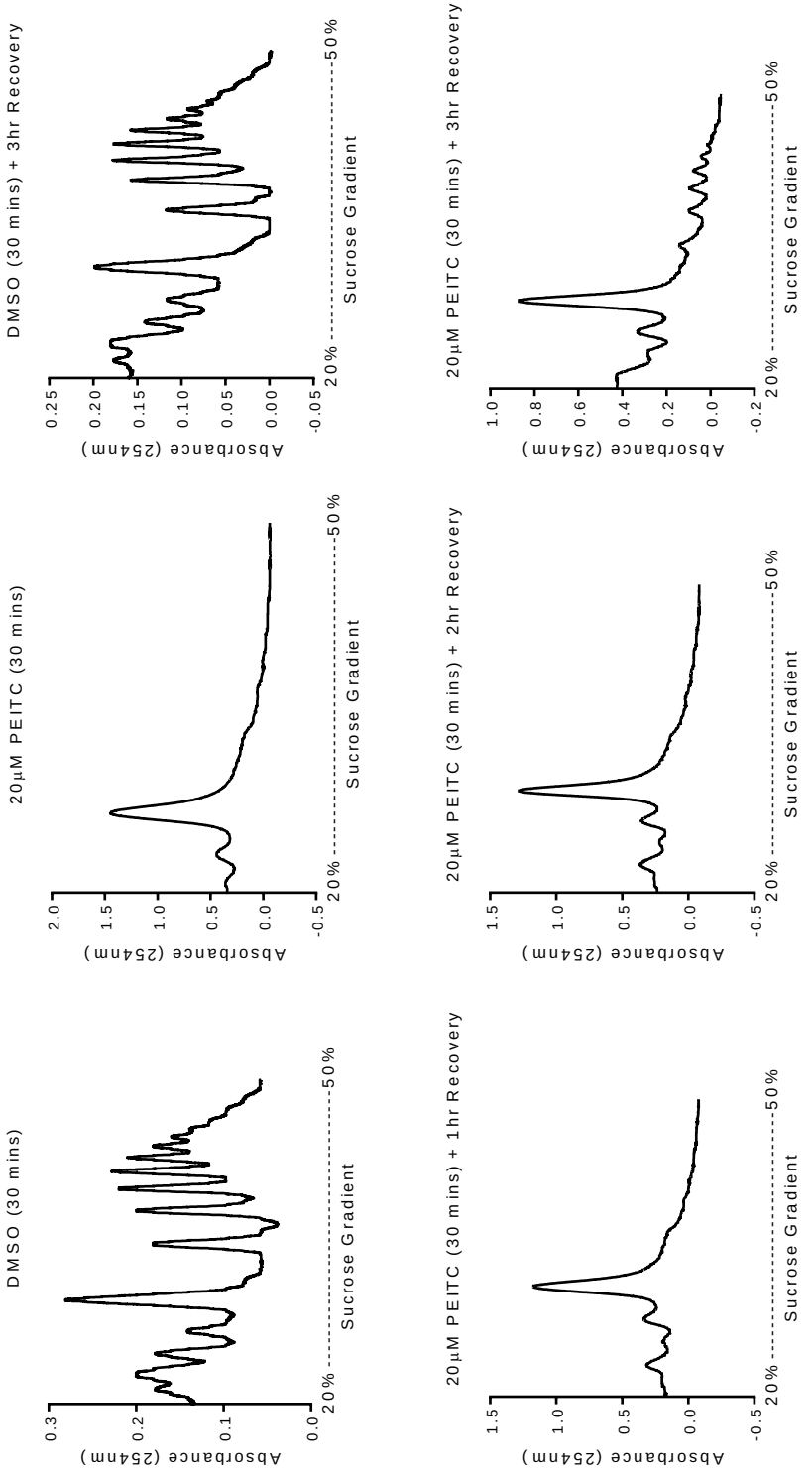

Figure 3-7: Effect of PEITC Removal on Polysome Profiles

MCF7 cells were treated with 20µM PEITC or equivalent DMSO for 30 minutes prior to washing cells with PBS and replacing with fresh complete DMEM. MCF7 cells were then incubated for one, two or three hours prior to polysome profiling. Data presented are representative of three independent experiments.

3. 3. 5. Effect of PEITC and Hypoxia

The initial studies demonstrated that PEITC inhibited global mRNA translation were performed in normoxia. However, PEITC has also been shown to interfere with hypoxia-induced pro-angiogenic responses, and the ability of PEITC to decrease hypoxia-induced HIF-1α protein expression has previously been linked to inhibition of *HIF1A* mRNA translation. Given the key role of hypoxia-induced changes in protein expression in promoting tumour growth, it was important to investigate the effects of PEITC on mRNA translation under hypoxic conditions.

I first investigated the effects of PEITC on expression of HIF1α protein. HIF-1α is important for promoting angiogenesis in hypoxic conditions and the expression/stabilisation of HIF-1α is highly dependent on oxygen levels (see Chapter 1. 2. 5.). Therefore the HIF-1α protein level in MCF7 cells was analysed following treatment with 20μM PEITC, equivalent DMSO (solvent control) or left untreated as a control. The experiment was performed using cells maintained in normoxic or hypoxic conditions for five hours before HIF-1α protein expression was analysed by immunoblotting. To model hypoxia, cells were maintained in 1% O_2, with physiological hypoxia known to be between 1-10% O_2 and pathological hypoxia being less than 1% (Hadjipanayi et al., 2010).

As expected in normoxic conditions (20% O_2) HIF-1α protein was very low or undetectable by immunoblotting (Figure 3-8A) and there was a significant increase in HIF-1α protein in cells incubated in hypoxic (1% O_2) conditions (Figure 3-8B). The hypoxic induction in HIF-1α expression was significantly inhibited by PEITC treatment, resulting in HIF-1α protein expression similar to that seen in normoxic conditions (Figure 3-8). In contrast neither hypoxia or PEITC treatment altered β-actin protein expression, used as a housekeeping control. Although actin has a longer protein half-life compared to HIF-1α therefore this result (Figure 3-8) indicated that PEITC did not alter the stability of actin over the five hour time course. In order to verify that PEITC inhibited the production of HIF-1α a radiolabelled (^{35}S) Co-immunoprecipiatation would give a more detailed view on HIF-1α protein levels, this was carried out in MCF7 and demonstrated that PEITC prevented the synthesis of HIF-1α (Cavell et al., 2012).

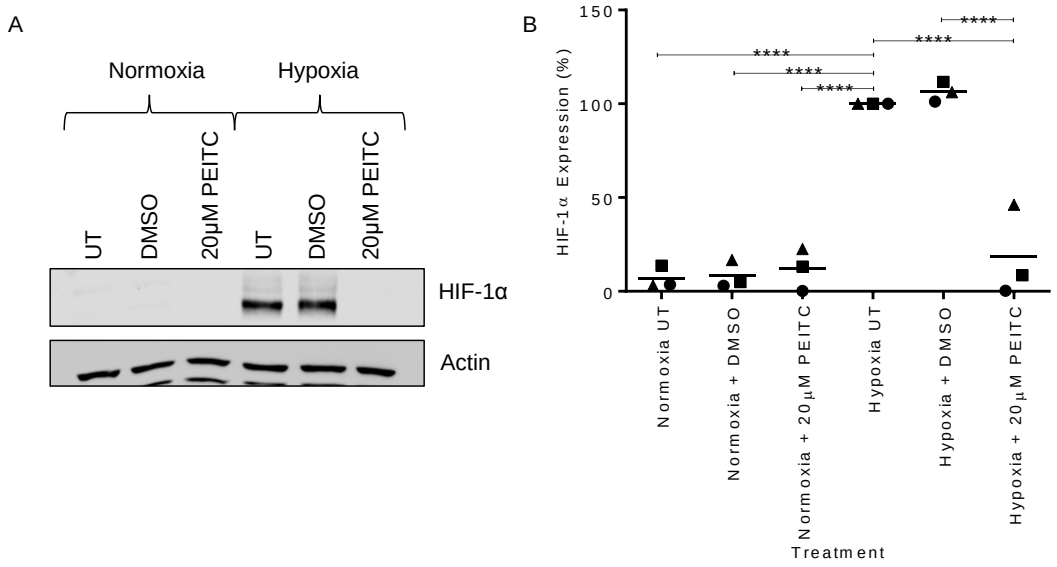

Figure 3-8: HIF-1α Protein Expression Following PEITC Treatment in Normoxic and Hypoxic Conditions

MCF7 cells were either untreated (UT), treated with 20μM PEITC or equivalent DMSO and incubated in normoxic (20% O_2) or hypoxic (1% O_2) conditions for five hours prior to cell harvest. (A) Representative western blot from three independent experiments using primary anti-HIF-1α and anti-β actin antibodies. (B) Densitometry data for HIF-1α protein expression from three independent experiments, each symbol represents once experiment with the line indicating the mean expression. Statistically significant differences are indicated **** ≤ 0.001, two-way ANOVA.

To confirm the inhibitory effect of PEITC, I also investigated the effect of PEITC treatment on expression of VEGF, a known HIF1 target gene that is also subject to tight translational control (Morris et al., 2010). VEGF contains a hypoxic response element (HRE) within the promoter region and is a target of the HIF transcription factor (Michel et al., 2002). VEGF protein expression was analysed by an ELISA assay to quantify secreted VEGF protein in the culture medium of MCF7 cells. Media was collected from MCF7 cells that had been incubated in normoxic (20% O_2) or hypoxic (1% O_2) conditions and either treated with 20µM PEITC, equivalent DMSO or left untreated as a control for five hours.

VEGF production increased in all three independent experiments in hypoxic conditions compared to normoxic conditions (Figure 3-9 A-C – normoxia UT vs hypoxia UT). However, there was some variation between experiments and in experiment three basal VEGF levels were relatively high and the increase induced by hypoxia was minor (Figure 3-9 C), therefore the hypoxic induction of VEGF did not reach statistical significance. However, even with this variation, VEGF expression was increased approximately 4 fold in both untreated and DMSO treated cells in hypoxic conditions compared to normoxic conditions (Figure 3-9 D). This increase in VEGF secretion in hypoxic conditions was prevented in the presence of 20µM PEITC (Figure 3-9 D), where VEGF levels were reduced to levels seen in normoxic untreated conditions. Thus, PEITC prevented the accumulation of both HIF-1α and VEGF protein in hypoxic MCF7 cells.

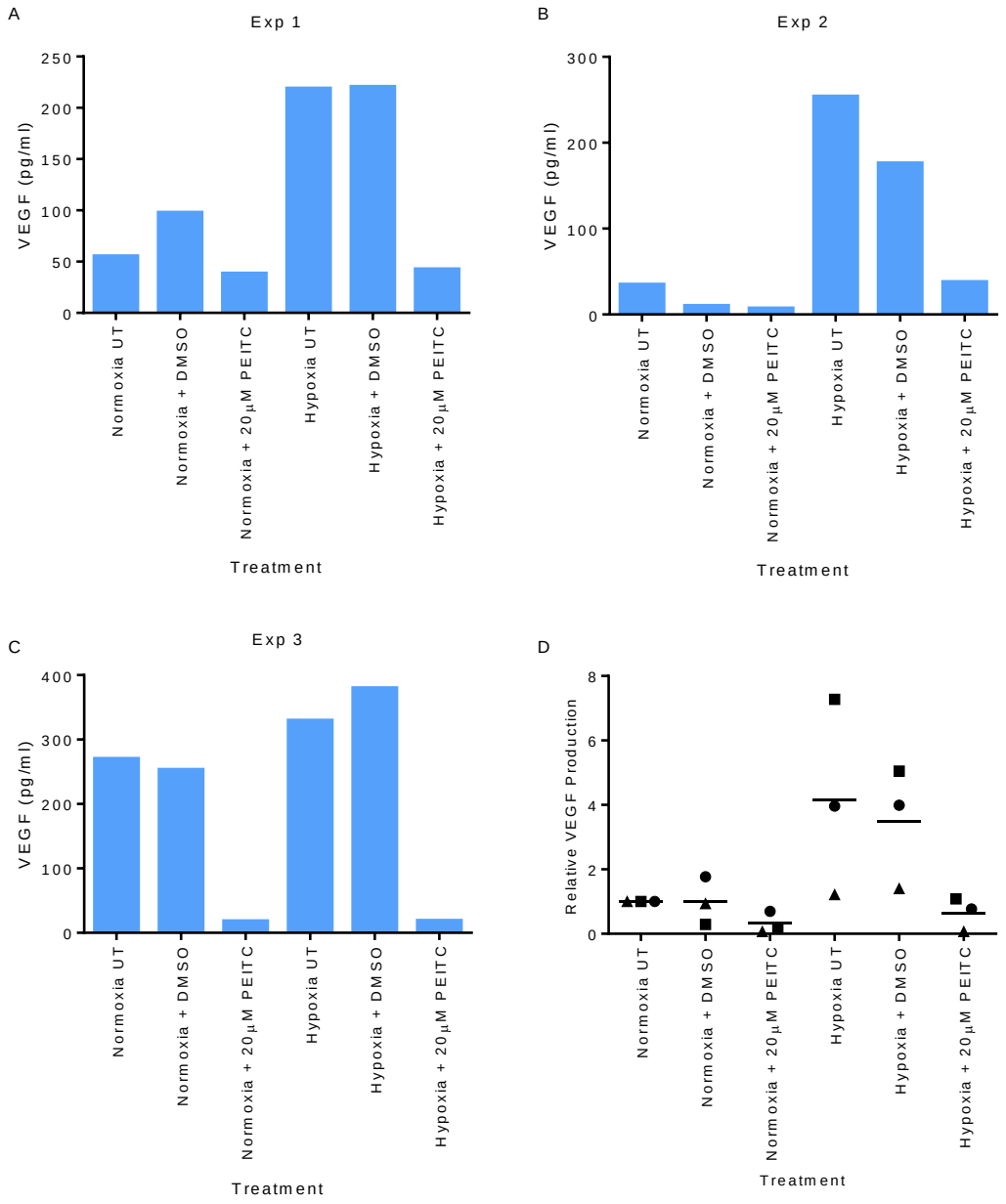

Figure 3-9: VEGF Production Following PEITC Treatment in Normoxic and Hypoxic Conditions

MCF7 cells were either untreated (UT), treated with 20μM PEITC or equivalent DMSO and incubated in normoxic (20% O_2) or hypoxic (1% O_2) conditions for five hours prior to collection of the media. VEGF expression was analysed by ELISA. (A-C) VEGF expression in each individual experiment (D) VEGF expression relative to Normoxic UT in each experiment, where the symbols indicate the individual experiment and the line represents the mean, n=3.

3. 3. 6. Effect of PEITC and Hypoxia on mRNA Translation

Having established experimental conditions in which PEITC effectively blocked hypoxia responses, I next investigated effects on mRNA translation under these conditions by analysing the effects on polysome profiles. Overall, hypoxia caused a modest change in the polysome profiles of MCF7 cells with a reduction in the number of polysomes and an increase in the 80S peak (Figure 3-10 – normoxic and hypoxic untreated samples). Similar changes were seen following treatment with DMSO in normoxic and hypoxic conditions. As shown before (Figure 3-3), in normoxic conditions PEITC (20µM) caused an almost complete loss of polysomes after five hours of treatment. A similar response to PEITC (20µM) was seen in hypoxic conditions (Figure 3-10). The modest increase in the 80S peak in response to hypoxia alone was in agreement with the response seen by others (Fahling, 2009; Koritzinsky et al., 2006). The presence of polysome peaks in hypoxia indicated that some mRNA molecules were still actively translated. However, any proteins expressed during hypoxia were also sensitive to decreased production in response to PEITC treatment, due to an almost complete loss of the polysome peaks.

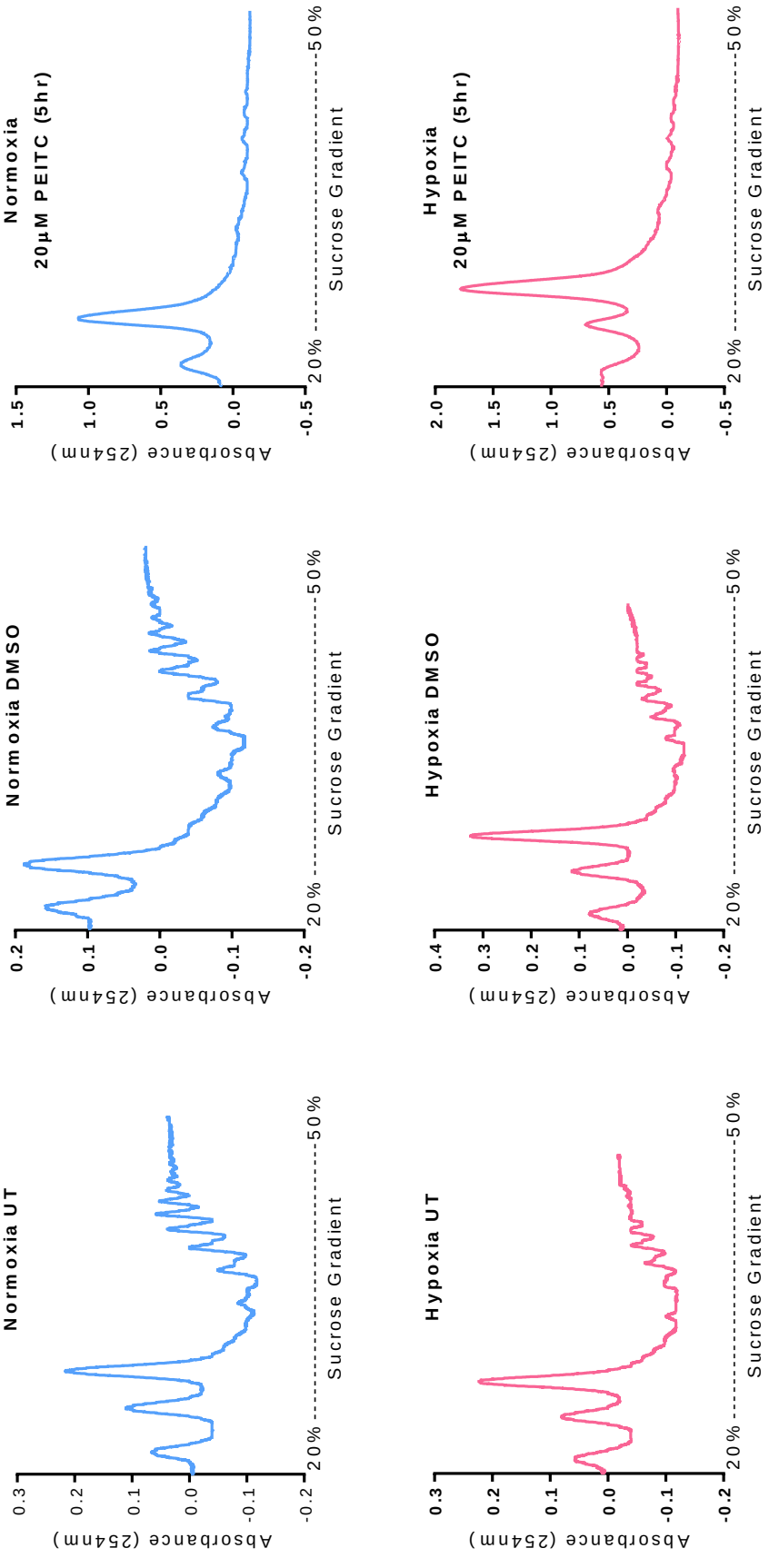

Figure 3-10: Effect of PEITC and Hypoxia on Polysome Profiles

MCF7 cells were untreated, treated with 20µM PEITC or equivalent DMSO before incubating in normoxic (20% O_2) or hypoxic (1% O_2) conditions for five hours. Polysome profiling was then carried out. Data presented represents three independent experiments.

3. 3. 7. Effect of PEITC on HIF-1α and VEGF mRNA Translation

Since PEITC inhibited the hypoxic accumulation of HIF-1α protein (Figure 3-8), I directly investigated the effect of PEITC on *HIF-1A* mRNA translation. Similar to the previous experiment MCF7 cells were treated with 20μM PEITC, equivalent DMSO or left untreated and incubated in normoxic (20% O_2) or hypoxic (1% O_2) conditions for five hours prior to polysome profiling. In this analysis, RNA was purified from each fraction, as indicated in Figure 3-11 and the abundance of *HIF-1A* mRNA was analysed by qPCR. I also investigated the translation of *VEGF* mRNA and ACTB (β-actin mRNA) as a control.

The qPCR data was then analysed in four ways to elucidate the translational effect from any changes in transcription. Firstly, the total amount of mRNA in all fractions (for each gene) is shown to determine whether there were any transcriptional changes in each gene. Secondly, the total amount of mRNA in each fraction of the profile is presented to establish where the mRNA was located on the polysome profile. Thirdly, the amount of mRNA in each fraction of the profile is presented as a percentage of the total mRNA, to remove any transcriptional regulation, and finally, the proportion of mRNA in the highest polysome fractions (fractions 3-5) is shown relative to the lower fractions (fractions 1-2), to ascertain whether the mRNA was highly translated.

The total amount of ribosomal associated *VEGF* mRNA significantly increased in response to hypoxic incubation ($p \leq 0.001$), whereas both *HIF-1A* and *ACTB* total mRNA levels remained constant between hypoxic and normoxic conditions (Figure 3-12 B - D). The total mRNA levels of all three genes were unaltered with DMSO treatment in both normoxic or hypoxic incubation. Treatment with PEITC (20μM) resulted in a significant reduction in total mRNA levels of all three genes analysed in both normoxic and hypoxic conditions (Figure 3-12).

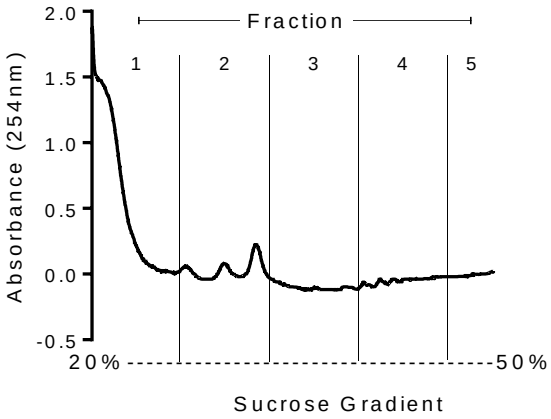

Figure 3-11: Collecting Polysome Fractions

The RNA from the profiles were collected into five different fractions as indicated before RNA extraction and qPCR was carried out.

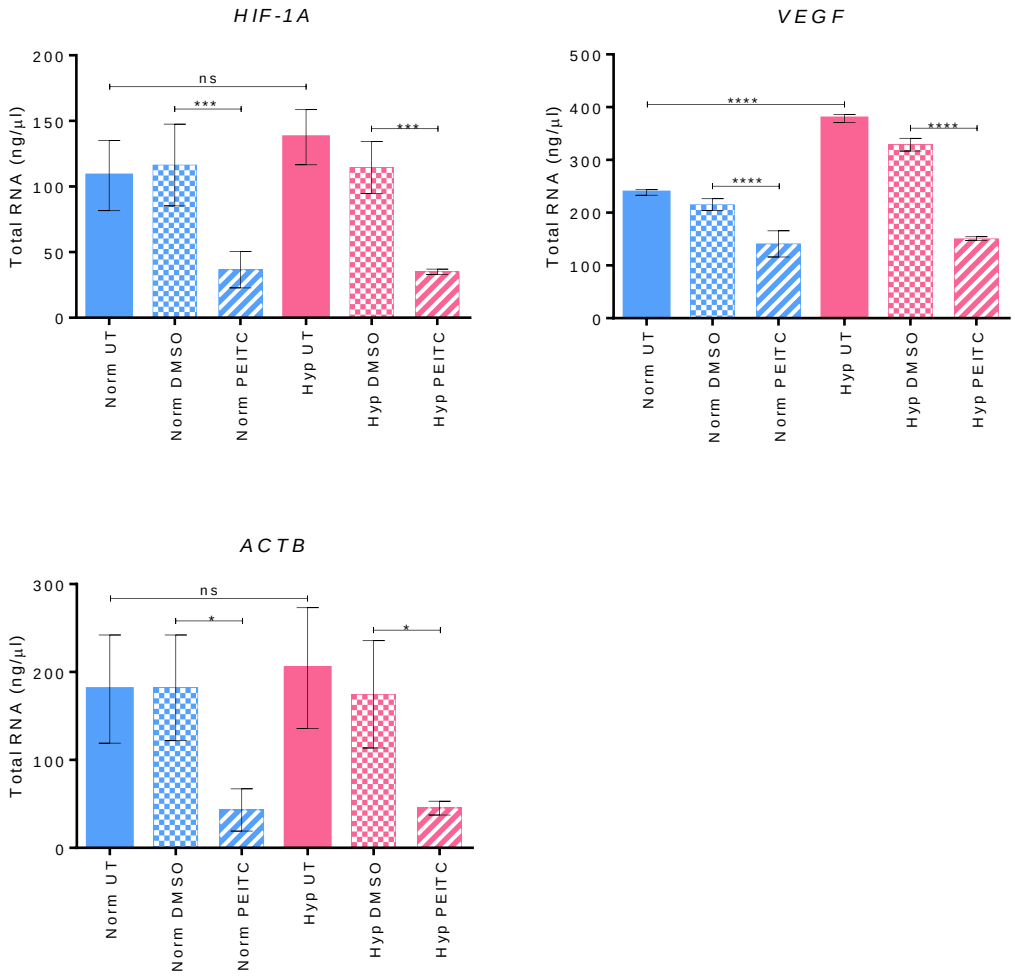

Figure 3-12: Effect of Hypoxia and PEITC on the Abundance of Total *HIF-1A*, *VEGF* and *ACTB* mRNA Levels

Following polysome profiling of MCF7 cells that were untreated (UT), treated with 20µM PEITC or equivalent DMSO and incubated in normoxic (20% O_2) or hypoxic (1% O_2) conditions for five hours (Figure 3-10) qPCR analysis was undertaken to investigate the abundance of *HIF-1A*, *VEGF* and *ACTB* mRNA levels in the whole profile. Bars represent the average total mRNA. Error bars indicate the standard deviation and significantly different data is indicated, * = $p \leq 0.05$, *** = $p \leq 0.005$, **** = $p \leq 0.001$, one-way ANOVA (n=2 independent experiments).

The positioning of each mRNA on the polysome profile indicated how actively translated the mRNA was. Initial comparison of normoxic and hypoxic profiles (untreated samples) indicated that hypoxic conditions had little effect on the amount of *HIF-1A* and *ACTB* mRNA per fraction compared to normoxia (Figure 3-13). While hypoxic conditions increased *VEGF* mRNA in all fractions (except fraction 1) compared to normoxic conditions (Figure 3-13). Thus indicating that *HIF-1A* translation does not increase in hypoxic conditions, rather translation is maintained in hypoxic conditions, when global translation is believed to decrease (van den Beucken et al., 2006). PEITC significantly decreased *HIF-1A*, *VEGF* and *ACTB* mRNA in many fractions of the polysome profiles (Figure 3-13). In order to determine whether the decrease in response to PEITC was due to decreased translation or changes in transcription were responsible for the changes seen the amount of mRNA associated to each fraction was calculated as a percentage of the total mRNA from the whole fraction (Figure 3-14). It was important to remove any transcriptional effects as PEITC decreased total mRNA extracted from polysome profiles (Figure 3-12).

The only significant changes seen in response to PEITC compared to DMSO, independent of any transcriptional effects, was a decrease in *HIF-1A* in fraction 4 in normoxic conditions and an increase in *VEGF* mRNA in fraction 3 (Figure 3-14). A final analysis of the data was carried out to determine whether the mRNA localisation on the polysome profile altered following PEITC treatment. The amount of mRNA associated with polysomes (fractions 3-5 which includes everything denser than an 80S peak) was compared to the amount of mRNA associated with sub-polysome fractions (fractions 1 and 2 up to and including the 80S peak) (Figure 3-15). This indicated that PEITC significantly decreased translation of *HIF-1A* and *ACTB* mRNA but had no significant effect on *VEGF* mRNA translation (Figure 3-15).

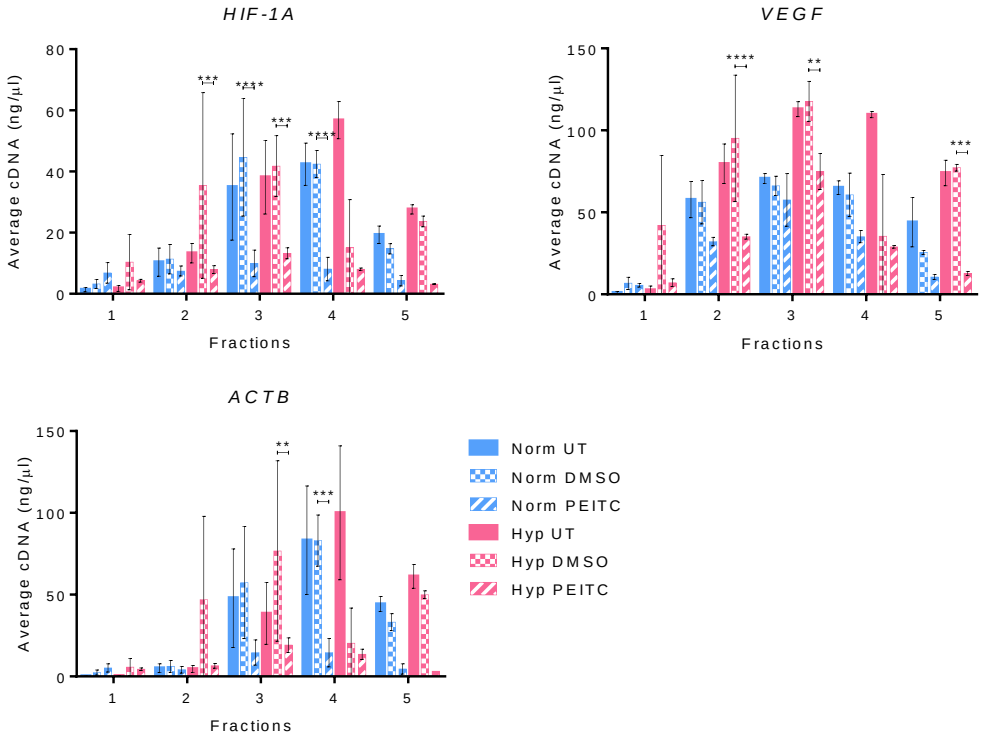

Figure 3-13: Polysome Distribution of *HIF-1A*, *VEGF* and *ACTB* mRNA Following Treatment with PEITC and Incubation in Hypoxic Conditions

Following polysome profiling of MCF7 cells that were untreated (UT), treated with 20µM PEITC or equivalent DMSO and incubated in normoxic (20% O_2) or hypoxic (1% O_2) conditions for five hours (Figure 3-10) qPCR analysis was undertaken to investigate the abundance of *HIF-1A*, *VEGF* and *ACTB* mRNA levels in each fraction of the profile. Bars represent the average mRNA present in each fraction of the polysome profile. Error bars indicate the standard deviation and significantly different data is indicated, ** = $p \leq 0.01$, *** = $p \leq 0.005$, **** = $p \leq 0.001$, one-way ANOVA (n=2 independent experiments).

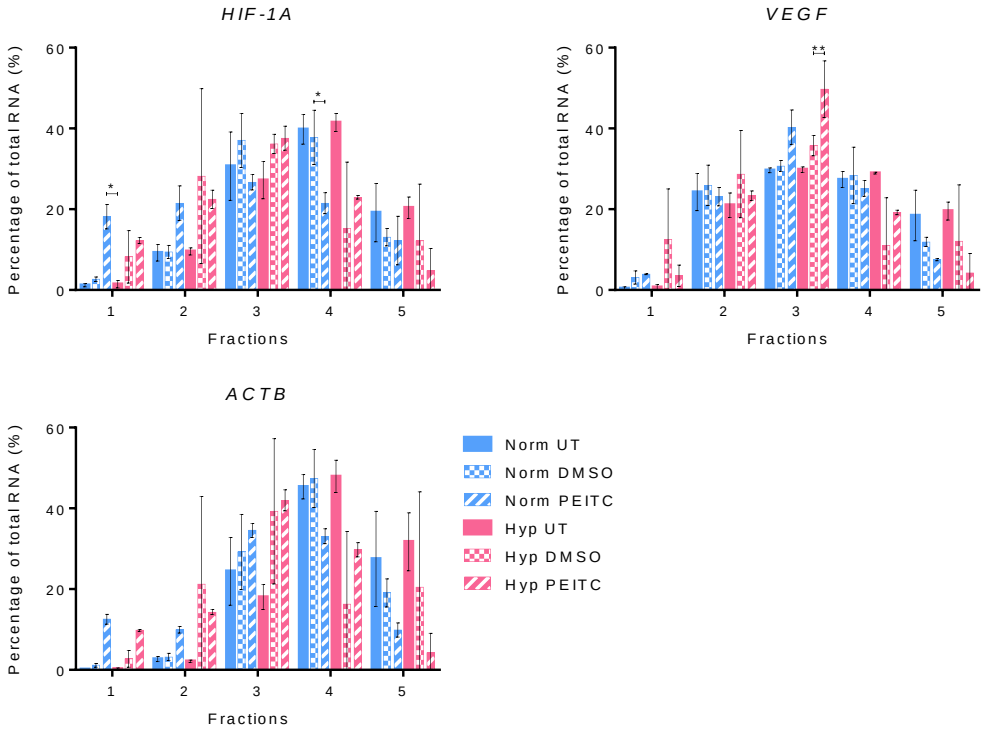

Figure 3-14: Percentage of *HIF-1A*, *VEGF* and *ACTB* mRNA within Polysome Fractions

Following polysome profiling of MCF7 cells that were untreated (UT), treated with 20μM PEITC or equivalent DMSO and incubated in normoxic (20% O_2) or hypoxic (1% O_2) conditions for five hours (Figure 3-10) qPCR analysis was undertaken to investigate the abundance of *HIF-1A*, *VEGF* and *ACTB* mRNA levels as a percentage of the total mRNA isolated from the profile. Bars represent the perecentage of total mRNA present in each fraction of the polysome profile. Error bars indicate the standard deviation and significantly different data is indicated, * = $p \leq 0.05$, ** = $p \leq 0.01$, one-way ANOVA (n=2 independent experiments).

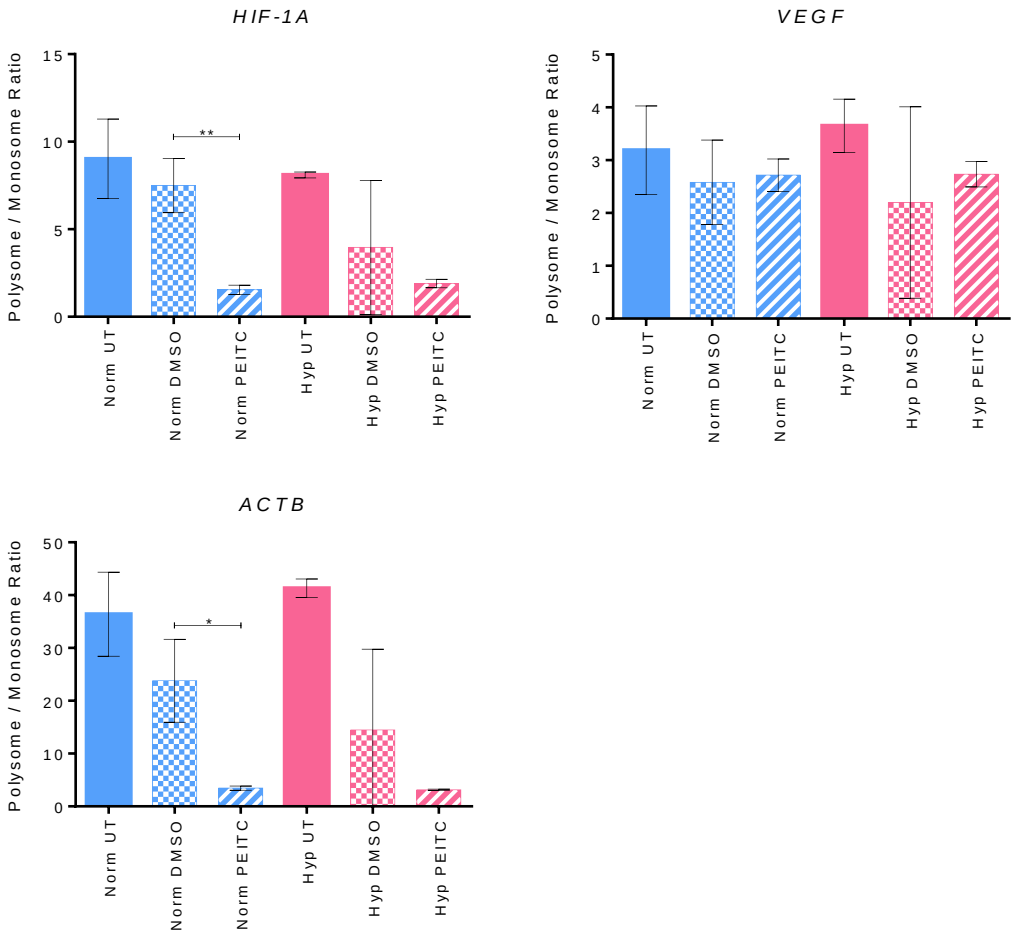

Figure 3-15: Polysome Association of *HIF-1A*, *VEGF* and *ACTB* mRNA Following PEITC Treatment and Incubation in Hypoxic Conditions

Following polysome profiling of MCF7 cells that were untreated (UT), treated with 20μM PEITC or equivalent DMSO and incubated in normoxic (20% O_2) or hypoxic (1% O_2) conditions for five hours (Figure 3-10) qPCR analysis was undertaken to investigate the abundance of *HIF-1A*, *VEGF* and *ACTB* mRNA levels in the whole profile. Bars represent the average ratio of polysomally associated mRNA (fractions 3-5) with respect to sub-polysome associated mRNA (fractions 1 and 2). Error bars indicate the standard deviation and significantly different data is indicated, * = $p \leq 0.05$, ** = $p \leq 0.01$, one-way ANOVA (n=2 independent experiments).

3. 3. 8. Maintenance of HIF-1α mRNA Translation

It is known that in hypoxic conditions overall translation rates are significantly reduced (Fahling, 2009; Koumenis et al., 2002; McEwen et al., 2005; Wouters et al., 2005), even though in hypoxic conditions expression levels of HIF-1α as well as VEGF and other HIF-1α targets increase. A possible mechanism for increased expression of these proteins is due to the presence of an IRES (Lang et al., 2002; Mathews et al., 2007; Schepens et al., 2005), but the presence of an IRES is still debated and other elements may contribute to translational regulation of *HIF-1A*.

HIF-1α protein expression was enhanced following hypoxic incubation (Figure 3-8), while mRNA levels were unaltered (Figure 3-12). Indicating decreased oxygen-dependent degradation of HIF-1α protein as well as maintained translation. Translation following hypoxic incubation resulted in a decrease in global translation (Figure 3-10), yet *HIF-1A* mRNA stayed associated with polysomes (Figure 3-13), indicating active translation of *HIF-1A* mRNA. This raised the question of how *HIF-1A* mRNA translation was maintained when global translation was reduced. Analysis of the association of *HIF-1A* mRNA with ribosomes was carried out using qPCR (Figure 3-12 - Figure 3-15), which analysed the presence of the coding sequence of the mRNA, but the UTRs are important in regulating translation therefore it was important to analyse whether any changes in the UTRs of *HIF-1A* mRNA facilitated the maintenance of *HIF-1A* mRNA translation. The published sequence for *HIF-1A* (NCBI gene, www.ncbi.nlm.nih.gov/nuccore/NM_001530.3) was updated in the last three years resulting in a 5'extension of the 5'UTR by 120 nucleotides (Figure 3-16). In order to determine the mRNA sequence of *HIF-1A* expressed following incubation in hypoxic or normoxic conditions RACE (rapid amplification of cDNA ends) was carried out on both the 5' and 3'UTRs, as described in section 2. 19. Following RACE the PCR product underwent restriction enzyme digestion to determine that the product was HIF-1α (Figure 3-17).

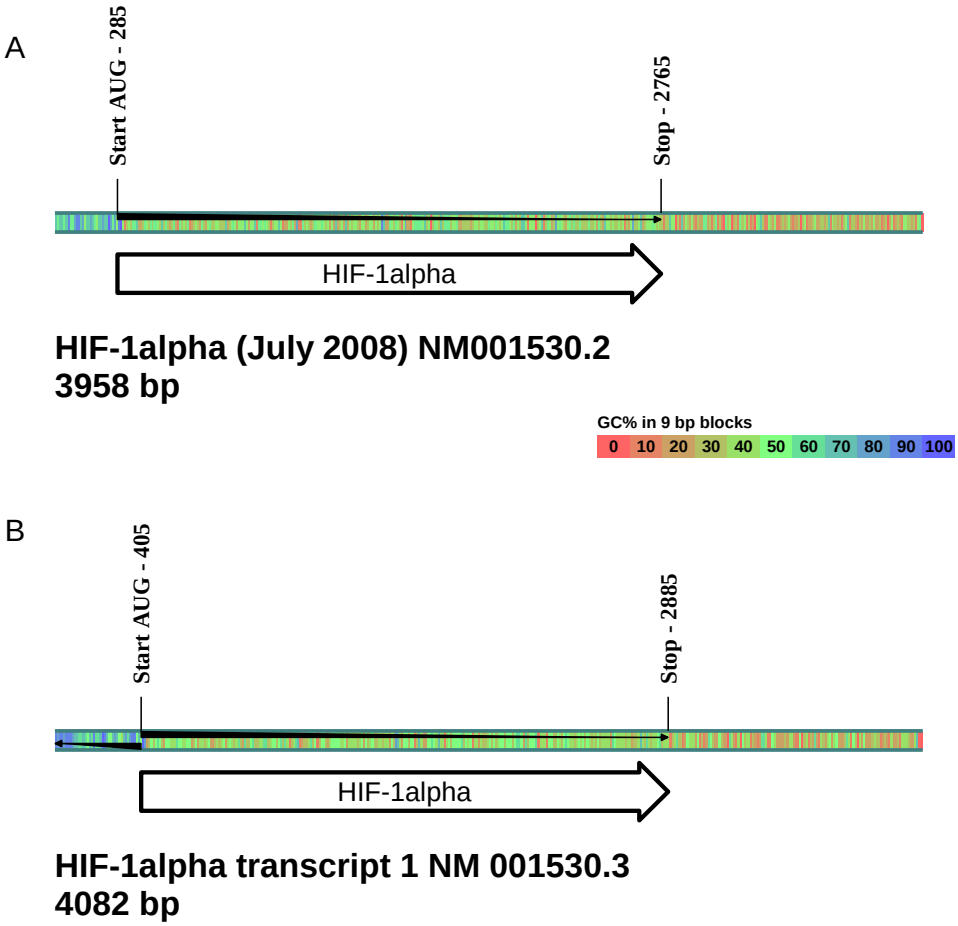

Figure 3-16: 5'Untranslated Region Sequence Extension of *HIF-1A* mRNA

Schematic of the *HIF-1A* sequence before (A) and after (B) the sequence up-date resulting in an extension in the 5'UTR.

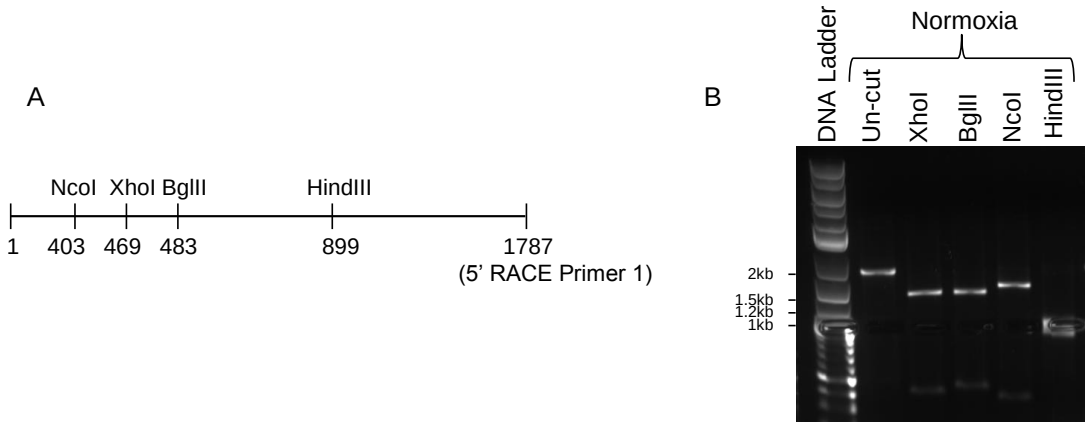

Figure 3-17: Analysis of 5' *HIF-1A* Untranslated Region by Restriction Enzyme Digest

(A) Schematic representation of the restriction enzyme cut sites in the 5'UTR of *HIF-1A*. (B) Following 5' RACE of *HIF-1A* mRNA the RACE PCR product was subjected to restriction enzyme digestion by XhoI, BgIII, NcoI or HindIII as indicated, or un-cut. The products from restriction enzyme digestion were run on a 0.8% agarose gel alongside the DNA ladder (2 log ladder).

The results indicated that the 5' RACE product from cells incubated in normoxic conditions was *HIF-1A* (Figure 3-17), similar experiments were performed from mRNA extracted from cells incubated in hypoxic conditions as well as on 3'RACE PCR products. It was important to characterise both the 5' and 3' UTRs as both regions can modulate translation, with an anti-sense HIF-1α transcript known to bind to the 3'UTR of renal cell carcinoma cells and lymphocytes (Thrash-Bingham and Tartof, 1999). Hence the 3'UTR may also influence translation and required further investigation.

The RACE PCR products were ligated into pJet1.2 by blunt end ligation for sequencing to confirm that the products seen were *HIF-1A* as well as to determine the sequence of the 5' and 3'UTR of *HIF-1A* expressed in normoxic and hypoxic conditions. Sequencing was carried out by Eurofins MWG Operon and indicated that following normoxic incubation MCF7 cells only expressed *HIF-1A* mRNA that started 120 nucleotides downstream of the published sequence, while MCF7 cells incubated in hypoxic conditions expressed three variants starting at 120, 137 and 363 of the published sequence (NCBI Reference Sequence: NM_001530.3), see Supplementary data, section 9. 1. Whereas sequencing data confirmed that regardless of hypoxic incubation the 3'UTR was unaltered, see Supplementary data, section 9. 1.

Primers were designed to amplify the *HIF-1A* 5'UTRs and 3'UTR from the pJet1.2 plasmids to be re-cloned into pGLp, a reporter plasmid. These primers also contained restriction enzyme cut sites immediately flanking the HIF-1α sequence to enable sticky-end ligation into pGLp (Figure 3-18A). Following amplification of the 5' and 3'UTRs the PCR products were cleaned up and digested with restriction enzymes to generate complementary sticky ends to pGLp that was digested with EcoRI and NcoI (for 5' UTR insertion) and XbaI (for 3' UTR insertion) (Figure 3-18). The pGLp plasmid (kindly provided by Dr. Mark Coldwell, University of Southampton, UK) is a luciferase reporter plasmid that contains firefly luciferase flanked with a PEST (Proline–Glutamic acid–Serine–Threonine) motif. The presence of the PEST domain decreased luciferase half-life from the native three hours down to one hour (Figure S9-1). The pGLp plasmid was used as a reporter construct as the shorter half-life of luciferase in this construct allowed rapid

modifications in translation to be measured. The plasmids were transfected into MCF7 cells and incubated in normoxic or hypoxic conditions for two hours prior to determination of luciferase activity (Figure 3-19). As a control the 5' and 3'UTR of globin was also cloned into pGLp and the luciferase activity of cells transfected with 5'globin–pGLp–3'globin was set to one. Addition of the HIF-1α 5' 363 UTR enhanced luciferase activity in normoxic conditions, but a greater increase was seen with the addition of 5' 137 and 120 UTR (Figure 3-19 A). The subsequent addition of the HIF-1α 3'UTR prevented the increase in luciferase activity, in 5' 120-, or 5' 137- HIF UTR containing plasmids, while addition of the HIF-1α 3' UTR in 5' 363- HIF plasmids completely abolished luciferase activity in normoxic conditions (Figure 3-19 A). Similar results were seen following incubation in hypoxic conditions (Figure 3-19 B). Comparison between luciferase activity mediated by the different UTRs indicated that only the 5' 137 HIF UTR enhanced translation significantly in hypoxic conditions compared to normoxic conditions (Figure 3-20). While addition of PEITC significantly decreased luciferase activity in the presence of all the plasmids in normoxic and hypoxic conditions (Figure 3-21 and Figure 3-22). This indicated that PEITC did not just decrease *HIF-1A* translation as translation regulated by the globin UTRs was also inhibited. Although it cannot be ruled out that PEITC may have inhibited transcription and further analysis would be required to uncouple the translation and transcription effect of PEITC.

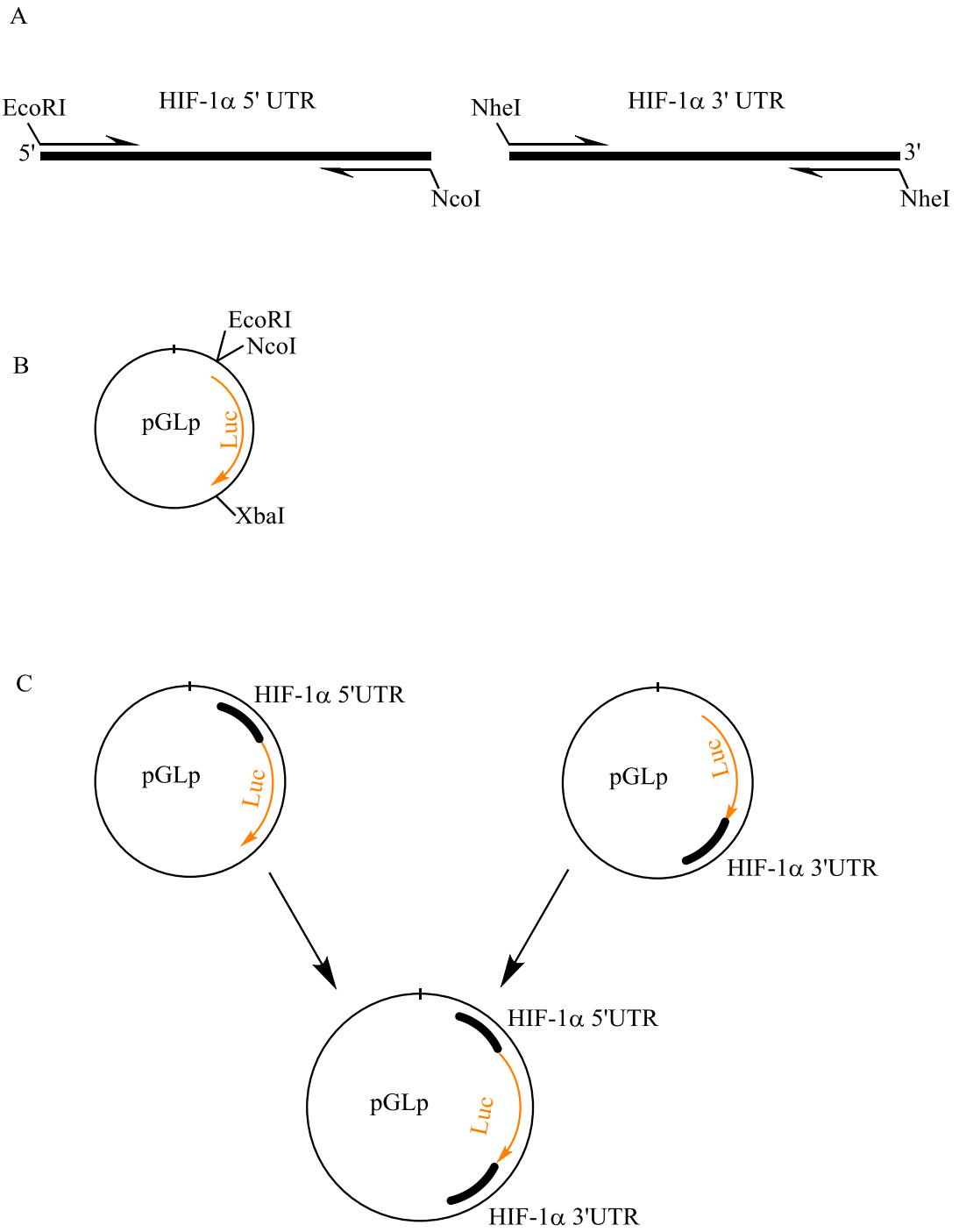

Figure 3-18: Primer Design and Cloning of *HIF-1A* Untranslated Regions into pGLp

(A) Primers were designed to be complementary to the *HIF-1A* UTR and immediately following this restriction enzyme sites were added that would not match the starting pJet1.2 plasmid. Following restriction enzyme digestion of PCR products and the pGLp vector (B), *HIF-1A* UTRs were ligated into pGLp to generate pGLp plasmids (C).

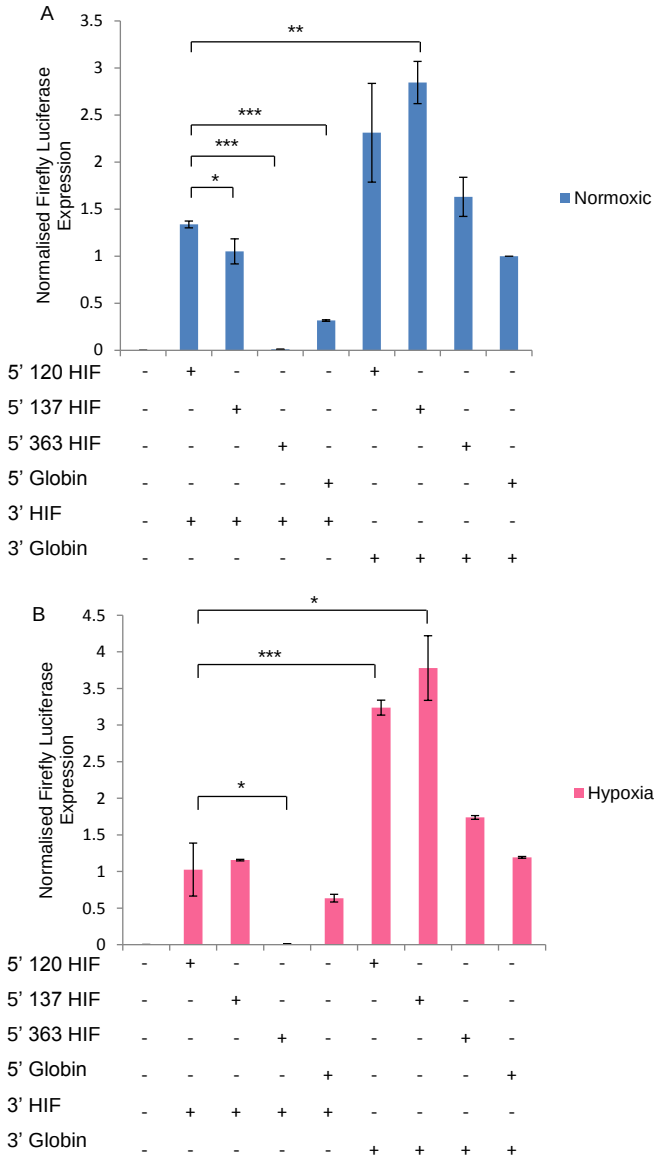

Figure 3-19: Effect of Different *HIF-1A* 5'Untranslated Regions on Translation using Luciferase Reporter Constructs

MCF7 cells were transfected with pGLp plasmids with the different *HIF-1A* and globin UTRs in the 5' and 3' region of luciferase along with *Renilla* luciferase. Cells were then incubated in (A) normoxic (20% O_2) or (B) hypoxic (1% O_2) conditions for two hours before firefly and *Renilla* luciferase activity was analysed. Data shown is firefly luciferase relative to protein concentration and then normalised to the 5'globin-pGLp-3'globin transfected cells. Bars represent the average of duplicate conditions in three independent experiments. Error bars are the standard deviation from the mean and statistically different data is indicated (* = $p \leq 0.05$, ** = $p \leq 0.01$, *** = $p \leq 0.001$), student's t-test n=6.

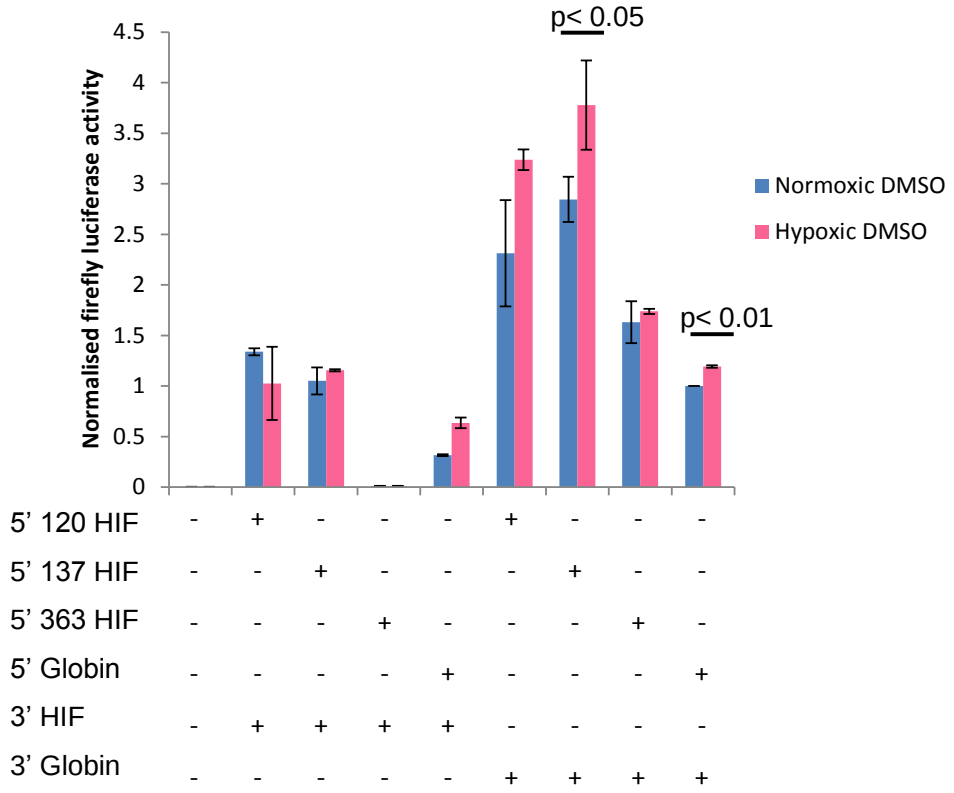

Figure 3-20: Effect of Hypoxic Conditions on *HIF-1A* Translation using Luciferase Reporter Constructs

MCF7 cells were transfected with pGLp plasmids with the different *HIF-1A* and globin UTRs in the 5' and 3' region of luciferase along with *Renilla* luciferase. Cells were then incubated in normoxic (20% O_2) or hypoxic (1% O_2) conditions for two hours before firefly and *Renilla* luciferase activity was analysed. Data shown is firefly luciferase relative to protein concentration and then normalised to the 5'globin-pGLp-3'globin transfected cells incubated in normoxic conditions. Bars represent the average of duplicate conditions in three independent experiments. Error bars are the standard deviation from the mean and statistically different data is indicated, student's t-test n=6.

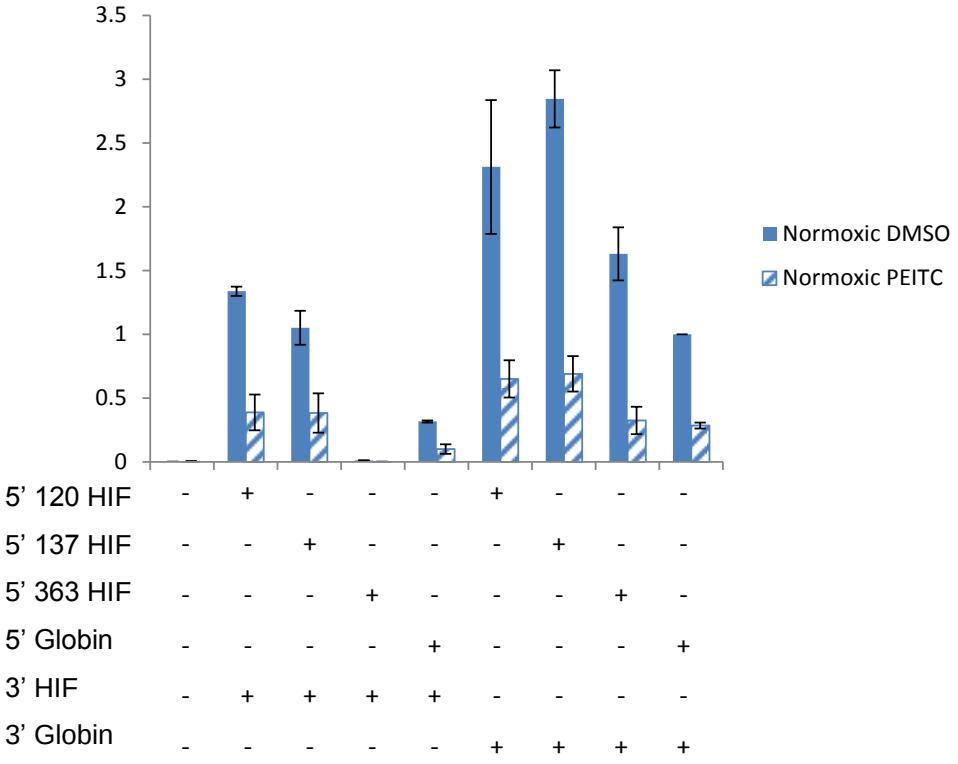

Figure 3-21: Effect of PEITC on *HIF-1A* Translation using Luciferase Reporter Constructs in Normoxic Conditions

MCF7 cells were transfected with pGLp plasmids with the different *HIF-1A* and globin UTRs in the 5' and 3' region of luciferase along with *Renilla* luciferase. Cells were treated with 20µM PEITC or equivalent DMSO and then were incubated in normoxic (20% O_2) conditions for two hours. Firefly and *Renilla* luciferase activity was then determined. Data shown is firefly luciferase relative to protein concentration and then normalised to the 5'globin-pGLp-3'globin transfected cells incubated in normoxic conditions. Bars represent the average of duplicate conditions in three independent experiments. Error bars are the standard deviation from the mean and statistically different data is indicated, student's t-test n=6.

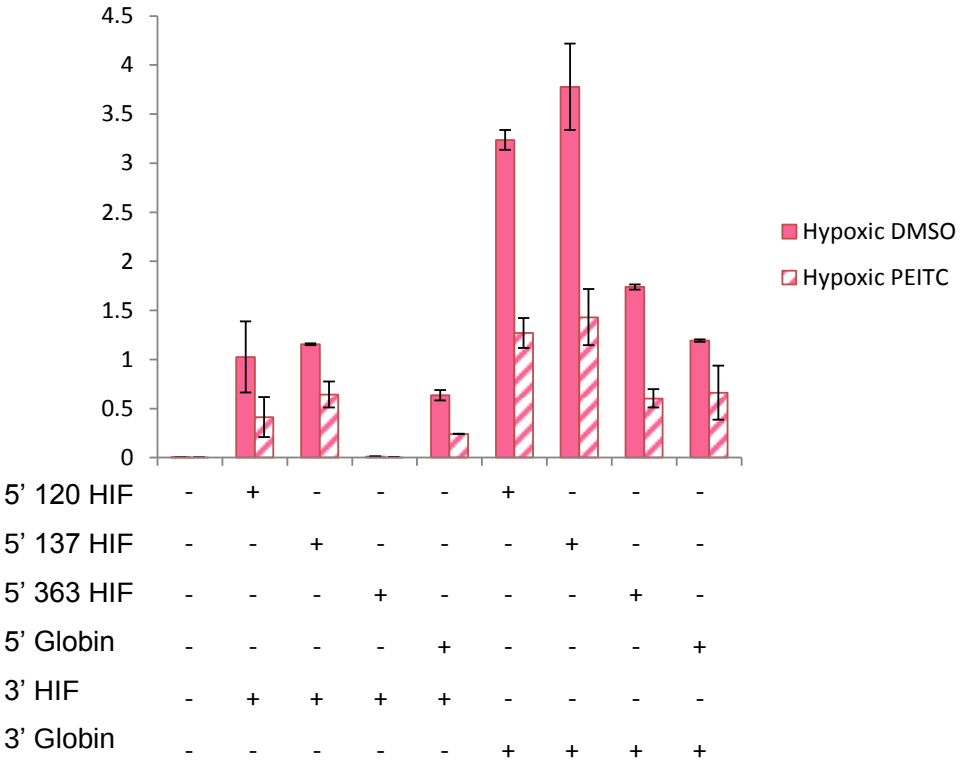

Figure 3-22: Effect of PEITC on *HIF-1A* Translation in Hypoxic Conditions using Luciferase Reporter Constructs

MCF7 cells were transfected with pGLp plasmids with the different *HIF-1A* and globin UTRs in the 5' and 3' region of luciferase along with *Renilla* luciferase. Cells were treated with 20μM PEITC or equivalent DMSO and then were incubated in hypoxic (1% O_2) conditions for two hours. Firefly and *Renilla* luciferase activity was then determined. Data shown is firefly luciferase relative to protein concentration and then normalised to the 5'globin-pGLp-3'globin transfected cells incubated in normoxic conditions. Bars represent the average of duplicate conditions in three independent experiments. Error bars are the standard deviation from the mean and statistically different data is indicated, student's t-test n=6.

3. 4. Summary of Main Findings

- PEITC treatment caused a large accumulation in the 80S peak in normoxic and hypoxic conditions
- Inhibition of translation by PEITC occurred rapidly and was dose dependent
- Inhibition of translation partially recovered following PEITC wash out
- Hypoxic induction of HIF-1α protein and VEGF was inhibited by PEITC treatment
- Hypoxic incubation had no effect on *HIF-1A* and *ACTB* transcription but increased *VEGF* transcription
- Translation of *HIF-1A* was maintained in hypoxic conditions
- PEITC decreased *HIF-1A*, *VEGF* and *ACTB* transcription
- PEITC treatment decreased translation of *HIF-1A* and *ACTB* mRNA
- The 5'UTR may be altered in hypoxic conditions, with longer 5'UTRs enabling efficient *HIF-1A* translation
- The 3'UTR of *HIF-1A* has a detrimental effect on *HIF-1A* translation

3. 5. Discussion

Inhibition of translation by PEITC was expected as it had been previously shown that PEITC inhibited the translation of *HIF-1A* mRNA (Cavell et al., 2012; Wang et al., 2009) but it was unclear as to whether the decrease in translation was specific to *HIF-1A* mRNA or whether the decrease in translation would have a global effect. The data presented here indicated that PEITC decreased translation in a global manner with an accumulation of mRNA into the 80S fraction and a loss of mRNA associated with polysomes (Figure 3-3 - Figure 3-6, inclusive and Figure 3-12). The global block in translation as a result of PEITC treatment occurred rapidly, with decreased polysome peaks seen within 10 minutes as well as a large accumulation in the 80S peak (Figure 3-4). The time dependent decrease in translation indicated that PEITC only inhibited new rounds of translation, those ribosomes that were already in the process of translating the mRNA were allowed to complete that round of

translation, as the polysome peaks diminish with amplitude rather than an immediate collapse. This may also indicate the time delay for PEITC incorporation into the cell and the rate of translational blockage. This would require further investigation in order to determine whether PEITC disrupts translating ribosomes causing them to dissociate from the mRNA, or whether translating ribosomes are able to complete that round of translation.

The dose dependent decrease in translation in response to PEITC treatment was in agreement with previous work in our group, which showed that the IC_{50} for inhibition of *HIF-1A* translation by PEITC to be around 5-7.5µM (Cavell et al., 2012). These concentrations of PEITC resulted in decreased polysome peaks and a large accumulation in the 80S peak (Figure 3-6). The IC_{50} for growth inhibition of MCF7 cells by PEITC has been shown to be around 11µM (Wang et al., 2009), therefore the concentration of PEITC required to inhibit translation was not in excess of the IC_{50} values for other anti-cancer activities. The concentration of PEITC required to inhibit translation is achievable *in vivo* with fats fed daily dietary PEITC resulting in plasma concentrations reaching up to 42µM (Cheung and Kong, 2010).

I also analysed the effect of PEITC on specific genes especially those involved in angiogenesis, as PEITC had previously been shown to inhibit angiogenesis (Xiao and Singh, 2007). The effect of PEITC on specific mRNA translation is summarised in sections 3.5.1 – 3.5.3.

3. 5. 1. Effect of PEITC and Hypoxia on HIF-1α

PEITC decreased the protein expression of HIF-1α in hypoxic conditions (Figure 3-8) that was hypothesised to occur due to decreased translation. Previous data indicated that HIF-1α protein production was inhibited without changes in *HIF-1A* mRNA levels (Wang et al., 2009). Hypoxia has previously been shown to decrease mRNA translation as a result of increased cellular stress, with decreased mRNA translation acting as a survival mechanism (Fahling, 2009; Koumenis et al., 2002;

McEwen et al., 2005; Wouters et al., 2005). mRNA translation utilises 20-30% of the total cellular energy, whereas during hypoxia this expenditure is reduced to just 10%. The hypoxic decrease in protein synthesis previously seen was rapid therefore was not believed to be a consequence of changes in gene transcription and occurred in response to a block in initiation of translation (Fahling, 2009; Wouters et al., 2005). However, some proteins are preferentially expressed under hypoxia and mRNA translation under these conditions could be differentially sensitive to PEITC inhibition.

Hypoxic conditions had a small inhibitory effect on polysome formation (Figure 3-10), which contradicts the literature. This could possibly be due to the percentage of oxygen stated as 'hypoxia', many papers claim changes in translation are due to the effect of hypoxia on the cells when in fact the cells are incubated in anoxic condition (0% oxygen) (Koritzinsky et al., 2006; Thomas and Johannes, 2007), which is not physiologically relevant (Hadjipanayi et al., 2010). The modest change seen in polysome profiles in response to hypoxia indicated that in order for the cell to survive the hypoxic environment many genes are still translated. Genes may include *HIF-1A* (and downstream HIF-1 target genes, including VEGF) known to promote angiogenesis. Treatment with PEITC and incubation in hypoxic conditions resulted in significant inhibition of translation (Figure 3-10). This was in agreement with decreased *HIF-1A* mRNA translation in response to PEITC (Cavell et al., 2012; Wang et al., 2009) as well as providing a mechanism for decreased angiogenesis in response to PEITC treatment. Reduced translation of proteins expressed in hypoxic conditions by PEITC would result in decreased survival to hypoxic stress, as proteins up-regulated in response to hypoxia are known to enable cell survival during hypoxia.

PEITC reduced the association of *HIF-1A* mRNA with ribosomes in both normoxic and hypoxic conditions, seen by reduced total *HIF-1A* mRNA levels collected from polysome profiles (Figure 3-12). This appeared to contradict the published data that showed PEITC did not alter *HIF-1A* mRNA levels (Wang et al., 2009), but here only the mRNA levels associated with ribosomes were analysed therefore it was only possible to conclude that ribosomally associated *HIF-1A* mRNA was significantly reduced in response to PEITC treatment. In response to

hypoxia ribosomally associated *HIF-1A* total mRNA levels were unchanged compared to normoxic conditions (Figure 3-12) and hypoxia did not enhance the association of *HIF-1A* mRNA to heavier density ribosomes (Figure 3-13 and Figure 3-14). Indicating that translation of *HIF-1A* was not enhanced in hypoxic conditions, rather *HIF-1A* translation was maintained (Figure 3-13 - Figure 3-15).

Investigation into how *HIF-1A* mRNA translation was maintained when global translation was reduced was undertaken using RACE to determine the sequence of the 5' and 3'UTRs of *HIF-1A* following incubation in normoxic or hypoxic conditions. This revealed during hypoxia three *HIF-1A* mRNAs were presence that differ in the length of their 5'UTRs, while the 3'UTR was maintained regardless of oxygen levels (see supplementary data, section 9. 1.). The longest form of the 5'UTR expressed in hypoxia was the same as that expressed in normoxic conditions. The longer *HIF-1A* 5'UTRs enabled translation to be enhanced in hypoxic conditions compared to normoxic conditions, compared to the shorter 5'UTR sequences (Figure 3-19). The presence of the 3'UTR had a detrimental effect on translation (Figure 3-19). The inhibitory action of the *HIF-1A* 3'UTR on translation may have occurred due to the presence of the complementary sequence in the 3'UTR with the anti-sense HIF-1α, that is expressed in hypoxic conditions (Thrash-Bingham and Tartof, 1999), although verification of this would be required. The stability of the RNA produced from each plasmid was not analysed and the 3'UTR of HIF-1α is known to have a complementary sequence to the anti-sense HIF-1α (Thrash-Bingham and Tartoff, 1999), which may have altered stability of the RNA rather than the translational efficiency of the message. Translation of *HIF-1A* was inhibited by PEITC in both normoxic and hypoxic conditions regardless of the length of the 5'UTR (Figure 3-20 and Figure 3-21) and occurred independently of any changes in transcription (Figure 3-15). Suggesting that the PEITC-decreased translation of *HIF-1A* may provide a mechanism for PEITC to decrease angiogenesis.

3. 5. 2. Effect of PEITC and Hypoxia on VEGF

To determine whether PEITC only modulated translation of *HIF-1A* analysis on the effect of PEITC on the downstream target, *VEGF*, was carried out. In response to hypoxia *VEGF* mRNA (total levels) increased (Figure 3-12). This indicated that hypoxia had enhanced the activity of HIF-1α to promote transcription of *VEGF*. Translation of *VEGF* was also maintained in hypoxic conditions, through unknown mechanisms (Figure 3-13 and Figure 3-14). This allowed the expression of VEGF to be enhanced following hypoxic incubation (Figure 3-9). Although *VEGF* translation was not enhanced in hypoxic conditions the fact that transcription was enhanced resulted in elevated VEGF levels (Figure 3-9).

VEGF mRNA translation was unaltered in response to PEITC in both normoxic and hypoxic conditions (Figure 3-15). A possible mechanism for *VEGF* being insensitive to PEITC treatment could be due to *VEGF* translation being IRES driven as well as modulated by G-quadruplex formation (Morris et al., 2010). It would be interesting to determine whether certain mRNA molecules are insensitive to decreased translation modulated by PEITC treatment, although this would require further investigation.

3. 5. 3. Effect of PEITC and Hypoxia on ACTB

Hypoxia had minimal effect on transcription of *ACTB* compared to normoxic incubation, with total *ACTB* mRNA levels maintained (Figure 3-12). Hypoxia also had little effect on the association of *ACTB* mRNA with ribosomes and the distribution of *ACTB* along the polysome profile was maintained (Figure 3-13 and Figure 3-14). It was unexpected that translation of *ATCB* would be unaltered following hypoxic incubation although previous work in adipose cells incubated in hypoxic conditions also indicated that *ACTB* translation was maintained (Fink et al., 2008) therefore supporting the findings presented in Figure 3-13 and Figure 3-14. Treatment with PEITC decreased translation of *ACTB* mRNA in both normoxic and hypoxic conditions independently of any changes in transcription (Figure 3-15).

In conclusion the fact that total mRNA levels of all three genes analysed decreased in response to PEITC treatment indicated that transcription was inhibited in a global manner. PEITC also decreased translation and the decrease in translation, independent of transcription, appears to be specific to certain mRNA molecules. The modulation of transcription as well as translation makes analysis difficult to determine the exact effect of PEITC on translation and requires further investigation.

Chapter Four

Results – Mechanism of Decreased Translation in Response to PEITC Treatment

4. Mechanism of Decreased Translation in Response to PEITC Treatment

4. 1. Introduction

PEITC was shown to inhibit translation of *HIF-1A* (Figure 3-15 and (Cavell et al., 2012)) as well as translation in a global manner (Figure 3-3). The mechanisms behind the rapid inhibition of translation following treatment with PEITC required investigation (Figure 3-4). Our group had previously determined that PEITC modulated mTORC1 activity to decrease translation (Cavell et al., 2012), although this does not rule out the possibility that PEITC may act via many different pathways to cause such a dramatic inhibition of translation seen (Figure 3-3). The mTORC1 pathway is able to modulate cap-dependent translation (see section 1. 3. 2.) whereas cap-independent translation can overcome mTORC1 inhibition. As PEITC treatment caused the polysome peaks to collapse (Figure 3-3), this suggested that translation was inhibited in a global manner therefore may inhibit both cap-dependent and cap-independent pathways. It was important to determine whether PEITC acts via inhibition of mTORC1 alone or whether multiple pathways were modulated by PEITC treatment, another potential candidate is eIF2α. Phosphorylation of eIF2α is known to be enhanced under cellular stress to inhibit translation (Mathews et al., 2007), therefore PEITC may induce the phosphorylation of eIF2α due to enhanced ROS, causing cellular stress.

4. 2. Hypothesis and Aims

4. 2. 1. Hypothesis

PEITC inhibited mRNA translation at the initiation stage of translation due to inhibition of mTORC1 and/or via the phosphorylation of the initiation factor, eIF2α.

4. 2. 2. Aims

The overall aim of this chapter was to determine the molecular target of PEITC that resulted in altered mRNA translation. This was carried out by investigating the effect of:

- mTORC1 inhibition on translation by polysome profiling
- PEITC treatment on eIF2α phosphorylation status
- eIF2α phosphorylation on translation by polysome profiling
- PEITC treatment on stress granule formation

4. 3. Results

4. 3. 1. Effect of Rapamycin on Downstream Signalling

Previous data had demonstrated that PEITC decreased P70S6K and 4E-BP1 phosphorylation as a consequence of mTORC1 inhibition (Cavell et al., 2012). In order to determine whether PEITC inhibited translation via mTORC1 alone the mTORC1 inhibitor, rapamycin, was used (Sarbassov et al., 2006). If mTORC1 was responsible for the decrease in translation in response to PEITC treatment then inhibition of mTORC1 by rapamycin should produce similar effects on polysome profiles as those produced in response to PEITC treatment. Before determining the consequence of mTORC1 inhibition on translation, analysed by polysome profiling (see section 4. 3. 2.), it was important to determine the correct concentration of rapamycin to use to inhibit mTORC1 activity. MCF7 cells were treated with 1, 10, 25 or 50nM rapamycin, equivalent DMSO or left untreated for three hours prior to cell lysis and western blotting. Western blotting was used to determine the phosphorylation status of P70S6K and 4E-BP1, known downstream targets of mTORC1. In the untreated or DMSO (solvent control) treated samples P70S6K was phosphorylated at Thr 389 and 4E-BP1 was in the hyperphosphorylated state (Figure 4-1), both indicated that mTORC1 was active. Following treatment with rapamycin, at all concentrations, there was a significant reduction in p70S6K phosphorylation and 4E-BP1 migrated further through the gel that indicated hypophosphorylation (Figure 4-1). Therefore mTORC1 was significantly inhibited after three hours of incubation with as little as 1nM rapamycin.

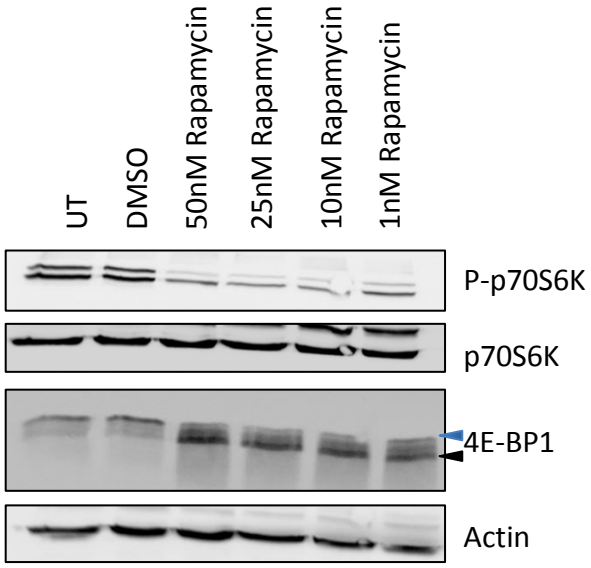

Figure 4-1: mTORC1 Inhibition by Rapamycin

MCF7 cells were either untreated (UT), treated with rapamycin at the concentrations indicated or treated with DMSO (equivalent to the highest concentration of rapamycin) for three hours prior to cell lysis and western blotting. Hyperphosphorylation of 4E-BP1 is indicated by the blue arrow, while hypophosphorylation is indicated by the black arrow. Blot is representative of three independent experiments.

4. 3. 2. Role of mTORC1 in PEITC-Induced Inhibition of mRNA Translation

To investigate whether the mTORC1 pathway was responsible for the profound decreased in global mRNA translation in response to PEITC treatment the mTORC1 pathway was inhibited with rapamycin prior to polysome analysis. MCF7 cells were treated with rapamycin (25nM) for one, two or three hours prior to polysome profiling. This time course was used to ensure incorporation into the cells as well as inhibition of mTORC1 signalling (section 4. 3. 1.). Following treatment with rapamycin, PEITC (20µM) or DMSO (equivalent to the highest concentration) polysome profiling was undertaken.

The results confirmed that PEITC maintained mRNA translation inhibition at two and three hours, again showing the characteristic accumulation in the 80S peak and absence of polysome peaks (Figure 4-2). Incubation with rapamycin for one, two or three hours had minimal effect on mRNA translation, as polysome peaks were still present, with only a slight increase in 80S accumulation seen after three hours incubation (Figure 4-2). To identify any changes in amplitude of the peaks following rapamycin treatment the profiles were overlaid (Figure 4-3). There appeared to be a slight increase in the 80S peak after three hours incubation with rapamycin but there was no decrease in the polysome peaks indicating that active translation had still occurred (Figure 4-3), unlike the profiles seen in response to PEITC treatment. This indicated that mTORC1 inhibition alone was insufficient to decrease mRNA translation to the same extent as PEITC treatment. Therefore multiple pathways are likely to be involved in the inhibition of mRNA translation in response to PEITC treatment.

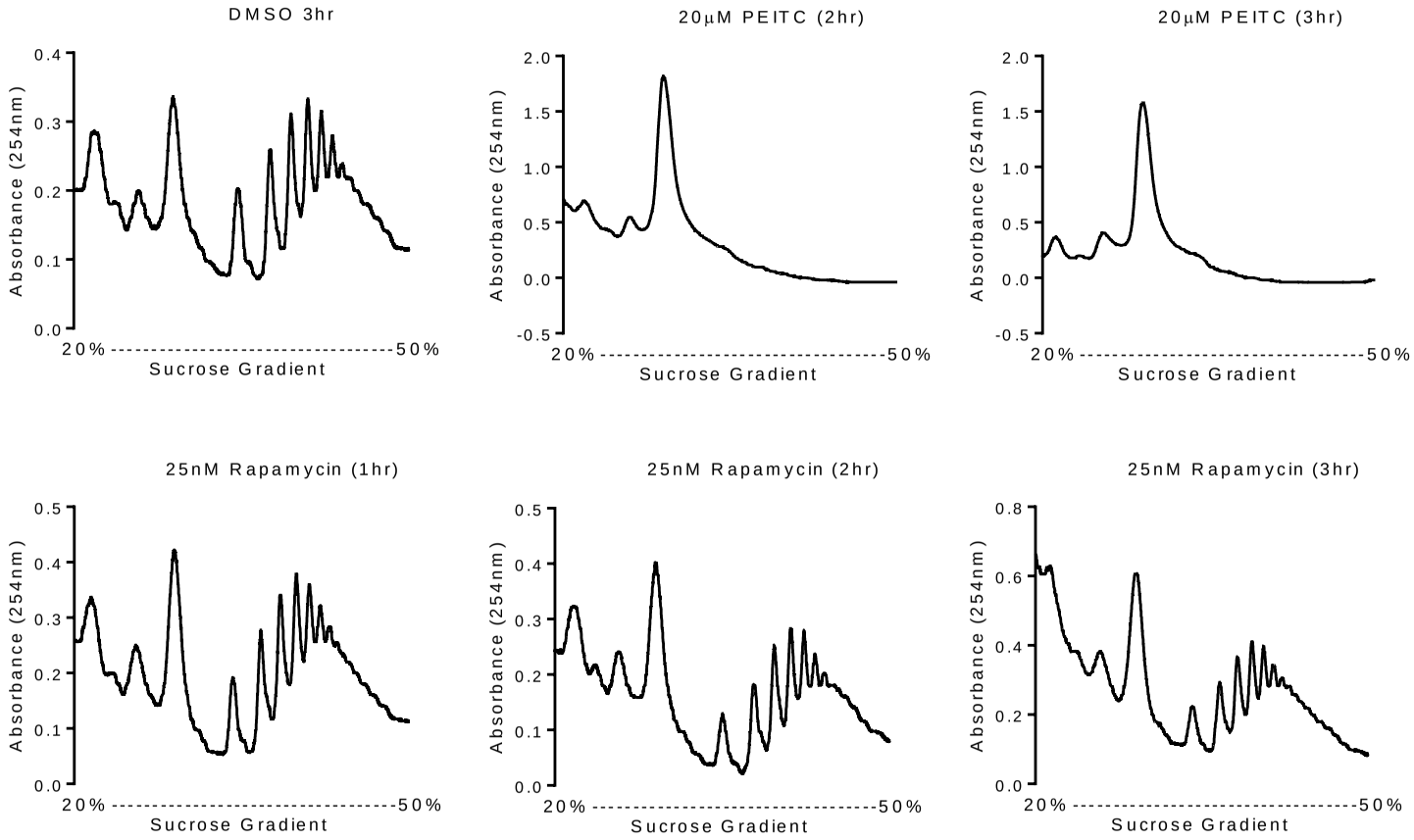

Figure 4-2: Effect of mTORC1 Inhibition on Polysome Profiling

MCF7 cells were treated with 20μM PEITC, 25nM Rapamycin or equivalent DMSO for one, two or three hours prior to polysome profiling. Data presented are representative of three independent repeats.

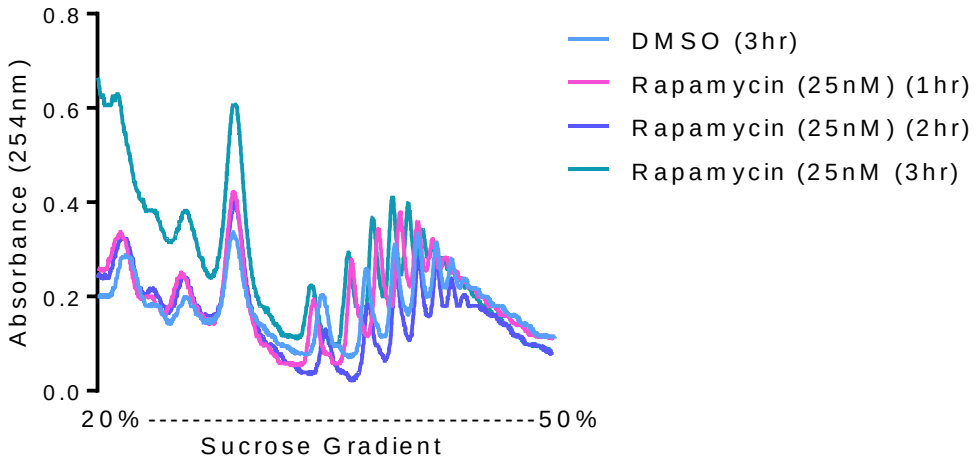

Figure 4-3: Overlay of Polysome Profiles Following mTORC1 Inhibition

MCF7 cells were treated with 25nM Rapamycin or equivalent DMSO for one, two or three hours prior to polysome profiling. Profiles were overlaid to compare any changes in amplitude of peaks. Data presented is representative of three independent repeats.

4. 3. 3. Determining Phosphorylation Status of eIF2α Following PEITC Treatment

Having established that mTORC1 inhibition alone was not responsible for the PEITC-induced decrease in mRNA translation, I next analysed the effect of PEITC on the eIF2α pathway. To determine whether eIF2α was involved in the response to PEITC MCF7 cells were treated with PEITC (ranging from 10-20µM), DMSO (equivalent to 20µM) or untreated prior to western blotting. A time course was carried out with PEITC treatment from five minutes to two hours. The phosphorylation status of eIF2α at Ser51 was analysed by western blotting, as phosphorylation of Ser51 inhibits TC formation and ultimately translation (see sections 1. 3. 7. 2. and 1. 3. 7. 3.). Untreated samples or DMSO treatment, at all-time points, produced low/undetectable levels of eIF2α phosphorylation (Figure 4-4). Following 5 to 15 minutes of treatment with PEITC (20µM) there was an increase in phospho-eIF2α levels. The phospho-eIF2α levels increased over time with PEITC treatment (20µM) and dose dependently increased at 30 minutes (Figure 4-4), with an average 14-fold increase in phosphorylation of eIF2α seen at 30 minutes with 20µM PEITC treatment ($p=0.0551$, $n=9$, paired t-test). Therefore PEITC induced the phosphorylation of eIF2α, which could provide a mechanism for decreased mRNA translation.

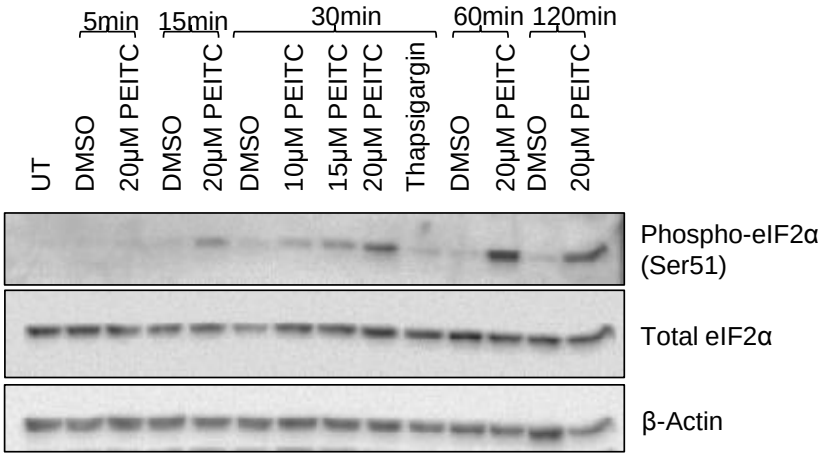

Figure 4-4: Phosphorylation Status of eIF2α Following PEITC Treatment

MCF7 cells were either untreated (UT), treated with PEITC at the indicated doses or DMSO equivalent to 20μM (blank lane contains lysate of cells treated with a compound that had no effect on eIF2α phosphorylation). Western blotting was carried out and eIF2α phosphorylation was detected using rabbit anti-phospho-eIF2α (ser51), alongside rabbit anti-total eIF2α and rabbit anti-β actin antibodies. Representative blot from three independent experiments.

4. 3. 4. Role of PERK in PEITC-Induced Phosphorylation of eIF2α

Having established that PEITC induced the phosphorylation of eIF2α it was important to determine the mechanism for increased eIF2α phosphorylation. To determine that PEITC activated one of the four eIF2α kinases (PKR, PERK, GCN2 and HRI) cells were treated with PEITC (20µM) in combination with 2-aminopurine (2-AP). 2-AP has been shown to inhibit the ATP dependent phosphorylation of eIF2α catalysed by PKR, HRI (Jarrous et al., 1996; Pervin et al., 2008) and PERK (Wu et al., 2008). Untreated and solvent control treated cells (DMSO, solvent for PEITC, and PBS:glacial acetic acid (GAA), solvent for 2-AP) had undetectable levels of eIF2α phosphorylation (Figure 4-5). Whereas treatment with PEITC (20µM) and PEITC in combination with PBS:GAA (solvent control for 2-AP) resulted in a significant increase in eIF2α phosphorylation (Figure 4-5A), confirmed by densitometry (Figure 4-5B). Treatment with PEITC (20µM) in combination with either 0.5mM or 1mM 2-AP resulted in undetectable eIF2α phosphorylation levels (Figure 4-5A). Treatment with 2-AP significantly prevented PEITC-induced eIF2α phosphorylation, analysed by densitometry (Figure 4-5B), therefore PEITC activated one (or more) of the eIF2α kinases.

Cells treated with PEITC (20µM) in the presence or absence of 2-AP were also analysed for PERK levels. It was hypothesised that PERK was the kinase activated due to the fact that PEITC is known to induced oxidative stress, due to depleted glutathione levels (Cavell et al., 2011). This may activate the unfolded protein response, which in turn would activate PERK. Also PEITC can covalently bind to thiol groups which may initiate the unfolded protein response or cause endoplasmic reticulum stress, again a trigger to activate PERK. PERK activation occurs by phosphorylation that can be detected by immunoblotting as a slower migrating form. Treatment with PEITC resulted in a slower migrating form of PERK, indicated by the black arrow (Figure 4-5). The presence of the slower migrating form was maintained in the presence of the solvent control, PBS:GAA, in combination with PEITC treatment. Combination treatment with PEITC and 1mM 2-AP resulted in a shift back to the basal state of PERK, indicated by the blue arrow (Figure 4-5A), suggesting PERK could be involved in PEITC-induced phosphorylation of eIF2α.

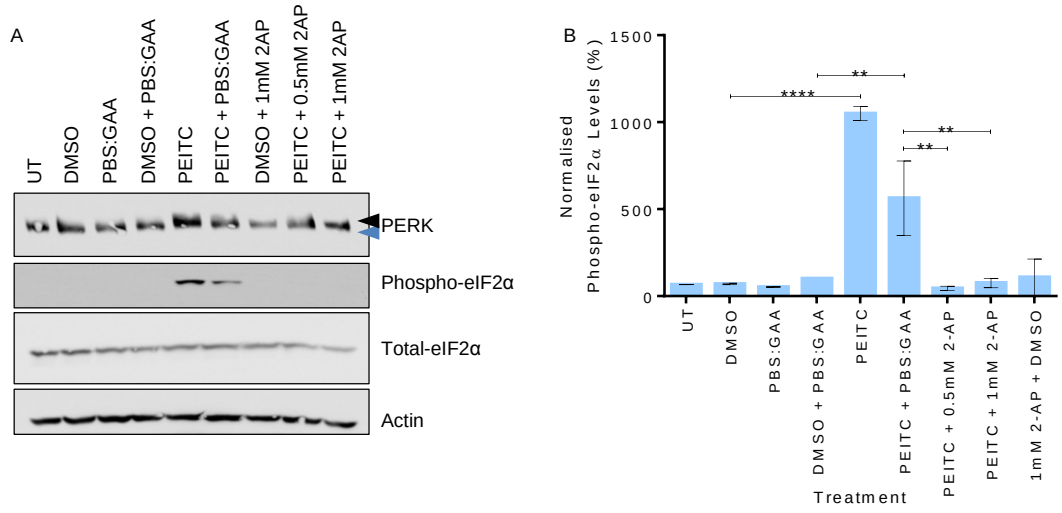

Figure 4-5: Effect of PEITC in Combination with 2-Aminopurine on eIF2α Phosphorylation

MCF7 cells were untreated (UT) or treated with 20μM PEITC in combination with 2-aminopurine or the solvent controls, DMSO and PBS: glacial acetic acid (PBS:GAA), respectively, for 30 minutes prior to cell harvest. (A) Protein levels of PERK, phospho-eIF2α, total eIF2α and β-actin. Data represents two independent experimental repeats. Blue arrow indicates basal PERK and the black arrow indicates a slower migrating form of PERK. (B) Densitometry data of phospho-eIF2α normalised to total eIF2α, relative to DMSO + PBS:GAA set to 100%. Bars represent the average expression and error bars indicate the standard deviation, n=2. Statistically significant data is indicated, **≤0.01, ****≤0.001, One-way ANOVA GraphPad Prism 6.

4. 3. 5. Effect of PEITC in PERK Knock Down Cells

The involvement of PERK in PEITC-induced eIF2α phosphorylation required further investigation. To determine whether PERK was essential for eIF2α phosphorylation in response to PEITC treatment PERK was knocked down using siRNA targeted against PERK. Knock down of PERK was allowed to occur for 48 hours prior to treatment with PEITC (20μM) for five minutes to one hour. Transfection of cells with control siRNA had no effect on PERK levels. Whereas transfection with siRNA targeted against PERK resulted in a significant decrease in PERK levels, although a small proportion of PERK (average 26%) was still detectable (Figure 4-6). In control siRNA transfected cells PEITC increased eIF2α phosphorylation in a time dependent manner (Figure 4-6). The increase in eIF2α phosphorylation was slightly decreased in PERK siRNA transfected cells (Figure 4-6). The ability of the cells to phosphorylate eIF2α in response to PEITC in PERK knock down cells indicated that either the knock down of PERK was insufficient or multiple kinases were involved.

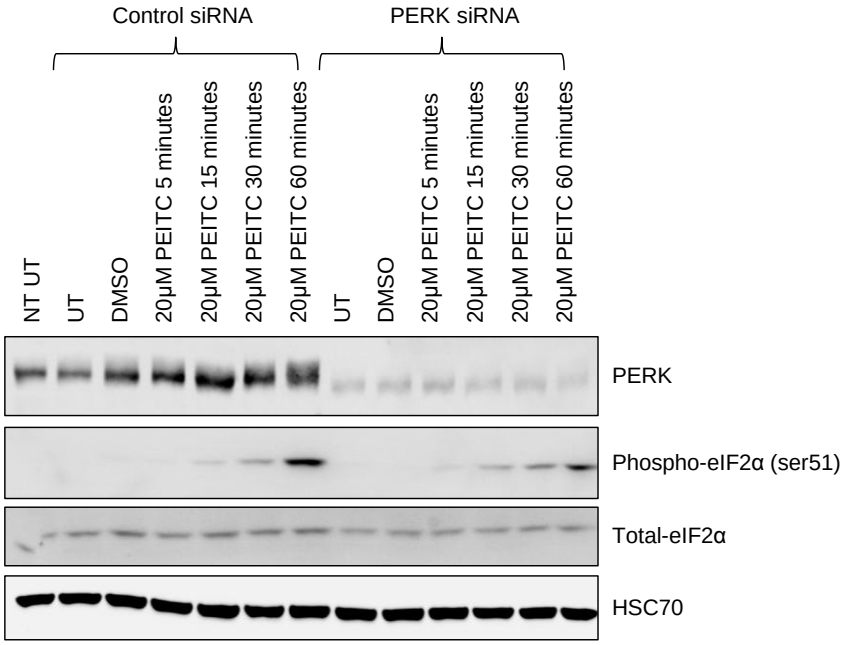

Figure 4-6: Effect of PEITC on eIF2α Phosphorylation in PERK Knock Down Cells

MCF7 cells were reverse transfected with 50μM siRNA targeted against PERK or control siRNA or non-transfected (NT) and incubated for 48 hours. Cells were then treated with 20μM PEITC for the times indicated, equivalent DMSO for one hour or untreated (UT) prior to cell harvest. Representative western blot from two independent experiments, showing levels of PERK, eIF2α (Ser51 phosphorylation), total eIF2α and HSC70, as a loading control.

4. 3. 6. Analysing the Involvement of HRI in PEITC-Induced eIF2α Phosphorylation

I next investigated whether HRI was involved in the phosphorylation of eIF2α in response to PEITC. HRI was the next logical kinase to analyse as HRI is activated by heme deficiency, and due to the role PEITC had in inhibiting angiogenesis this seemed to be an appropriate kinase to investigate. It was originally thought that HRI was only present in hemeocytes but has also been shown to be present in other tissues including breast epithelial cells (Pervin et al., 2008). HRI was the next logical kinase to investigate as PKR is activated by viral infection and GCN2 is activated by amino acid deficiency, therefore these were unlikely targets as the cells were uninfected and the media contained an excess of amino acids. A specific inhibitor of HRI, hemin chloride, was used to determine the involvement of HRI in the cellular response to PEITC. Hemin chloride was added to the media of cells for two passages, to enable entry of hemin chloride into the cells due to the large size of hemin chloride. After hemin chloride (25 or 50µM) treatment for two passages, or solvent control 0.1M NaOH equivalent to 50µM, cells were treated with PEITC (20µM) for one hour prior to western blotting. Detection of HRI inhibition was difficult to determine due to the poor specific nature of the HRI antibody available (Figure 4-7). HRI is a 72kDa protein, although the antibody available bound to multiple proteins of different sizes, which could be the dimerization product of HRI, although it is unclear which band corresponds to HRI specifically (Figure 4-7). Untreated and solvent control treated cells had undetectable levels of eIF2α phosphorylation. Cells treated with PEITC in the presence or absence of hemin chloride resulted in eIF2α phosphorylation (Figure 4-7). This result indicated that either HRI was not inhibited sufficiently, was not involved in PEITC-induced eIF2α phosphorylation or multiple kinases were involved.

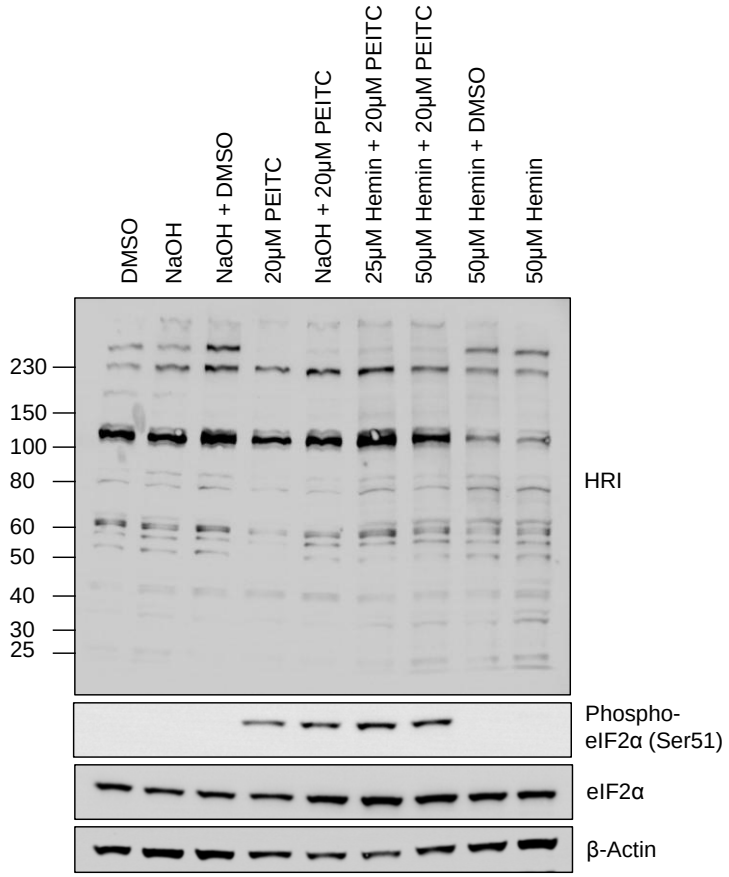

Figure 4-7: Effect of PEITC and HRI Inhibition on eIF2α Phosphorylation

MCF7 cells were treated with Hemin Chloride (hemin) at the doses indicated, or equivalent sodium hydroxide (0.1M NaOH) equivalent to 50µM for two passages prior to the addition of 20µM PEITC or equivalent DMSO for one hour prior to cell harvest. Western blots represent three independent experiments.

4. 3. 7. Role of Multiple Kinases in eIF2α Phosphorylation in Response to PEITC Treatment

Individual inhibition or knock down of PERK and HRI was insufficient to block PEITC-induced eIF2α phosphorylation. To investigate whether multiple kinases were involved in the response to PEITC, cells were treated with hemin chloride and were transfected with siRNA targeted against PERK. PERK knock down was allowed to occur for 48 hours in the presence of hemin chloride prior to treatment with PEITC (20μM) for 30 minutes. PEITC treatment for 30 minutes had previously been shown to be sufficient to induce robust eIF2α phosphorylation (Figure 4-4). Treatment with hemin chloride resulted in a decrease in the higher band of HRI compared to NaOH control treated cells (Figure 4-8). But as mentioned previously the non-specific nature of this antibody made it not possible to determine whether this indicated decreased HRI activity. Transfection of PERK siRNA resulted in a significant decrease in total PERK levels compared to control siRNA transfected cells in NaOH control treated cells (Figure 4-8). Whereas in hemin chloride treated cells only a slight decrease in total PERK levels was detected in PERK siRNA transfected cells compared to control siRNA transfected cells (Figure 4-8). This may suggest that the effectiveness of the siRNA was decreased with hemin chloride treatment. Treatment with PEITC in all cases resulted in the phosphorylation of eIF2α (Figure 4-8).

Due to the issue of specificity of eIF2α kinase inhibitors it was difficult to determine the kinase responsible for eIF2α phosphorylation as a result of PEITC treatment. Stable knock out cells for each of the individual kinase would have been required to determine whether one kinase specifically was responsible for the response to PEITC. Although, it is possible that PEITC activated multiple kinases to ensure phosphorylation of eIF2α, or PEITC may have inhibited the phosphatase responsible for removing the phosphate group from eIF2α. From these results it was clear that eIF2α was robustly phosphorylated in response to PEITC treatment but whether this phosphorylation was essential for decreased translation in response to PEITC was not yet known.

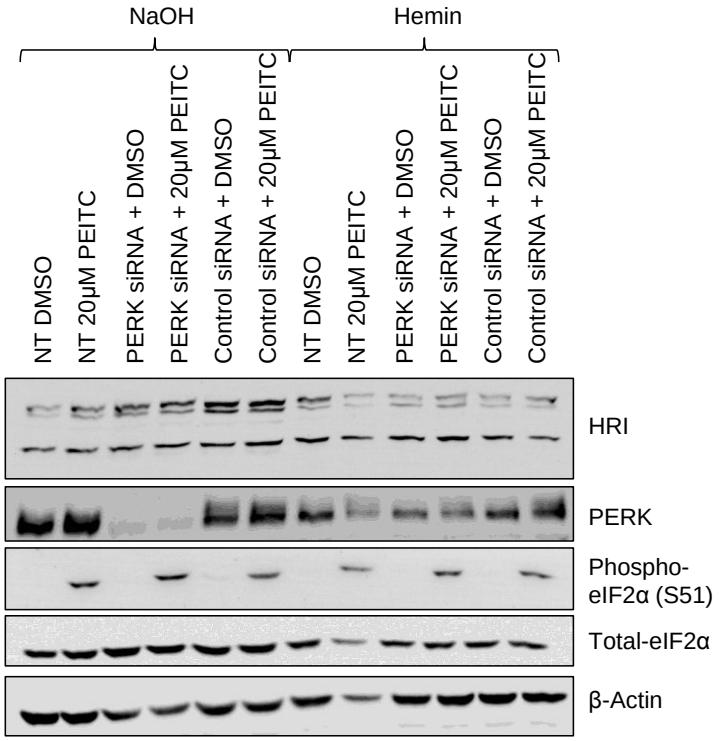

Figure 4-8: Effect of PEITC in PERK Knock Down and HRI Inhibited MCF7 Cells

MCF7 cells were treated with 50µM Hemin Chloride or equivalent sodium hydroxide (0.1M NaOH) for two passages prior to reverse transfection with 50µM siRNA targeted against PERK or control siRNA. Cells were incubated for a further 48 hours in the presence of 50µM Hemin Chloride or NaOH. Cells were then treated with 20µM PEITC or equivalent DMSO for 30 minutes prior to cell harvest. Western blot representative of two independent experiments.

4. 3. 8. Importance of eIF2α Phosphorylation for PEITC-Induced Inhibition of mRNA Translation

To further investigate the involvement of eIF2α phosphorylation in the response to PEITC treatment it was important to determine whether eIF2α phosphorylation was essential for decreased mRNA translation. Non-phosphorylatable eIF2α mouse embryonic fibroblasts (MEFs) were used to investigate the involvement of eIF2α phosphorylation. These stable knock in MEFs were homozygous for the eIF2α Ser51Ala mutation, which prevented eIF2α phosphorylation at this site. Non-phosphorylatable MEFs (S51A) and MEFs containing wild type eIF2α (S51S MEFs) (Scheuner et al., 2001) were treated with PEITC (20μM) for five minutes to one hour, treated with equivalent DMSO or left untreated prior to western blotting. Levels of phospho-PERK were analysed to measure activated PERK, which was not carried out in previous experiments due to the anti-phospho-PERK antibody only being sensitive to mouse PERK. Non-phosphorylatable eIF2α MEFs had elevated levels of phospho-PERK, or activated PERK, compared to the wild type MEFs (Figure 4-9). This could be a compensatory mechanism as phosphorylation of eIF2α is essential for the cell to respond to cellular stress and alter translation accordingly. Hence as the non-phosphorylatable cells cannot phosphorylate eIF2α PERK activity may be enhanced. PEITC induced the phosphorylation of eIF2α in the wild type MEFs (Figure 4-9), just like in MCF7 cells. Unlike non-phosphorylatable eIF2α MEFs that could not be phosphorylated on eIF2α in response to PEITC treatment (Figure 4-9).

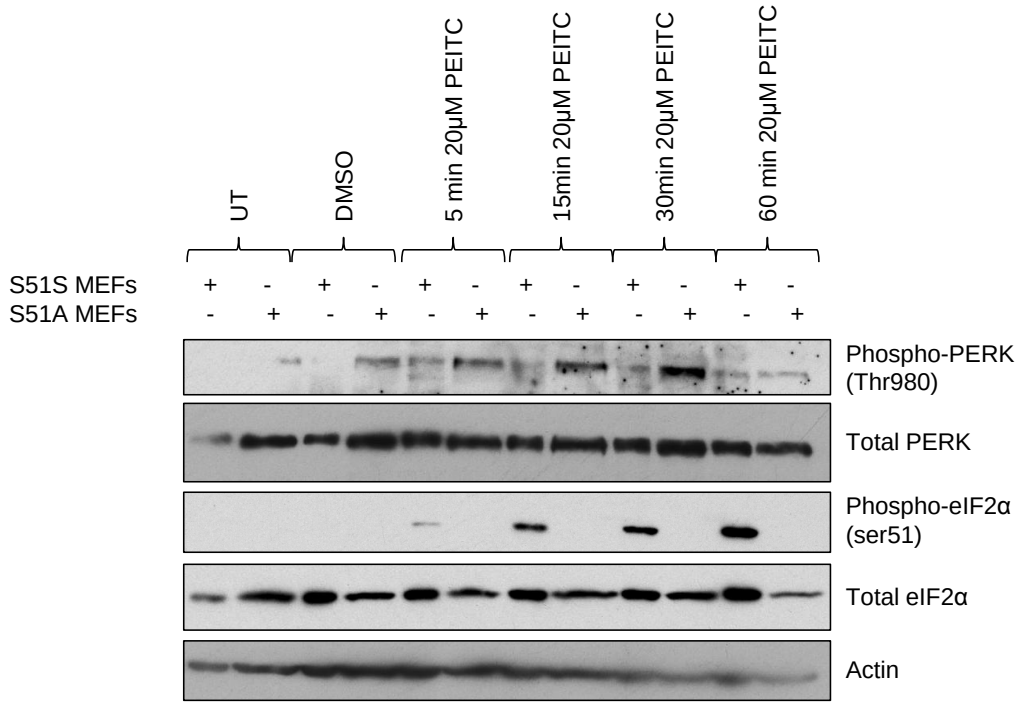

Figure 4-9: Phosphorylation Status of eIF2α in Non-Phosphorylatable eIF2α MEFs

Knock in eIF2α non-phosphorylatable MEFs (S51A) and control MEFs (S51S) were either untreated (UT), treated with 20μM PEITC for the times indicated or treated with equivalent DMSO for 60 minutes. Protein levels of phospho-PERK, total PERK, phospho-eIF2α (Ser51), total eIF2α and β-actin were analysed, blot represents three independent experiments.

Following confirmation that non-phosphorylatable eIF2α MEFs could not be phosphorylated in response to PEITC treatment, analysis of translation, by polysome profiling, was carried out. Wild type and non-phosphorylatable eIF2α MEFs were treated with PEITC (20μM), equivalent DMSO or left untreated for 30 minutes, which was sufficient to phosphorylate eIF2α in wild type MEFs (Figure 4-9), prior to polysome profiling. The wild type MEFs produced similar polysome profiles to MCF7 cells; untreated and DMSO treated samples had 40, 60 and 80S peaks followed by multiple polysome peaks (Figure 4-10). Treatment with PEITC in wild type MEFs resulted in a severe decrease in polysome peaks and a large accumulation in the 80S peak (Figure 4-10). This indicated that the wild type MEFs were also susceptible to decreased translation in response to PEITC treatment, similar to that seen in MCF7 cells. Untreated and DMSO treated non-phosphorylatable eIF2α MEFs produced very similar polysome profiles to the wild type MEFs. In non-phosphorylatable eIF2α MEFs PEITC treatment did not result in a collapse of the polysome peaks and there was no accumulation in the 80S peak (Figure 4-10). This result indicated that in the absence of eIF2α phosphorylation PEITC could not inhibit translation.

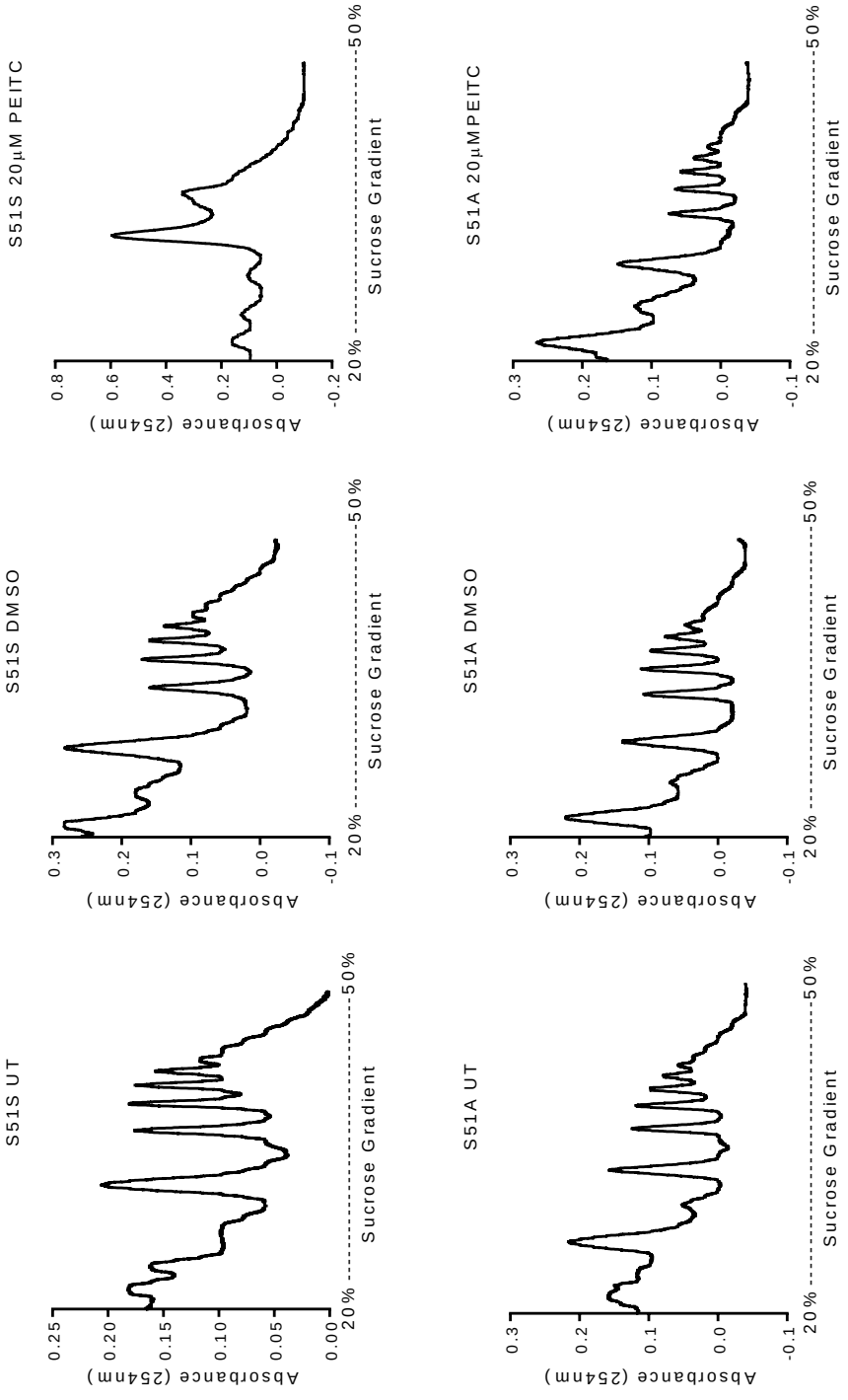

Figure 4-10: Polysome Profiling of Non-Phosphorylatable eIF2α MEFs in Response to PEITC Treatment

Knock in eIF2α non-phosphorylatable MEFs (S51A) and wild type (S51S) MEFs were either untreated (UT), treated with 20µM PEITC or equivalent DMSO for 30 minutes prior to cell lysates being collected and polysome profiling performed. Data represents three independent experiments.

4. 3. 9. Effect of PEITC on Stress Granule Formation

The phosphorylation of eIF2α is known to reduce translation initiation but eIF2α phosphorylation is also known to be important in the formation of stress granules. Stress granules are believed to enable the cell to react to transient cellular stress by aggregating stalled pre-initiation complexes. Stress granules are storage sites for mRNA and occur following eIF2α phosphorylation at Ser51, which acts as a competitive inhibitor preventing ternary complex (TC) recycling (see section 1. 3. 7. 2.) (Chernov et al., 2009; Mathews et al., 2007; Mokas et al., 2009). Stress granules are important cytoplasmic bodies as they are sites of mRNA storage and stability and may promote translation of certain mRNA molecules that may enable the cell to survive and respond to the cellular stress (Thomas et al., 2011).

Previous results indicated PEITC inhibited mRNA translation due to eIF2α phosphorylation (Figure 4-10) therefore investigation into the formation of stress granules in response to PEITC treatment was carried out. Stress granules were identified by immunofluorescence using two known stress granule markers; TIA-1 and eIF3. MCF7 cells were treated with PEITC (20μM), equivalent DMSO or untreated for 30 minutes prior to immunofluorescence analysis. Immunofluorescence visualisation following treatment with DMSO or untreated cells showed eIF3 was evenly distributed throughout the cytoplasm and did not enter the nucleus, visualised using DAPI nuclear stain (Figure 4-11). TIA-1 in untreated and DMSO treated cells was evenly distributed in the cytoplasm with some localisation also found in the nucleus (Figure 4-11). With PEITC treatment eIF3 and TIA-1 were not evenly distributed throughout the cytoplasm, there were sites of intense staining (Figure 4-11). Merging of the eIF3 and TIA-1 images indicated that these sites of intense staining were in a similar location, which suggested that stress granules were present following PEITC treatment.

To confirm that the staining seen following PEITC treatment was due to stress granule assembly, confocal microscopy was carried out. Following PEITC (20μM) treatment for 30 minutes in MCF7 cells the localisation of eIF3 and TIA-1 was analysed. Analysis of a single z-stack (1μm thick) enabled the co-localisation of eIF3 and TIA-1 to be analysed. Treatment with PEITC resulted in eIF3 and TIA-1 to

co-localise within the same z-stack (Figure 4-12). This indicated that eIF3 and TIA-1 were present at the same point within a cell. This was further confirmed by measuring the intensity of the signal produced by eIF3 and TIA-1 individually. Within a single z-stack where eIF3 signal intensity increased TIA-1 signal intensity increased (Figure 4-13). Therefore the intense staining spots of eIF3 and TIA-1, visualised by immunofluorescence (Figure 4-11) occurred due to the formation of stress granules following PEITC treatment.

4. 3. 10. Kinetics and Concentration Dependency of PEITC-Induced Stress Granule Formation

The production of stress granules in response to PEITC treatment had not previously been investigated and further investigation was required to determine whether the formation of stress granules was dose and time dependent. Thapsigargin (TG) was used as a positive control for stress granule assembly. MCF7 cells were treated with PEITC, TG (40µM), equivalent DMSO or untreated for five minutes to two hours prior to immunofluorescence. Within five minutes of treatment no/very few stress granules were present regardless of treatment (Figure 4-14). Treatment of TG for 15 minutes resulted in increased stress granule assembly, with multiple stress granules seen in some cells (Figure 4-14). Treatment with PEITC (20µM) for 15 minutes resulted in increased stress granule formation in the majority of cells (Figure 4-14). Whereas treatment with DMSO for 15 minutes did not induce the formation of stress granules (Figure 4-14).

Following 30 minutes of treatment DMSO had not promoted stress granule assembly, whereas the majority of cells treated with TG had formed stress granules (Figure 4-15). Treatment with PEITC had induced the formation of stress granules to a similar extent as TG and dose dependently increased the number of stress granules per cell as well as the number of cells that contained stress granules (Figure 4-15 and Table 4-1). The formation of stress granules was maintained up to two hours of treatment with PEITC without any other morphological changes to the cell

detected, with DMSO treatment up to two hours having little effect on stress granule formation (Figure 4-16).

Table 4-1: Stress Granule Count in Response to 20µM PEITC Treatment for 30 Minutes

Condition	Number of Cells	Total Number of Stress Granules	Stress Granules per Cell
DMSO	378	25	<1
PEITC	425	3992	10

4. 3. 11. Involvement of eIF2α Kinases in PEITC-Induced Stress Granule Assembly

PEITC induced the formation of stress granules, which are known to form as a consequence of eIF2α phosphorylation as well as independently of eIF2α phosphorylation (Kedersha et al., 2002). In order to determine whether stress granules produced in response to PEITC treatment were dependent on eIF2α phosphorylation MCF7 cells were treated with PEITC (20µM) in combination with 2-AP (0.5 or 1mM), which was shown previously to prevent PEITC-induced eIF2α phosphorylation (Figure 4-5). Treatment with PEITC for 30 minutes resulted in the formation of stress granules, whereas treatment with the solvent controls, DMSO or PBS:GAA alone or in combination had no effect on stress granule formation (Figure 4-17). Combined treatment of PEITC and the solvent control PBS:GAA still enabled stress granules to form (Figure 4-17). Treatment with PEITC in combination with either 0.5mM or 1mM 2-AP prevented the formation of stress granules (Figure 4-17). These results indicated that PEITC enhanced stress granule assembly in a phospho-eIF2α dependent manner.

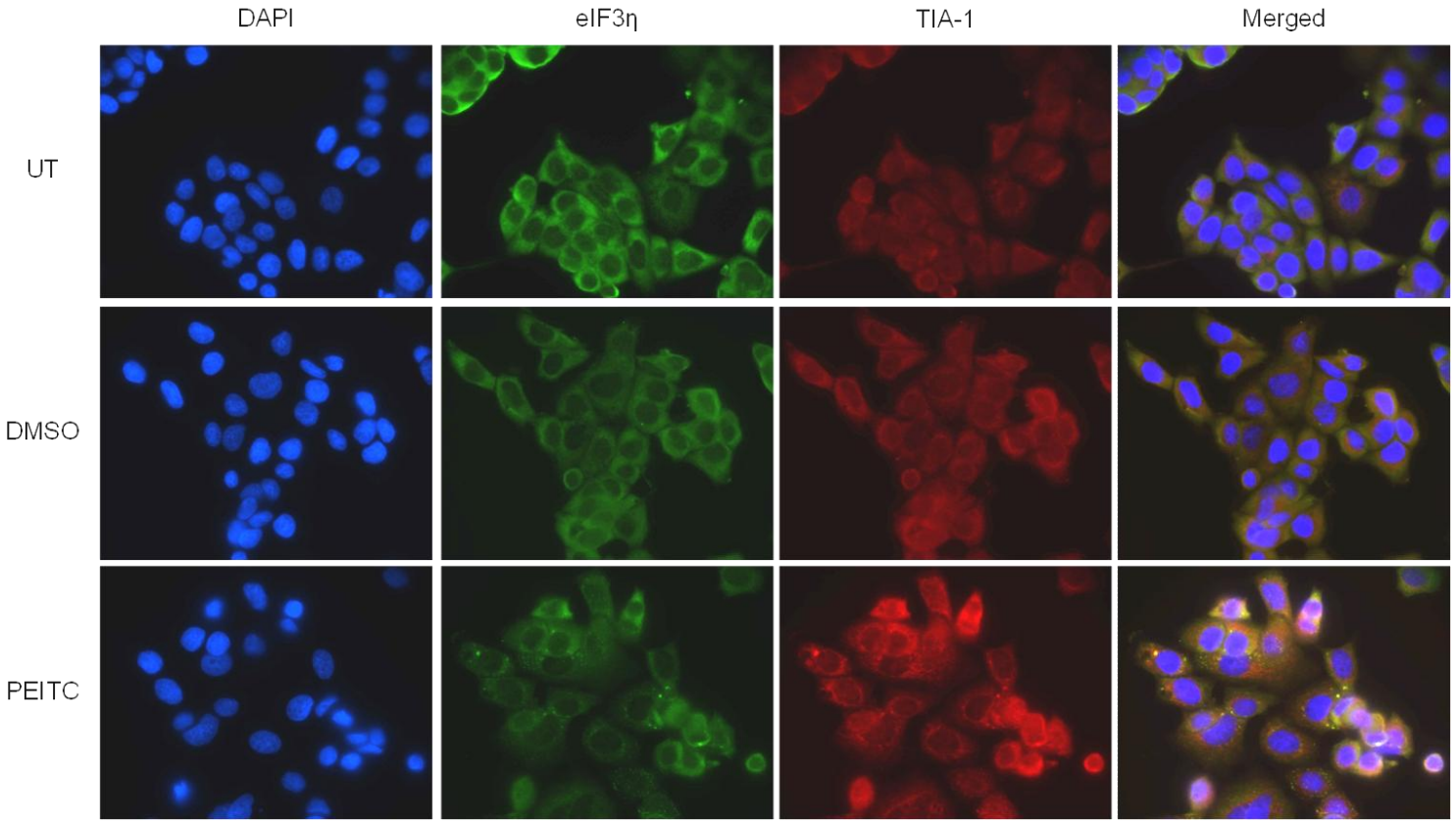

Figure 4-11: Effect of PEITC on Stress Granule Formation

MCF7 cells were either untreated, treated with 20μM PEITC or equivalent DMSO for 30 minutes prior to fixing and staining with goat anti-eIF3 and mouse anti-TIA-1 antibodies. Secondary rabbit anti-goat FITC labelled antibody was used to detect eIF3 and donkey anti-mouse Alex fluor 594 was used to detect TIA-1. Representative images from three independent experiments.

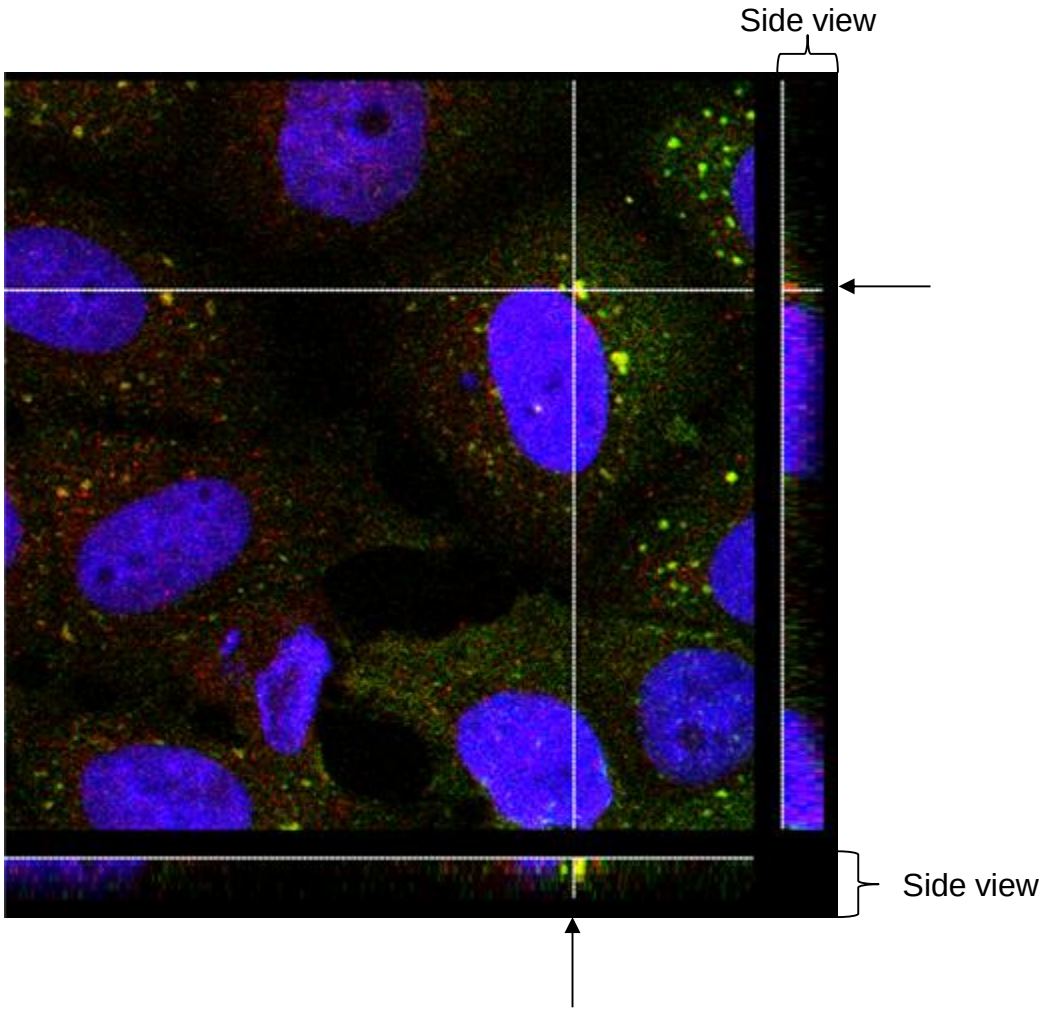

Figure 4-12: Confocal Analysis of Stress Granules Produced by PEITC Treatment

MCF7 cells were treated with 20μM PEITC for 30 minutes prior to confocal analysis. Stress granules were marked with goat anti-eIF3 and mouse anti- TIA-1, FITC labelled rabbit anti-goat secondary was used to detect eIF3, while Alexa Fluor 594 labelled donkey anti-mouse was used to detect TIA-1. Data represents four fields of view from a single z-stack. Side views indicate the thickness of the z-stack and indicate the position of eIF3 and TIA-1 within the Z-stack.

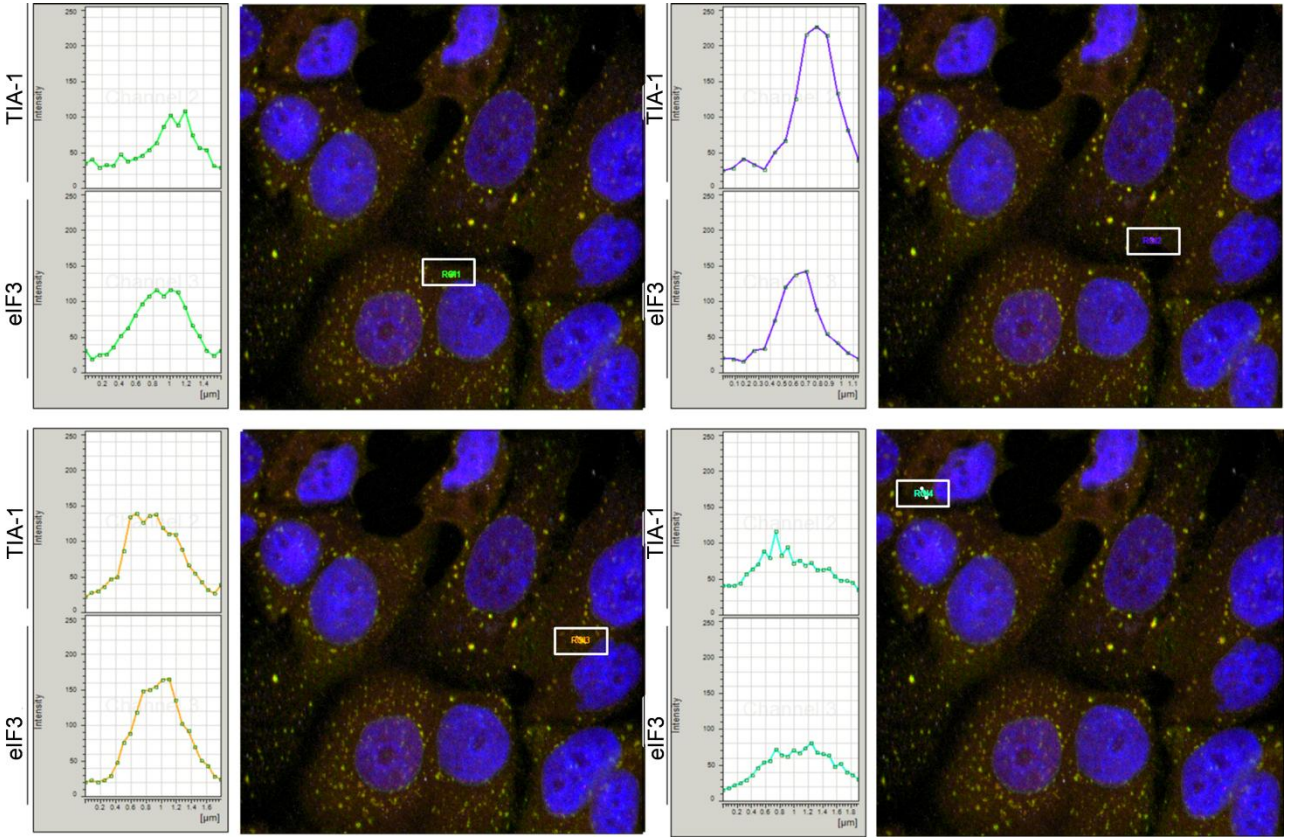

Figure 4-13: Alignment Data for Stress Granules Induced by PEITC

MCF7 cells were treated with 20µM PEITC of 30 minutes before staining for stress granules. Stress granules were marked with goat anti-eIF3 and mouse anti- TIA-1, FITC labelled rabbit anti-goat secondary was used to detect eIF3, while Alexa Fluor 594 labelled donkey anti-mouse was used to detect TIA-1. Stress granules were randomly selected and the intensity of eIF3 and TIA-1 staining was quantified in the graphs to the left of each image, where the white box indicates which stress granules were selected.

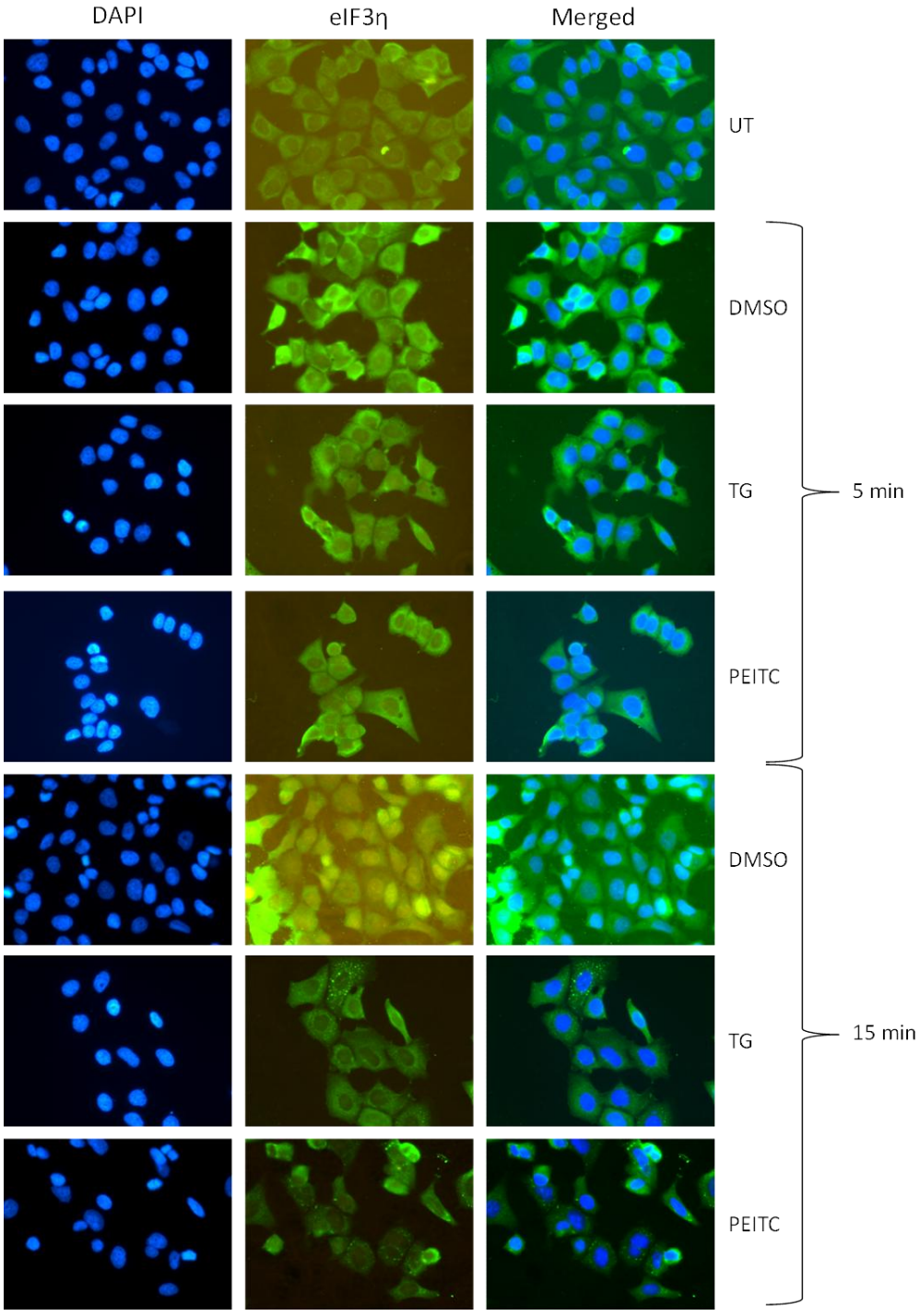

Figure 4-14: Stress Granule Formation in a Time Dependent Manner (Part 1 of 3)

MCF7 cells were either untreated, treated with 20µM PEITC, 40µM thapsigargin (TG) or equivalent DMSO for 5 or 15 minutes, as indicated, prior to fixing and staining with goat anti-eIF3 antibody. Secondary rabbit anti-goat FITC labelled antibody was used to detect eIF3 and DAPI was used as a nuclear stain. Images are representative from three independent experiments.

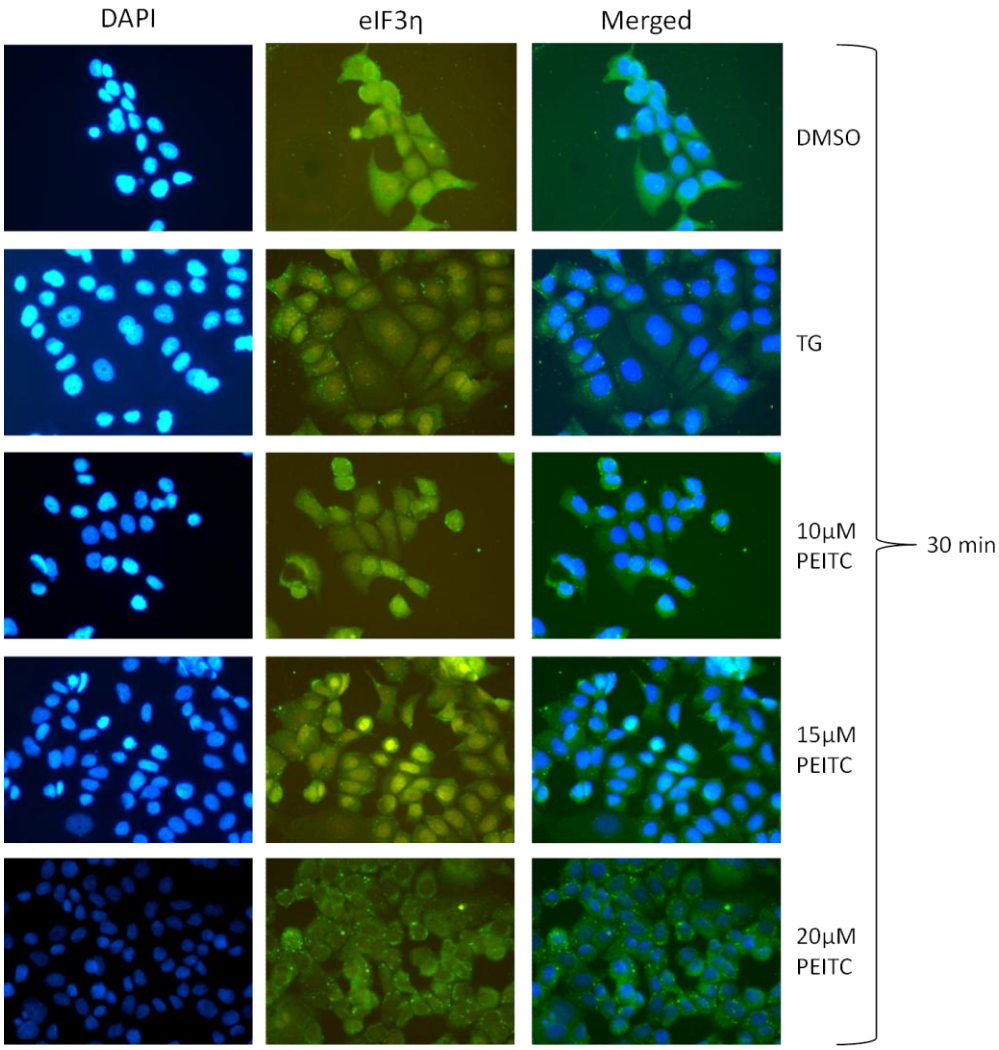

Figure 4-15: Stress Granule Formation in a Time Dependent Manner (Part 2 of 3)

MCF7 cells were either treated with the indicated doses of PEITC, 40μM thapsigargin (TG) or equivalent DMSO for 30 minutes, prior to fixing and staining with goat anti-eIF3 antibody. Secondary rabbit anti-goat FITC labelled antibody was used to detect eIF3 and DAPI was used as a nuclear stain. Images are representative from three independent experiments.

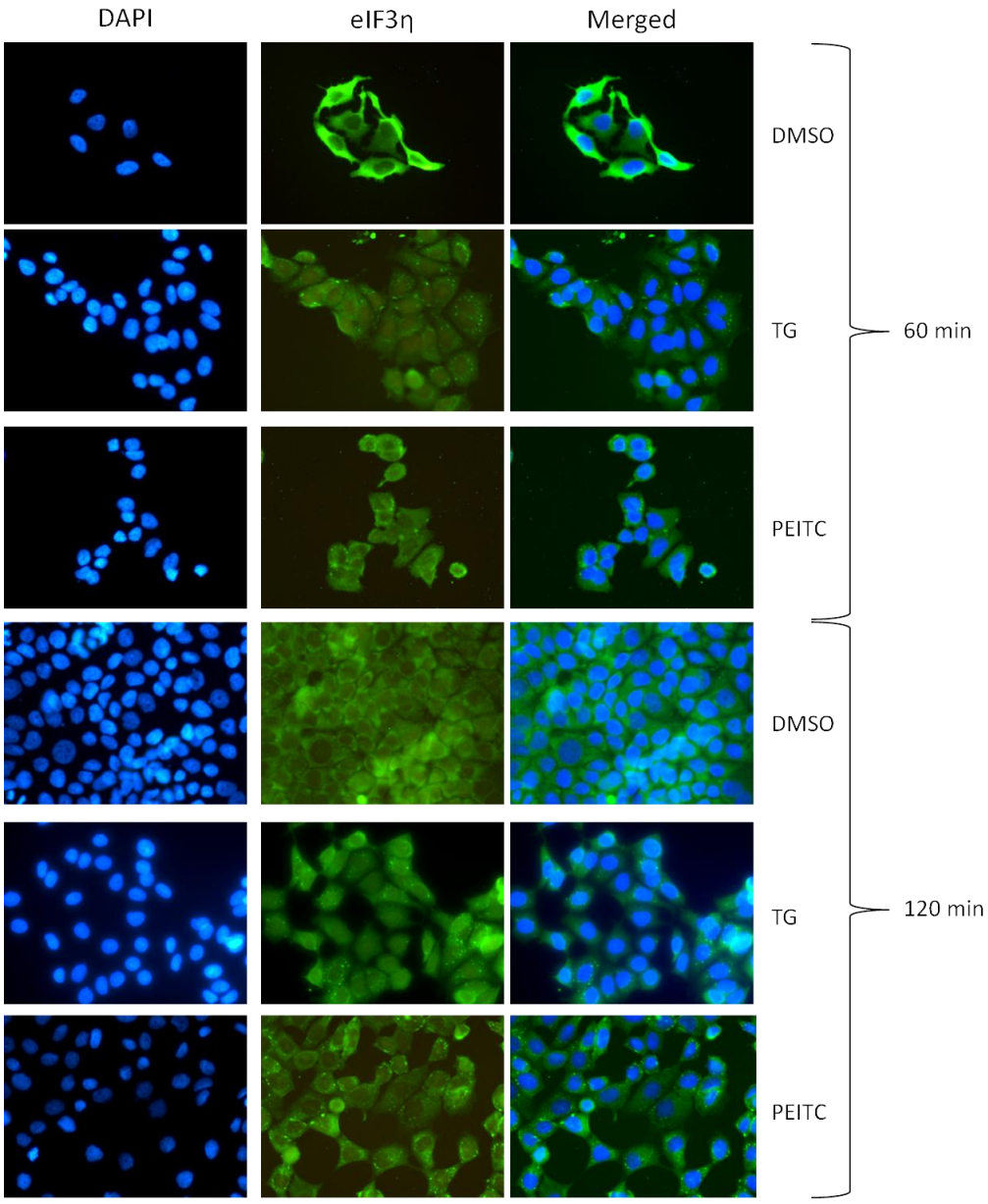

Figure 4-16: Stress Granule Formation in a Time Dependent Manner (Part 3 of 3)

MCF7 cells were either treated with 20µM PEITC, 40µM thapsigargin (TG) or equivalent DMSO for 60 or 120 minutes, as indicated, prior to fixing and staining with goat anti-eIF3 antibody. Secondary rabbit anti-goat FITC labelled antibody was used to detect eIF3 and DAPI was used as a nuclear stain. Images are representative from three independent experiments.

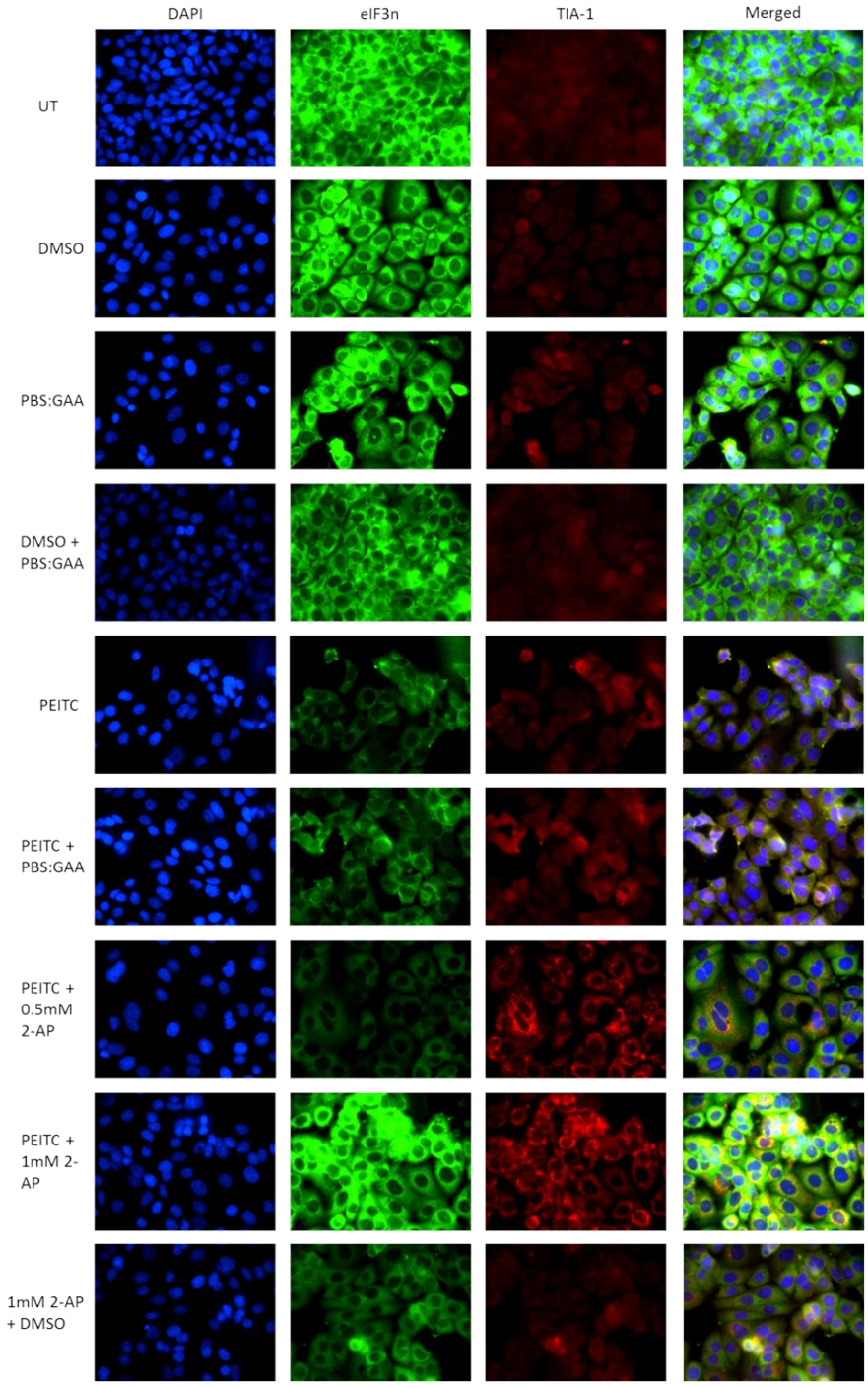

Figure 4-17: Involvement of eIF2α Phosphorylation in Stress Granule Formation

MCF7 cells were either untreated or treated with PEITC alone or in combination with 0.5mM or 1mM 2-Aminopurine, or the solvent controls (DMSO or PBS: glacial acetic acid (200:1)) for 30 minutes. Stress granules were marked with goat anti-eIF3 and mouse anti- TIA-1, FITC labelled rabbit anti-goat secondary was used to detect eIF3, while Alexa Fluor 594 labelled donkey anti-mouse was used to detect TIA-1. Data represents three independent experimental repeats.

4. 4. Summary of Main Findings

- mTOR inhibition was not sufficient to inhibit translation to the same extent as PEITC alone
- PEITC induced eIF2α phosphorylation (at Ser51)
- In the absence of eIF2α phosphorylation translation was not inhibited by PEITC
- PEITC induced the formation of stress granules in a phospho-eIF2α dependent manner.

4. 5. Discussion

It was important to determine the molecular target of PEITC in order to elucidate how PEITC manipulated translation. Previous work indicated that PEITC inhibited mTORC1 signalling (Cavell et al., 2012), which provided a possible mechanism for decreased translation. But inhibition of mTORC1 by rapamycin did not inhibit polysome formation to the same extent as PEITC treatment (Figure 4-2). Therefore even though PEITC inhibited mTORC1 this was not solely responsible for decreased translation and other pathways were involved in PEITC-induced translational repression. PEITC increased the phosphorylation of eIF2α on Ser51 in a dose and time dependent manner (Figure 4-4), providing an alternative mechanism for decreased translation in response to PEITC treatment. Phosphorylation of eIF2α is known to regulate translation initiation. Phospho-eIF2α acts as a competitive inhibitor of eIF2B, thereby preventing the exchange of GDP for GTP on eIF2α resulting in inhibition of ternary complex (TC) recycling (see section 1. 3. 2. and section 1. 3. 7. 2.). If eIF2α-GTP was phosphorylated translation initiation could occur but the subsequent round of initiation would be blocked, due to TC recycling, which could account for the fact that the polysome peaks diminished rather than immediately collapsed following PEITC treatment (Figure 3-4).

The ability of PEITC to phosphorylate eIF2α on Ser51 was essential for decreased translation (Figure 4-4, Figure 4-9 and Figure 4-10). The importance of PEITC-induced eIF2α phosphorylation was shown using non-phosphorylatable MEFs. In the absence of eIF2α phosphorylation PEITC did not decrease polysome formation (Figure 4-10) therefore eIF2α phosphorylation is fundamental in PEITC-induced translational repression.

There are four known kinases that phosphorylate eIF2α; GCN2, HRI, PERK and PKR (see section 1. 3. 7. 3.). Of these four kinases the kinases most likely to be implicated in phosphorylating eIF2α in response to PEITC treatment were PERK then HRI, whereas neither GCN2 nor PKR were expected to be active as cells were maintained in media with an excess of amino acids and were free of infection. HRI was originally thought to only be present in lymphocytes, but HRI is also present in many other tissue types including breast epithelial (Pervin et al., 2008), therefore HRI could be implicated in the phosphorylation of eIF2α by PEITC in MCF7 cells. PERK is activated by ER stress, due to the unfolded protein response, while HRI is activated in heme deficiency and may have implications for angiogenesis, which PEITC is known to inhibit (Xiao and Singh, 2007). It was difficult to determine whether these two kinases were activated in response to PEITC treatment. Inhibitors and siRNA directed against these kinases were used to determine the involvement of PERK and HRI in eIF2α phosphorylation in response to PEITC treatment, but unfortunately it was difficult to knock down PERK completely therefore it was problematic to determine the involvement of PERK (Figure 4-6). The involvement of HRI was also difficult to determine due to the quality of the anti-HRI antibody available (Figure 4-7). In the presence of both hemin chloride treatment and PERK siRNA, PEITC was able to induce the phosphorylation of eIF2α (Figure 4-8), suggesting that either both kinase had not been inhibited or knocked down, neither kinase was involved or the phosphatase responsible for the removal of the phosphate group from eIF2α was inhibited by PEITC. Ideally knock out MEFs for each of the four eIF2α kinases, individually and in combination, would be required to determine the involvement of the eIF2α kinases in response to PEITC treatment.

Decreased mRNA translation by PEITC was mediated by eIF2α phosphorylation and this phosphorylation could also induce the formation of stress granules to

prevent translation. Stress granules are aggregates of stalled pre-initiation complexes and are often induced by the phosphorylation of eIF2α (Chernov et al., 2009; Mathews et al., 2007; Mokas et al., 2009). The ability of PEITC to induce eIF2α phosphorylation indicated that PEITC would promote stress granule assembly. The formation of stress granules was shown to occur in MCF7 cells in a time and dose dependent manner following PEITC treatment (Figure 4-11 and Figure 4-14 - Figure 4-16, inclusive). Induction of stress granules by PEITC was prevented when cells were additionally treated with 2-AP to inhibit the phosphorylation of eIF2α (Figure 4-17), indicating the importance of eIF2α phosphorylation in stress granule assembly. Non-phosphorylatable eIF2α MEFs were not used to demonstrate the importance of eIF2α phosphorylation in PEITC-induced stress granule assembly due to technical difficulties in visualisation of stress granules in these cells. These data indicate that PEITC induced stress granule assembly in a phospho-eIF2α dependent manner.

The main function of stress granules is believed to be storage of mRNA, although stress granules contain eIF3 as well as IRES trans-activating factors to enable translation of specific mRNAs to occur (Thomas et al., 2011). An example is the mRNA for GADD34/PPP1R15a, the regulatory subunit of protein phosphatase 1 (PP1), a key phosphatase for eIF2α (Thomas et al., 2011). The mRNA for GADD34/PPP1R15a is found in stress granules and contains multiple uORFs enabling the mRNA to be translationally enhanced following eIF2α phosphorylation (Thomas et al., 2011). This raises the question of whether *HIF-1A* requires the formation of stress granules to ensure mRNA translation occurs following hypoxic stress.

PEITC enabled stress granules to form but it is not known whether PEITC disrupts which mRNA molecules accumulate in stress granules or whether the composition of the stress granules has changed, for example are IRES trans-activating factors still present? PEITC may alter the composition of stress granules, thereby inhibiting the translation of those specific mRNAs whose expression is enhanced upon stress granule assembly. This may provide an alternative mechanism for decreased translation following PEITC treatment, PEITC may prevent the expression of PP1 from initiating in stress granules therefore resulting in the

accumulation of eIF2α phosphorylation. In order to determine the consequence of PEITC on stress granules further investigation would be required, for example fluorescence *in situ* hybridisation could be carried out to investigate the localisation of specific mRNA molecules into stress granules. Further immunofluorescence studies could be carried out to determine whether IRES trans-activating factors are still recruited to stress granules following PEITC treatment.

In conclusion, PEITC induced the formation of stress granules in a phospho-eIF2α dependent manner, which provides additional evidence for inhibited initiation of translation following PEITC treatment. The formation of stress granules following PEITC treatment provides evidence that PEITC inhibits initiation of translation rather than elongation as stress granules do not form in the presence of translation elongation inhibitors (Mokas et al., 2009).

Chapter Five

Results – Regulation of mRNA Translation in CLL

5. Regulation of mRNA Translation in CLL

5. 1. Introduction

Having identified mechanisms by which PEITC inhibited mRNA translation in an established cancer cell line, my next goal was to investigate these pathways in primary cancer cells. I selected CLL for this study since this disease provides access to large numbers of malignant cells from blood samples of patients allowing detailed investigation *in vitro*. Moreover, PEITC selectively promotes apoptosis of CLL cells and has been proposed as a potential therapeutic agent (Zhang et al., 2012). Although it is known that some of the key proteins involved in CLL cell proliferation and survival, such as MYC and MCL-1, respectively, are enhanced following sIgM stimulation (Krysov et al., 2012; Petlickovski et al., 2005) and are tightly controlled at the level of transcription (Vallat et al., 2007), mRNA translation has not been fully investigated in this disease. Therefore, prior to analysis of PEITC, I first investigated the regulation of mRNA translation. I focused on the effects of BCR stimulation since antigen signalling is thought to play a major role in the development and progression of CLL (Stevenson et al., 2011). Interactions with antigen *in vivo* can be mimicked by stimulation of cells with anti-IgM or anti-IgD antibodies *in vitro* (Lanham et al., 2003; Mockridge et al., 2007).

5. 2. Hypothesis and Aims

5. 2. 1. Hypothesis

Stimulation of CLL cells via surface IgM (sIgM) or sIgD, to mimic antigen engagement *in vivo*, increases mRNA translation.

5. 2. 2. Aims

The aims of this chapter were to determine the effects of sIgM or sIgD stimulation on global mRNA translation and to determine the effect of sIgM stimulation on translation of *MYC* and *MCL-1* mRNAs. These aims were addressed by:

- Measuring translation by metabolic labelling at basal levels and following stimulation with anti-IgM or anti-IgD beads in signalling responsive and non-responsive CLL samples
- Polysome profiling of samples following sIgM stimulation
- Quantifying the mRNA associated with fractions of the polysome profile to determine whether sIgM stimulation altered translation of *MYC* and *MCL-1*.

Due to limited primary material availability the samples were treated with anti-IgM or anti-IgD and were incubated in the presence or absence of inhibitors. This chapter presents and discusses the effect of sIgM or sIgD stimulation on translation, whereas the subsequent chapter will analyse the effect of the inhibitors on translation using these sIgM and sIgD values as controls, rather than repeating these samples. Therefore large experiments were performed on each sample and the analysis has been split into the effect of sIgM or sIgD stimulation on translation in this chapter and the effect of BCR kinase inhibitors and PEITC on sIgM stimulated translation in chapter 6.

5. 3. Results

5. 3. 1. Effect of BCR Stimulation on mRNA Translation

To investigate mRNA translation in CLL, basal and BCR stimulated translation was first measured by ^{35}S metabolic labelling as compared to polysome profiling this method required significantly fewer cells. CLL samples can be sub-divided into 'responders' and 'non-responders' depending on their ability to promote intracellular Ca^{2+} mobilisation following treatment with soluble anti-IgM (Mockridge et al., 2007). Samples that can elicit intracellular Ca^{2+} mobilisation in at least 5% of the malignant clone have been classified as 'responders', whereas 'non-responders' are below the 5% threshold (Mockridge et al., 2007) (see Table 2-2 for Ca^{2+} response to soluble anti-IgM and anti-IgD). The difference in responsiveness to sIgM stimulation is considered to be clinically relevant as retained signalling capacity is associated with poor prognosis and outcome (Lanham et al., 2003; Le Roy et al., 2012; Mockridge et al., 2007). The first analysis carried out was to determine the translational response to sIgM stimulation using 11 responsive CLL samples.

Cryopreserved CLL cells were recovered and allowed to rest for 1 hour prior to stimulation using bead-bound anti-IgM. The antibody was a $F(ab')_2$ fragment of a goat polyclonal antibody (to circumvent potential binding of Fc receptors on CLL cells) covalently bound to Dynabeads. Compared to soluble antibodies, bead-bound antibodies are not endocytosed and therefore result in a longer-lasting and stronger signalling response (Coelho et al., 2013). Cells were stimulated for a total of 24 hours and metabolic labelling was performed during the final four hours of this incubation. As a control, cells were treated with bead-bound isotype control antibody. Cells were also left untreated to determine basal levels of mRNA translation in the absence of stimulation. Figure 5-1 shows metabolic labelling data for all the samples whereas Figure 5-2 shows data normalised to untreated cells.

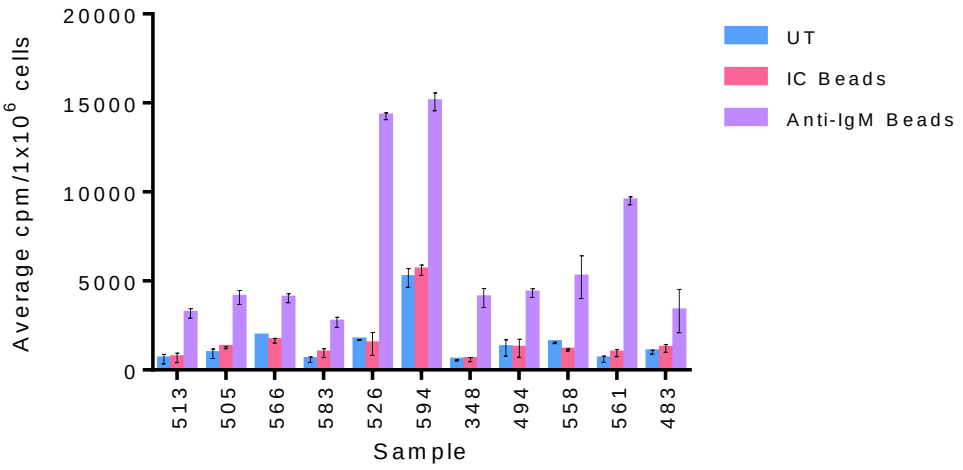

Figure 5-1: Effect of sIgM Stimulation on mRNA Translation in Signalling Responsive CLL Samples

CLL cells were recovered from cryopreservation and incubated with either anti-IgM beads, isotype control beads (IC beads) or left untreated (UT) for 24 hours prior to metabolic labelling. Bars represent the average incorporation with error bars representing the standard deviation from the mean, samples carried out in duplicate.

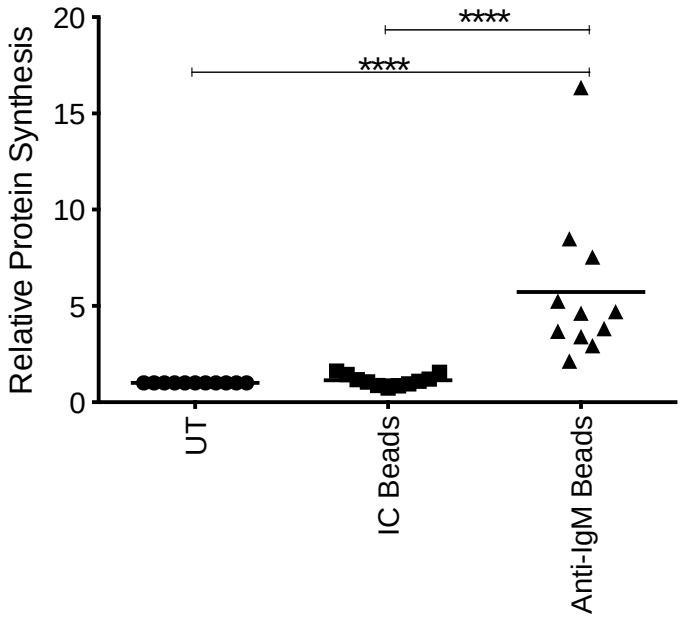

Figure 5-2: Quantitation of the Effect of sIgM Stimulation on mRNA Translation in Signal Responsive CLL Samples

Metabolic labelling of the 11 signal responsive CLL samples (Figure 5-1) was made relative to untreated (UT) for each sample to quantify the relative change in mRNA translation following treatment with anti-IgM beads or isotype control (IC) beads. Points represent the average incorporation per sample with the line representing the mean. Statistically significant data is indicated (p=**** < 0.001, Two way ANOVA, Prism6).

Variable levels of basal mRNA translation was detected in untreated CLL samples with 9.5 fold higher basal mRNA translation in sample 594 compared to the sample with the lowest basal mRNA translation, sample 348 (Figure 5-1). Treatment of CLL samples with anti-IgM beads increased mRNA translation at least 2-fold in all samples (Figure 5-1 and Figure 5-2). The mean increase in all 11 samples was 5.6-fold and the overall effect of IgM stimulation was significantly different compared to untreated ($p<0.001$) or isotype control treated cells ($p<0.001$) (two way ANOVA). Therefore stimulation of sIgM increased mRNA translation in signalling responsive CLL samples.

Similar experiments were performed to determine whether sIgD stimulation also increased mRNA translation. In contrast to sIgM the vast majority of CLL samples retain their ability to signal (analysed by intracellular Ca^{2+} flux) following sIgD stimulation (Lanham et al., 2003; Mockridge et al., 2007). However, sIgM and sIgD responses are distinct; sIgD stimulation only results in short-lived responses and signalling capacity does not correlate with prognostic markers (Lanham et al., 2003; Mockridge et al., 2007).

Effects of sIgM and sIgD stimulation were compared in 5 out of the 11 samples previously analysed for sIgM responses (Figure 5-1 and Figure 5-2). Following treatment with isotype control beads there was no increase in translation compared to untreated cells, while incubation with anti-IgM beads promoted translation (Figure 5-1 - Figure 5-4). Overall responses to anti-IgD were low compared to anti-IgM and the mean fold increase in mRNA translation was 2-fold. The maximum fold increase in mRNA translation following sIgD stimulation was seen in sample 483 with a 2.8-fold induction in mRNA translation (Figure 5-3 and Figure 5-4). Anti-IgD-induced translation was not significantly different from isotype control bead treated cells and was significantly lower than sIgM stimulated cells ($p<0.001$, Two-way ANOVA) (Figure 5-4). Therefore sIgD stimulation had only modest effects on mRNA translation.

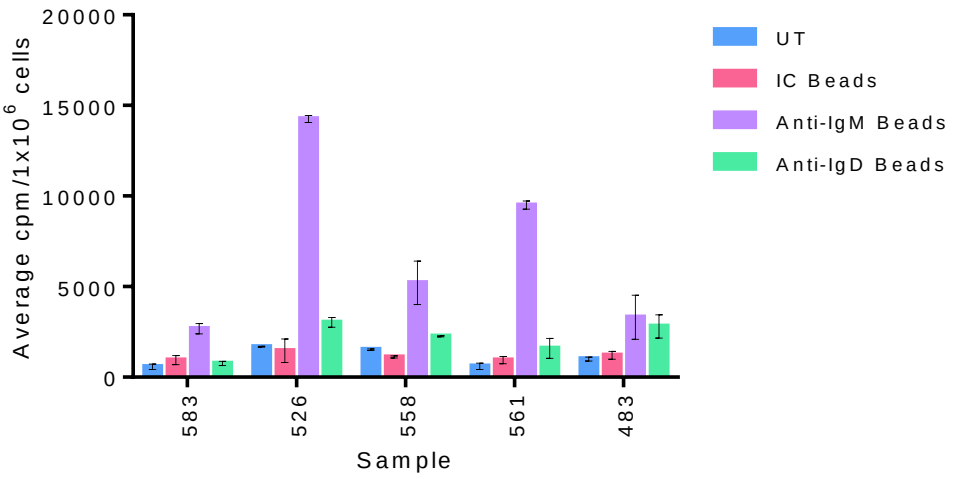

Figure 5-3: Effect of sIgM and sIgD Stimulation on mRNA Translation in Signal Responsive CLL Samples

CLL cells were recovered from cryopreservation and incubated with either anti-IgM beads, anti-IgD beads, isotype control beads (IC beads) or left untreated (UT) for 24 hours prior to metabolic labelling. Bars represent the average incorporation with error bars representing the standard deviation from the mean, samples carried out in duplicate.

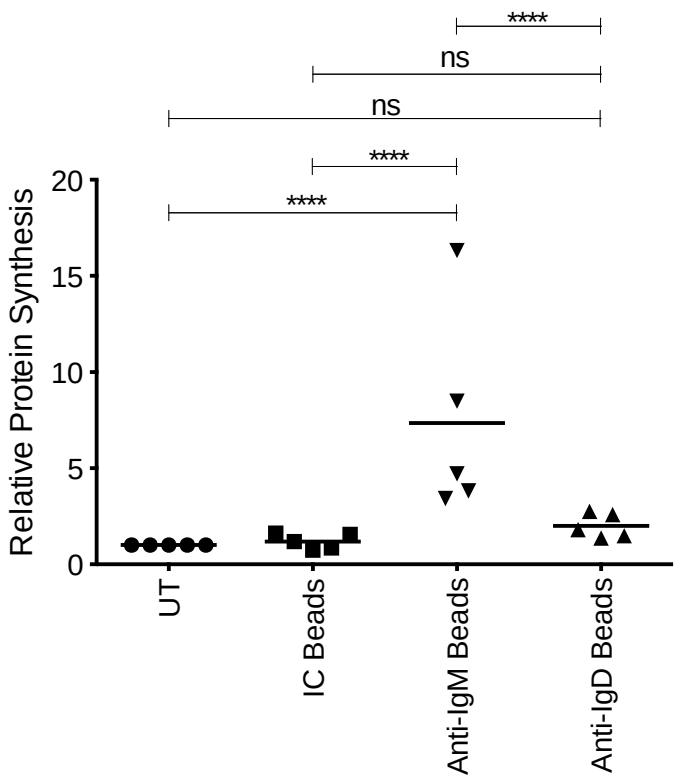

Figure 5-4: Quantitation of the Effect of sIgM and sIgD Stimulation on mRNA Translation in Signal Responsive CLL Samples

Metabolic labelling of the 5 signal responsive CLL samples (Figure 5-3) were made relative to untreated (UT) for each sample to quantify the relative change in mRNA translation following treatment with anti-IgM beads, anti-IgD beads or isotype control (IC) beads. Points represent the average incorporation per sample with the line representing the mean of all samples. Statistically significant data is indicated (p=**** < 0.001, n=5, Two way ANOVA, Prism6).

5. 3. 2. Determining Translation in 'Non-Responders' Following BCR Stimulation

Having established that sIgM stimulation enhanced mRNA translation in signalling responsive samples, I next investigated the response in four non-responsive samples. Similar to responsive samples, basal levels of mRNA translation were detected in all samples and basal mRNA translation was not different between signalling responsive and non-responsive samples ($p=0.37$, t-test $n=15$) (Figure 5-1 and Figure 5-5). However, in contrast to the effects in signalling responsive samples, there was only a very modest effect on mRNA translation following sIgM stimulation (Figure 5-5 and Figure 5-6). Overall the mean induction of mRNA translation was 2.6 fold and translation in anti-IgM treated cells was not statistically different from translation in untreated cells ($p=0.30$, t-test) or isotype control ($p=0.32$, t-test) treated cells. sIgD stimulation also did not significantly increase mRNA translation in two sIgM non-responsive samples, when compared to untreated cells ($p=0.35$, t-test) or isotype control treated cells ($p=0.17$, t-test) (Figure 5-7 and Figure 5-8), which is similar to the response to sIgD in signalling responsive samples (Figure 5-4).

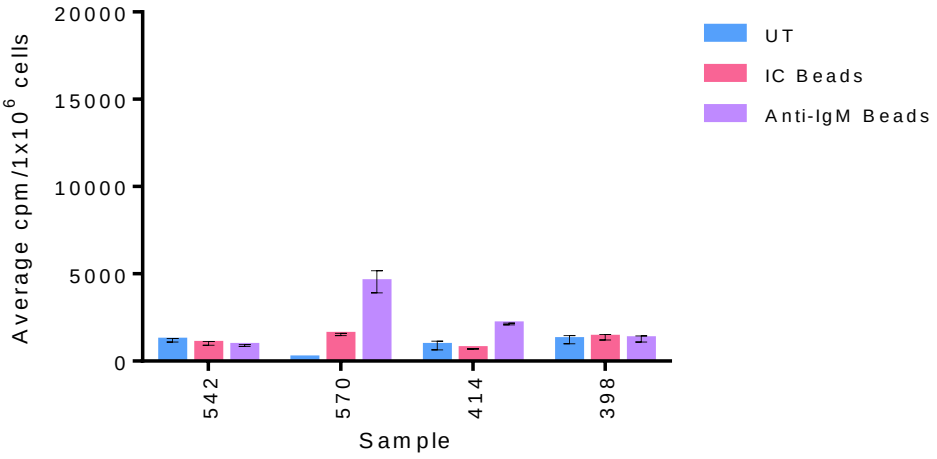

Figure 5-5: Effect of sIgM Stimulation on mRNA Translation in Non-Responsive CLL Samples

CLL cells were recovered from cryopreservation and incubated with either anti-IgM beads, isotype control beads (IC beads) or left untreated (UT) for 24 hours prior to metabolic labelling. Bars represent the average incorporation with error bars representing the standard deviation from the mean, samples carried out in duplicate.

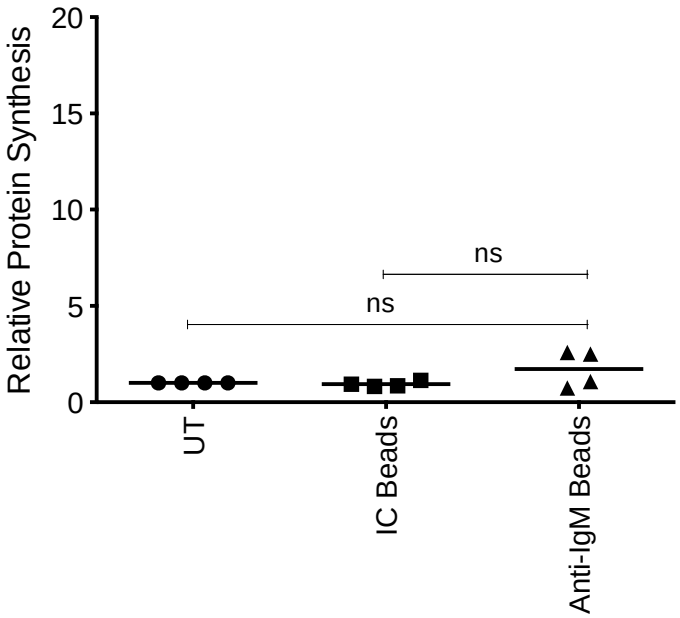

Figure 5-6: Quantitation of the Effect of sIgM Stimulation on mRNA Translation in Non-Responsive CLL Samples

Metabolic labelling of the 4 non-responsive CLL samples (Figure 5-5) were made relative to untreated (UT) for each sample to quantify the relative change in mRNA translation following treatment with anti-IgM beads or isotype control (IC) beads. Points represent the average incorporation per sample with the line representing the mean, n=4.

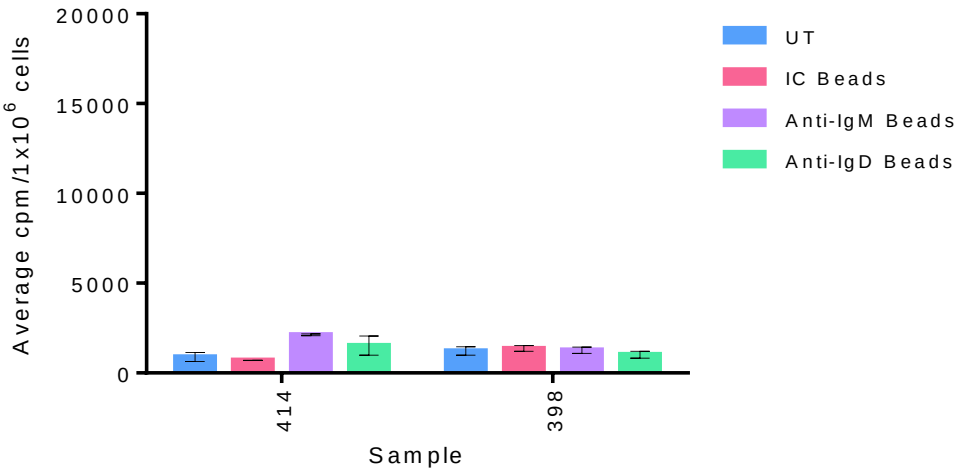

Figure 5-7: Effect of sIgM and sIgD Stimulation on mRNA Translation in Non-Responsive CLL Samples

CLL cells were recovered from cryopreservation and incubated with either anti-IgM beads, anti-IgD beads, isotype control beads (IC beads) or left untreated (UT) for 24 hours prior to metabolic labelling. Bars represent the average incorporation with error bars representing the standard deviation from the mean, samples carried out in duplicate.

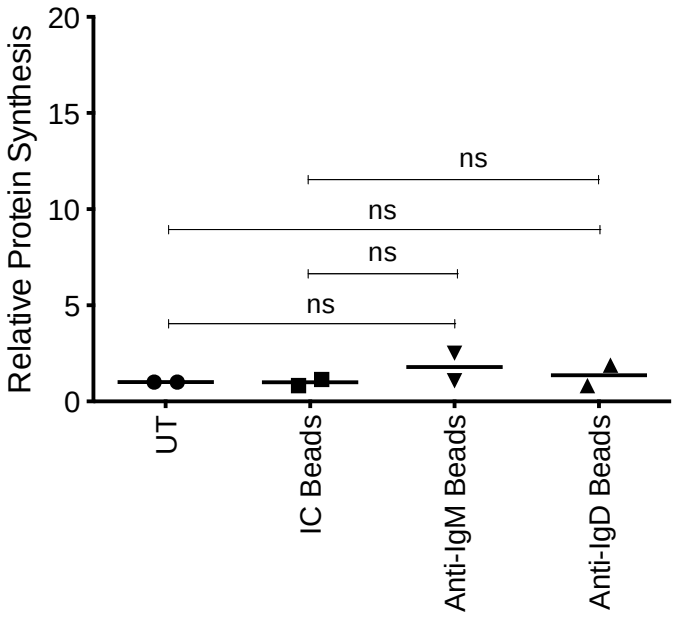

Figure 5-8: Quantitation of the Effect of sIgM and sIgD Stimulation on mRNA Translation in Non-Responsive CLL Samples

Metabolic labelling of two non-responsive CLL samples (Figure 5-7) were made relative to untreated (UT) for each sample to quantify the relative change in mRNA translation following treatment with anti-IgM beads, anti-IgD beads or isotype control (IC) beads. Points represent the average incorporation per sample with the line representing the mean, n=2.

5. 3. 3. Correlation of Stimulated mRNA Translation with Clinical Features of CLL

Data in the previous sub-sections (sections 5. 3. 1. and 5. 3. 2.) demonstrated that sIgM stimulation effectively increased mRNA translation in a subset of CLL samples that were classified as signalling responsive. Although overall numbers were small, I combined the data from signalling responsive and non-responsive samples and investigated whether the variations in mRNA translation correlated with any clinical feature of the samples. However, there were no significant correlations between basal or anti-IgM induced mRNA translation and *IGVH* mutational status, or expression of CD38 or ZAP70 (Figure 5-9).

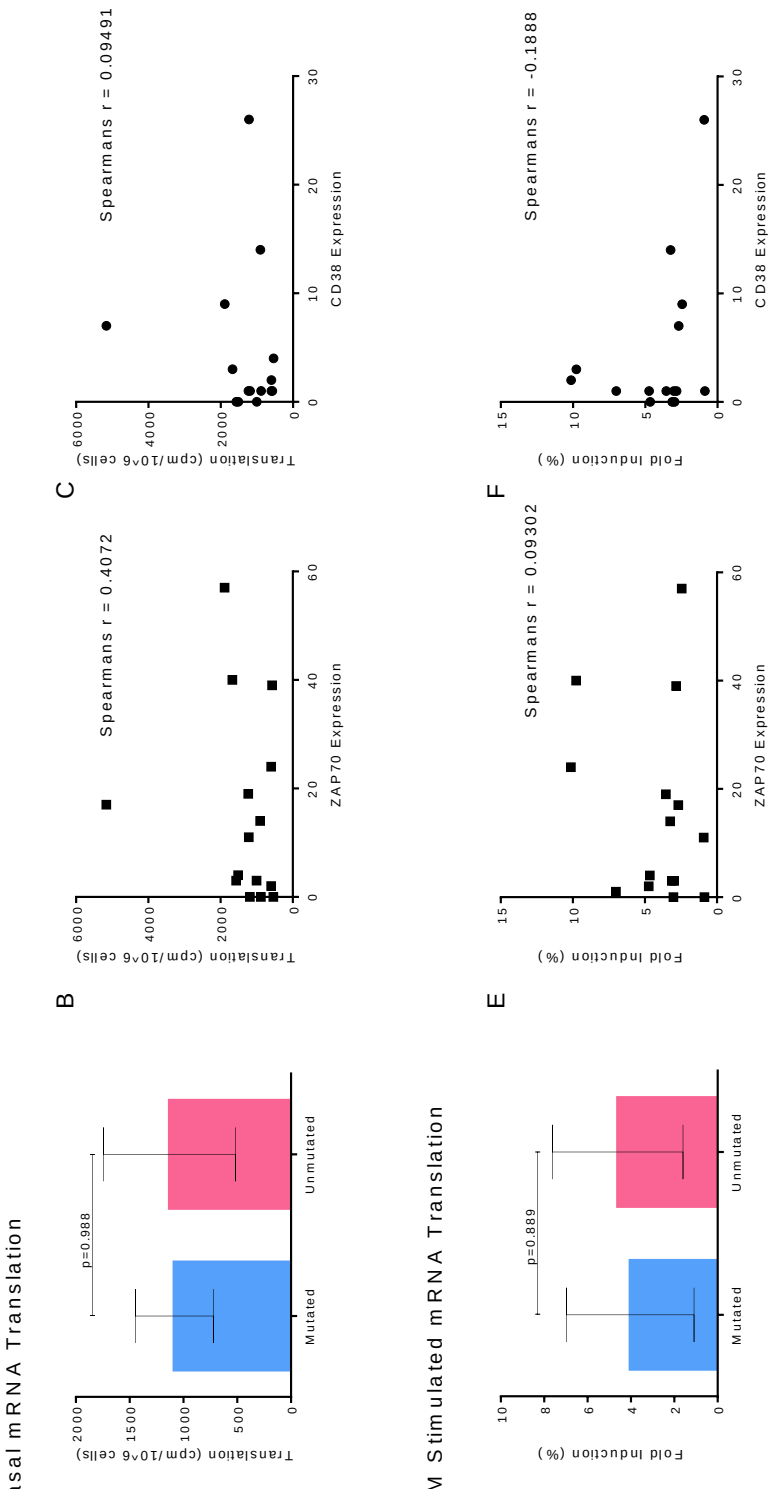

Figure 5-9: Correlation of mRNA Translation with Clinical Features of CLL

Analysis of basal mRNA translation correlation to *IGVH* mutational status (A), ZAP70 expression (B) and CD38 expression (C) (top panel). sIgM stimulated mRNA translation was analysed for correlation to *IGVH* mutational status (D), ZAP70 expression (E) and CD38 expression (F) (bottom panel). Mann-Whitney analysis was carried out to analyse the correlation with *IGVH* mutational status and the p-value is indicated Spearman's rank correlation was used to analyse any correlation with ZAP70 and CD38 expression and the r value is indicated, n=15 Prism 6.

5. 3. 4. CLL Translation Profiles

Further experiments were performed to investigate mRNA translation in CLL in more depth. Here polysome profiling was carried out to specifically determine the effect of sIgM stimulation on translation of *MYC* and *MCL-1* mRNAs. MYC and MCL-1 proteins are known to be induced following sIgM stimulation (Krysov et al., 2012; Petlickovski et al., 2005), with enhanced MYC expression present in proliferation centres in the lymph nodes (Krysov et al., 2012). These are subject to tight transcriptional regulation (Vallat et al., 2007), but could also be regulated by translation therefore analysis into the translational regulation of these mRNAs following sIgM stimulation was required. Before I could investigate the effect of sIgM stimulation on translation of specific mRNA molecules it was important to determine the technical feasibility of polysome profiling CLL samples. It was also important to establish whether CLL B cells previously isolated and cryopreserved were suitable for polysome profiling or whether freshly isolated CLL B cells were required.

One sample (594) was selected for initial validation studies since we had sufficient material from this patient for analysis of both cryopreserved and freshly isolated cells. This sample had high levels of basal translation when analysed by metabolic labelling (Figure 5-1). Polysome profiling of cryopreserved cells revealed very low polysome peaks and an abundance of RNA in the 80S peak (Figure 5-10). The results were very similar in freshly isolated CLL B cells from the same blood sample (Figure 5-10). The low polysome peaks were calculated as 3.2% of the total amplitude of the profile in both freshly isolated cells and cryopreserved cells, indicating that the results were comparable regardless of previous storage (Figure 5-10). The polysome peaks were calculated as a percentage of the total amplitude of the profile as absorbance readings can alter due to changes in cell numbers as well as the sensitivity of the equipment. Thus the very low level of mRNA translation seen (Figure 5-1, Figure 5-5 and Figure 5-10) was not a consequence of cryopreservation but appeared to be a feature of CLL cells.

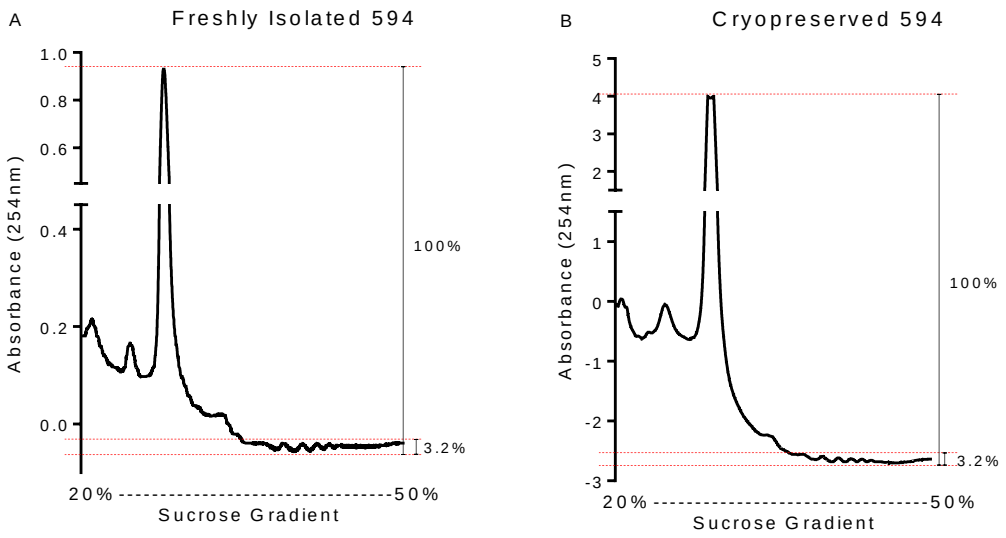

Figure 5-10: Polysome Profiling of CLL Cells

Cells from patient 594 were either freshly isolated from the blood (A) or cells were recovered from liquid nitrogen storage (B) allowed to recover for one hour prior to cell lysis and polysome profiling. Polysome peak amplitude was calculated as a percentage of the total amplitude of the profiles.

Polysome profiling of CLL samples was expected to be difficult due to the anergic nature of circulating CLL cells (Stevenson et al., 2011). Having established that cryopreserved samples can be used successfully to investigate polysome profiles the effect of sIgM stimulation was next analysed. Five samples characterised as sIgM responsive (494, 513, 566, 505 and 348) and had been used previously to analyse the effect of anti-IgM treatment on metabolic labelling were used for polysome profiling. Cells were recovered from liquid nitrogen storage and were allowed to rest for one hour before treatment with bead-bound anti-IgM or isotype control antibody for 24 hours. The polysome profiles demonstrate that the response to sIgM stimulation varied between the samples (Figure 5-11, Figure S9-2 and Figure S9-3). By contrast metabolic labelling indicated a similar level of induced translation following anti-IgM bead treatment (Figure 5-1); therefore metabolic labelling was the main focus to determine the global effect on mRNA translation. Figure 5-11 shows the polysome profile from one sample that showed a clear increase in polysome peaks following sIgM stimulation. Results for a further four samples are shown in Figure S9-2 and Figure S9-3, showing that overall responses were modest and variable but enhanced polysome peaks were indicated in three out of the five samples tested.

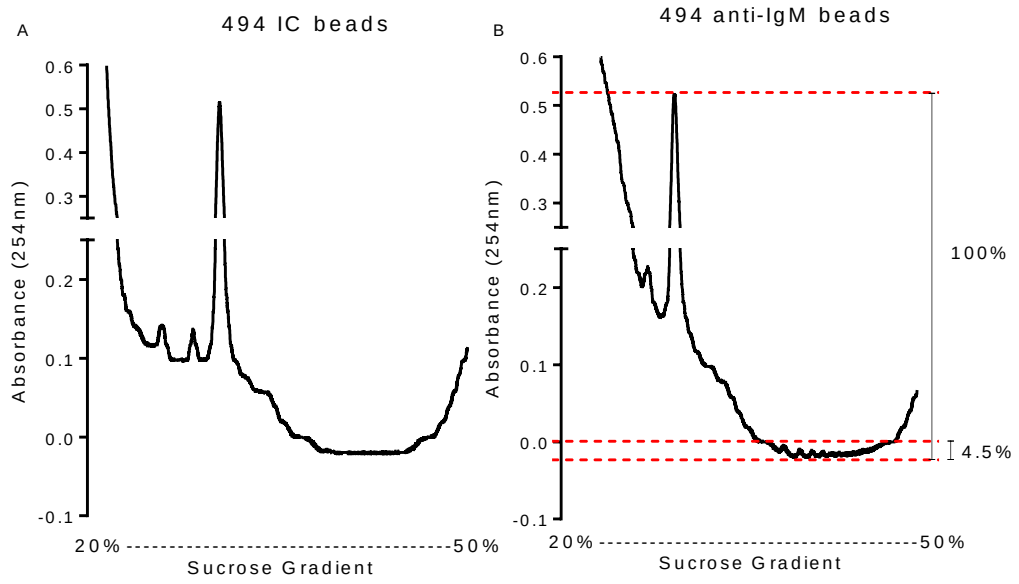

Figure 5-11: Polysome Profiling of CLL cells Treated with anti-IgM Beads

CLL sample 494 was recovered from cryopreservation and allowed to recover for one hour prior to incubation with anti-IgM beads or isotype control beads (IC) for 24 hours before polysome cell lysates were collected and profiled.

5. 3. 5. Effect of sIgM Stimulation on MYC, MCL-1 and ACTB mRNA localisation on Polysome profiles

Having confirmed that polysome profiling could be used successfully to monitor changes in mRNA translation in CLL samples, I next investigated the effect of sIgM stimulation on translation of *MYC*, *MCL-1* and *ACTB* RNA using q-PCR analysis of polysome fractions. I selected five samples that were known to be signal responsive and were used in metabolic labelling experiments and positively responded to anti-IgM treatment (Figure 5-1 – samples 348, 494, 505, 513 and 566). Samples were prepared and treated as in previous experiments; CLL samples were thawed and allowed to recover for one hour prior to incubation with bead-bound anti-IgM or isotype control antibody for 24 hours before polysome profiling. The profile was fractionated as indicated in Figure 3-11. The collected fractions were subjected to RNA extraction, cDNA synthesis and TaqMan qPCR for *MYC*, *MCL-1* and *ACTB*.

As for MCF7 cells (section 3. 3. 7.) the qPCR data was analysed in four ways to elucidate the translational effect from any changes in transcription. Firstly, the total amount of mRNA (for each gene) is shown to determine whether there were any transcriptional changes in each gene. Secondly, the total amount of mRNA in each fraction of the profile is presented to establish where the mRNA was located on the polysome profile. Thirdly, the amount of mRNA in each fraction of the profile is presented as a percentage of the total mRNA, to remove any transcriptional regulation, and finally, the proportion of mRNA in the highest polysome fractions (fractions 3-5) is shown relative to the lower fractions (fractions 1-2), to ascertain whether the mRNA was highly translated. This data will be shown for a representative sample as well as all 5 samples combined to summarise all findings.

For *MYC* mRNA there was a significant increase in total abundance of *MYC* mRNA across all fractions of the polysome profile in all five samples analysed following sIgM stimulation ($p = 0.035$, $n=5$, t-test) (Figure 5-12, Figure 5-13, Figure S9-4 and Figure S9-5). *MCL-1* and *ACTB* total mRNA also significantly increased in all samples, except in sample 348 *MCL-1* mRNA decreased (Figure 5-12, Figure 5-13, Figure S9-4 and Figure S9-5).

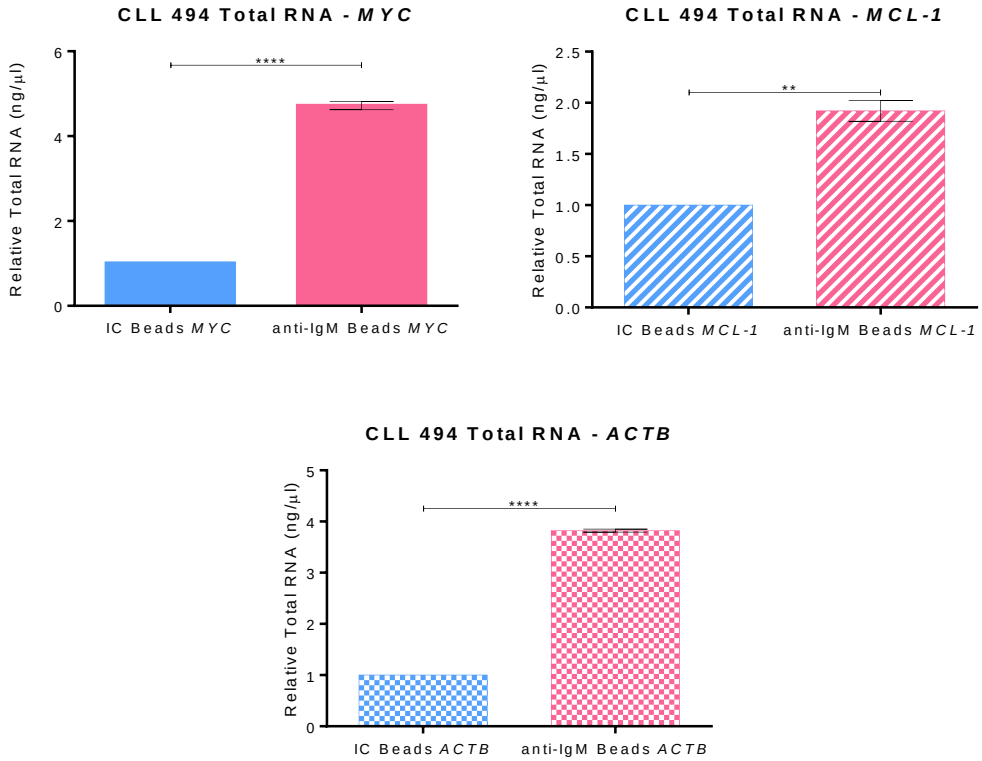

Figure 5-12: Abundance of *MYC, MCL-1* and *ACTB* mRNA Following sIgM Stimulation

Following polysome profiling of CLL sample 494 (Figure 5-11) qPCR analysis was undertaken to investigate the abundance of *MYC, MCL-1* and *ACTB* mRNA levels in the whole profile. Bars represent the average total mRNA relative to isotype control (IC) beads. Error bars indicate the standard deviation and significantly different data is indicated, ** = $p \leq 0.01$, *** = $p \leq 0.005$, **** = $p \leq 0.001$, t-test (n=2).

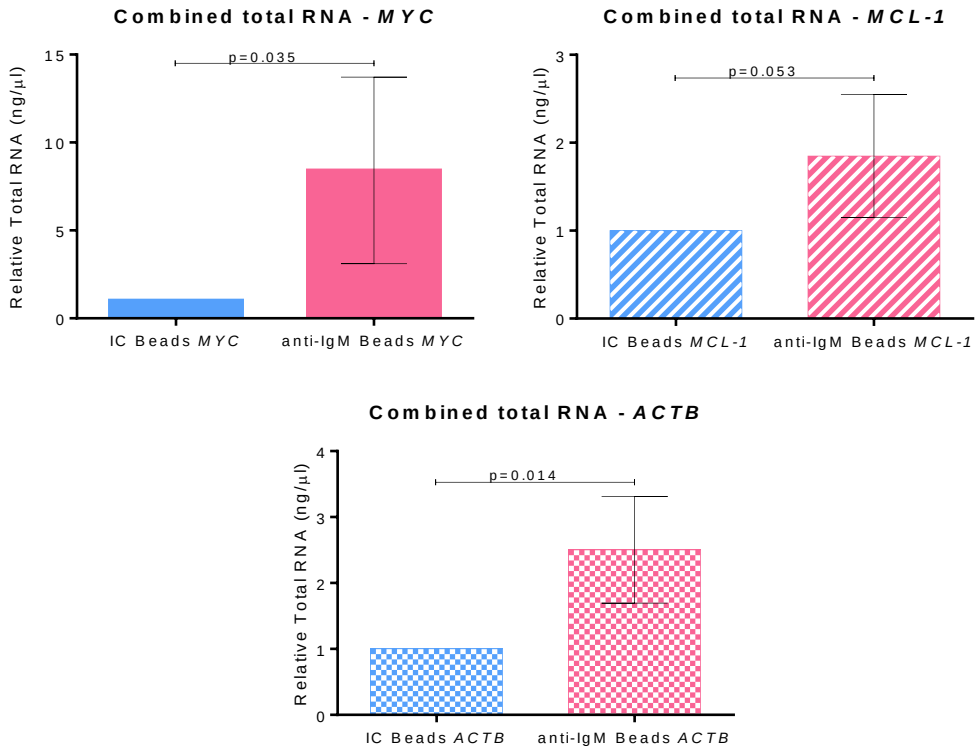

Figure 5-13: Average Abundance of *MYC*, *MCL-1* and *ACTB* mRNA Following sIgM Stimulation

Following polysome profiling of CLL samples (Figure 5-11, Figure S9-4 and Figure S9-5), qPCR analysis was undertaken to investigate the abundance of *MYC*, *MCL-1* and *ACTB* mRNA levels in the whole profile. Bars represent the average total mRNA relative to isotype control (IC) beads, n=5. Error bars indicate the standard deviation and significantly different data is indicated, ** = $p \leq 0.01$, *** = $p \leq 0.005$, **** = $p \leq 0.001$, t-test.

The increase in *MYC* mRNA following sIgM stimulation was consistent with the observation that MYC is transcriptional up-regulated (Krysov et al., 2012; Vallat et al., 2007). It was surprising to see that *ACTB* mRNA was enhanced following sIgM stimulation as this is often used as a reference gene. But recent data has shown that *ACTB* expression can be altered in different culturing conditions, as well as other well-known housekeeping genes (Fink et al., 2008). The clear increase in the abundance of *MYC, MCL-1* and *ACTB* mRNA following sIgM stimulation indicated that there could also have been enhanced translation of these mRNA molecules to promote protein expression of these genes.

Having established that treatment with bead-bound anti-IgM enhanced levels of *MYC, MCL-1* and *ACTB* mRNA I next analysed the amount of mRNA associated with each fraction of the profile (Figure 5-14, Figure S9-6 and Figure S9-7). All three mRNAs were significantly enhanced in all fractions, with the greatest increase seen in the higher fractions (fractions 3-5). The only exception was in sample 348 where *MCL-1* mRNA had decreased association with the higher fractions (Figure S9-7), which is in agreement with decreased total *MCL-1* mRNA in this sample (Figure S9-5). In summary these data indicated that there was more mRNA associated with ribosomes following sIgM stimulation but the distribution along the profile was unaltered. In order to determine whether the changes seen were just due to transcriptional changes further analysis of the data was carried out. To remove any transcriptional effects the amount of mRNA per fraction was calculated as a percentage of the total mRNA (Figure 5-15). *MYC* mRNA significantly decreased in lower density fractions (fractions 2 and 3) and increased in higher density fractions, following sIgM stimulation (Figure 5-15). There was a similar change seen for *MCL-1* and *ACTB* mRNA in sample 494 (Figure 5-15). This change was not as clearly seen in the other four samples therefore sample variation indicated that there was variability in translational regulation of these genes analysed (Figure 9-8-Figure S9-10, inclusive) and collecting more fractions from the polysome profile may have provided a more detailed analysis to be carried out.

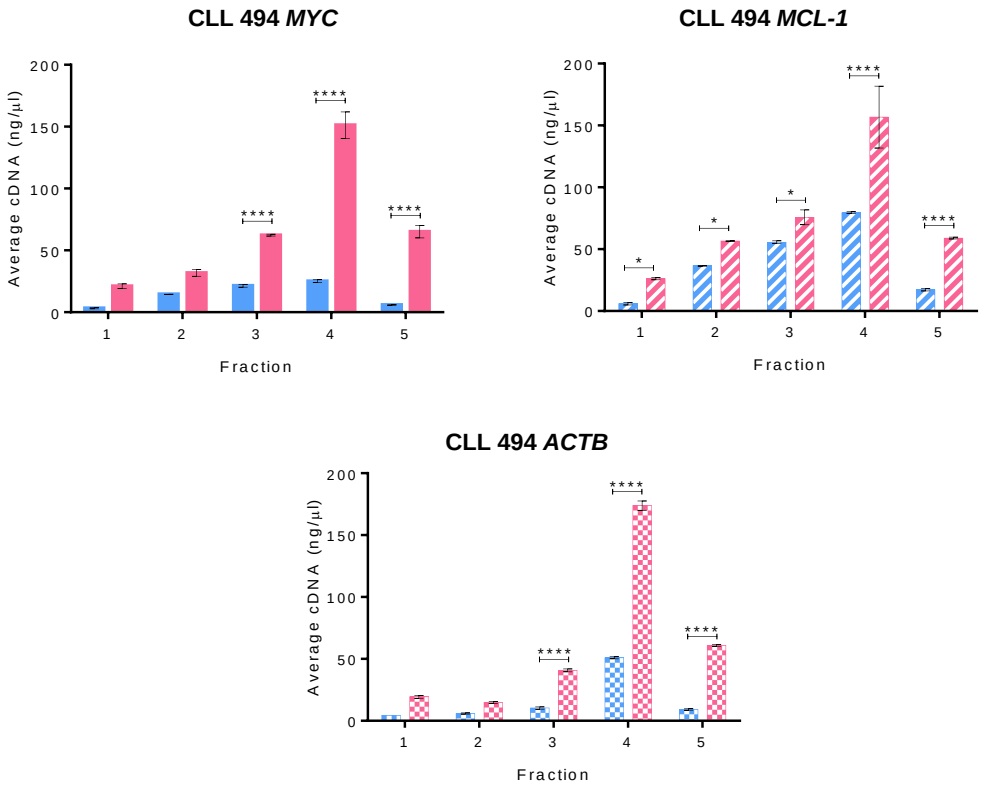

Figure 5-14: Polysome Distribution of *MYC, MCL-1* and *ACTB* mRNAs

Following polysome profiling of CLL sample 494 (Figure 5-11) qPCR analysis was undertaken to investigate the abundance of *MYC, MCL-1* and *ACTB* mRNA levels in each fraction of the polysome profile. Bars represent the average mRNA in each fraction, blue bars indicate cells treated with isotype control beads and pink bars indicate cells treated with anti-IgM beads. Error bars indicate the standard deviation and significantly different data is indicated, * = p≤ 0.05,*** = p≤ 0.005, **** = p≤ 0.001, Two-way ANOVA (n=2).

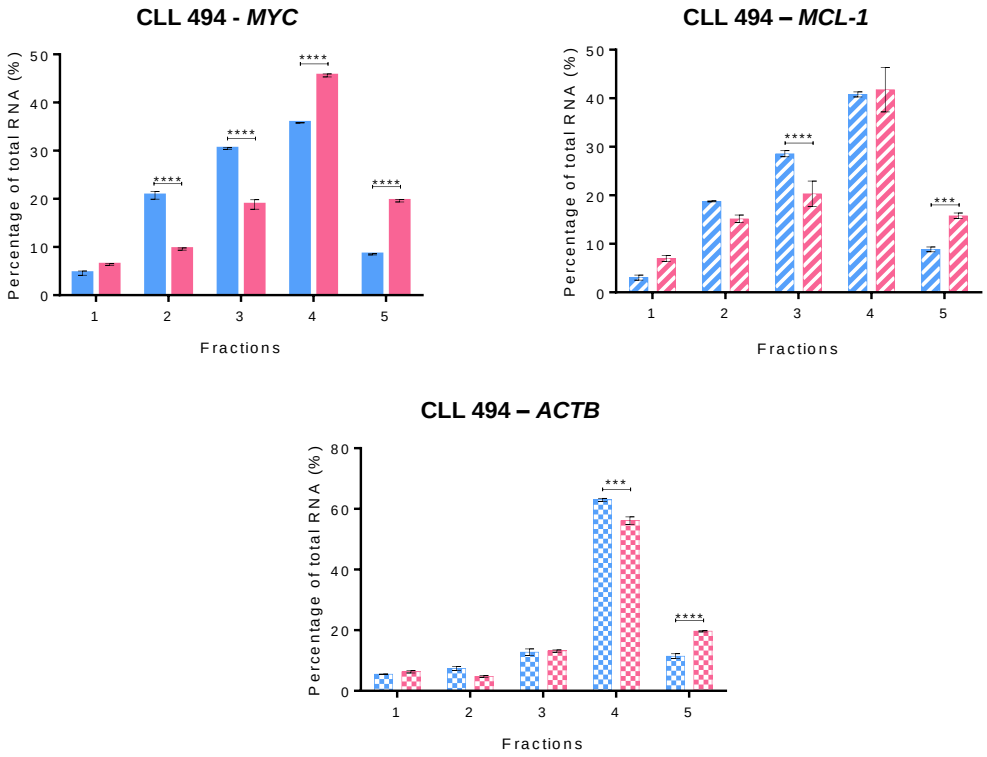

Figure 5-15: Percentage of *MYC, MCL-1* and *ACTB* mRNA Associated with Polysome Fractions

Following polysome profiling of CLL sample 494 (Figure 5-11) qPCR analysis was undertaken to investigate the abundance of *MYC, MCL-1* and *ACTB* mRNA levels in each fraction of the polysome profile. Bars represent the average percentage of mRNA in each fraction as a percentage of total mRNA, blue bars indicate cells treated with isotype control beads and pink bars indicate cells treated with anti-IgM beads. Error bars indicate the standard deviation and significantly different data is indicated, *** = $p \leq 0.005$, **** = $p \leq 0.001$, Two-way ANOVA (n=2).

A final analysis of the data was carried out to determine whether the mRNA localisation on the polysome profile altered following sIgM stimulation. The amount of mRNA associated with polysomes (fractions 3-5 which includes everything denser than an 80S peak) was compared to the amount of mRNA associated with sub-polysome fractions (fractions 1 and 2 up to and including the 80S peak) (see Figure 3-11). This analysis again removed transcriptional regulation and began to resolve whether sIgM stimulation shifts *MYC, MCL-1* and *ACTB* mRNA into heavier density polysome fractions. sIgM stimulation significantly increased the association of *MYC* and *ACTB* mRNA with polysomes in all five samples analysed (Figure 5-16), with individual changes shown in Figure S9-11, whereas *MCL-1* distribution was unaltered following treatment with bead-bound anti-IgM (Figure 5-16).

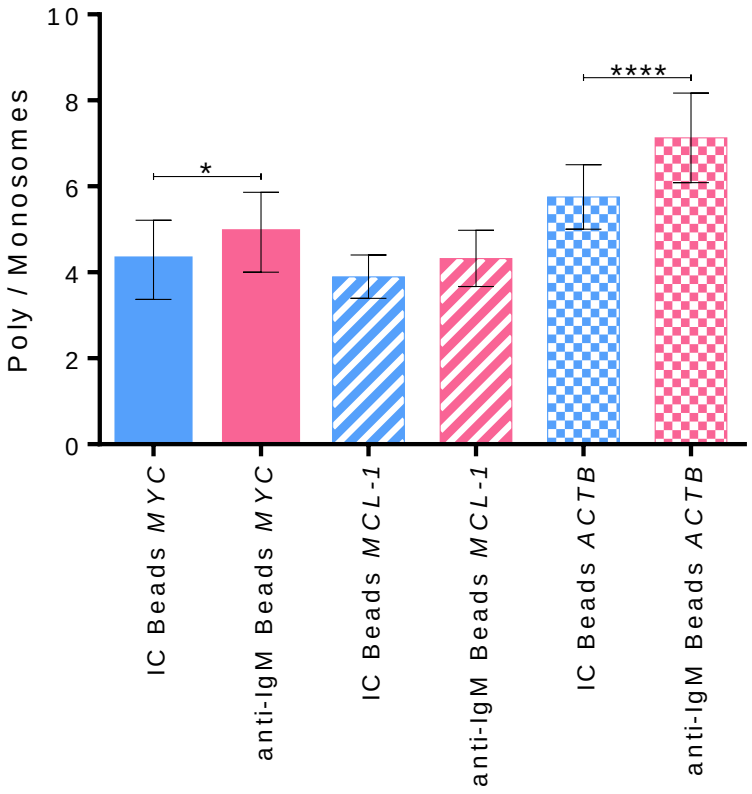

Figure 5-16: Polysome Association of *MYC*, *MCL-1* and *ACTB* mRNA

Following polysome profiling of CLL samples (Figure 5-1, Figure S9-2 and Figure S9-3) qPCR analysis was undertaken to investigate the accumulation of *MYC*, *MCL-1* and *ACTB* mRNA levels in polysome fractions (fractions 3-5). Bars represent the average ratio of polysome associated mRNA (fractions 3-5) with respect to sub-polysome associated mRNA (fractions 1 and 2). Error bars indicate the standard deviation and significantly different data is indicated, * = $p \leq 0.05$, **** = $p \leq 0.001$, Two-way ANOVA (n=5).

5. 4. Summary of Main Findings

- Stimulation of sIgM with bead-bound anti-IgM enhanced translation, measured by polysome profiling and ^{35}S-Met/Cys incorporation
- Treatment with bead-bound anti-IgD had little effect on translation
- sIgM stimulation of 'non-responders' had less effect on translation
- sIgM stimulation increased transcription of *MYC*, *MCL-1* and *ACTB* mRNA
- Stimulation of sIgM increased translation of *MYC*, *MCL-1* and *ACTB* mRNA
- Treatment with bead-bound anti-IgM enhanced translation of *MYC* and *ACTB* mRNA by increasing association with higher molecular weight polysome fractions

5. 5. Discussion

The key observation from this chapter was the finding that BCR stimulation enhanced translation (Figure 5-1, Figure 5-2 and Figure 5-11). This finding may have clinical implications as BCR signalling has been linked to disease progression, with signalling responsive samples having a worse prognosis compared to non-responsive samples (Mockridge et al., 2007). CLL samples classified as 'responsive' showed enhanced translation following incubation with bead-bound anti-IgM, although the response to sIgM stimulation varied between samples (Figure 5-1). These samples did not have elevated translation following treatment with bead-bound anti-IgD (Figure 5-3). This is in agreement with published data showing that production of the oncogene, MYC, was only enhanced following sIgM stimulation and not with sIgD stimulation (Krysov et al., 2012). Samples classified as 'non-responsive' did not have elevated translation following sIgM stimulation (Figure 5-5). The 'non-responders' tested did not show significantly enhanced translation following anti-IgD bead incubation (Figure 5-7 and Figure 5-8). This either demonstrated that these samples did not signal through sIgD, although calcium flux indicated that one sample (sample 414) would signal and one sample would not

signal after IgD stimulation (Table 2-2), or that stimulation of sIgD did not alter translation.

Basal translation levels as well as translation following sIgM stimulation in signal responsive samples varied by as much as 9.5 fold, but the variation was independent of any clinical feature of CLL (Figure 5-9). The sample numbers were small which may have prevented any correlation from being detected, hence more samples need to be analysed. To investigate translation further in CLL polysome profiling was carried out and it was confirmed that translation in CLL could be followed by polysome profiling. Cryopreservation had minimal effect on translation therefore cryopreserved samples could be used to analyse translation (Figure 5-10). It was difficult to detect changes in the polysome profile of sIgM stimulated cells compared to cells treated with bead-bound isotype control antibody due to the large accumulation in the 80S peak, but subsequent qPCR provided insight into the transcriptional and translational regulation of *MYC, MCL-1* and *ACTB* mRNA.

It was important to investigate the effect of sIgM stimulation on translation of *MYC* and *MCL-1* as these genes have been linked with poor clinical outcome (Krysov et al., 2012; Paterson et al., 2012; Pepper et al., 2008; Petlickovski et al., 2005). The protein expression of MYC is elevated following sIgM stimulation resulting in enhanced proliferation (Krysov et al., 2012). Elevated MYC protein expression was thought to have occurred, at least in part, due to increased transcription (Krysov et al., 2012; Vallat et al., 2007). Following sIgM stimulation transcription of *MYC* was enhanced (Figure 5-12 and Figure 5-13) confirming these findings. Levels of *MYC* mRNA associated with different fractions of the polysome profile were also enhanced following sIgM stimulation especially in the higher density fractions (Figure 5-14), indicating the increased *MYC* mRNA was being translated. Analysis showed that *MYC* mRNA also had elevated translation following sIgM stimulation after compensation for any transcriptional effects (Figure 5-16). These data suggest that increased MYC protein expression following BCR signalling occurred due to increased transcription as well as enhanced translation, thus implying that following BCR signalling proliferation is enhanced due to increased translation of *MYC*.

Enhanced expression of MCL-1 protein in response to sIgM stimulation has also been linked with poor clinical outcome, due to increased survival (Paterson et al., 2012; Pepper et al., 2008; Petlickovski et al., 2005). MCL is overexpressed in samples from patients that respond poorly to chemotherapy and signalling responsive samples have been shown to have elevated levels of MCL-1 following stimulation with immobilised anti-IgM (Petlickovski et al., 2005). Therefore the increase in *MCL-1* mRNA was not unexpected following sIgM stimulation (Figure 5-12 and Figure 5-13). The levels of *MCL-1* mRNA associated with the different polysome fractions were also enhanced following sIgM stimulation (Figure 5-14), indicating increased translation. After removing any transcriptional effects *MCL-1* did not have elevated translation (Figure 5-16), suggesting that the increase in MCL-1 in CLL is regulated at the level of transcription and translation rather than translation alone. Although, these results may not provide an accurate indication of the translational effect as one sample differed from the other samples analysed therefore to determine whether *MCL-1* is also translational regulated following sIgM stimulation greater samples numbers are required.

The changes in *ACTB* mRNA expression and association with polysome fractions was unexpected as *ACTB* was chosen as a housekeeping gene, but the data showed that following sIgM stimulation transcription was enhanced and *ACTB* mRNA shifted to higher density fractions indicated enhanced translation (Figure 5-12 and Figure 5-16). Others have also shown that *ACTB* can vary with incubation conditions (Fink et al., 2008), therefore it is interesting that *ACTB* translation was enhanced following sIgM stimulation.

Data in this chapter suggested that signalling via the BCR enhanced translation especially of *MYC* and *MCL-1*, providing a link between BCR signalling, translation and clinical outcome.

Chapter Six

Results – Effect of PEITC and Kinase Inhibitors on Translation in CLL

6. Effect of PEITC and Kinase Inhibitors on Translation in CLL

6. 1. Introduction

Having established the conditions required for the study of mRNA translation in primary CLL samples, the next step was to investigate the effects of PEITC using sIgM stimulation as a means to mimic growth promoting antigen stimulation. I also investigated the effects of novel inhibitors targeted against BCR-associated kinases to determine if the effects of these compounds on mRNA translation could contribute to their therapeutic efficacy. As before, investigations focused on both global mRNA translation as well as specific translation of *MYC* and *MCL-1* mRNAs.

6. 2. Hypothesis and Aims

6. 2. 1. Hypothesis

PEITC, and inhibitors of BCR-associated kinases, will inhibit mRNA translation in sIgM stimulated CLL cells.

6. 2. 2. Aims

The aims of this chapter were to investigate the effects of PEITC, and the SYK inhibitor tamatinib and the BTK inhibitor Ibrutinib, on basal and sIgM-induced mRNA translation. These aims were investigated by:

- Metabolic labelling experiments to determine whether PEITC or kinase inhibitors prevented sIgM-induced translation
- Quantifying the mRNA associated with fractions of the polysome profile to determine whether PEITC or kinase inhibitors altered sIgM-induced translation of *MYC* and *MCL-1*.
- Determining the signalling pathway altered by PEITC to decrease basal and sIgM-induced translation in CLL

6. 3. Results

6. 3. 1. Analysing the Effect of PEITC on mRNA Translation Rates Following BCR Stimulation

To investigate the effect of PEITC on mRNA translation experiments were first performed using metabolic labelling. Cells were stimulated using bead-bound anti-IgM as carried out in previous experiments (section 5. 3.) but cells were also additional treated with PEITC (10µM). PEITC was added in the final five hours of the 24 hour incubation with anti-IgM beads or cells were left untreated as a control. In parallel, cells were treated with bead-bound isotype control antibody (with and without PEITC) in order to investigate the effect of PEITC on basal mRNA translation. Cells were treated for the final five hours of the incubation with PEITC, thus allowing one hour of PEITC treatment prior to initiation of metabolic labelling. Signal responsive CLL samples were selected that had shown enhanced mRNA translation following sIgM stimulation previously (Figure 5-1). Metabolic labelling data for individual samples are shown in Figure 6-1 and data obtained from all samples analysed are summarised in Figure 6-2.

Stimulation of the sIgM enhanced RNA translation compared to isotype control antibody (Figure 6-1 and Figure 6-2) with a mean increase of 5.5 fold ($p<0.001$, t-test, n=7). PEITC inhibited both basal and sIgM stimulated translation (Figure 6-3). Overall the mean reduction in basal translation induced by PEITC was 2.7 fold ($p<0.001$ for the difference between isotype control treated cells in the presence or absence of 10µM PEITC, paired t-test, n=7). The mean reduction in anti-IgM induced translation in response to PEITC treatment was 1.8 fold ($p=0.011$ for the difference between anti-IgM treated cells in the presence of absence of 10µM PEITC, paired t-test, n=7).

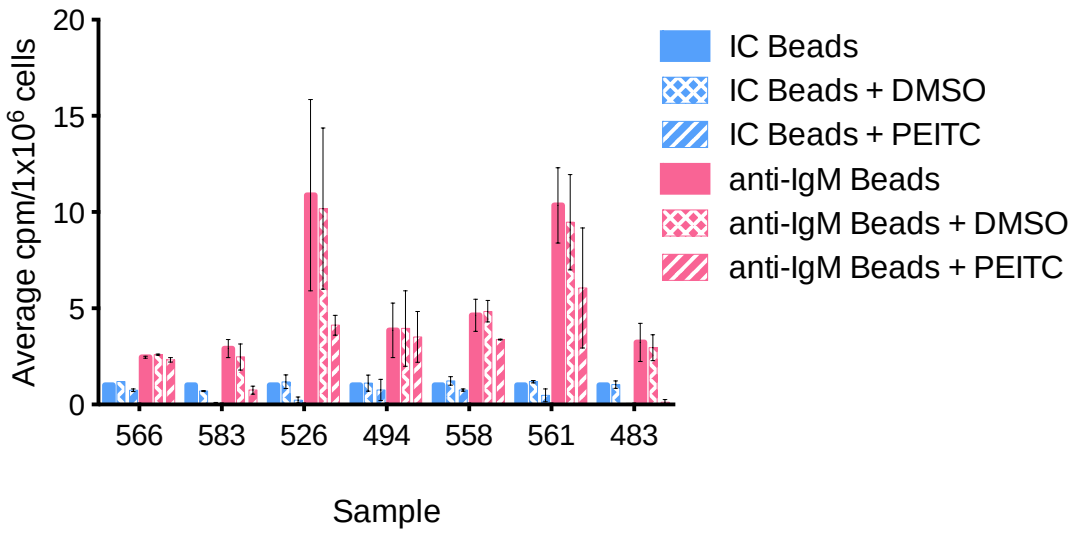

Figure 6-1: Effect of anti-IgM Stimulation in Combination with PEITC Treatment on Translation

CLL cells were recovered from cryopreservation and incubated with either anti-IgM beads, isotype control beads (IC beads) or left untreated (UT) for 24 hours. Cells were treated with 10µM PEITC, equivalent DMSO or left UT for five hours. Metabolic labelling was carried out in the final four hours. Bars represent the average incorporation with error bars representing the standard deviation from the mean, samples carried out in duplicate.

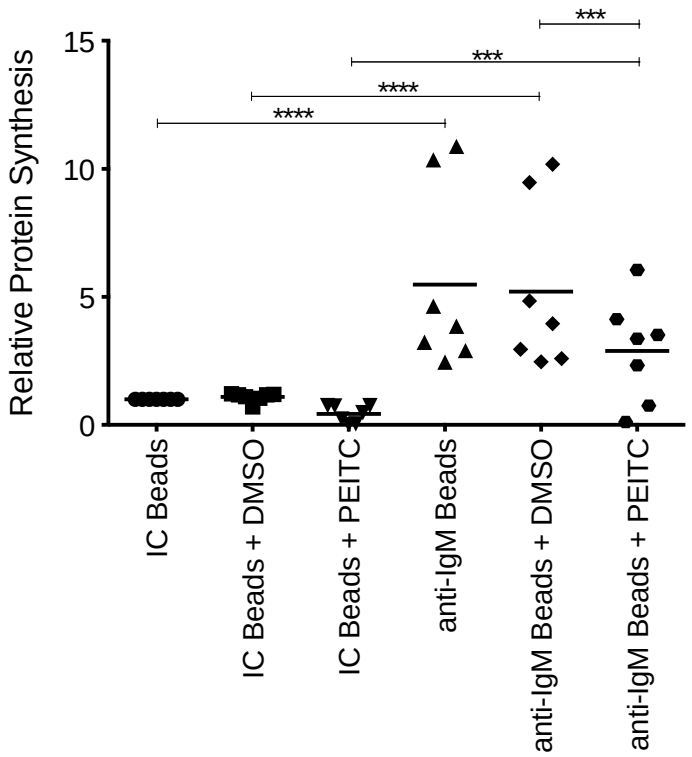

Figure 6-2: Effect of PEITC on Translation Following IgM Stimulation

Metabolic labelling of seven signal responsive CLL samples treated with anti-IgM or isotype control (IC) beads alone or in combination with 10µM PEITC or equivalent DMSO (Figure 6-1) were made relative to IC bead treatment alone for each sample to quantify the relative change in mRNA translation. Points represent the average incorporation per sample with the line representing the mean of all samples. Statistically significant data is indicated (p=*** ≤ 0.005, p=**** ≤ 0.001, Two way ANOVA, Prism6).

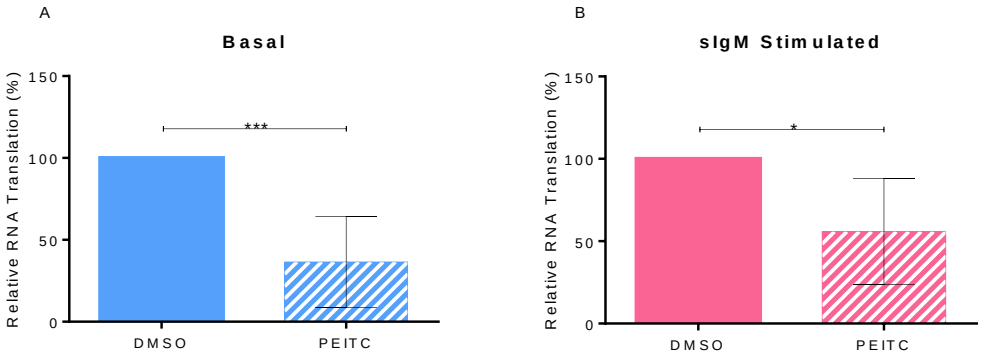

Figure 6-3: Effect of PEITC on Basal and sIgM-Induced mRNA Translation

Metabolic labelling of seven signal responsive CLL samples treated with anti-IgM (sIgM Stimulated) or isotype control beads (Basal) alone or in combination with 10µM PEITC or equivalent DMSO was carried out, see Figure 6-1. The DMSO treated samples were set to 100% and the effect of PEITC on basal and sIgM was calculated as a percentage. Bars represent the average metabolic incorporation, with DMSO set to 100%, error bars indicate the standard deviation. Statistically significant data is indicated (p=*≤ 0.05, p=*** ≤ 0.005, paired t-test, n=7, Prism6).

6. 3. 2. Effect of PEITC on Polysome Profiles Following BCR Stimulation

To confirm the results obtained by metabolic labelling, polysome profiling was carried out in signalling responsive samples that had been used in the experiments shown in Figure 6-1. Firstly profiles were analysed from a sample that was recovered from cryopreservation and allowed to recover for one hour prior to the addition of 10µM PEITC or equivalent DMSO for a short time point of 30 minutes. PEITC decreased the amplitude of the polysome peaks by approximately 20% compared to DMSO treatment (Figure 6-4). This confirmed the metabolic labelling data that PEITC decreased basal translation (Figure 6-3). Further experiments were performed on four signalling responsive samples, in these experiments cells were recovered from cryopreservation and allowed one hour to recover prior to the addition of anti-IgM beads or isotype control beads for 24 hours. In the final five hours PEITC (10µM), or equivalent DMSO, was added prior to collection of polysome lysates. Following anti-IgM treatment there was no detectable increase in polysome peaks, which made changes hard to detect in response to PEITC treatment (Figure S9-12).

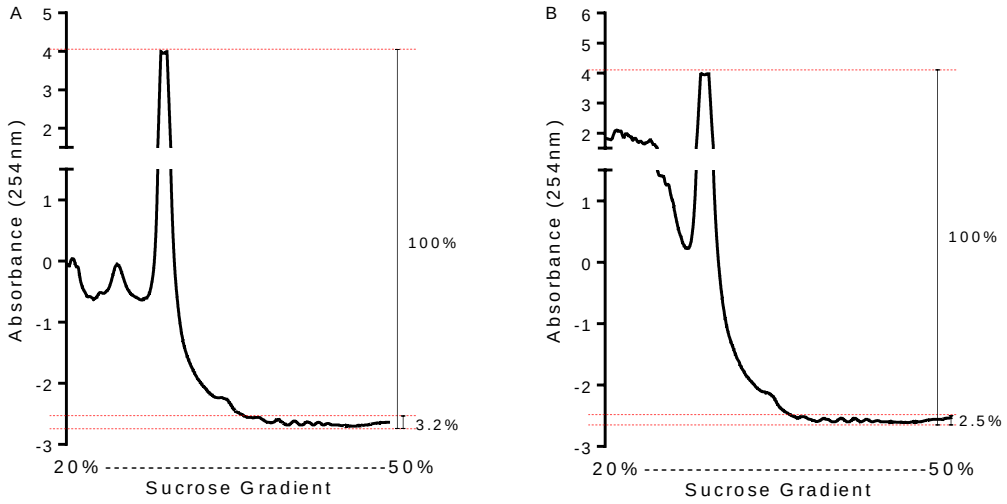

Figure 6-4: Effect of PEITC on Polysome Profiles Following sIgM Stimulation

CLL cells were recovered for one hour before treatment with 10µM PEITC (B) or equivalent DMSO (A) for 30 minutes before polysome cell lysates were collected and profiled. Polysome peak amplitude was calculated as a percentage of the total amplitude of the profiles. Profiles are representative of two samples.

To further investigate the effect of PEITC on sIgM-induced translation qPCR was carried out as described in section 5. 3. 5. I investigated the effect of PEITC treatment on the translation of *MYC* and *MCL-1* mRNAs on polysome fractions, collected as illustrated in Figure 3-11. The data are presented in a similar manner to section 5. 3. 5. PEITC treatment inhibited sIgM-induced increase in *MYC, MCL-1* and *ACTB* total mRNA levels (Figure 6-5, Figure 6-6 and Figure S9-13). Treatment with PEITC decreased total mRNA levels of these genes to a similar level as un-stimulated (isotype control bead treated) cells. The decrease in total mRNA levels following PEITC treatment did not reach significance when all four samples were combined, which could be due to insufficient samples numbers or that PEITC only had a minor influence on transcription (Figure 6-6).

The amount of *MYC, MCL-1* and *ACTB* mRNA per fraction of the polysome profile significantly decreased in fractions 2-5 inclusive following treatment of PEITC compared to incubation with anti-IgM beads alone (Figure 6-7 and Figure S9-14). After removal of any transcriptional effects PEITC significantly reduced the association of mRNA associated with the highest density polysomes, for *MYC, MCL-1* and *ACTB* (Figure 6-8 and Figure S9-15). Although when data from all samples were combined the PEITC-induced decrease in mRNA association with polysome fractions did not reach significance (Figure 6-9). Finally analysis into the ratio of mRNA associated with polysomes compared to monosomes was carried out. This analysis indicated that following PEITC treatment the mRNAs of *MYC, MCL-1* and *ACTB* were less associated with polysomes compared to sIgM stimulated cells alone (Figure 6-10 and Figure S9-16). This data indicated that translation induced by sIgM stimulation was significantly inhibited by PEITC treatment. The inhibition of translation was independent of transcription, although PEITC may also modulate transcription as well as specifically translation.

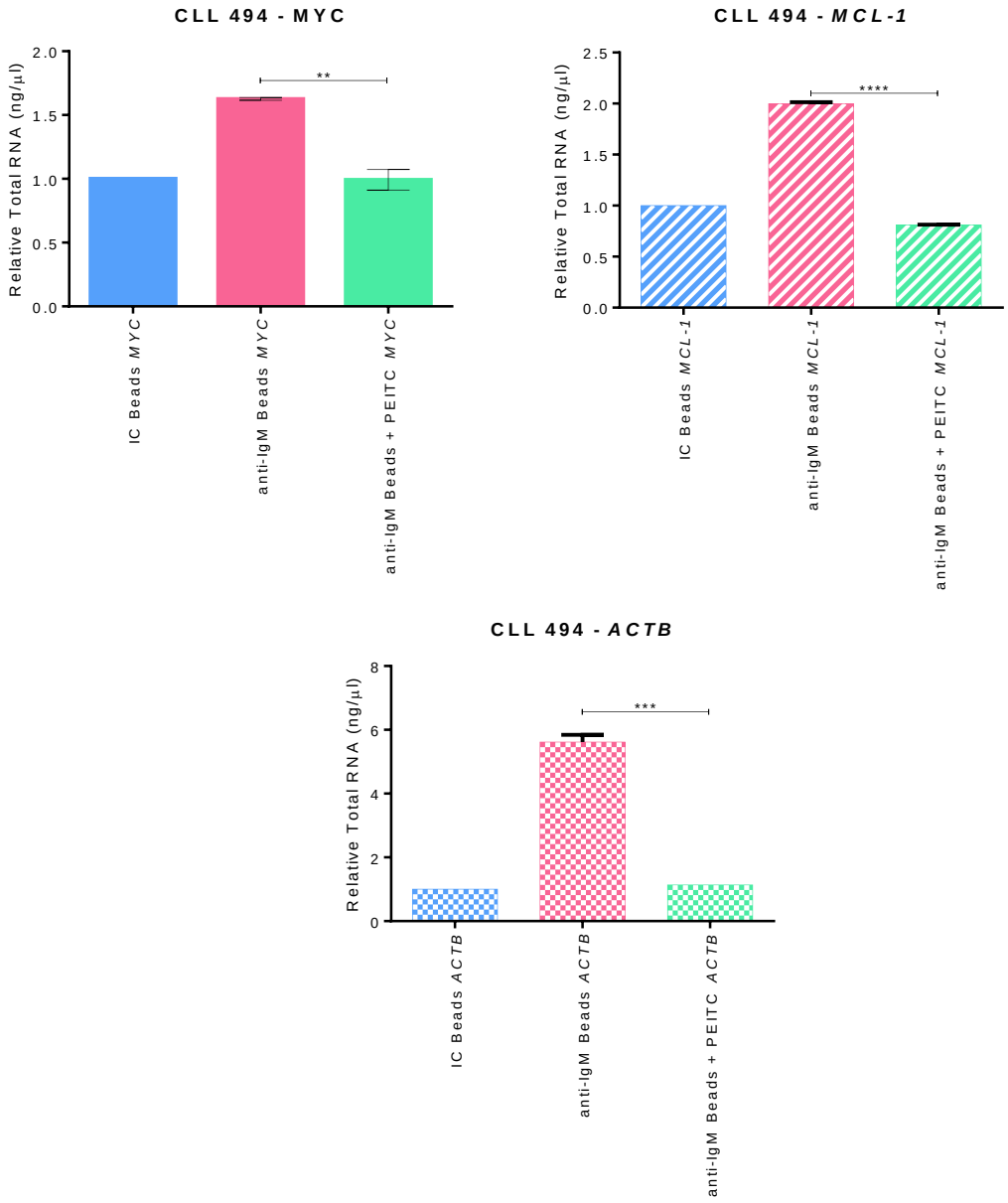

Figure 6-5: Abundance of *MYC*, *MCL-1* and *ACTB* mRNA Following sIgM Stimulation and Treatment with PEITC

CLL sample 494 was incubated with anti-IgM beads or isotype control (IC) beads for a total of 24 hours and during the final five hours 10µM PEITC was added, prior to polysome profiling. Following polysome profiling qPCR analysis was undertaken to investigate the abundance of *MYC*, *MCL-1* and *ACTB* mRNA levels in the whole profile. Bars represent the average total mRNA relative to isotype control (IC) beads. Error bars indicate the standard deviation and significantly different data is indicated, ** = $p \leq 0.01$, *** = $p \leq 0.005$, **** = $p \leq 0.001$, t-test (n=2).

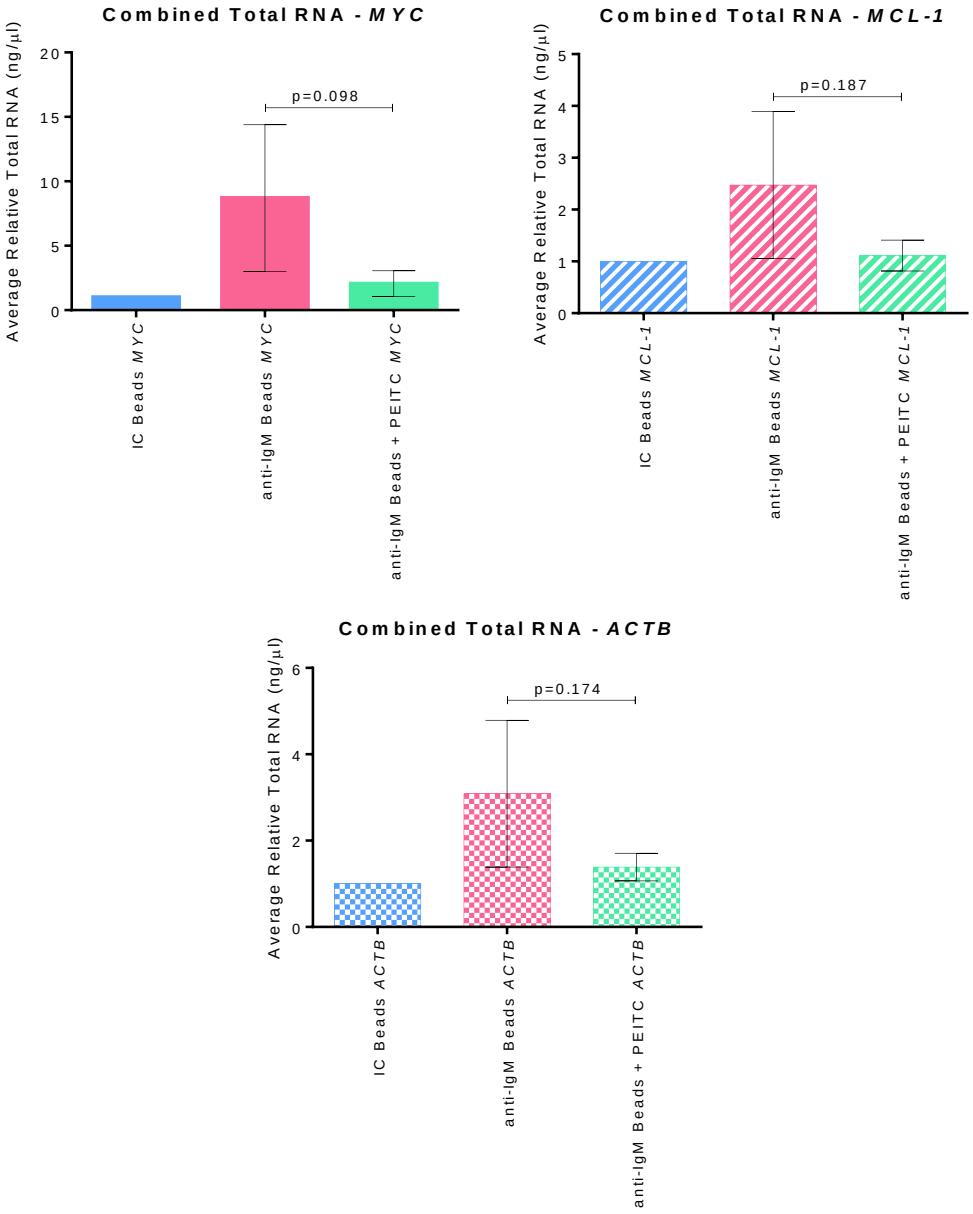

Figure 6-6: Average Abundance of *MYC, MCL-1* and *ACTB* mRNA Following sIgM Stimulation and Treatment with PEITC

CLL samples were incubated with anti-IgM beads or isotype control (IC) beads for a total of 24 hours and during the final five hours 10µM PEITC was added, prior to polysome profiling. Following polysome profiling qPCR analysis was undertaken to investigate the abundance of *MYC, MCL-1* and *ACTB* mRNA levels in the whole profile. Bars represent the average total mRNA relative to isotype control (IC) beads. Error bars indicate the standard deviation and significantly different data is indicated, ** = $p \leq 0.01$, *** = $p \leq 0.005$, **** = $p \leq 0.001$, t-test (n=4).

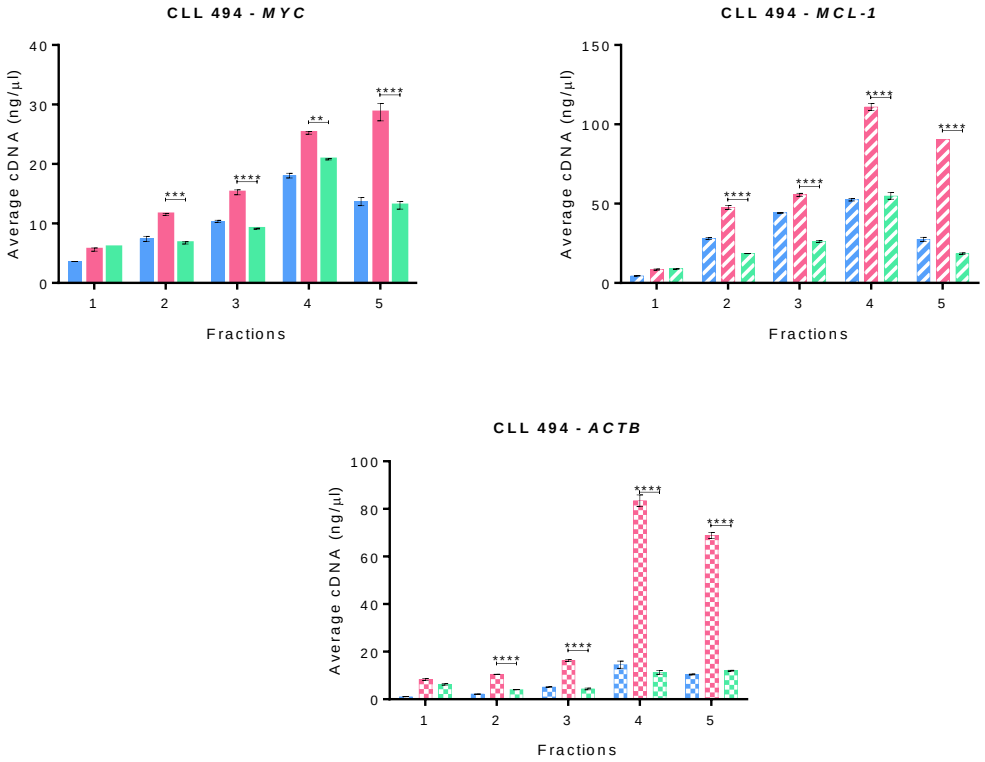

Figure 6-7: Polysome Distribution of *MYC, MCL-1* and *ACTB* mRNA After Treatment with PEITC

Following polysome profiling of CLL sample 494 qPCR analysis was undertaken to investigate the abundance of *MYC*, *MCL-1* and *ACTB* mRNA levels in each fraction of the polysome profile. Bars represent the average mRNA in each fraction following treatment with isotype control beads and DMSO (blue bars), treatment with anti-IgM beads (pink bars) or treatment with anti-IgM beads in combination with 10µM PEITC (green bars). Error bars indicate the standard deviation and significantly different data is indicated, ** = p≤ 0.01, *** = p≤ 0.005, **** = p≤ 0.001, Two-way ANOVA (n=2).

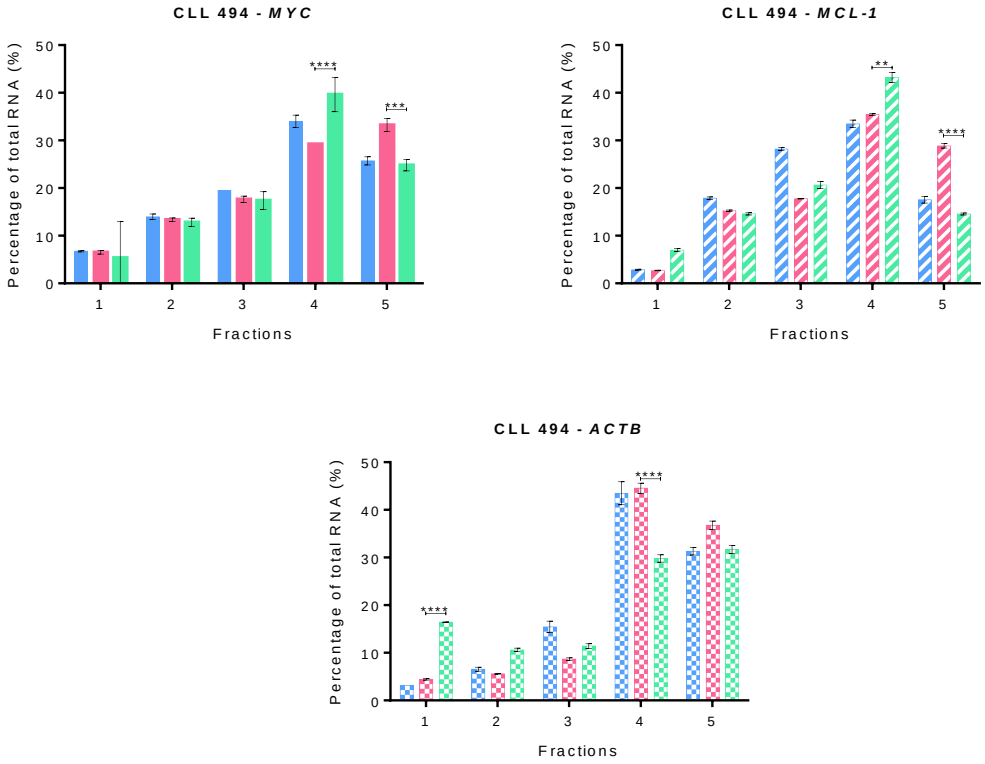

Figure 6-8: Percentage of *MYC, MCL-1* and *ACTB* mRNA Associated with Polysome Profile Fractions Following Treatment with PEITC

Following polysome profiling of CLL sample 494 qPCR analysis was undertaken to investigate the abundance of *MYC, MCL-1* and *ACTB* mRNA levels in each fraction as a percentage of the total mRNA. Bars represent the average percentage of mRNA in each fraction following treatment with isotype control beads and DMSO (blue bars), treatment with anti-IgM beads (pink bars) or treatment with anti-IgM beads in combination with 10µM PEITC (green bars). Error bars indicate the standard deviation and significantly different data is indicated, ** = p≤ 0.01, *** = p≤ 0.005, **** = p≤ 0.001, Two-way ANOVA (n=2).

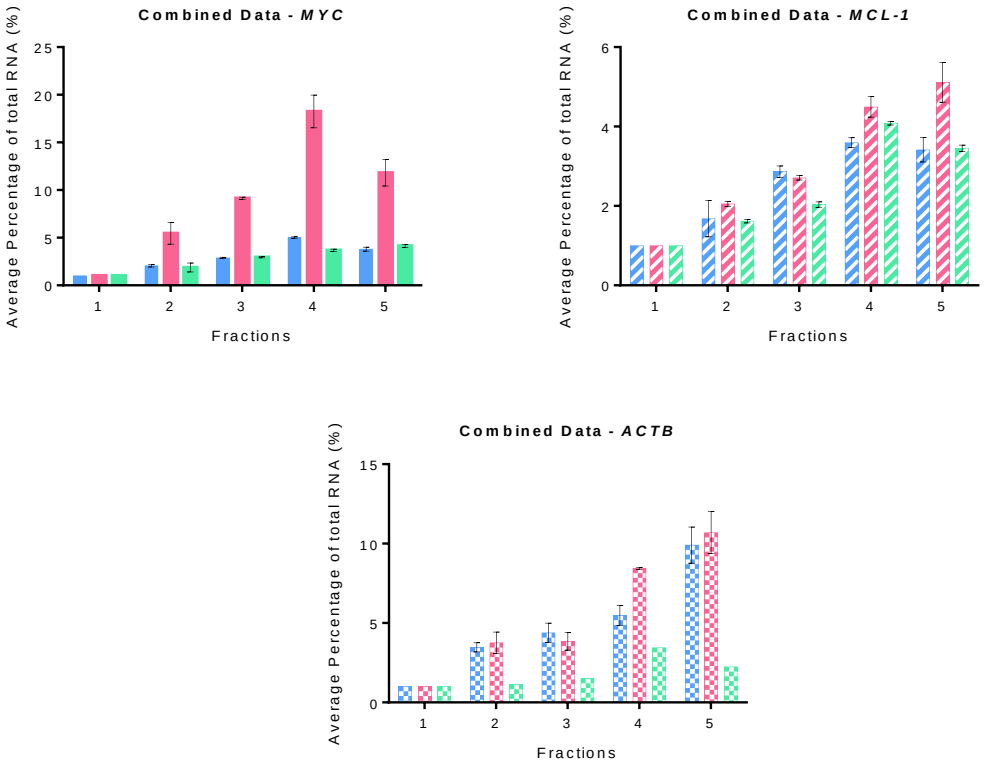

Figure 6-9: Average Percentage of *MYC*, *MCL-1* and *ACTB* mRNA Associated with Polysome Profile Fractions Following Treatment with PEITC

Following polysome profiling of CLL samples qPCR analysis was undertaken to investigate the abundance of *MYC*, *MCL-1* and *ACTB* mRNA levels in each fraction of the polysome profile. Bars represent the average percentage of mRNA in each fraction for all four samples analysed. With isotype control beads and DMSO treatment in blue, treatment with anti-IgM beads in pink and treatment with anti-IgM beads in combination with 10µM PEITC in green. Error bars indicate the standard deviation. No significant differences were identified by Two-way ANOVA.

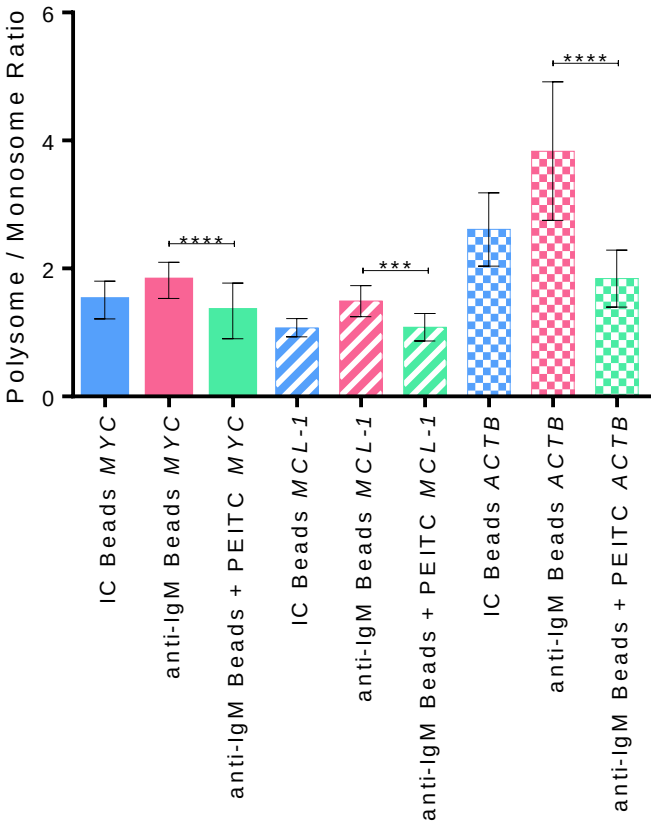

Figure 6-10: Polysome Association of *MYC, MCL-1* and *ACTB* mRNA Following sIgM Stimulation and Treatment with PEITC

Following polysome profiling of CLL samples qPCR analysis was undertaken to investigate the accumulation of *MYC, MCL-1* and *ACTB* mRNA levels in polysome fractions (fractions 3-5). Bars represent the average ratio of polysomally associated mRNA (fractions 3-5) with respect to sub-polysome associated mRNA (fractions 1 and 2). Error bars indicate the standard deviation and significantly different data is indicated, *** = $p \leq 0.005$, **** = $p \leq 0.001$, Two-way ANOVA (n=4).

6. 3. 3. Investigation into the Mechanism for Decreased Translation Following PEITC Treatment in CLL Cells

Having determined that PEITC inhibited sIgM-induced translation as well as basal translation (Figure 6-1 and Figure 6-3) it was important to determine which molecular pathways were altered by PEITC treatment. Previous data demonstrated the importance of eIF2α phosphorylation in PEITC induced translational repression (Chapter 4) and mTORC1 inhibition was also thought to be involved (Cavell et al., 2012). To investigate the effect of PEITC on signalling pathways CLL cells were recovered from cryopreservation and allowed to recover for one hour before incubating with anti-IgM beads or isotype control beads in the presence or absence of PEITC for 30 or 60 minutes. Western blotting analysis indicated that following sIgM stimulation P70S6K was phosphorylated at both time points, indicating that the mTORC1 pathway was activated following BCR signalling (Figure 6-11). The phosphorylation of P70S6K was reduced by PEITC treatment (Figure 6-11), indicating a decrease in mTORC1 activity that was in agreement with the published data showing that PEITC inhibited mTORC1 activity (Cavell et al., 2012). Stimulation of sIgM also increased the phosphorylation of Akt at Ser473 (Figure 6-11), the target site for mTORC2 phosphorylation (see section 1. 3. 7. 1.). Phosphorylation of Akt will ultimately decrease mTORC1 activity (see Figure 1-15) forming a negative feedback loop. PEITC treatment did not effect Akt phosphorylation (Figure 6-11) therefore indicating that PEITC works downstream of mTORC2, in agreement with the Cavell et al paper, which showed that TSC2 was essential for decreased mTORC1 activity in response to PEITC (Cavell et al., 2012). PEITC also induced the phosphorylation of eIF2α at Ser51 following sIgM stimulation for a minimum of 30 minutes (Figure 6-11). PEITC also induced the phosphorylation of eIF2α in unstimulated cells (Figure 6-11). Additional supportive experiments were carried out to confirm this finding and can be found in Figure S9-17, carried out by Dr Marina Sanchez Hidalgo. These data together indicated that similar pathways were modulated by PEITC in CLL cells and MCF7 cells. The data suggested that BCR signalling increases translation via increased mTORC1 activity, which was negated by PEITC not only by decreased mTORC1 activity but also via increased eIF2α phosphorylation.

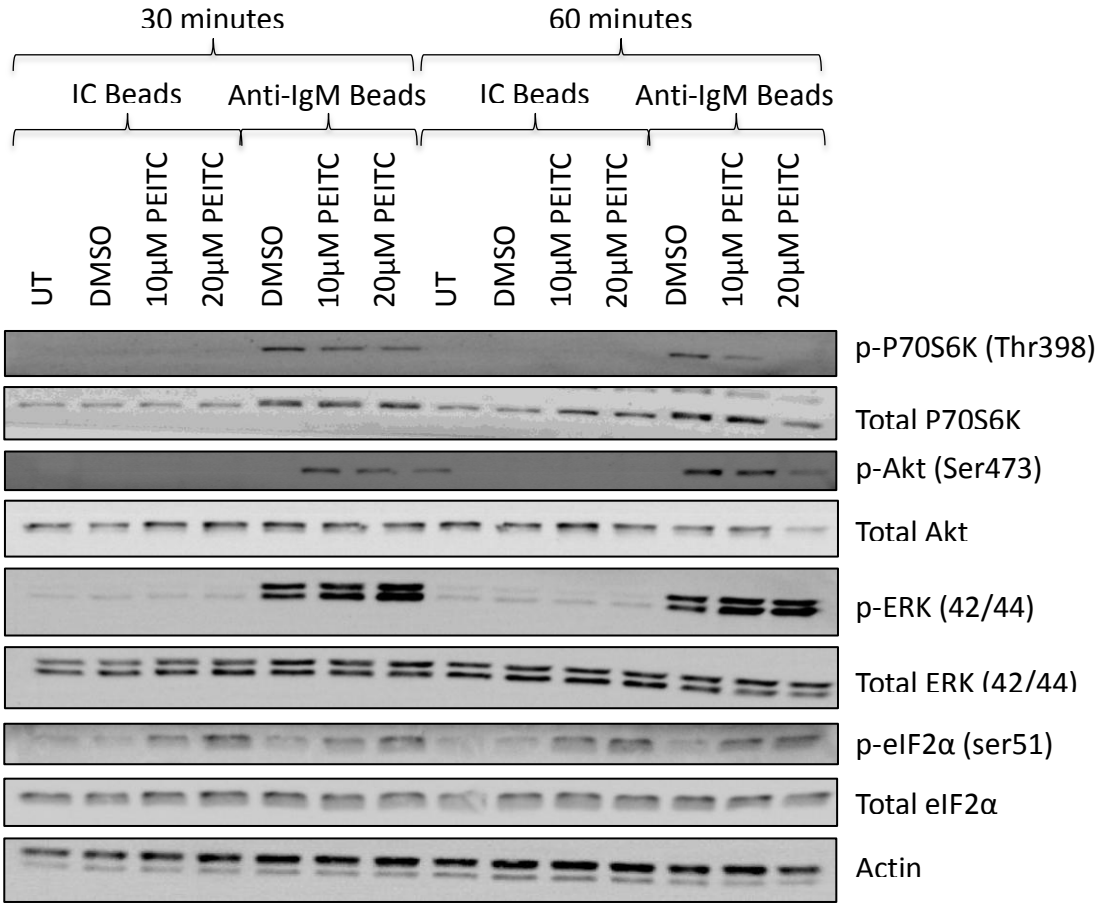

Figure 6-11: Effect of PEITC on Basal and sIgM Stimulated Signalling Pathways

CLL cells (sample 558) were either untreated (UT) or incubated with anti-IgM beads (IgM beads) or isotype control beads (I.C beads) and treated with the indicated concentration of PEITC or equivalent DMSO to 20µM for 30 or 60 minutes. Western blotting was carried out to determine the phosphorylation status of P70S6K, Akt and eIF2α, total levels of these proteins along with β-actin was also determined. Representative western blot from two samples.

6. 3. 4. Analysing the Effect of BCR Inhibitors on Translation by Metabolic Labelling

Stimulation of CLL B cells by anti-IgM beads significantly enhanced translation, although further investigation was required to determine the importance of BCR signalling. Similar experiments were performed to investigate the effects of inhibitors of BCR associated kinases on mRNA translation in CLL cells. The compounds selected for this study were the BTK inhibitor, ibrutinib, and tamatinib, the active form of the SYK inhibitor pro-drug fostamatinib. Both ibrutinib and fostamatinib have been evaluated in clinical trials in CLL. Ibrutinib is currently in 24 clinical trials, including phase II and phase III trials for the use of ibrutinib as a monotherapy as well as in combination with rituximab (anti-CD20 monoclonal antibody) treatment (NCT01886872 clinical trials.gov). Fostamatinib is currently in a phase II clinical trial to evaluate the effectiveness of SYK inhibition in lymphoma patients (NCT01499303).

CLL samples were selected that had previously been analysed for translation following sIgM stimulation and were all ‘responders’ (Figure 5-1). Following recovery from cryopreservation samples were pre-treated with 10µM Ibrutinib (BTKi), 10µM Tamatinib (SYKi), equivalent DMSO or left untreated for one hour before the addition of bead-bound anti-IgM or isotype control antibody. Cells were incubated with anti-IgM beads or isotype control beads for a total of 24 hours and metabolic labelling was carried out in the final four hours of the incubation time.

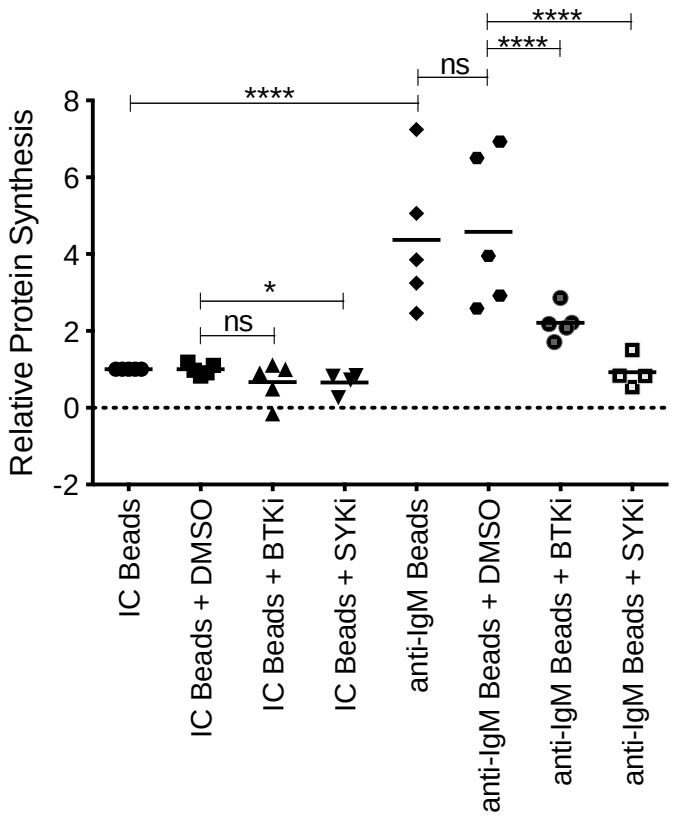

Figure 6-12: Effect of BTK and SYK Inhibitors on sIgM Stimulated Translation

Metabolic labelling of five signal responsive CLL samples treated with 10µM Ibrutinib (BTKi), 10µM Tamatinib (SYKi), equivalent DMSO or untreated for one hour prior to incubation with anti-IgM or isotype control (IC) beads for 24 hours (Figure S9-18) were made relative to IC bead treatment alone for each sample to quantify the relative change in mRNA translation. Points represent the average incorporation per sample with the line representing the mean of all samples. Statistically significant data is indicated (p=* ≤ 0.05, p=**** ≤ 0.001, Two way ANOVA, Prism6).

As in previous analyses stimulation of the sIgM with bead-bound anti-IgM significantly increased metabolic incorporation compared to isotype control beads and additional treatment with the solvent control, DMSO, had minimal effect on translation (Figure 6-12). Like PEITC, ibrutinib and tamatinib inhibited sIgM-induced mRNA translation (Figure 6-12 and Figure S9-18). Tamatinib was particularly effective and on average reduced sIgM-induced mRNA translation by approximately 80% ($p=0.0005$ for tamatinib treated CLL samples in combination with anti-IgM beads versus cells treated with equivalent DMSO in combination with anti-IgM beads) (Figure 6-13 B). Tamatinib was also able to decrease basal translation by approximately 40% ($p=0.0348$ for tamatinib treated cells in combination with isotype control beads versus cells treated with equivalent DMSO and isotype control beads) (Figure 6-13 A). Ibrutinib was less effective, reducing translation by approximately 50% ($p=0.045$ for ibrutinib treated cells in combination with anti-IgM beads versus cells treated with equivalent DMSO in combination with anti-IgM beads) (Figure 6-13 B). In contrast to PEITC ibrutinib did not have a significant effect on basal translation ($p=0.1886$ for ibrutinib treated cells in combination with isotype control beads versus cells treated with equivalent DMSO and isotype control beads) (Figure 6-13 A). In conclusion, PEITC was able to inhibit basal translation to a greater extent than sIgM-induced translation, while the kinase inhibitors (ibrutinib and tamatinib) inhibited sIgM-induced translation to a greater extent than basal translation.

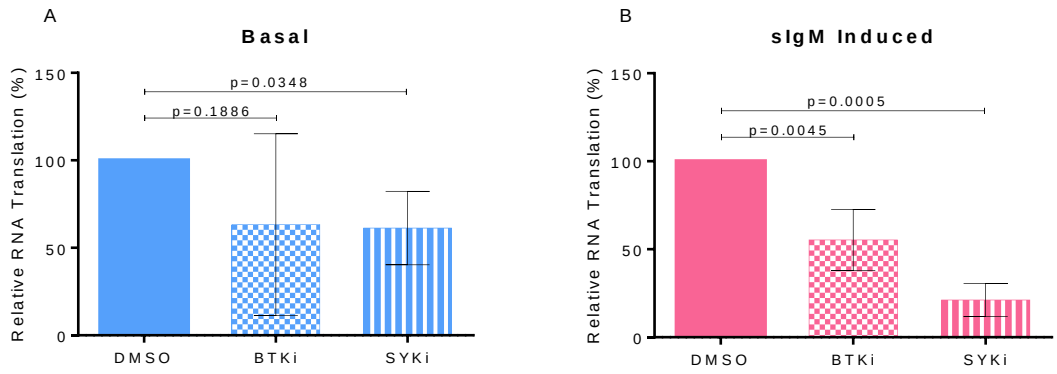

Figure 6-13: Effect of BTK and SYK Inhibition on Basal and sIgM-Induced Translation

Metabolic labelling of five signal responsive CLL samples treated with 10µM Ibrutinib (BTKi), 10µM Tamatinib (SYKi), equivalent DMSO or untreated for one hour prior to incubation with anti-IgM or isotype control (IC) beads for 24 hours, see Figure S9-18. The DMSO treated samples were set to 100% and the effect of BTKi and SYKi on basal and sIgM-induced translation was calculated as a percentage. Bars represent the average percentage of metabolic incorporation with DMSO treated cells set to 100%, error bars indicate the standard deviation. Statistically significant data is indicated, paired t-test, n=5, Prism6.

6. 3. 5. Effect of BCR Kinase Inhibitors on Polysome Profiles

Having established that inhibition of BTK or SYK decreased translation I next investigated the effect of inhibition of these kinases on the translation of *MYC, MCL-1* and *ACTB* following sIgM stimulation. As before, CLL samples were recovered from cryopreservation and allowed to recover for one hour prior to the addition of 10µM ibrutinib (BTKi), 10µM tamatinib (SYKi), equivalent DMSO or untreated. Bead-bound anti-IgM or isotype control beads were added to the samples and incubated for a further 24 hours. In the final five hours of incubation cells treated with anti-IgM alone were also treated with 10µM PEITC, prior to collection of polysome lysates. Polysome profiling was carried out (Figure S9-19 and Figure S9-20) on two responsive CLL samples, used in metabolic labelling experiments (Figure 6-12). The profiles were fractionated and q-PCR was carried out for *MYC, MCL-1* and *ACTB*. The data was analysed in a similar way as described in section 5. 3. 5. Similar to PEITC, BTK inhibition decreased sIgM stimulated induction of *MYC* total mRNA (Figure 6-14, Figure S9-21 and Figure 6-15). Inhibition of SYK had a more profound effect on *MYC* total mRNA levels, with *MYC* mRNA levels decreased back down to levels seen in unstimulated (isotype control) cells (Figure 6-14, Figure S9-21 and Figure 6-15).

BTK inhibition significantly decreased *MCL-1* total mRNA levels in one sample (Figure 6-14), but combined analysis showed that BTK inhibition had no effect on *MCL-1* total mRNA levels compared to anti-IgM bead treated cells (Figure 6-15). Whereas inhibition of SYK significantly decreased *MCL-1* total mRNA levels compared to sIgM stimulation alone (Figure 6-14 and Figure 6-15). *ACTB* total mRNA levels were not significantly different in BTK inhibited cells compared to sIgM stimulation alone, whereas SYK inhibition decreased sIgM-induced *ACTB* mRNA levels (Figure 6-14, Figure 6-15 and Figure S9-21).

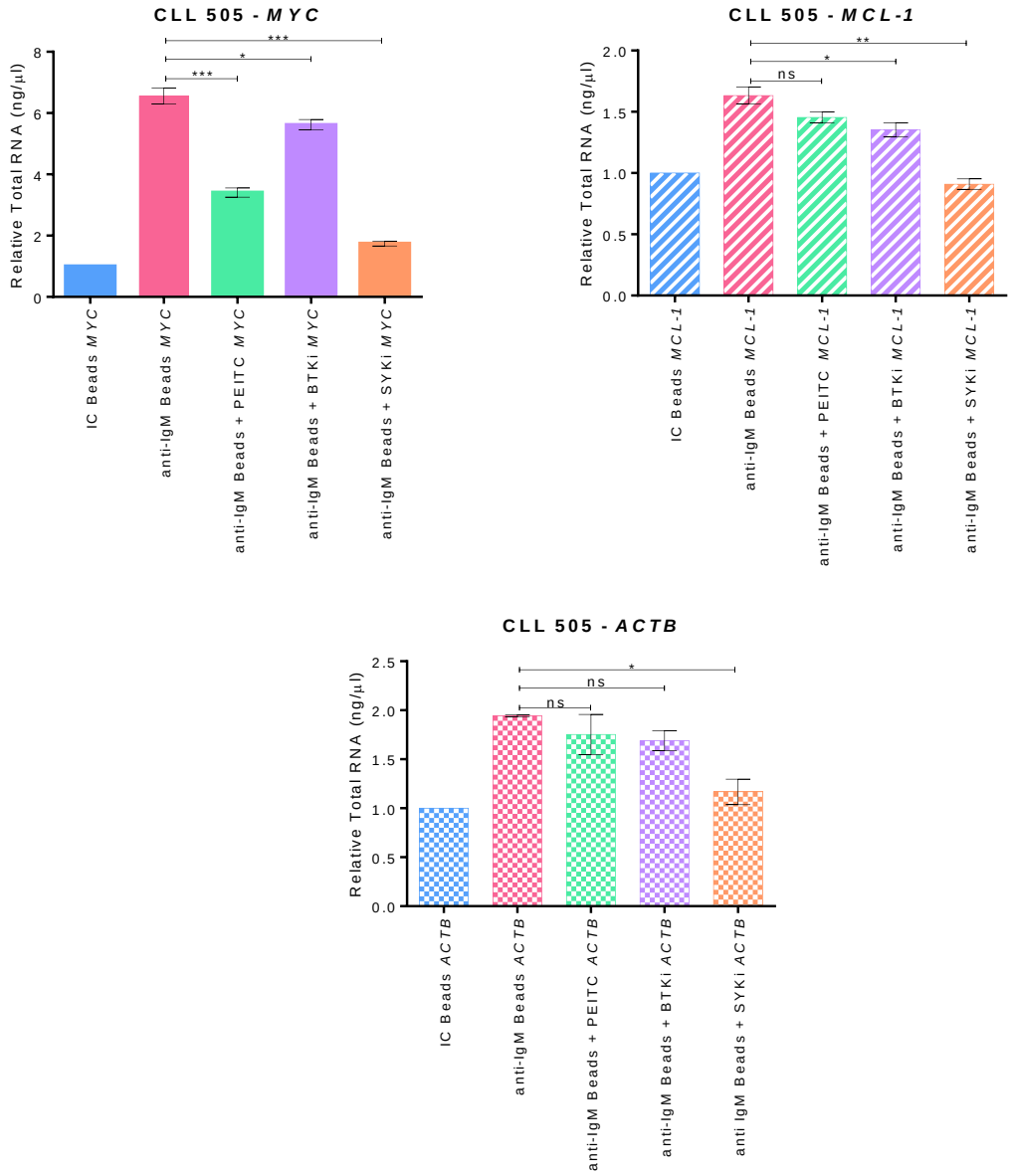

Figure 6-14: Abundance of *MYC, MCL-1* and *ACTB* mRNA Following Inhibition of BTK or SYK and Treatment with anti-IgM Beads

CLL sample 505 was treated with 10µM ibrutinib (BTKi) or 10µM tamatinib (SYKi) for one hour prior to incubation with anti-IgM beads or isotype control (IC) beads for a total of 24 hours and during the final five hours 10µM PEITC was added, prior to polysome profiling. Following polysome profiling, qPCR analysis was undertaken to investigate the abundance of *MYC, MCL-1* and *ACTB* mRNA levels in the whole profile. Bars represent the average total mRNA relative to isotype control (IC) beads. Error bars indicate the standard deviation and significantly different data is indicated, * = $p \leq 0.05$, ** = $p \leq 0.01$, *** = $p \leq 0.005$, t-test (n=2).

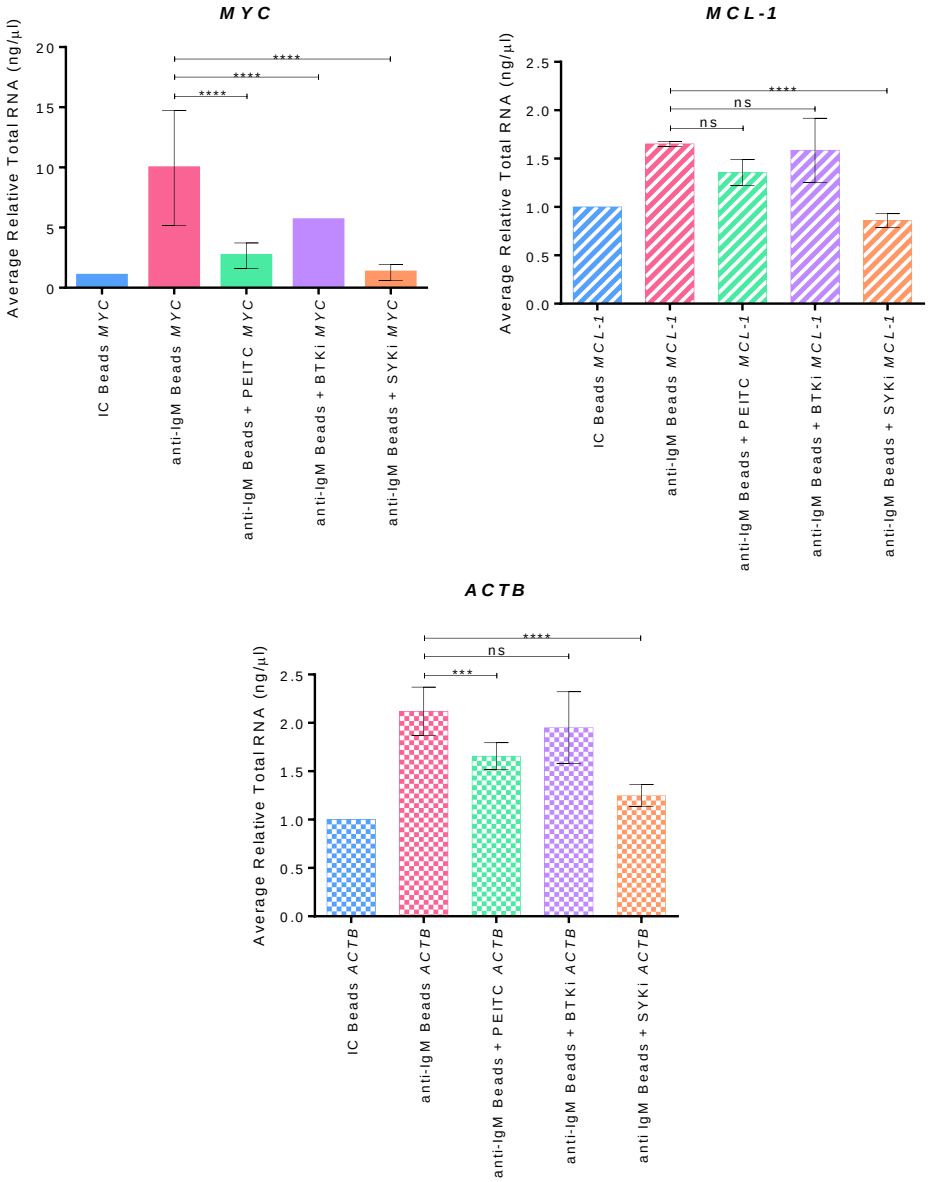

Figure 6-15: Average Abundance of *MYC*, *MCL-1* and *ACTB* mRNA Following Inhibition of BTK or SYK and Treatment with anti-IgM Beads

CLL samples were treated with 10µM ibrutinib (BTKi) or 10µM tamatinib (SYKi) or 10µM PEITC in combination with anti-IgM beads or isotype control beads (Figure S9-19 and Figure S9-20). Following polysome profiling, qPCR analysis was undertaken to investigate the abundance of *MYC*, *MCL-1* and *ACTB* mRNA levels in the whole profile. Bars represent the average total mRNA relative to isotype control (IC) beads. Error bars indicate the standard deviation and significantly different data is indicated, *** = $p \leq 0.005$, **** = $p \leq 0.001$, t-test (n=2 samples with duplicate readings).

Next analysis was undertaken to determine the polysome distribution of mRNA in response to sIgM stimulation in combination with BTK or SYK inhibition. Inhibition of BTK significantly decreased *MYC* mRNA in the highest density fraction and increased in the lowest density fraction, indicating decreased translation (Figure 6-16 and Figure S9-22). BTK inhibition had less of an effect on polysomal distribution of *MCL-1* and *ACTB* mRNA compared to sIgM stimulation alone (Figure 6-16 and Figure S9-22). Inhibition of SYK and sIgM stimulation resulted in a significant reduction in *MYC, MCL-1* and *ACTB* mRNA associated with all fractions of the profile compared to sIgM stimulation alone (Figure 6-16 and Figure S9-22).

In order to remove any transcriptional effect that inhibition of BTK or SYK may have had the data was analysed as a percentage of the total mRNA for each fraction. This indicated that BTK inhibition decreased mRNA associated with the highest density fraction and increased mRNA associated with fraction 4 (Figure 6-17, Figure 6-18 and Figure S9-23). This may suggest that BTK inhibition decreased translation. SYK inhibition had a similar effect as BTK in all three mRNAs analysed as SYK inhibition shifted mRNAs into lower density fractions (Figure 6-17, Figure 6-18 and Figure S9-23).

Analysis of polysomal associated mRNA (in fractions 3-5) compared to sub-polysome associated mRNA (fractions 1 and 2) indicated that inhibition of BTK decreased translation of all three genes, but did not reach significance due to low sample numbers (Figure 6-19 and Figure S9-16). Inhibition of SYK caused a more profound decrease in translation, especially on *MYC* mRNA (Figure 6-19 and Figure S9-16). Decreased translation following BTK and SYK inhibition indicated that anti-IgM beads signal via the BCR signalling pathway to stimulate translation, to increase expression of *MYC, MCL-1* and *ACTB*.

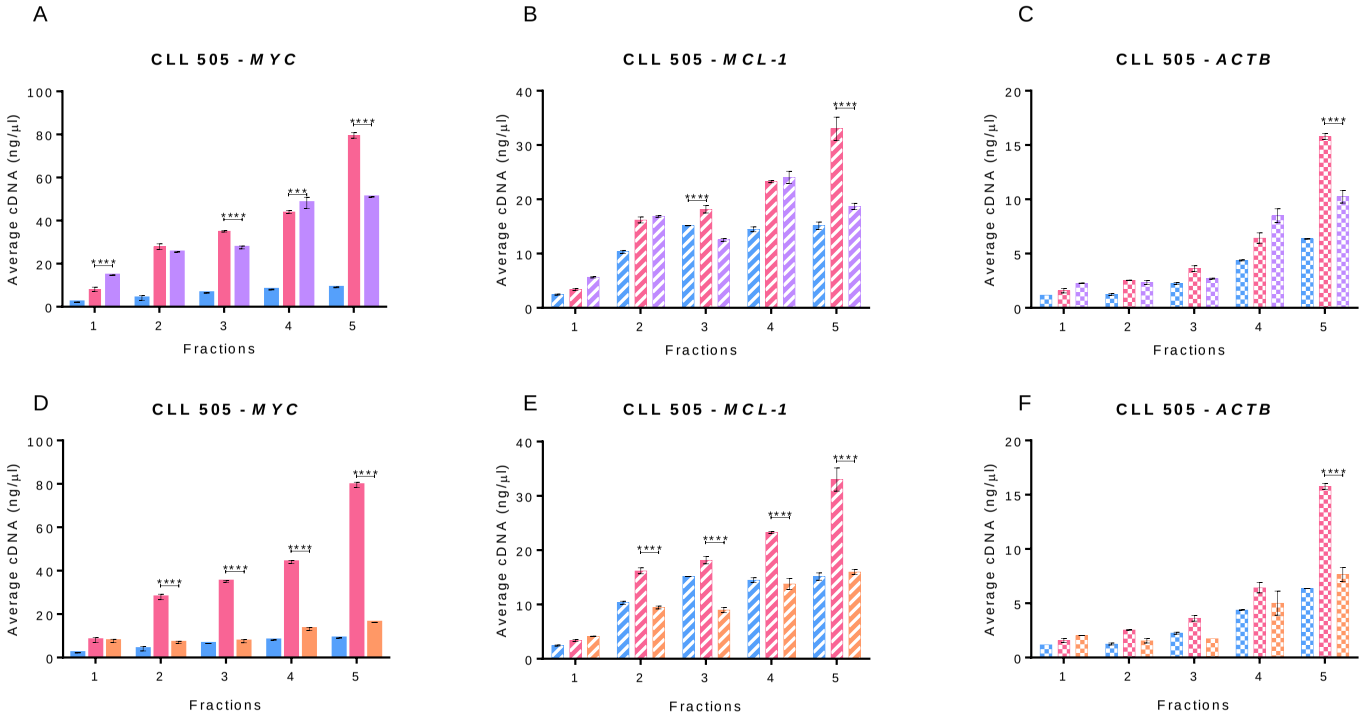

Figure 6-16: Polysome Distribution of *MYC, MCL-1* and *ACTB* mRNA Following BTK or SYK Inhibition in Combination with sIgM Stimulation

Following polysome profiling of CLL sample 505 qPCR analysis was undertaken to investigate the abundance of *MYC, MCL-1* and *ACTB* mRNA levels in each fraction of the polysome profile. Bars represent the average mRNA in each fraction following treatment with isotype control beads and DMSO (blue bars), treatment with anti-IgM beads (pink bars), treatment with anti-IgM beads in combination with 10µM Ibrutinib (purple bars – A to C) or treatment with anti-IgM beads in combination with 10µM Tamatinib (orange bars – D to E). Error bars indicate the standard deviation and significantly different data is indicated, **** = $p \leq 0.001$, Two-way ANOVA (n=2).

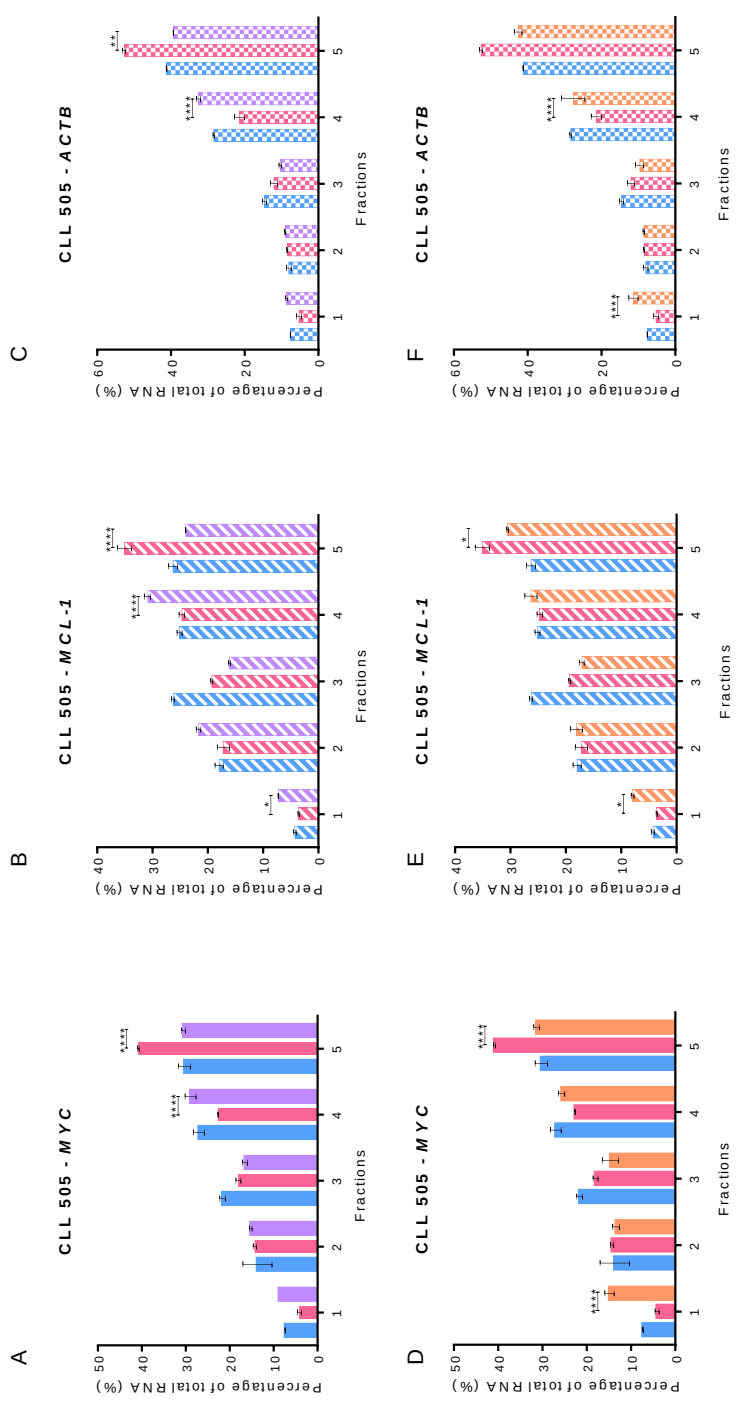

Figure 6-17: Percentage of *MYC*, *MCL-1* and *ACTB* mRNA Associated with Polysome Fractions Following Inhibition of BTK and SYK

Following polysome profiling of CLL sample 505 qPCR analysis was undertaken to investigate the abundance of *MYC*, *MCL-1* and *ACTB* mRNA levels in each fraction of the polysome profile. Bars represent the average percentage of mRNA in each fraction following treatment with isotype control beads and DMSO (blue bars), treatment with anti-IgM beads (pink bars), treatment with anti-IgM beads in combination with 10μM Ibrutinib (purple bars), or treatment with anti-IgM beads in combination with 10μM Tamatinib (orange bars). Error bars indicate the standard deviation and significantly different data is indicated, * = $p \leq 0.05$, ** = $p \leq 0.01$, **** = $p \leq 0.001$, Two-way ANOVA (n=2).

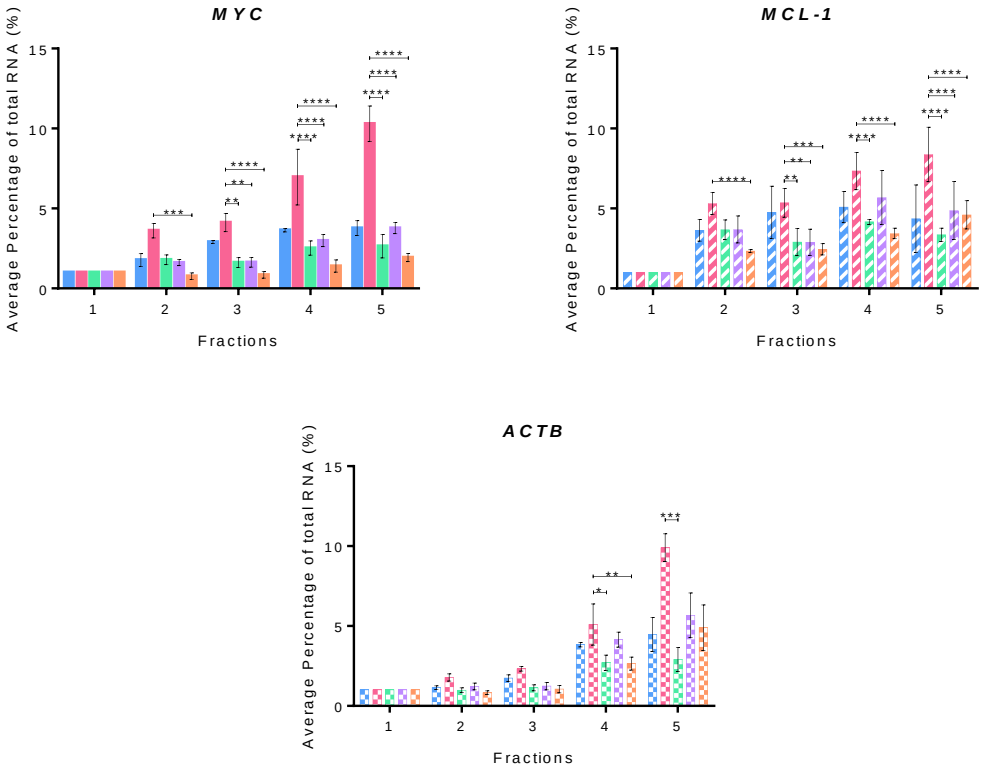

Figure 6-18: Average Percentage of *MYC*, *MCL-1* and *ACTB* mRNA Associated with Polysome Fractions Following Inhibition of BTK and SYK

Following polysome profiling of CLL samples qPCR analysis was undertaken to investigate the abundance of *MYC*, *MCL-1* and *ACTB* mRNA levels in each fraction of the polysome profile. Bars represent the average percentage of mRNA in each fraction following treatment with isotype control beads and DMSO (blue bars), treatment with anti-IgM beads (pink bars), treatment with anti-IgM beads in combination with 10µM Ibrutinib (purple bars), or treatment with anti-IgM beads in combination with 10µM Tamatinib (orange bars). Error bars indicate the standard deviation and significantly different data is indicated, * = $p \leq 0.05$, ** = $p \leq 0.01$, *** = $p \leq 0.005$, **** = $p \leq 0.001$, Two-way ANOVA (n=2).

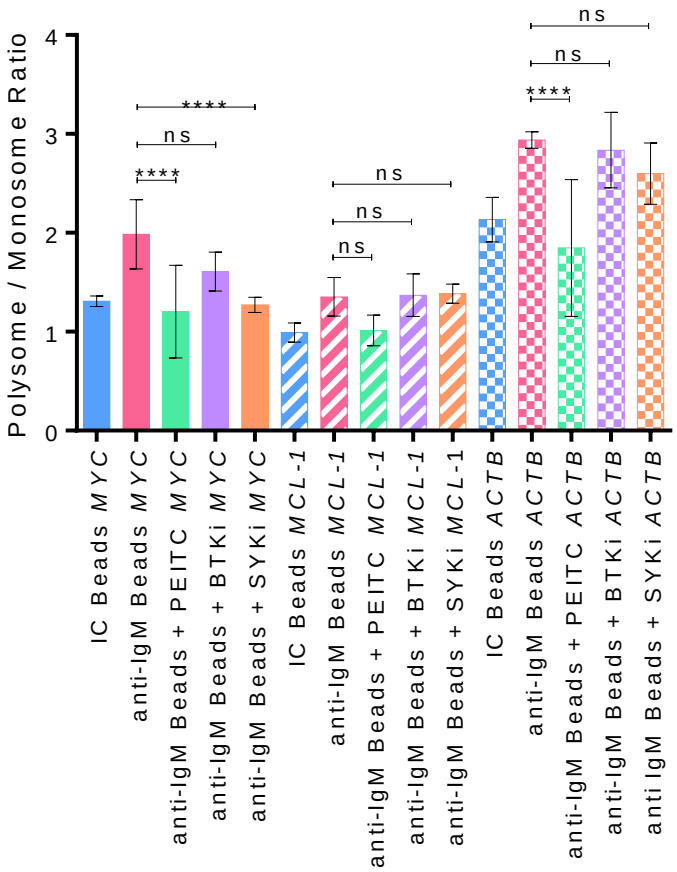

Figure 6-19: Polysome Association of *MYC, MCL-1 and ACTB* Following Inhibition of BTK or SYK

Following polysome profiling of CLL samples qPCR analysis was undertaken to investigate the accumulation of *MYC*, *MCL-1* and *ACTB* mRNA levels in polysome fractions (fractions 3-5). Bars represent the average ratio of polysomally associated mRNA (fractions 3-5) with respect to sub-polysome associated mRNA (fractions 1 and 2). Error bars indicate the standard deviation and significantly different data is indicated, *** = $p \leq 0.005$, **** = $p \leq 0.001$, Two-way ANOVA (n=4).

6. 4. Summary of Main Findings

- PEITC treatment decreased basal and sIgM-induced translation
- PEITC treatment decreased translation of *MYC, MCL-1* and *ACTB* mRNA compared to incubation with anti-IgM beads alone
- PEITC decreased sIgM stimulated mTORC1 activity and increased eIF2α phosphorylation
- Inhibition of BTK and SYK decreased sIgM-induced translation
- BTK inhibition decreased sIgM-induced transcription of *MYC* and *MCL-1* mRNA
- BTK inhibited translation of *MYC* and *MCL-1*
- Inhibition of SYK decreased sIgM-induced transcription of *MYC, MCL-1* and *ACTB*
- SYK inhibition decreased sIgM stimulated translation in a global manner and specifically decreased translation of *MYC*.

6. 5. Discussion

The enhanced translation following sIgM stimulation was inhibited by PEITC treatment (Figure 6-1-Figure 6-2). PEITC decreased basal translation to a greater extent than sIgM-induced translation (Figure 6-3). Thus suggesting that PEITC may inhibit the BCR pathway to decrease stimulated translation as well as inhibit translation independently of the BCR pathway. PEITC decreased the sIgM-induced transcription of *MYC, MCL-1* and *ACTB* (Figure 6-6) although this did not reach significance, possibly due to small sample numbers. PEITC had a greater effect on translation of *MYC, MCL-1* and *ACTB* as PEITC decreased the amount of mRNA associated with the highest density fractions of the polysome profile (Figure 6-8 and Figure 6-9). Thus resulting in a shift in the polysome:monosome ratio (Figure 6-10) such that these mRNAs were associated with lower density fractions, hence translation was lower following PEITC treatment compared to stimulation with anti-IgM beads alone. This provided a mechanism for decreased expression of MYC and

MCL-1 following PEITC treatment and stimulation with anti-IgM beads compared to stimulation alone, as seen by members of our group (Dr. Sergey Krysov, unpublished data).

6. 5. 1. Mechanisms for Decreased Translation

PEITC decreased translation in CLL in part by disrupting the BCR signalling pathway. The BCR signalling pathway leads to the activation of mTORC1 visualised by increased P70S6K phosphorylation (Figure 6-11) to enhance translation. PEITC decreased this sIgM-induced phosphorylation of P70S6K, without affecting the phosphorylation status of Akt (Figure 6-11). The fact that PEITC did not decrease sIgM-induced Akt phosphorylation indicated that PEITC worked further down the BCR signalling pathway to disrupt mTORC1 activity. Previous data had implicated TSC2 in mTORC1 inhibition in response to PEITC treatment (Cavell et al., 2012), this would require verification in CLL cells. The disruption to BCR signalling at mTORC1 in CLL was in agreement with decreased mTORC1 activity in response to PEITC treatment in other malignant cells (Cavell et al., 2012). Disruption of mTORC1 activity provides a mechanism for decreased BCR-induced translation in response to PEITC treatment (Figure 6-3). Previous data had shown that the mTORC1 inhibitor, rapamycin, suppressed stimulated lymphocyte proliferation, due to decreased protein synthesis (measured by ^{35}S-Met incorporation) as well as decreased DNA replication (measured by ^{3}H-thymidine incorporation) (Kay et al., 1991; Limon and Fruman, 2012). Rapamycin blocked cell cycle entry and B cell differentiation through unknown mechanisms (Limon and Fruman, 2012). Decreased proliferation following rapamycin treatment could provide an effective treatment for B cell disease but the inhibition of mTORC1 and mTORC2 by rapamycin is time and dose dependent. Hence alternative therapies to decrease proliferation and differentiation are required to treat B cell malignancies.

In MCF7 cells PEITC induced the phosphorylation of eIF2α (Figure 4-4) and this was also seen in CLL cells (Figure 6-11) providing another mechanism for decreased translation. The phosphorylation of eIF2α may enable PEITC to decrease translation

independently of the BCR signalling pathway, thereby providing a mechanism for decreased basal translation (Figure 6-3).

6. 5. 2. Importance of BCR Signalling on Translation

Targeting the BCR signalling pathway has become an attractive therapy for CLL, with BTK and SYK inhibitors in multiple clinical trials. Inhibition of BTK, using Ibrutinib, has prevented BCR induced adhesion and migration as well as retention of CLL cells in the bone marrow and lymph node (de Rooij et al., 2012). This deprives the cells of mircoenvironmental stimuli to enhance growth and survival that ultimately leads to tumour regression. Inhibition of SYK has previously been demonstrated to induce apoptosis in a caspase dependent manner (Gobessi et al., 2009). The effect of disrupted BCR signalling on translation had not previously been analysed. Inhibition of BTK or SYK decreased BCR induced translation by 50 and 80% respectively (Figure 6-12). SYK inhibition was also able to significantly decrease basal translation to a lesser extent than stimulated translation (Figure 6-12) therefore indicating the importance of the BCR signalling pathway in induction of translation. SYK inhibition prevented sIgM-induced MCL-1 expression (Gobessi et al., 2009), which could be due to decreased translation of *MCL-1* mRNA (Figure 6-19).

Inhibition of the BCR signalling pathway using both BTK and SYK inhibitors decreased transcription of *MYC* and *MCL-1* (Figure 6-13). The transcription of *MYC* is known to be up-regulated following sIgM stimulation (Krysov et al., 2012; Vallat et al., 2007) and inhibition of BTK or SYK further indicates the importance of the BCR signalling cascade in promoting transcription of these genes, which are linked to proliferation and survival of CLL cells. sIgM-induced translation of *MYC*, *MCL-1* and *ACTB* were decreased following BTK or SYK inhibition (Figure 6-17). SYK inhibition had a more profound effect on translation as SYK inhibition decreased *MYC* translation independently of transcriptional effects (Figure 6-18). Inhibition of SYK was likely to have a greater effect on translation as SYK is the first kinase in the BCR signalling cascade.

These data presented here indicated that translation was enhanced in CLL cells following stimulation through the BCR, via sIgM. This suggested that CLL cells within proliferation centres in the lymph node or in the germinal centre reaction will have elevated translation, as cells in this environment will be continuously exposed to antigen that will stimulate the BCR. BCR controlled translation was inhibited by Ibrutinib and Fostamatinib, indicating the importance of this pathway in promoting translation in CLL cells. PEITC also decreased BCR induced translation, although this may also be independent of the BCR signalling pathway via eIF2α phosphorylation.

6. 5. 3. Clinical Implications

The ability of PEITC, Ibrutinib and Tamatinib to decrease translation has important clinical relevance. Increased MYC expression is linked to enhanced proliferation (Krysov et al., 2012) and enhanced MCL-1 expression leads to increased survival of CLL cells (Paterson et al., 2012) therefore by preventing the basal and sIgM-induced translation of *MYC* and *MCL-1* PEITC may inhibit cell cycle progression and survival of both signalling responsive and non-responsive CLL samples. The ability of PEITC to inhibit basal translation is important as this may prevent survival of CLL cells in the absence of stimulation. Basal translation possibly occurs to maintain cell survival while the CLL cell is in the peripheral blood, whereas following stimulation in proliferation centres translation will be enhanced to promote disease progression. Decreased basal translation by PEITC may inhibit cell survival, due to decreased *MCL-1* translation (Figure 6-10). PEITC would have minimal effect on 'normal' B cell survival as malignant cells are more susceptible to the effects of PEITC possibly due to their elevated ROS levels rendering the cell unable to cope with additional stress as well as the fact that many oncogenes rely heavily on translation for enhanced expression.

The ability of Ibrutinib and Tamatinib to inhibit sIgM-induced translation may provide another mechanism for decreased proliferation and survival, due to decreased expression of MYC and MCL-1 (Dr. Sergey Krysov, unpublished data).

All of the mRNA molecules translationally up-regulated in response to BCR stimulation is currently unknown, therefore the effect of BTK or SYK inhibition on disease progression is unknown as inhibition of translation by these compounds may inhibit expression of many proteins associated with cancer progression.

Chapter Seven

Final Discussion

7. Final Discussion

At the beginning of this thesis my primary hypothesis stated that PEITC will inhibit mRNA translation, in either a gene specific or global manner. The secondary hypothesis stated that BCR stimulation of primary leukaemic cells will enhance mRNA translation. In order to investigate this hypothesis I had several aims. Listed below are the key findings related to each aim.

Aim: Analyse the effect of PEITC on mRNA translation in MCF7 cells

Key findings:

- PEITC rapidly and dose dependently caused a profound decrease in translation
- PEITC treatment decreased translation in a global manner whereas *VEGF* mRNA stayed associated with polysomes
- Translation of *HIF-1A* mRNA was maintained in hypoxic conditions and *VEGF* transcription was enhanced, both of which were inhibited with PEITC treatment providing a mechanism for decreased angiogenesis in response to PEITC treatment

Aim: Investigate the mechanism of decreased translation in response to PEITC

Key findings:

- mTORC1 inhibition was not sufficient to inhibit translation to the same extent as PEITC alone
- PEITC induced eIF2α phosphorylation that was essential to inhibit translation
- PEITC induced the formation of stress granules in a phospho-eIF2α dependent manner.

Aim: Investigate the effect of sIgM stimulation on translation in CLL samples

Key findings:

- Stimulation of sIgM with bead-bound anti-IgM enhanced translation, measured by polysome profiling and ^{35}S-Met/Cys incorporation only in signalling responsive CLL samples
- Treatment with bead-bound anti-IgD had little effect on translation
- sIgM stimulation increased transcription and translation of *MYC, MCL-1* and *ACTB* mRNA
- Treatment with bead-bound anti-IgM enhanced translation of *MYC* and *ACTB* mRNA by increasing association with higher molecular weight polysome fractions

Aim: Investigate the effect of PEITC on mRNA translation in CLL

Key findings:

- PEITC treatment decreased basal and sIgM-induced translation
- PEITC treatment decreased translation of *MYC, MCL-1* and *ACTB* mRNA compared to incubation with anti-IgM beads alone
- PEITC decreased sIgM stimulated mTORC1 activity and increased eIF2α phosphorylation

Aim: Investigate the effect of BCR kinase inhibitors on mRNA translation in CLL

Key findings:

- Inhibition of BTK and SYK decreased sIgM-induced translation
- BTK inhibition decreased sIgM-induced transcription of *MYC* and *MCL-1* mRNA
- Ibrutinib inhibited translation of *MYC* and *MCL-1*

- Inhibition of SYK decreased sIgM-induced transcription of *MYC*, *MCL-1* and *ACTB*
- SYK inhibition decreased sIgM stimulated translation in a global manner and specifically decreased translation of *MYC*.

The data presented in this thesis supports the hypothesis as PEITC was shown to decrease translation in both a breast cancer cell line as well as in primary CLL samples. The decrease in translation appeared to be global, although it is possible that certain mRNA molecules were more sensitive to PEITC decreased translation than others, determining which mRNAs PEITC effected requires further investigation. The use of BCR kinase inhibitors highlighted the importance of BCR signalling in promoting translation in CLL, again supporting the hypothesis. PEITC decreased BCR-induced translation, supporting the hypothesis, but also decreased basal translation which was unexpected. Overall the results revealed two important findings (1) the mechanism of action of PEITC and (2) the importance of BCR signalling to enhance translation in CLL.

7. 1. Mechanism of Action of PEITC

It has recently been shown that PEITC had a detrimental effect on CLL survival (Trachootham et al., 2008; Zhang et al., 2012). PEITC has been demonstrated to disrupt the protective potential that the microenvironment provides, due to decreased production of glutathione within CLL cells, rendering the CLL cells susceptible to oxidative stress and death (Zhang et al., 2012). Co-culture of CLL cells with stromal cells inhibited ROS dependent apoptosis because the release of cysteine from stromal cells enhanced survival of CLL cells as cysteine uptake stimulated CLL cells to produce glutathione, resulting in decreased oxidative stress (Zhang et al., 2012). This was inhibited by PEITC treatment (Zhang et al., 2012). Whether this was the only detrimental effect of PEITC on CLL cells was unknown and required further investigation. Data in this thesis indicated that this was not the only mechanism for disrupting CLL survival, PEITC was shown to inhibit translation in CLL cells including translation of *MYC* and *MCL-1*.

Work in our group had previously indicated that PEITC inhibited translation of *HIF-1A* with mTORC1 shown to be implicated (Cavell et al., 2012). This required further investigation to determine whether PEITC specifically inhibited translation of certain mRNA molecules or whether PEITC affected global translation. It was also important to determine the pathways involved in the regulation of translation. Chapters 3 and 4 addressed these issues and it was demonstrated that PEITC inhibited translation in a global manner indicated by the complete collapse of polysome peaks in polysome profiles (Figure 3-4). A collapse in the polysome peaks indicated that translation could not be initiated and the finding that PEITC induced the phosphorylation of eIF2α (Figure 4-4), along with the effects PEITC had on mTOR signalling, supported the conclusion the PEITC blocked translation at initiation. Previous data indicated that PEITC could negate many of the 'hallmarks' of cancer (see Table 1-1 and references therein) although the mechanisms of this were unclear. Decreased global translation could potentially provide a mechanism that PEITC utilises for its anti-cancer activity as protein synthesis was reduced in a global manner which would affect many pathways enabling PEITC to have a broad range of anti-cancer effects.

The phosphorylation of eIF2α induced by PEITC was important as eIF2α non-phosphorylatable MEFs continued to initiate translation in the presence of PEITC (Figure 4-10). Therefore the phosphorylation of eIF2α was key for translational-repression by PEITC. Phosphorylation of eIF2α may be mediated via one (or more) of the four eIF2α kinases; GCN2, HRI, PERK and PKR. I was unable to determine which kinase specifically phosphorylated eIF2α following PEITC treatment, although the two kinases most likely to be activated are PERK and HRI. PERK is activated in response to ER stress due to oxidative stress and the unfolded protein response (Mathews et al., 2007). It is known that during PEITC accumulation in the cell glutathione is depleted (Syed Alwi et al., 2012), resulting in oxidative stress. This is particularly important for cancerous cells that depend on their anti-oxidant system. Oxidative stress has a proliferative advantage therefore the majority of cancerous cells have elevated ROS (Hu et al., 2005). PEITC is also able to covalently modify redox regulated cysteines on proteins (Mi et al., 2011), which may interfere with protein synthesis and folding in the endoplasmic reticulum. This would result in BiP chaperoning the unfolded proteins, thus activating PERK

(Mathews et al., 2007), see section 1. 3. 7. 3. Both effects potentially activate PERK to phosphorylate eIF2α. The other likely kinase to be activated by PEITC was HRI. HRI is activated not only by heme deficiency but also by osmotic stress, heat shock and has been shown to be activated in response to oxidative stress by arsenite (Fournier et al., 2010).

It is also possible that PEITC does not affect the activity of the eIF2α kinases but may affect the phosphatase responsible for removing the phosphate group from eIF2α, PP1 (Thomas et al., 2011). Phosphatases are sensitive to oxidative stress therefore their activity may be modulated by PEITC treatment. Oxidative stress has been shown to inhibit the activity of PP1, while the addition of N-acetylcysteine or Cys-reducing agents (GSH) has been shown to recover the activity of PP1 (Kim et al., 2003). PP1 contains redox sensitive Cys residues (Fetrow et al., 1999) that could possibly be a target for PEITC thiocarbamoylation, which may result in decreased activity of PP1 thus increasing the phosphorylation status of eIF2α. This would require further investigation to determine whether PEITC inhibits PP1 activity.

PEITC was also shown to induce the formation of stress granules in a phospho-eIF2α dependent manner (Figure 4-17). Stress granules are storage sites for mRNA, although they can also initiate translation of certain mRNA molecules in order to enable cell to response to cellular stress (Thomas et al., 2011). The finding that *HIF-1A* mRNA translation was maintained in hypoxic conditions when global translation rates are low is well known, although the mechanisms for this are not understood. It may be that *HIF-1A* mRNA is one of those mRNAs whose translation is initiated from stress granules, although this would require further investigation. If this were true it would be interesting that PEITC decreased translation of *HIF-1A* in hypoxic conditions as this would indicate changes in translation regulated by stress granules.

7. 1. 1. Suggestions for Future Work to Analyse the Mechanism of Action of PEITC

In order to establish whether PEITC induced the phosphorylation of eIF2α via activation of an eIF2α kinase, or multiple kinases, knock out MEFs could be used.

The MEFs would either have each kinase individually, or in combination, knocked out. Western blotting would need to be carried out to determine whether PEITC induced eIF2α phosphorylation and polysome profiling along with ^{35}S-metabolic labelling would be carried out in these cells to confirm their importance in decreased translation in response to PEITC treatment.

To determine whether PEITC inhibits the activity of the phosphatase PP1 the phosphorylation status of other PP1 targets could be analysed by western blotting, for example the phosphorylation status of Ser15 on p53 (Haneda et al., 2004). PP1 could also be knocked down using siRNA targeted against PP1 to determine whether decreased PP1 would mimic the action of PEITC. If this indicated the involvement of PP1 further investigations could be carried out to determine the importance of PP1 in the response to PEITC treatment. The activity of PP1 in response to PEITC treatment could be measured in a phosphatase activity assay. A commercially available kit from Promega can measure phosphatase activity (ProFluor Ser/Thr PPase Assay). This kit briefly measures the phosphatase activity by using phosphorylated bisamide rhodamine 110 (non-fluorescent) as a substrate. The supplied phosphatase can then be added to the substrate in the presence or absence of PEITC and reaction allowed to occur. The phosphatase reaction is stopped and protease digestion is carried out. The bisamide rhomadime 110 will only undergo proteolytic digestion in the absence of phosphate groups (if the phosphatase was active) and will produce fluorescent rhomadine 110. Therefore this would determine whether PEITC inhibits PP1 activity, although further verification would be required to determine whether the effects seen in this experiment also occurred in the intracellular environment.

Further studies are required to analyse the consequence of stress granule assembly following PEITC treatment. Analysis of mRNA localisation into stress granules is required to determine whether certain mRNA molecules, that are sensitive to PEITC-decreased translation (such as *HIF-1A* and *MYC*), are located in stress granules. This could be carried out by fluorescence *in situ* hybridisation, where a fluorescently labelled anti-sense RNA probe would be synthesised against the mRNA of interest. The RNA probe would then be allowed to hybridise to the mRNA of interest in fixed and permeabilised cells. The cells would then be stained

for stress granules using the immunofluorescence protocol used in this thesis. It would also be interesting to determine whether PEITC induces stress granules in CLL cells as this may provide another mechanism for decreased translation in CLL.

It would be important to investigate whether PEITC directly effects the ribosomes as there is some discrepancy between the timing of polysome collapse and eIF2α phosphorylation. Mi et al had identified two ribosomal proteins S21 and P2 that can covalently couple to PEITC (Mi et al., 2011) but the effect of this on ribosome function is unknown. PEITC treatment for 10 minutes resulted in a significant decrease in polysome formation (Figure 3-4) whereas phosphorylation of eIF2α was detectable after 15 minutes (Figure 4-4). Due to this inconsistency it would be important to determine whether PEITC in addition to altering eIF2α phosphorylation also disrupts the ribosome in a more direct manner. To determine whether PEITC causes the ribosomes to dissociate due to direct interaction PEITC treatment could be given following cycloheximide treatment. This would provide insight into whether the decrease in polysome peaks in response to PEITC treatment was solely due to the inability to re-initiate translation (due to eIF2α phosphorylation), if this was the mechanism used by PEITC then the addition of cycloheximide first would result in no change in the polysome profile compared to the untreated control. Whereas if PEITC directly interacts with the ribosome causing dissociation then a collapse of the polysome peaks would still be visualised with prior cycloheximide treatment.

7. 2. Importance of sIgM Stimulation in Translation in CLL

It was an important finding that sIgM increased mRNA translation (Figure 5-1) as this supports the hypothesis that antigen is a main driving force in CLL disease progression (Chiorazzi et al., 2005). This was supported by the fact that sIgM increased translation of *MYC* and *MCL-1* both of which are linked to poor clinical outcome (Pepper et al., 2008; Zhang et al., 2010).

PEITC clearly decreased translation in a breast cancer cell line (Figure 3-4) as well as in primary CLL samples (Figure 5-1). PEITC was shown to disrupt the

microenvironment-induced survival of CLL cells (Zhang et al., 2012) providing further evidence for the importance of the microenvironment in CLL survival. CLL cells are known to proliferate in proliferation centres, whereas they do not undergo proliferation in the peripheral blood. This indicated that the microenvironment in the proliferation centres were able to stimulate CLL cells but it was unknown whether this would enhance translation.

Recent work has indicated that enhanced mRNA translation occurred following culturing of CLL cells on stromal cells and stromal cells with CD154 (Willimott et al., 2013), supporting the hypothesis that the microenvironment or stimulation of the CLL cell may promote translation. Culturing CLL cells on stromal cells resulted in a six-fold increase in ^{35}S-Met/Cys incorporation and enhanced the eIF4G – eIF4E interaction, which indicated that co-cultured CLL cells had elevated translation compared to CLL cells culture alone (Willimott et al., 2013). The idea that the microenvironment was important in stimulating the CLL cells to proliferate was not unique as previously it has been shown that BCR stimulation was important for cell survival with sIgM stimulation shown to enhance survival and proliferation (Krysov et al., 2012; Paterson et al., 2012). The data linking the microenvironment to mRNA translation (Willimott et al., 2013) further supports the data presented in this thesis that sIgM stimulation enhanced mRNA translation (Figure 5-1).

The observation that both sIgM and microenvironmental stimulation enhanced translation to promote cell survival suggests that translation may be a good target for therapeutic attack. PEITC decreased sIgM-induced translation as well as basal translation (Figure 6-3), which may provide an attractive therapy for BCR 'non-responsive' samples. The two kinase inhibitors, ibrutinib and tamatinib, currently in clinical trials also decreased sIgM-induced translation (Figure 6-12), demonstrating the importance of the BCR signalling pathway in promoting translation. Although not fully characterised translation appears to be regulated by BCR stimulation in the pathway indicated in Figure 7-1.

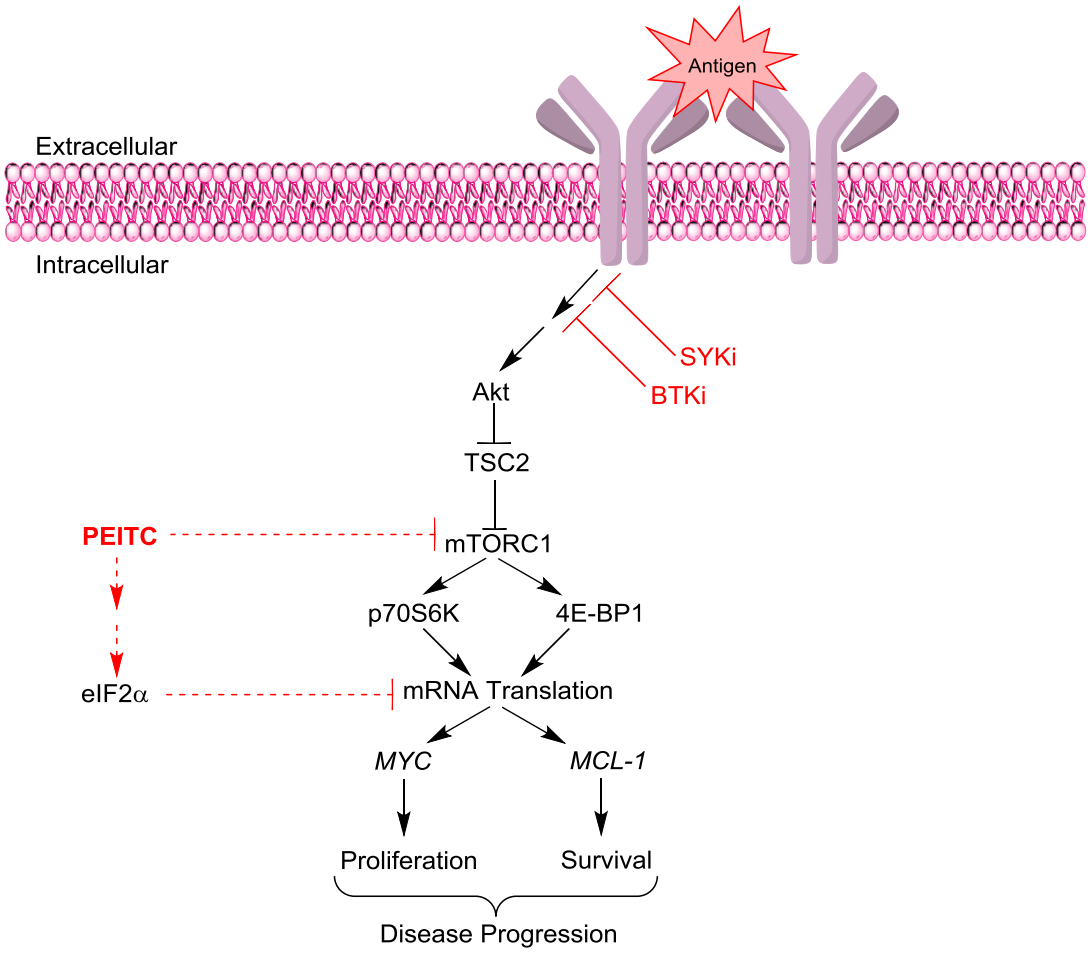

Figure 7-1: BCR Signalling Pathway Involved in Regulating mRNA Translation

Following BCR activation by antigen (Figure 1-20) Akt is activated. The activation of Akt relieves the inhibitory effect of TSC2 on mTORC1, resulting in activation. mTORC1 activation increases translation, aiding proliferation and survival of CLL cells. This pathway is inhibited upstream of Akt by BTK and SYK inhibitors, whereas PEITC inhibits the BCR signalling pathway at mTORC1 as well as modulating translation via eIF2α phosphorylation.

7. 2. 1. Suggestions for Future Work to Investigate the Importance of sIgM Stimulation on Translation in CLL

More samples are required to analyse the effect of sIgM stimulation on translation, to determine any potential clinical significance. Greater sample numbers will provide better insight into any correlation with clinical features as well as indicate the clinical significance of elevated basal translation levels or whether the degree of stimulated translation leads to a worse prognosis.

Investigating specifically translation in CLL using blood samples was difficult due to stimulation altering translation levels as well as altering transcription. For example *MYC* and *MCL-1* had increased transcription as well as translation following sIgM stimulation; therefore to decipher the effect of sIgM on translation independently of changes in transcription was problematic. The question of which mRNA molecules are translationally regulated in CLL still requires further investigation. The data presented demonstrated that sIgM-induced translation of *MYC* and *ACTB* (Figure 5-16) but whether these are the only mRNA molecules that were translational up-regulated requires further investigation. In order to analyse ribosomal association with mRNAs a technique known as ribosome profiling needs to be carried out. This technique involves isolation of ribosomes by sucrose gradient centrifugation, digestion of the mRNA surrounding the approximate 30 nucleotide footprint protected by the ribosome and gel electrophoresis to purify the footprints. Once the mRNA is isolated next generation sequencing can be carried out to provide a measure of ribosome density on any given mRNA at a codon-level resolution. This will enable all mRNAs to be analysed to determine whether they are differentially translated in response to sIgM stimulation. This could also be used to characterise the efficacy of decreased sIgM-induced translation in response to drugs, including PEITC, Ibrutinib and Tamatinib.

It will be important to determine which mRNAs have enhanced translation following sIgM stimulation as sIgM stimulation has been linked with poor clinical outcome. The identification of which mRNAs are linked with poor prognosis will have important clinical implications as the expression or activity of these genes could then be targeted therapeutically. The identification may also provide another

mechanism for determining disease progression and prognosis. The current system used to determine whether a sample is a responder or non-responder to BCR stimulation is based on calcium flux and indicates the ability of the cell to signal via the BCR, but does not indicate the degree of response as calcium flux did not correlate with increased translation following sIgM stimulation (Figure 5-9). Therefore determining whether translation of specific mRNA molecules is enhanced following sIgM stimulation may provide a more detailed understanding in the ability of the cell to respond to BCR stimulation and may provide a better link to disease progression.

Once mRNA molecules that are translationally up-regulated in response to sIgM stimulation have been identified *in vitro* studies could be carried out to determine whether these mRNAs/proteins are increased in proliferation centres in lymph nodes by immunohistochemical analysis, which could provide a link with proliferation and disease progression. Polysome profiling and the identification of translation as an important feature of CLL survival and proliferation may provide another mechanism to test potential drugs for the treatment of CLL.

It is important to characterise the signalling pathway that regulates translation in response to sIgM stimulation further. I have demonstrated that P70S6K was phosphorylated following sIgM stimulation to promote translation, whereas decreased P70S6K phosphorylation and enhanced eIF2α phosphorylation by PEITC decreased translation (Figure 6-11 and Figure 7-1). These markers could be used to determine whether patients previously treated with Ibrutinib and Fostamatinib in the phase II clinical trials have phosphorylated P70S6K, which would provide insight into the modulation of translation *in vivo*. Further work to investigate the control of translation *in vivo* would involve immunohistochemistry of proliferation centres from lymph nodes staining for phospho-P70S6K and phospho-eIF2α.

Chapter Eight

References

8. References

Agathangelidis, A., Darzentas, N., Hadzidimitriou, A., Brochet, X., Murray, F., Yan, X.J., Davis, Z., van Gastel-Mol, E.J., Tresoldi, C., Chu, C.C., *et al.* (2012). Stereotyped B-cell receptors in one-third of chronic lymphocytic leukemia: a molecular classification with implications for targeted therapies. Blood *119*, 4467-4475.

Alberts, B. (2002). Molecular biology of the cell, 4th edn (New York: Garland Science).

Algire, M.A., Maag, D., and Lorsch, J.R. (2005). Pi release from eIF2, not GTP hydrolysis, is the step controlled by start-site selection during eukaryotic translation initiation. Mol Cell *20*, 251-262.

Bargis-Surgey, P., Lavergne, J.P., Gonzalo, P., Vard, C., Filhol-Cochet, O., and Reboud, J.P. (1999). Interaction of elongation factor eEF-2 with ribosomal P proteins. European journal of biochemistry / FEBS *262*, 606-611.

Berg, J.M., Tymoczko, J.L., Stryer, L., and Stryer, L. (2007). Biochemistry, 6th edn (New York: W.H. Freeman).

Bert, A.G., Grepin, R., Vadas, M.A., and Goodall, G.J. (2006). Assessing IRES activity in the HIF-1alpha and other cellular 5' UTRs. RNA *12*, 1074-1083.

Bertolotti, A., Zhang, Y., Hendershot, L.M., Harding, H.P., and Ron, D. (2000). Dynamic interaction of BiP and ER stress transducers in the unfolded-protein response. Nat Cell Biol *2*, 326-332.

Bushell, M., Stoneley, M., Kong, Y.W., Hamilton, T.L., Spriggs, K.A., Dobbyn, H.C., Qin, X., Sarnow, P., and Willis, A.E. (2006). Polypyrimidine tract binding protein regulates IRES-mediated gene expression during apoptosis. Mol Cell *23*, 401-412.

Cande, C., Vahsen, N., Metivier, D., Tourriere, H., Chebli, K., Garrido, C., Tazi, J., and Kroemer, G. (2004). Regulation of cytoplasmic stress granules by apoptosis-inducing factor. J Cell Sci *117*, 4461-4468.

Carmeliet, P., and Jain, R.K. (2000). Angiogenesis in cancer and other diseases. Nature *407*, 249-257.

Cavell, B.E., Syed Alwi, S.S., Donlevy, A., and Packham, G. (2011). Anti-angiogenic effects of dietary isothiocyanates: mechanisms of action and implications for human health. Biochem Pharmacol *81*, 327-336.

Cavell, B.E., Syed Alwi, S.S., Donlevy, A.M., Proud, C.G., and Packham, G. (2012). Natural Product-Derived Antitumor Compound Phenethyl Isothiocyanate Inhibits mTORC1 Activity via TSC2. J Nat Prod *75*, 1051-1057.

Chen, J.J., Yang, J.M., Petryshyn, R., Kosower, N., and London, I.M. (1989). Disulfide bond formation in the regulation of eIF-2 alpha kinase by heme. J Biol Chem *264*, 9559-9564.

Chernov, K.G., Barbet, A., Hamon, L., Ovchinnikov, L.P., Curmi, P.A., and Pastre, D. (2009). Role of microtubules in stress granule assembly: microtubule dynamical instability favors the formation of micrometric stress granules in cells. J Biol Chem *284*, 36569-36580.

Cheung, K.L., and Kong, A.N. (2010). Molecular targets of dietary phenethyl isothiocyanate and sulforaphane for cancer chemoprevention. AAPS J *12*, 87-97.

Chiorazzi, N., and Ferrarini, M. (2003). B cell chronic lymphocytic leukemia: Lessons learned from studies of the B cell antigen receptor. Annu Rev Immunol *21*, 841-894.

Chiorazzi, N., Rai, K.R., and Ferrarini, M. (2005). Chronic lymphocytic leukemia. The New England journal of medicine *352*, 804-815.

Chung, F.L., Morse, M.A., Eklind, K.I., and Lewis, J. (1992). Quantitation of human uptake of the anticarcinogen phenethyl isothiocyanate after a watercress meal. Cancer epidemiology, biomarkers & prevention : a publication of the American Association for Cancer Research, cosponsored by the American Society of Preventive Oncology *1*, 383-388.

Circu, M.L., and Aw, T.Y. (2012). Glutathione and modulation of cell apoptosis. Biochimica et biophysica acta *1823*, 1767-1777.

Coelho, V., Krysov, S., Steele, A., Sanchez Hidalgo, M., Johnson, P.W., Chana, P.S., Packham, G., Stevenson, F.K., and Forconi, F. (2013). Identification in CLL of circulating intraclonal subgroups with varying B-cell receptor expression and function. Blood.

Dann, C.E., 3rd, and Bruick, R.K. (2005). Dioxygenases as O2-dependent regulators of the hypoxic response pathway. Biochem Biophys Res Commun *338*, 639-647.

de Rooij, M.F., Kuil, A., Geest, C.R., Eldering, E., Chang, B.Y., Buggy, J.J., Pals, S.T., and Spaargaren, M. (2012). The clinically active BTK inhibitor PCI-32765 targets B-cell receptor- and chemokine-controlled adhesion and migration in chronic lymphocytic leukemia. Blood *119*, 2590-2594.

Deng, J., Harding, H.P., Raught, B., Gingras, A.C., Berlanga, J.J., Scheuner, D., Kaufman, R.J., Ron, D., and Sonenberg, N. (2002). Activation of GCN2 in UV-irradiated cells inhibits translation. Current biology : CB *12*, 1279-1286.

Dewhirst, M.W. (2009). Relationships between cycling hypoxia, HIF-1, angiogenesis and oxidative stress. Radiat Res *172*, 653-665.

Dinkova-Kostova, A.T., Holtzclaw, W.D., Cole, R.N., Itoh, K., Wakabayashi, N., Katoh, Y., Yamamoto, M., and Talalay, P. (2002). Direct evidence that sulfhydryl groups of Keap1 are the sensors regulating induction of phase 2 enzymes that protect against carcinogens and oxidants. Proc Natl Acad Sci U S A *99*, 11908-11913.

Fahey, J.W., Zalcmann, A.T., and Talalay, P. (2001). The chemical diversity and distribution of glucosinolates and isothiocyanates among plants. Phytochemistry *56*, 5-51.

Fahling, M. (2009). Cellular oxygen sensing, signalling and how to survive translational arrest in hypoxia. Acta Physiol (Oxf) *195*, 205-230.

Fetrow, J.S., Siew, N., and Skolnick, J. (1999). Structure-based functional motif identifies a potential disulfide oxidoreductase active site in the serine/threonine protein phosphatase-1 subfamily. FASEB J *13*, 1866-1874.

Fink, T., Lund, P., Pilgaard, L., Rasmussen, J.G., Duroux, M., and Zachar, V. (2008). Instability of standard PCR reference genes in adipose-derived stem cells during propagation, differentiation and hypoxic exposure. BMC molecular biology *9*, 98.

Fogg, V.C., Lanning, N.J., and Mackeigan, J.P. (2011). Mitochondria in cancer: at the crossroads of life and death. Chinese journal of cancer *30*, 526-539.

Forconi, F., Potter, K.N., Wheatley, I., Darzentas, N., Sozzi, E., Stamatopoulos, K., Mockridge, C.I., Packham, G., and Stevenson, F.K. (2010). The normal IGHV1-69-derived B-cell repertoire contains stereotypic patterns characteristic of unmutated CLL. Blood *115*, 71-77.

Forsythe, J.A., Jiang, B.H., Iyer, N.V., Agani, F., Leung, S.W., Koos, R.D., and Semenza, G.L. (1996). Activation of vascular endothelial growth factor gene transcription by hypoxia-inducible factor 1. Mol Cell Biol *16*, 4604-4613.

Fournier, M.J., Gareau, C., and Mazroui, R. (2010). The chemotherapeutic agent bortezomib induces the formation of stress granules. Cancer Cell Int *10*, 12.

Fulda, S., and Debatin, K.M. (2004). Apoptosis signaling in tumor therapy. Annals of the New York Academy of Sciences *1028*, 150-156.

Gauld, S.B., Dal Porto, J.M., and Cambier, J.C. (2002). B cell antigen receptor signaling: roles in cell development and disease. Science *296*, 1641-1642.

Glassford, J., Soeiro, I., Skarell, S.M., Banerji, L., Holman, M., Klaus, G.G., Kadowaki, T., Koyasu, S., and Lam, E.W. (2003). BCR targets cyclin D2 via Btk and the p85alpha subunit of PI3-K to induce cell cycle progression in primary mouse B cells. Oncogene *22*, 2248-2259.

Gobessi, S., Laurenti, L., Longo, P.G., Carsetti, L., Berno, V., Sica, S., Leone, G., and Efremov, D.G. (2009). Inhibition of constitutive and BCR-induced Syk activation downregulates Mcl-1 and induces apoptosis in chronic lymphocytic leukemia B cells. Leukemia *23*, 686-697.

Goh, A.M., Coffill, C.R., and Lane, D.P. (2011). The role of mutant p53 in human cancer. The Journal of pathology *223*, 116-126.

Goldin, L.R., Slager, S.L., and Caporaso, N.E. (2010). Familial chronic lymphocytic leukemia. Current opinion in hematology *17*, 350-355.

Granziero, L., Ghia, P., Circosta, P., Gottardi, D., Strola, G., Geuna, M., Montagna, L., Piccoli, P., Chilosi, M., and Caligaris-Cappio, F. (2001). Survivin is expressed on CD40 stimulation and interfaces proliferation and apoptosis in B-cell chronic lymphocytic leukemia. Blood *97*, 2777-2783.

Green, S.R., and Mathews, M.B. (1992). Two RNA-binding motifs in the double-stranded RNA-activated protein kinase, DAI. Genes Dev *6*, 2478-2490.

Gross, S.R., and Kinzy, T.G. (2007). Improper organization of the actin cytoskeleton affects protein synthesis at initiation. Mol Cell Biol *27*, 1974-1989.

Hadjipanayi, E., Brown, R.A., Mudera, V., Deng, D., Liu, W., and Cheema, U. (2010). Controlling physiological angiogenesis by hypoxia-induced signaling. Journal of controlled release : official journal of the Controlled Release Society *146*, 309-317.

Hanahan, D., and Weinberg, R.A. (2000). The hallmarks of cancer. Cell *100*, 57-70.

Hanahan, D., and Weinberg, R.A. (2011). Hallmarks of cancer: the next generation. Cell *144*, 646-674.

Haneda, M., Kojima, E., Nishikimi, A., Hasegawa, T., Nakashima, I., and Isobe, K. (2004). Protein phosphatase 1, but not protein phosphatase 2A, dephosphorylates DNA-damaging stress-induced phospho-serine 15 of p53. FEBS letters *567*, 171-174.

Heesom, K.J., Avison, M.B., Diggle, T.A., and Denton, R.M. (1998). Insulin-stimulated kinase from rat fat cells that phosphorylates initiation factor 4E-binding protein 1 on the rapamycin-insensitive site (serine-111). Biochem J *336 (Pt 1)*, 39-48.

Hileman, E.O., Liu, J., Albitar, M., Keating, M.J., and Huang, P. (2004). Intrinsic oxidative stress in cancer cells: a biochemical basis for therapeutic selectivity. Cancer chemotherapy and pharmacology *53*, 209-219.

Hinnebusch, A.G. (2011). Molecular mechanism of scanning and start codon selection in eukaryotes. Microbiology and molecular biology reviews : MMBR *75*, 434-467, first page of table of contents.

Holz, M.K., Ballif, B.A., Gygi, S.P., and Blenis, J. (2005). mTOR and S6K1 mediate assembly of the translation preinitiation complex through dynamic protein interchange and ordered phosphorylation events. Cell *123*, 569-580.

Hong, F., Freeman, M.L., and Liebler, D.C. (2005). Identification of sensor cysteines in human Keap1 modified by the cancer chemopreventive agent sulforaphane. Chem Res Toxicol *18*, 1917-1926.

Hu, J., Straub, J., Xiao, D., Singh, S.V., Yang, H.S., Sonenberg, N., and Vatsyayan, J. (2007). Phenethyl isothiocyanate, a cancer chemopreventive constituent of cruciferous

vegetables, inhibits cap-dependent translation by regulating the level and phosphorylation of 4E-BP1. Cancer Res *67*, 3569-3573.

Hu, Y., Rosen, D.G., Zhou, Y., Feng, L., Yang, G., Liu, J., and Huang, P. (2005). Mitochondrial manganese-superoxide dismutase expression in ovarian cancer: role in cell proliferation and response to oxidative stress. J Biol Chem *280*, 39485-39492.

Huang, J., and Manning, B.D. (2009). A complex interplay between Akt, TSC2 and the two mTOR complexes. Biochem Soc Trans *37*, 217-222.

Huez, I., Creancier, L., Audigier, S., Gensac, M.C., Prats, A.C., and Prats, H. (1998). Two independent internal ribosome entry sites are involved in translation initiation of vascular endothelial growth factor mRNA. Mol Cell Biol *18*, 6178-6190.

Huong le, D., Shim, J.H., Choi, K.H., Shin, J.A., Choi, E.S., Kim, H.S., Lee, S.J., Kim, S.J., Cho, N.P., and Cho, S.D. (2011). Effect of beta-phenylethyl isothiocyanate from cruciferous vegetables on growth inhibition and apoptosis of cervical cancer cells through the induction of death receptors 4 and 5. Journal of agricultural and food chemistry *59*, 8124-8131.

Hwang, E.S., and Lee, H.J. (2006). Phenylethyl isothiocyanate and its N-acetylcysteine conjugate suppress the metastasis of SK-Hep1 human hepatoma cells. The Journal of nutritional biochemistry *17*, 837-846.

Jaramillo, M., Dever, T.E., Merrick, W.C., and Sonenberg, N. (1991). RNA unwinding in translation: assembly of helicase complex intermediates comprising eukaryotic initiation factors eIF-4F and eIF-4B. Mol Cell Biol *11*, 5992-5997.

Jarrous, N., Osman, F., and Kaempfer, R. (1996). 2-Aminopurine selectively inhibits splicing of tumor necrosis factor alpha mRNA. Mol Cell Biol *16*, 2814-2822.

Ji, Y., and Morris, M.E. (2003). Determination of phenethyl isothiocyanate in human plasma and urine by ammonia derivatization and liquid chromatography-tandem mass spectrometry. Analytical biochemistry *323*, 39-47.

Kay, J.E., Kromwel, L., Doe, S.E., and Denyer, M. (1991). Inhibition of T and B lymphocyte proliferation by rapamycin. Immunology *72*, 544-549.

Kedersha, N., Chen, S., Gilks, N., Li, W., Miller, I.J., Stahl, J., and Anderson, P. (2002). Evidence that ternary complex (eIF2-GTP-tRNA(i)(Met))-deficient preinitiation complexes are core constituents of mammalian stress granules. Mol Biol Cell *13*, 195-210.

Khor, T.O., Keum, Y.S., Lin, W., Kim, J.H., Hu, R., Shen, G., Xu, C., Gopalakrishnan, A., Reddy, B., Zheng, X., *et al.* (2006). Combined inhibitory effects of curcumin and phenethyl isothiocyanate on the growth of human PC-3 prostate xenografts in immunodeficient mice. Cancer Res *66*, 613-621.

Kim, H.S., Song, M.C., Kwak, I.H., Park, T.J., and Lim, I.K. (2003). Constitutive induction of p-Erk1/2 accompanied by reduced activities of protein phosphatases 1 and 2A and MKP3 due to reactive oxygen species during cellular senescence. J Biol Chem *278*, 37497-37510.

Kimball, S.R., Horetsky, R.L., Ron, D., Jefferson, L.S., and Harding, H.P. (2003). Mammalian stress granules represent sites of accumulation of stalled translation initiation complexes. Am J Physiol Cell Physiol *284*, C273-284.

Kong, X.Y., Kissen, R., and Bones, A.M. (2012). Characterization of recombinant nitrile-specifier proteins (NSPs) of Arabidopsis thaliana: dependency on Fe(II) ions and the effect of glucosinolate substrate and reaction conditions. Phytochemistry *84*, 7-17.

Konsue, N., and Ioannides, C. (2010). Phenethyl isocyanate is not the metabolite of phenethyl isothiocyanate responsible for mechanism-based inhibition of cytochrome P450. Archives of toxicology *84*, 751-759.

Koritzinsky, M., Magagnin, M.G., van den Beucken, T., Seigneuric, R., Savelkouls, K., Dostie, J., Pyronnet, S., Kaufman, R.J., Weppler, S.A., Voncken, J.W., *et al.* (2006). Gene expression during acute and prolonged hypoxia is regulated by distinct mechanisms of translational control. EMBO J *25*, 1114-1125.

Koromilas, A.E., Lazaris-Karatzas, A., and Sonenberg, N. (1992a). mRNAs containing extensive secondary structure in their 5' non-coding region translate efficiently in cells overexpressing initiation factor eIF-4E. EMBO J *11*, 4153-4158.

Koromilas, A.E., Roy, S., Barber, G.N., Katze, M.G., and Sonenberg, N. (1992b). Malignant transformation by a mutant of the IFN-inducible dsRNA-dependent protein kinase. Science *257*, 1685-1689.

Koumenis, C., Naczki, C., Koritzinsky, M., Rastani, S., Diehl, A., Sonenberg, N., Koromilas, A., and Wouters, B.G. (2002). Regulation of protein synthesis by hypoxia via activation of the endoplasmic reticulum kinase PERK and phosphorylation of the translation initiation factor eIF2alpha. Mol Cell Biol *22*, 7405-7416.

Krysov, S., Dias, S., Paterson, A., Mockridge, C.I., Potter, K.N., Smith, K.A., Ashton-Key, M., Stevenson, F.K., and Packham, G. (2012). Surface IgM stimulation induces MEK1/2-dependent MYC expression in chronic lymphocytic leukemia cells. Blood *119*, 170-179.

Kulathu, Y., Hobeika, E., Turchinovich, G., and Reth, M. (2008). The kinase Syk as an adaptor controlling sustained calcium signalling and B-cell development. EMBO J *27*, 1333-1344.

Lang, K.J., Kappel, A., and Goodall, G.J. (2002). Hypoxia-inducible factor-1alpha mRNA contains an internal ribosome entry site that allows efficient translation during normoxia and hypoxia. Mol Biol Cell *13*, 1792-1801.

Lanham, S., Hamblin, T., Oscier, D., Ibbotson, R., Stevenson, F., and Packham, G. (2003). Differential signaling via surface IgM is associated with VH gene mutational status and CD38 expression in chronic lymphocytic leukemia. Blood *101*, 1087-1093.

Laplante, M., and Sabatini, D.M. (2012). mTOR signaling in growth control and disease. Cell *149*, 274-293.

Laplante, M., and Sabatini, D.M. (2013). Regulation of mTORC1 and its impact on gene expression at a glance. J Cell Sci *126*, 1713-1719.

Lazaris-Karatzas, A., Montine, K.S., and Sonenberg, N. (1990). Malignant transformation by a eukaryotic initiation factor subunit that binds to mRNA 5' cap. Nature *345*, 544-547.

Le Roy, C., Deglesne, P.A., Chevallier, N., Beitar, T., Eclache, V., Quettier, M., Boubaya, M., Letestu, R., Levy, V., Ajchenbaum-Cymbalista, F., *et al.* (2012). The degree of BCR and NFAT activation predicts clinical outcomes in chronic lymphocytic leukemia. Blood *120*, 356-365.

LeBien, T.W., and Tedder, T.F. (2008). B lymphocytes: how they develop and function. Blood *112*, 1570-1580.

Levy, N.S., Chung, S., Furneaux, H., and Levy, A.P. (1998). Hypoxic stabilization of vascular endothelial growth factor mRNA by the RNA-binding protein HuR. J Biol Chem *273*, 6417-6423.

Limon, J.J., and Fruman, D.A. (2012). Akt and mTOR in B Cell Activation and Differentiation. Frontiers in immunology *3*, 228.

Mamane, Y., Petroulakis, E., LeBacquer, O., and Sonenberg, N. (2006). mTOR, translation initiation and cancer. Oncogene *25*, 6416-6422.

Martel, A., Fard, M.S., Van Rooij, P., Jooris, R., Boone, F., Haesebrouck, F., Van Rooij, D., and Pasmans, F. (2012). Road-killed common toads (Bufo bufo) in Flanders (Belgium) reveal low prevalence of ranaviruses and Batrachochytrium dendrobatidis. Journal of wildlife diseases *48*, 835-839.

Mathews, M., Sonenberg, N., and Hershey, J.W.B. (2007). Translational control in biology and medicine, 3rd edn (Cold Spring Harbor, N.Y.: Cold Spring Harbor Laboratory Press).

McEwen, E., Kedersha, N., Song, B., Scheuner, D., Gilks, N., Han, A., Chen, J.J., Anderson, P., and Kaufman, R.J. (2005). Heme-regulated inhibitor kinase-mediated phosphorylation of eukaryotic translation initiation factor 2 inhibits translation, induces stress granule formation, and mediates survival upon arsenite exposure. J Biol Chem *280*, 16925-16933.

Mi, L., Gan, N., Cheema, A., Dakshanamurthy, S., Wang, X., Yang, D.C., and Chung, F.L. (2009). Cancer preventive isothiocyanates induce selective degradation of cellular alpha- and beta-tubulins by proteasomes. J Biol Chem *284*, 17039-17051.

Mi, L., Hood, B.L., Stewart, N.A., Xiao, Z., Govind, S., Wang, X., Conrads, T.P., Veenstra, T.D., and Chung, F.-L. (2011). Identification of potential protein targets of isothiocyanates by proteomics. Chemical research in toxicology *24*, 1735-1743.

Mi, L., Wang, X., Govind, S., Hood, B.L., Veenstra, T.D., Conrads, T.P., Saha, D.T., Goldman, R., and Chung, F.L. (2007). The role of protein binding in induction of apoptosis by phenethyl isothiocyanate and sulforaphane in human non-small lung cancer cells. Cancer Res *67*, 6409-6416.

Michel, G., Minet, E., Mottet, D., Remacle, J., and Michiels, C. (2002). Site-directed mutagenesis studies of the hypoxia-inducible factor-1alpha DNA-binding domain. Biochimica et biophysica acta *1578*, 73-83.

Mockridge, C.I., Potter, K.N., Wheatley, I., Neville, L.A., Packham, G., and Stevenson, F.K. (2007). Reversible anergy of sIgM-mediated signaling in the two subsets of CLL defined by VH-gene mutational status. Blood *109*, 4424-4431.

Mokas, S., Mills, J.R., Garreau, C., Fournier, M.J., Robert, F., Arya, P., Kaufman, R.J., Pelletier, J., and Mazroui, R. (2009). Uncoupling stress granule assembly and translation initiation inhibition. Mol Biol Cell *20*, 2673-2683.

Morris, M.J., Negishi, Y., Pazsint, C., Schonhoft, J.D., and Basu, S. (2010). An RNA G-quadruplex is essential for cap-independent translation initiation in human VEGF IRES. Journal of the American Chemical Society *132*, 17831-17839.

Muller, P.A., and Vousden, K.H. (2013). p53 mutations in cancer. Nat Cell Biol *15*, 2-8.

Nakamura, T., Furuhashi, M., Li, P., Cao, H., Tuncman, G., Sonenberg, N., Gorgun, C.Z., and Hotamisligil, G.S. (2010). Double-stranded RNA-dependent protein kinase links pathogen sensing with stress and metabolic homeostasis. Cell *140*, 338-348.

Nishana, M., and Raghavan, S.C. (2012). Role of recombination activating genes in the generation of antigen receptor diversity and beyond. Immunology *137*, 271-281.

Packham, G., and Stevenson, F.K. (2005). Bodyguards and assassins: Bcl-2 family proteins and apoptosis control in chronic lymphocytic leukaemia. Immunology *114*, 441-449.

Palamarchuk, A., Efanov, A., Nazaryan, N., Santanam, U., Alder, H., Rassenti, L., Kipps, T., Croce, C.M., and Pekarsky, Y. (2010). 13q14 deletions in CLL involve cooperating tumor suppressors. Blood *115*, 3916-3922.

Parker, H., Rose-Zerilli, M.J., Parker, A., Chaplin, T., Wade, R., Gardiner, A., Griffiths, M., Collins, A., Young, B.D., Oscier, D.G., *et al.* (2011). 13q deletion anatomy and disease progression in patients with chronic lymphocytic leukemia. Leukemia *25*, 489-497.

Paterson, A., Mockridge, C.I., Adams, J.E., Krysov, S., Potter, K.N., Duncombe, A.S., Cook, S.J., Stevenson, F.K., and Packham, G. (2012). Mechanisms and clinical significance of BIM phosphorylation in chronic lymphocytic leukemia. Blood *119*, 1726-1736.

Pepper, C., Lin, T.T., Pratt, G., Hewamana, S., Brennan, P., Hiller, L., Hills, R., Ward, R., Starczynski, J., Austen, B., *et al.* (2008). Mcl-1 expression has in vitro and in vivo significance in chronic lymphocytic leukemia and is associated with other poor prognostic markers. Blood *112*, 3807-3817.

Pervin, S., Tran, A.H., Zekavati, S., Fukuto, J.M., Singh, R., and Chaudhuri, G. (2008). Increased susceptibility of breast cancer cells to stress mediated inhibition of protein synthesis. Cancer Res *68*, 4862-4874.

Petlickovski, A., Laurenti, L., Li, X., Marietti, S., Chiusolo, P., Sica, S., Leone, G., and Efremov, D.G. (2005). Sustained signaling through the B-cell receptor induces Mcl-1 and promotes survival of chronic lymphocytic leukemia B cells. Blood *105*, 4820-4827.

Pouyssegur, J., and Mechta-Grigoriou, F. (2006). Redox regulation of the hypoxia-inducible factor. Biol Chem *387*, 1337-1346.

Qiu, H., Garcia-Barrio, M.T., and Hinnebusch, A.G. (1998). Dimerization by translation initiation factor 2 kinase GCN2 is mediated by interactions in the C-terminal ribosome-binding region and the protein kinase domain. Mol Cell Biol *18*, 2697-2711.

Rafie-Kolpin, M., Chefalo, P.J., Hussain, Z., Hahn, J., Uma, S., Matts, R.L., and Chen, J.J. (2000). Two heme-binding domains of heme-regulated eukaryotic initiation factor-2alpha kinase. N terminus and kinase insertion. J Biol Chem *275*, 5171-5178.

Ramsay, A.D., and Rodriguez-Justo, M. (2013). Chronic lymphocytic leukaemia - the role of the microenvironment pathogenesis and therapy. British journal of haematology.

Richardson, S.J., Matthews, C., Catherwood, M.A., Alexander, H.D., Carey, B.S., Farrugia, J., Gardiner, A., Mould, S., Oscier, D., Copplestone, J.A., *et al.* (2006). ZAP-70 expression is associated with enhanced ability to respond to migratory and survival signals in B-cell chronic lymphocytic leukemia (B-CLL). Blood *107*, 3584-3592.

Rini, B.I., and Atkins, M.B. (2009). Resistance to targeted therapy in renal-cell carcinoma. The lancet oncology *10*, 992-1000.

Roitt, I.M. (1997). Roitt's Essential Immunology, Vol Ninth Edition.

Rosenwald, I.B. (2004). The role of translation in neoplastic transformation from a pathologist's point of view. Oncogene *23*, 3230-3247.

Rosenwald, I.B., Wang, S., Savas, L., Woda, B., and Pullman, J. (2003). Expression of translation initiation factor eIF-2alpha is increased in benign and malignant melanocytic and colonic epithelial neoplasms. Cancer *98*, 1080-1088.

Ruel, M., Song, J., and Sellke, F.W. (2004). Protein-, gene-, and cell-based therapeutic angiogenesis for the treatment of myocardial ischemia. Mol Cell Biochem *264*, 119-131.

Sambrook, J., Fritsch, E.F., and Maniatis, T. (1989). Molecular cloning, Vol 2 (Cold spring harbor laboratory press New York).

Sarbassov, D.D., Ali, S.M., Sengupta, S., Sheen, J.H., Hsu, P.P., Bagley, A.F., Markhard, A.L., and Sabatini, D.M. (2006). Prolonged rapamycin treatment inhibits mTORC2 assembly and Akt/PKB. Mol Cell *22*, 159-168.

Satyan, K.S., Swamy, N., Dizon, D.S., Singh, R., Granai, C.O., and Brard, L. (2006). Phenethyl isothiocyanate (PEITC) inhibits growth of ovarian cancer cells by inducing apoptosis: role of caspase and MAPK activation. Gynecologic oncology *103*, 261-270.

Schepens, B., Tinton, S.A., Bruynooghe, Y., Beyaert, R., and Cornelis, S. (2005). The polypyrimidine tract-binding protein stimulates HIF-1alpha IRES-mediated translation during hypoxia. Nucleic Acids Res *33*, 6884-6894.

Scheuner, D., Song, B., McEwen, E., Liu, C., Laybutt, R., Gillespie, P., Saunders, T., Bonner-Weir, S., and Kaufman, R.J. (2001). Translational control is required for the unfolded protein response and in vivo glucose homeostasis. Mol Cell *7*, 1165-1176.

Schwanhausser, B., Busse, D., Li, N., Dittmar, G., Schuchhardt, J., Wolf, J., Chen, W., and Selbach, M. (2011). Global quantification of mammalian gene expression control. Nature *473*, 337-342.

Shlomchik, M.J., and Weisel, F. (2012). Germinal center selection and the development of memory B and plasma cells. Immunological reviews *247*, 52-63.

Somers, J., Poyry, T., and Willis, A.E. (2013). A perspective on mammalian upstream open reading frame function. The international journal of biochemistry & cell biology *45*, 1690-1700.

Sonenberg, N., and Hinnebusch, A.G. (2009). Regulation of translation initiation in eukaryotes: mechanisms and biological targets. Cell *136*, 731-745.

Spriggs, K.A., Cobbold, L.C., Jopling, C.L., Cooper, R.E., Wilson, L.A., Stoneley, M., Coldwell, M.J., Poncet, D., Shen, Y.C., Morley, S.J., *et al.* (2009). Canonical initiation factor requirements of the Myc family of internal ribosome entry segments. Mol Cell Biol *29*, 1565-1574.

Stevenson, F.K., and Caligaris-Cappio, F. (2004). Chronic lymphocytic leukemia: revelations from the B-cell receptor. Blood *103*, 4389-4395.

Stevenson, F.K., Krysov, S., Davies, A.J., Steele, A.J., and Packham, G. (2011). B-cell receptor signaling in chronic lymphocytic leukemia. Blood *118*, 4313-4320.

Stoneley, M., Paulin, F.E.M., Le Quesne, J.P.C., Chappell, S.A., and Willis, A.E. (1998). C-Myc 5 ' untranslated region contains an internal ribosome entry segment. Oncogene *16*, 423-428.

Syed Alwi, S.S., Cavell, B.E., Donlevy, A., and Packham, G. (2012). Differential induction of apoptosis in human breast cancer cell lines by phenethyl isothiocyanate, a glutathione depleting agent. Cell Stress Chaperones *17*, 529-538.

Syed Alwi, S.S., Cavell, B.E., Telang, U., Morris, M.E., Parry, B.M., and Packham, G. (2010). In vivo modulation of 4E binding protein 1 (4E-BP1) phosphorylation by watercress: a pilot study. Br J Nutr *104*, 1288-1296.

Tang, L., and Zhang, Y. (2005). Mitochondria are the primary target in isothiocyanate-induced apoptosis in human bladder cancer cells. Mol Cancer Ther *4*, 1250-1259.

Thomas, J.D., and Johannes, G.J. (2007). Identification of mRNAs that continue to associate with polysomes during hypoxia. RNA *13*, 1116-1131.

Thomas, M.G., Loschi, M., Desbats, M.A., and Boccaccio, G.L. (2011). RNA granules: The good, the bad and the ugly. Cell Signal *23*, 324-334.

Thrash-Bingham, C.A., and Tartof, K.D. (1999). aHIF: a natural antisense transcript overexpressed in human renal cancer and during hypoxia. Journal of the National Cancer Institute *91*, 143-151.

Tomoo, K., Shen, X., Okabe, K., Nozoe, Y., Fukuhara, S., Morino, S., Sasaki, M., Taniguchi, T., Miyagawa, H., Kitamura, K., *et al.* (2003). Structural features of human initiation factor 4E, studied by X-ray crystal analyses and molecular dynamics simulations. Journal of molecular biology *328*, 365-383.

Tong, L., Heim, R.A., and Wu, S. (2011). Nitric oxide: a regulator of eukaryotic initiation factor 2 kinases. Free Radic Biol Med *50*, 1717-1725.

Torok, I., Herrmann-Horle, D., Kiss, I., Tick, G., Speer, G., Schmitt, R., and Mechler, B.M. (1999). Down-regulation of RpS21, a putative translation initiation factor interacting with P40, produces viable minute imagos and larval lethality with overgrown hematopoietic organs and imaginal discs. Mol Cell Biol *19*, 2308-2321.

Touriol, C., Bornes, S., Bonnal, S., Audigier, S., Prats, H., Prats, A.C., and Vagner, S. (2003). Generation of protein isoform diversity by alternative initiation of translation at non-AUG codons. Biol Cell *95*, 169-178.

Trachootham, D., Zhang, H., Zhang, W., Feng, L., Du, M., Zhou, Y., Chen, Z., Pelicano, H., Plunkett, W., Wierda, W.G., *et al.* (2008). Effective elimination of fludarabine-resistant CLL cells by PEITC through a redox-mediated mechanism. Blood *112*, 1912-1922.

Vallat, L.D., Park, Y., Li, C., and Gribben, J.G. (2007). Temporal genetic program following B-cell receptor cross-linking: altered balance between proliferation and death in healthy and malignant B cells. Blood *109*, 3989-3997.

van den Beucken, T., Koritzinsky, M., and Wouters, B.G. (2006). Translational control of gene expression during hypoxia. Cancer Biol Ther *5*, 749-755.

Vattem, K.M., and Wek, R.C. (2004). Reinitiation involving upstream ORFs regulates ATF4 mRNA translation in mammalian cells. Proc Natl Acad Sci U S A *101*, 11269-11274.

von Der Haar, T., Ball, P.D., and McCarthy, J.E. (2000). Stabilization of eukaryotic initiation factor 4E binding to the mRNA 5'-Cap by domains of eIF4G. J Biol Chem *275*, 30551-30555.

Wang, L.D., and Clark, M.R. (2003). B-cell antigen-receptor signalling in lymphocyte development. Immunology *110*, 411-420.

Wang, X.H., Cavell, B.E., Syed Alwi, S.S., and Packham, G. (2009). Inhibition of hypoxia inducible factor by phenethyl isothiocyanate. Biochem Pharmacol *78*, 261-272.

Weidemann, A., and Johnson, R.S. (2008). Biology of HIF-1alpha. Cell Death Differ *15*, 621-627.

Wek, R.C., Jiang, H.Y., and Anthony, T.G. (2006). Coping with stress: eIF2 kinases and translational control. Biochem Soc Trans *34*, 7-11.

Williams, D.D., Pavitt, G.D., and Proud, C.G. (2001). Characterization of the initiation factor eIF2B and its regulation in Drosophila melanogaster. J Biol Chem *276*, 3733-3742.

Willimott, S., Beck, D., Ahearne, M.J., Adams, V.C., and Wagner, S.D. (2013). Cap-Translation Inhibitor, 4EGI-1, Restores Sensitivity to ABT-737 Apoptosis through Cap-Dependent and -Independent Mechanisms in Chronic Lymphocytic Leukemia. Clinical cancer research : an official journal of the American Association for Cancer Research.

Wouters, B.G., van den Beucken, T., Magagnin, M.G., Koritzinsky, M., Fels, D., and Koumenis, C. (2005). Control of the hypoxic response through regulation of mRNA translation. Semin Cell Dev Biol *16*, 487-501.

Wu, D., Yang, H., Zhao, Y., Sharan, C., Goodwin, J.S., Zhou, L., Guo, Y., and Guo, Z. (2008). 2-Aminopurine inhibits lipid accumulation induced by apolipoprotein E-deficient lipoprotein in macrophages: potential role of eukaryotic initiation factor-2alpha phosphorylation in foam cell formation. J Pharmacol Exp Ther *326*, 395-405.

Wu, X., Zhu, Y., Yan, H., Liu, B., Li, Y., Zhou, Q., and Xu, K. (2010). Isothiocyanates induce oxidative stress and suppress the metastasis potential of human non-small cell lung cancer cells. BMC cancer *10*, 269.

Xiao, D., Johnson, C.S., Trump, D.L., and Singh, S.V. (2004). Proteasome-mediated degradation of cell division cycle 25C and cyclin-dependent kinase 1 in phenethyl isothiocyanate-induced G2-M-phase cell cycle arrest in PC-3 human prostate cancer cells. Mol Cancer Ther *3*, 567-575.

Xiao, D., and Singh, S.V. (2007). Phenethyl isothiocyanate inhibits angiogenesis in vitro and ex vivo. Cancer Res *67*, 2239-2246.

Yates, L.A., Norbury, C.J., and Gilbert, R.J. (2013). The long and short of microRNA. Cell *153*, 516-519.

Zhang, W., Kater, A.P., Widhopf, G.F., 2nd, Chuang, H.Y., Enzler, T., James, D.F., Poustovoitov, M., Tseng, P.H., Janz, S., Hoh, C., *et al.* (2010). B-cell activating factor and v-Myc myelocytomatosis viral oncogene homolog (c-Myc) influence progression of chronic lymphocytic leukemia. Proc Natl Acad Sci U S A *107*, 18956-18960.

Zhang, W., Trachootham, D., Liu, J., Chen, G., Pelicano, H., Garcia-Prieto, C., Lu, W., Burger, J.A., Croce, C.M., Plunkett, W., *et al.* (2012). Stromal control of cystine metabolism promotes cancer cell survival in chronic lymphocytic leukaemia. Nat Cell Biol *14*, 276-286.

Zhang, Y. (2004). Cancer-preventive isothiocyanates: measurement of human exposure and mechanism of action. Mutation research *555*, 173-190.

Zhang, Y., Yao, S., and Li, J. (2006). Vegetable-derived isothiocyanates: anti-proliferative activity and mechanism of action. Proc Nutr Soc *65*, 68-75.

Chapter Nine

Supplementary Figures and Data

9. Supplementary Figures and Data

9. 1. Sequencing Data

Sequencing data was provided by MWG Operon and aligned using a BLAST search (see Chapter 2. 23.). The sequences highlighted in yellow align with the known HIF-1α sequence (NCBI Reference Sequence: NM_001530.3) at positions indicated at the end of each sequence. Three hypoxic plasmids were sent for sequencing due to differences in restriction enzyme digestion products, but all three aligned with the known HIF-1α sequence.

Sequence Data for Normoxic pJet1.2 plasmid:

> Norm HIF R_pJET12r -- 13..941 of sequence

GGAGATCTTCTAGAAAGATCTAATACGACTCACTATAGGGCAAGCAGTGGTATCAACGC
AGAGTACATGGGGAGTGCTGCCTCGTCTGAGGGGACAGGAGGATCACCCTCTTCGTCGC
TTCGGCCAGTGTGTCGGGCTGGGCCCTGACAAGCCACCTGAGGAGAGGCTCGGAGCCGG
GCCCGGACCCCGGCGATTGCCGCCCGCTTCTCTCTAGTCTCACGAGGGGTTTCCCGCCTC
GCACCCCCACCTCTGGACTTGCCTTTCCTTCTCTTCTCCGCGTGTGGAGGGAGCCAGCGCT
TAGGCCGGAGCGAGCCTGGGGGCCGCCCGCCGTGAAGACATCGCGGGGACCGATTCACC
ATGGAGGGCGCCGGCGGCGCGAACGACAAGAAAAATAGGATAAGTTCTGAACGTCGAA
AAGAAAAGTCTCGAGATGCAGCCAGATCTCGGCGAAGTAAAGAATCTGAAGTTTTTTAT
GAGCTTGCTCATCAGTTGCCACTTCCACATAATGTGAGTTCGCATCTTGATAAGGCCTCT
GTGATGAGGCTTACCATCAGCTATTTGCGTGTGAGGAAACTTCTGGATGCTGGTGATTTG
GATATTGAAGATGACATGAAAGCACAGATGAATTGCTTTTATTTGAAAGCCTTGGATGGT
TTTGTTATGGTTCTCACAGATGATGGTGACATGATTTACATTTCTGATAATGTGAACAAA
TACATGGGATTAACTCAGTTTGAACTAACTGGACACAGTGTGTTTGATTTTACTCATCCA
TGTGACCATGAGGAAATGAGAGAAATGCTTACACACAGAAATGGCCTTGTGAAAAAGGG
TAAAGAACAAAACACACAGCGAAGCTTTTTTCTCAGAATGAAGTGTACCCTAACTAGCC
GAGGAAGAACTATGAACATAAAGTCTGCAACATGGAA

Sequence aligned with HIF-1α known sequence at +120.

Sequence Data for Hypoxic pJet1.2 plasmids:

> Hyp1_M13unil -- 13..1018 of sequence

TGATGTATACGACTCACTATAGGGCGAATTGGGCCCGACGTCGCATGCTCCCGGCCGCCA
TGGCGGCCGCGGGAATTCGATTCTAATACGACTCACTATAGGGCAAGCAGTGGTATCAA
CGCAGAGTACATGGGGGGGGCCGCCCGCCGTGAAGACATCGCGGGGACCGATTCACCAT
GGAGGGCGCCGGCGGCGCGAACGACAAGAAAAAGATAAGTTCTGAACGTCGAAAAGAA
AAGTCTCGAGATGCAGCCAGATCTCGGCGAAGTAAAGAATCTGAAGTTTTTTATGAGCTT
GCTCATCGGTTGCCACTTCCACATAATGTGAGTTCGCATCTTGATAAGGCCTCTGTGATG
AGGCTTACCATCAGCTATTTGCGTGTGAGGAAACTTCTGGATGCTGGTGATTTGGATATT
GAAGATGACATGAAAGCACAGATGAATTGCTTTTATTTGAAAGCCTTGGATGGTTTTGTT
ATGGTTCTCACAGATGATGGTGACATGATTTACATTTCTGATAATGTGAACAAATACATG
GGATTAACTCAGTTTGAACTAACTGGACACAGTGTGTTTGATTTTACTCATCCATGTGAC
CATGAGGAAATGAGAGAAATGCTTACACACAGAAATGGCCTTGTGAAAAAGGGTAAAG
AACAAAACACACAGCGAAGCTTTTTTCTCAGAATGAAGTGTACCCTAACTAGCCGAGGA
AGAACTATGAACATAAAGTCTGCAACATGGAAGGTATTGCACTGCACAGGCCACATTCA
CGTATATGATACCAACAGTAACCAACCTCAGTGTGGGTATAAGAAACCACCTATGACCT
GCTTGGTGCTGATTTGTGAACCCATTCCTCACCCATCAAATATTGAAATTCCTTTAGATAG
CAAGACTTTCCTCAGTCGACACAGCCTGGATATGAAATTTTCTTATTGTGATGAAAGAAT
TACCGAATTGATGGGATATGAGCCAGAAGACTTTTAGGCCGCTCAATTTATGAA

Sequence aligned with HIF-1α known sequence at +363.

> Hyp2_M13unil -- 13..211 of sequence

CCGGCTCGTCAGTGATGTATACGACTCACTATAGGGCGAATTGGGCCCGACGTCGCATGC

TCCCGGCCGCCATGGCGGCCGCGGGAATTCGATTCTAATACGACTCACTATAGGGCAAG
CAGTGGTATCAACGCAGAGTACATGGGGACAGGAGGATCACCCTCTTCGTCGCTTCGGC
CCCTGTGTCGGGCTGGGCCCTGACGAGCCACCTGAGGAGAGGCTCGGAGCCGGGCCCGG
ACCCCGGCGATTGCCGCCCGCTTCTCTCTAGTCTCACGAGGGGTTTCCCGCCTCGCACCC
CCACCTCTGGACTTGCCTTTCCTTCTCTTCTCCGCGTGTGGAGGGAGCCAGCGCTTAGGCC
GGACCGAGCCTGGGGGCCGCCCGCCGTGAATACATCGCGGGGACCGATTCACCATGGAG
GGCGCCGGCGGCGCGAACGACAAAAAAAAGATAAGTTCTGAACGTCGAAAAGAAAAGT
CTCGAGATGCATCCAGATCTCGGCGAATTAAAGAATCTGAAGTTTTTTATGACCTTGCTC
ATCAGTTGCCACTTCCACCTAATGTGAGTTCCCATCTTGATAAGGCCTCTGTGATGAGGC
TTACCATCGACTATTTGCGTGTGAGGAAACTTCTGGATGCTGGTGATTTGGATATTGAAG
ATGACATGAAAGCACATATGAATTGCTTTTATTTGAAAGCCTTGGATGGTTTTGTTATGG
TTCTCACATATGATGGTGACATGATTTACATTTCTGATAATGTGAACAAATACATGGGAT
TAACTCAGTTTGGACTAACTGTACACAGTGTGTTTGATTTTACTCATCCATGTGACCCATG
AGGAAATGAGAGAAATGCTTACACACAGAAGTGGCCTTGTGAAAAACGCTAAAGAGCA
TTTCTCACAGCGTAACTTTTTTCTCAGAATGAAGTGTACCCATATCTAACCGAGGAGTAT
CTATGATCATAAGGTCTGCAACGTGCAAGGTATTGCACTGCACATGCCACATTCACGTAT
ATGATACAATCAGTAATCTAGCATCCGTGCTGGGTATCAGAAATGCATGCTAGGATCTGC
ATCGCATGCTCGATTTCGTGAACCCAATTCTTCACTCATCAAATATTGCAAATTCTTCTAC
ATTGCAGGACGTTTCGTCAGTCGAACCTAGCTTGGATTGAAATTTACTAACTGATGATGA
ATACGAACTTGATGCAATTGAGCCGAGACTTTGTAG

Sequence aligned with HIF-1α known sequence at +137.

> Hyp3_M13unil -- 12..982 of sequence

TGATGTATACGACTCACTATAGGGCGAATTGGGCCCGACGTCGCATGCTCCCGGCCGCCA
TGGCGGCCGCGGGAATTCGATTCTAATACGACTCACTATAGGGCAAGCAGTGGTATCAA
CGCAGAGTACATGGGGAGTGCTGCCTCGTCTGAGGGGACAGGAGGATCACCCTCTTCGT
CGCTTCGGCCAGTGTGTCGGGCTGGGCCCTGACAAGCCACCTGAGGAGAGGCTCGGAGC
CGGGCCCGGACCCCGGCGATTGCCGCCCGCTTCTCTCTAGTCTCACGAGGGGTTTCCCGC
CTCGCACCCCCACCTCTGGACTTGCCTTTCCTTCTCTTCTCCGCGTGTGGAGGGAGCCAGC
GCTTAGGCCGGAGCGAGCCTGGGGGCCGCCCGCCGTGAAGACATCGCGGGGACCGATTC
ACCATGGAGGGCGCCGGCGGCGCGAACGACAAGAAAAATAGGATAAGTTCTGAACGTC
GAAAAGAAAAGTCTCGAGATGCAGCCAGATCTCGGCGAAGTAAAGAATCTGAAGTTTTT
TATGAGCTTGCTCATCAGTTGCCACTTCCACATAATGTGAGTTCGCATCTTGATAAGGCC
TCTGTGATGAGGCTTACCATCAGCTATTTGCGTGTGAGGAAACTTCTGGATGCTGGTGAT
TTGGATATTGAAGATGACATGAAAGCACAGATGAATTGCTTTTATTTGAAAGCCTTGGAT
GGTTTTGTTATGGTTCTCACAGATGATGGTGACATGATTTACATTTCTGATAATGTGAAC
AAATACATGGGATTAACTCAGTTTGAACTAACTGGACACAGTGTGTTTGATTTTACTCAT
CCATGTGACCATGAGGAAATGAGAGAAATGCTTACACACAGAAATGGCCTTGTGAAAAA
GGGTAAAGAACAAAACACACAGCGAAGCTTTTTTCTCAGAATGAAGTGTACCCTAACTA
GCCGAGGAAGAACTATGAC

Sequence aligned with HIF-1α known sequence at +137.

9. 2. Supplementary Figures

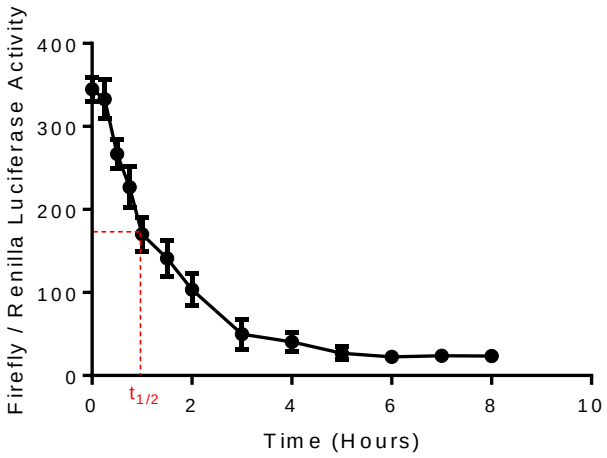

Figure S9-1: PEST-Luciferase Activity

Firefly luciferase activity was determined relative to renilla luciferase to determine the half-life of luciferase activity in the presence of the PEST sequence. The half-life of the PEST luciferase is shown to be approximately 1 hour. Data provided by Dr Mark Coldwell, University of Southampton, UK.

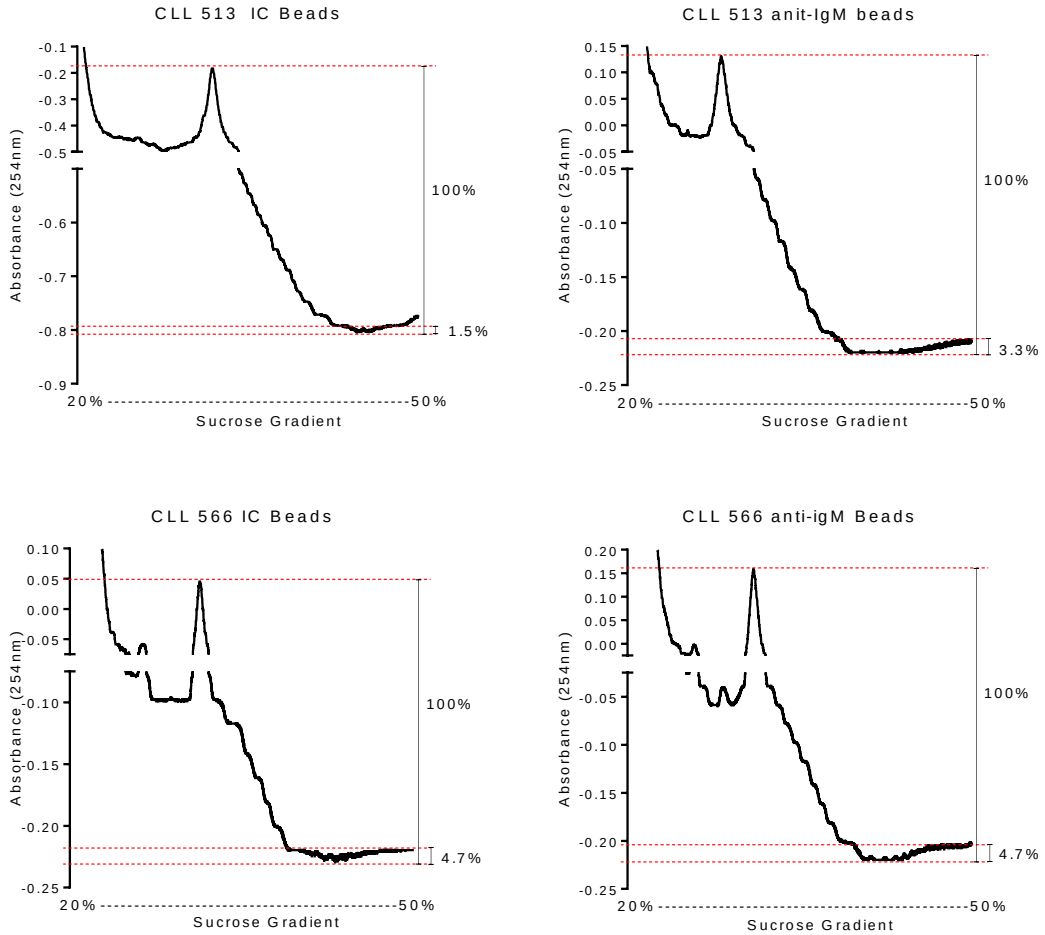

Figure S9-2: Polysome Profiling of CLL samples Stimulated with anti-IgM Beads (Part 1 of 2)

CLL samples were recovered and incubated with anti-IgM beads or isotype control beads (IC) for 24 hours before polysome cell lysates were collected and profiled.

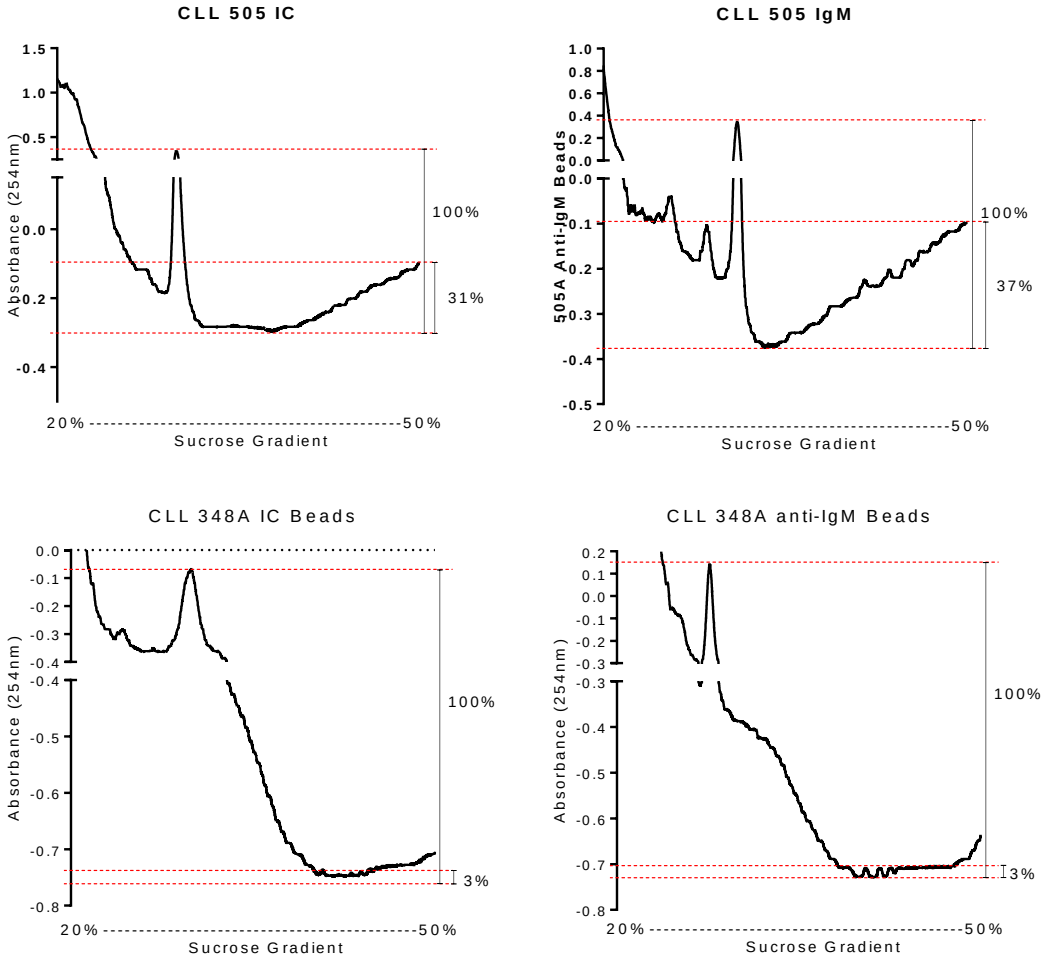

Figure S9-3: Polysome Profiling of CLL Samples Stimulated with anti-IgM Beads (Part 2 of 2)

CLL samples were recovered and incubated with anti-IgM beads or isotype control beads (IC) for 24 hours before polysome cell lysates were collected and profiled.

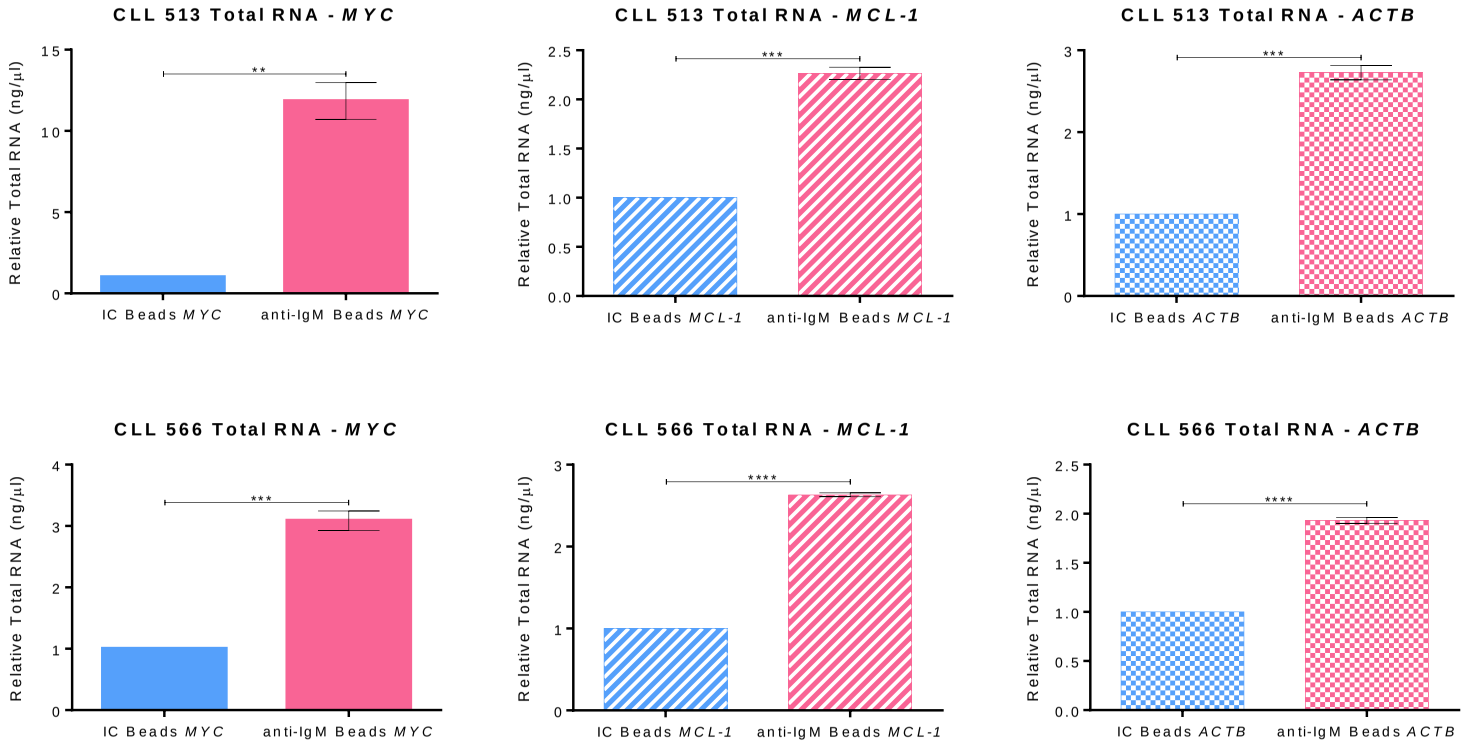

Figure S9-4: Abundance of *MYC, MCL-1* and *ACTB* mRNA Following sIgM Stimulation (part 1 of 2)

Following polysome profiling of CLL samples (Figure 5-11) qPCR analysis was undertaken to investigate the abundance of *MYC, MCL-1* and *ACTB* mRNA levels in the whole profile. Bars represent the average total mRNA relative to isotype control (IC) beads. Error bars indicate the standard deviation and significantly different data is indicated, ** = $p \leq 0.01$, *** = $p \leq 0.005$, **** = $p \leq 0.001$, t-test (n=2).

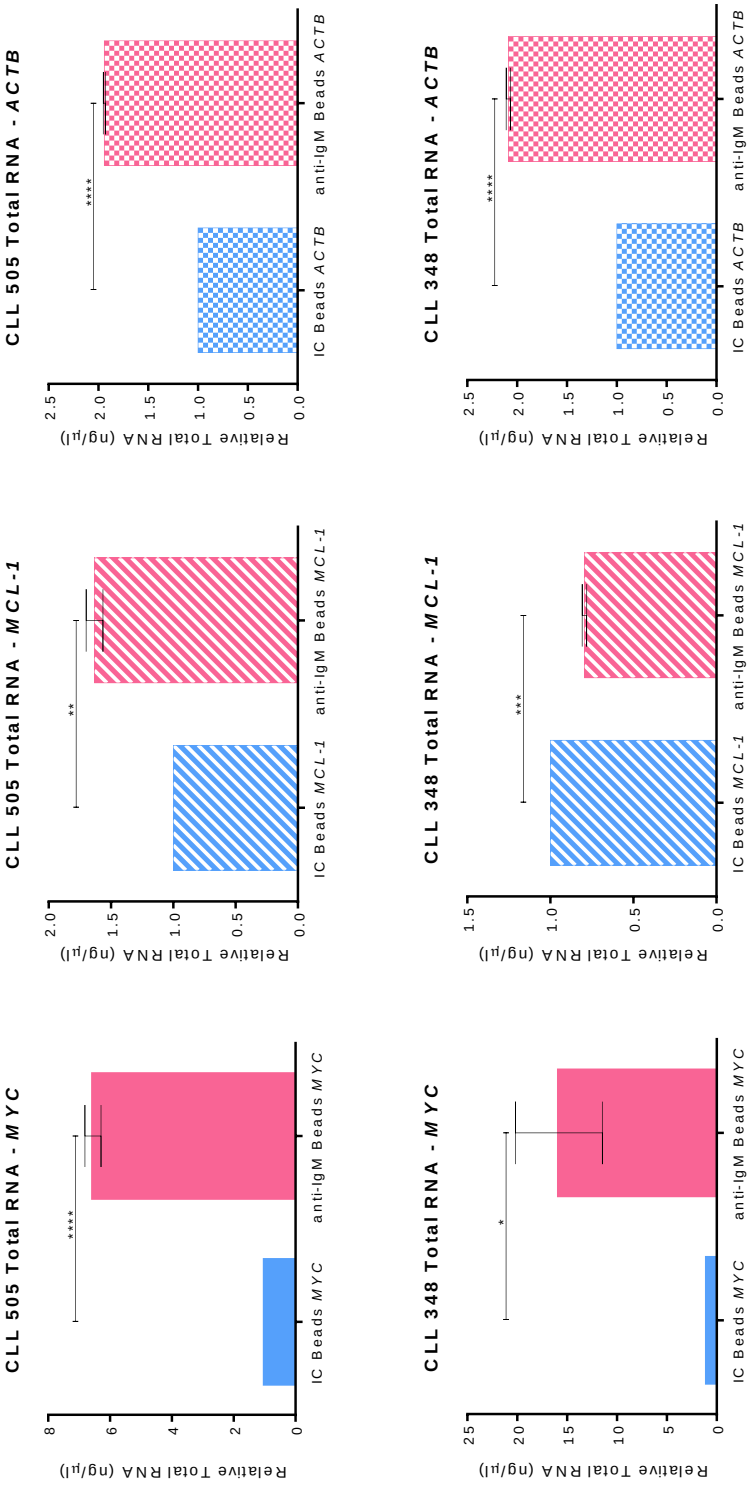

Figure S9-5: Abundance of *MYC*, *MCL-1* and *ACTB* mRNA Following sIgM Stimulation (part 2 of 2)

Following polysome profiling of CLL samples (Figure 5-11) qPCR analysis was undertaken to investigate the abundance of *MYC*, *MCL-1* and *ACTB* mRNA levels in the whole profile. Bars represent the average total mRNA relative to isotype control (IC) beads. Error bars indicate the standard deviation and significantly different data is indicated, ** = $p \leq 0.01$, *** = $p \leq 0.005$, **** = $p \leq 0.001$, t-test (n=2).

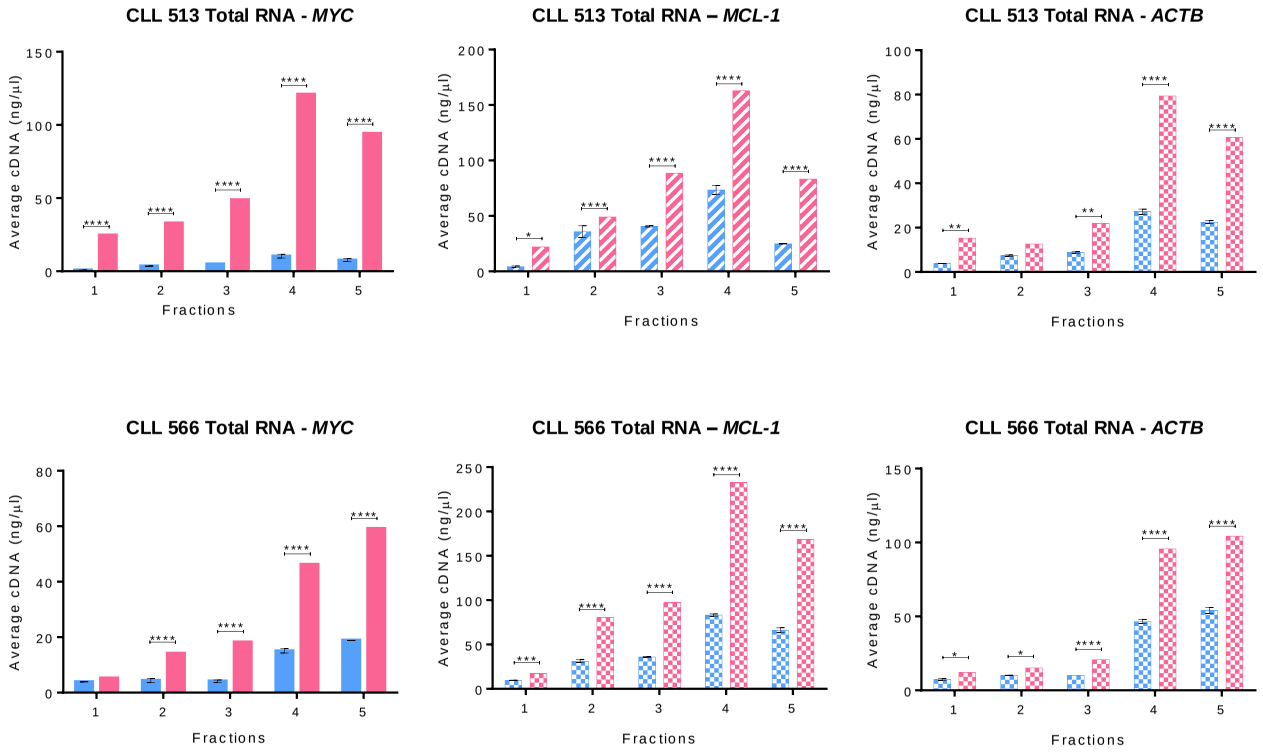

Figure S9-6: Polysome Distribution of *MYC, MCL-1* and *ACTB* mRNAs (Part 1 of 2)

Following polysome profiling of CLL samples (Figure S9-2 and Figure 5-11) qPCR analysis was undertaken to investigate the abundance of *MYC, MCL-1* and *ACTB* mRNA levels in each fraction of the polysome profile. Bars represent the average mRNA in each fraction. Error bars indicate the standard deviation and significantly different data is indicated, * = p≤ 0.05, ** = p≤ 0.01, *** = p≤ 0.005, **** = p≤ 0.001, Two-way ANOVA (n=2).

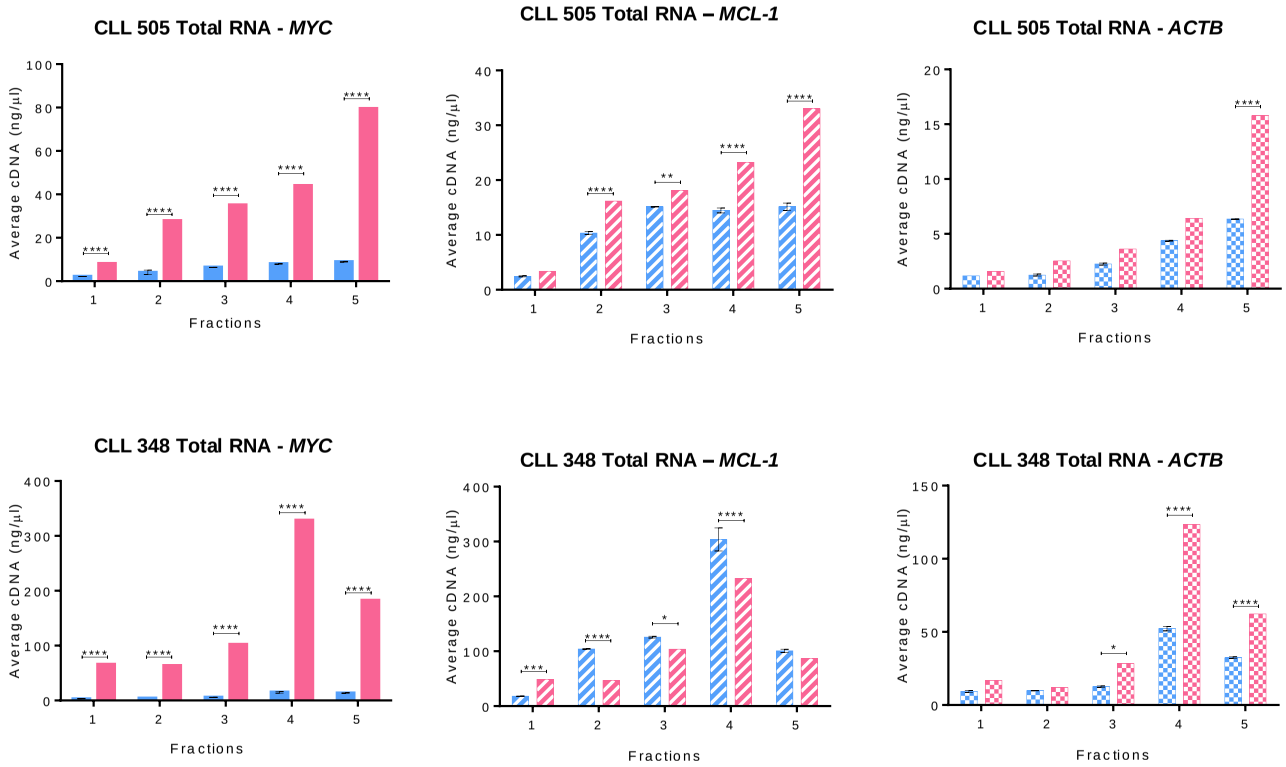

Figure S9-7: Polysome Distribution of *MYC*, *MCL-1* and *ACTB* mRNAs (Part 2 of 2)

Following polysome profiling of CLL samples (Figure S9-3 and Figure 5-11) qPCR analysis was undertaken to investigate the abundance of *MYC*, *MCL-1* and *ACTB* mRNA levels in each fraction of the polysome profile. Bars represent the average mRNA in each fraction. Error bars indicate the standard deviation and significantly different data is indicated, * = p≤ 0.05, ** = p≤ 0.01, *** = p≤ 0.005, **** = p≤ 0.001, Two-way ANOVA (n=2).

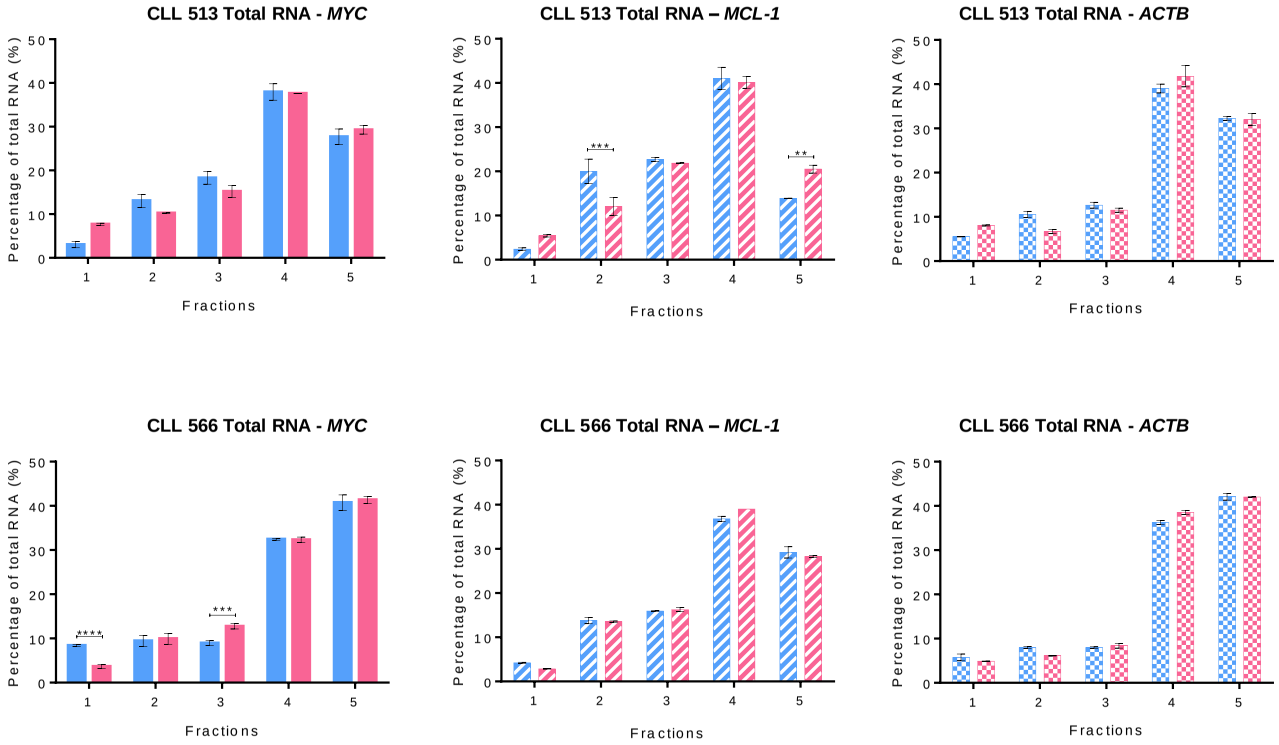

Figure 9-8: Percentage of *MYC*, *MCL-1* and *ACTB* mRNA Associated with Polysome Fractions (Part 1 of 2)

Following polysome profiling of CLL samples (Figure S9-2) qPCR analysis was undertaken to investigate the abundance of *MYC*, *MCL-1* and *ACTB* mRNA levels in each fraction of the polysome profile. Bars represent the average percentage of mRNA in each fraction. Error bars indicate the standard deviation and significantly different data is indicated, *** = p≤ 0.005, **** = p≤ 0.001, Two-way ANOVA (n=2).

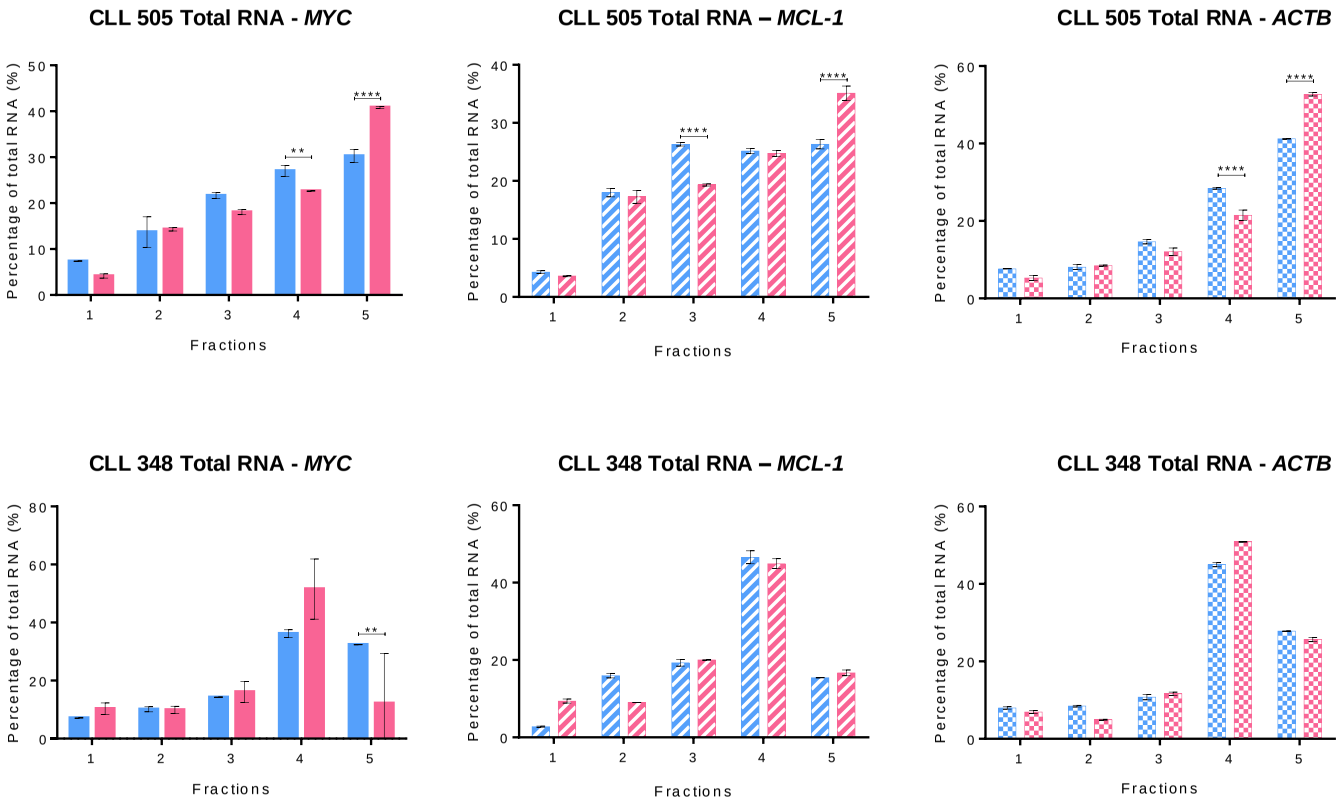

Figure S9-9: Percentage of *MYC*, *MCL-1* and *ACTB* mRNA Associated with Polysome Fractions (Part 2 of 2)

Following polysome profiling of CLL samples (Figure S9-3) qPCR analysis was undertaken to investigate the abundance of *MYC*, *MCL-1* and *ACTB* mRNA levels in each fraction of the polysome profile. Bars represent the average percentage of mRNA in each fraction. Error bars indicate the standard deviation and significantly different data is indicated, *** = $p \leq 0.005$, **** = $p \leq 0.001$, Two-way ANOVA (n=2).

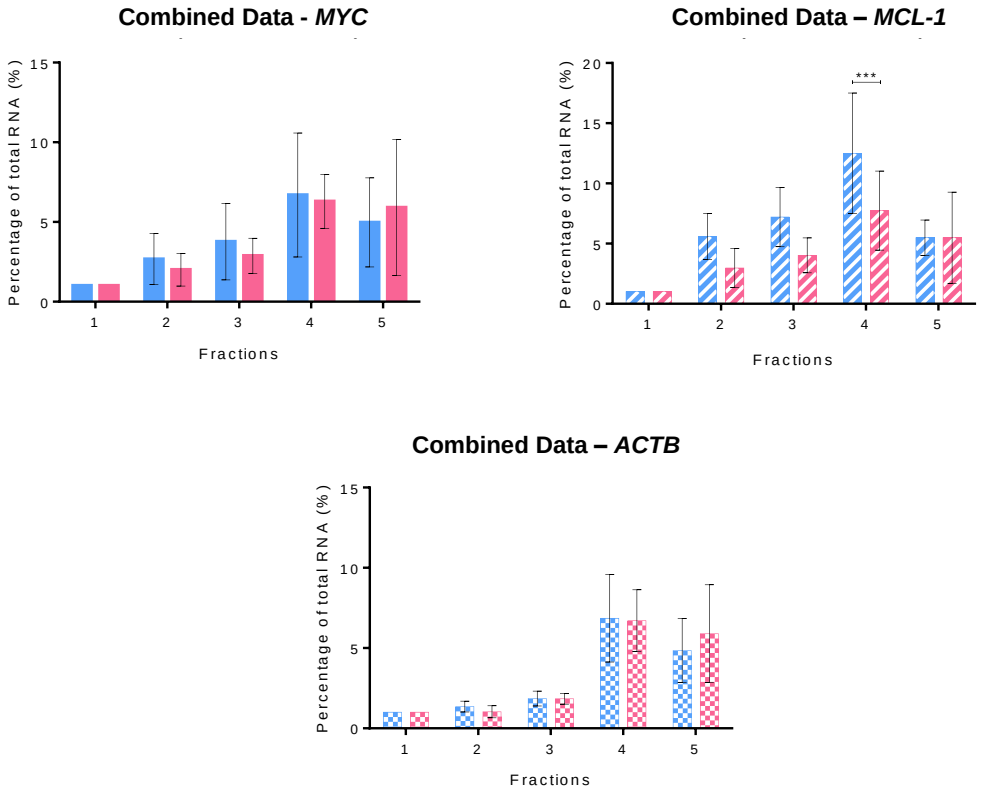

Figure S9-10: Average Percentage of *MYC, MCL-1* and *ACTB* mRNA Associated with Polysome Fractions

Following polysome profiling of CLL samples (Figure S9-2 and Figure S9-3) qPCR analysis was undertaken to investigate the abundance of *MYC*, *MCL-1* and *ACTB* mRNA levels in each fraction of the polysome profile. Bars represent the average percentage of mRNA in each fraction from all five samples. Error bars indicate the standard deviation. Significant data is indicated, *** = $p \leq 0.005$, Two-way ANOVA, n=5 carried out in duplicate.

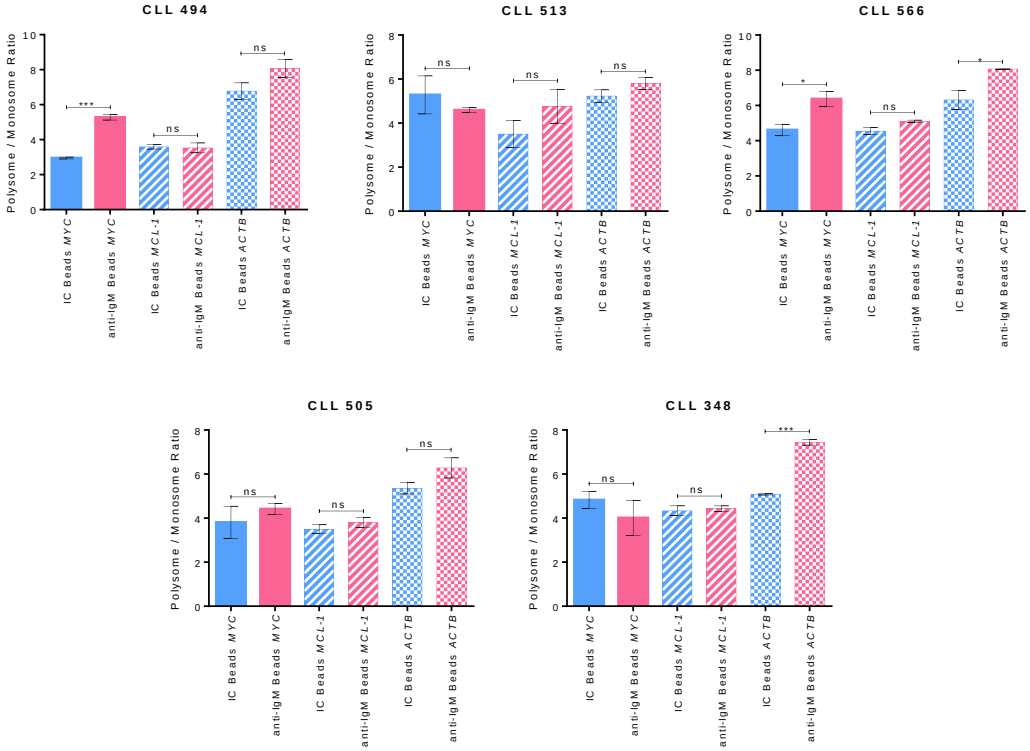

Figure S9-11: Polysome Association of *MYC*, *MCL-1* and *ACTB*

Following polysome profiling of CLL samples (Figure 5-1, Figure S9-2 and Figure S9-3) qPCR analysis was undertaken to investigate the accumulation of *MYC*, *MCL-1* and *ACTB* mRNA levels in polysome fractions (fractions 3-5). Bars represent the ratio of polysomally associated mRNA (fractions 3-5) with respect to sub-polysome associated mRNA (fractions 1 and 2). Error bars indicate the standard deviation and significantly different data is indicated, * = p≤ 0.05, *** = p≤ 0.005, Two-way ANOVA (n=2).

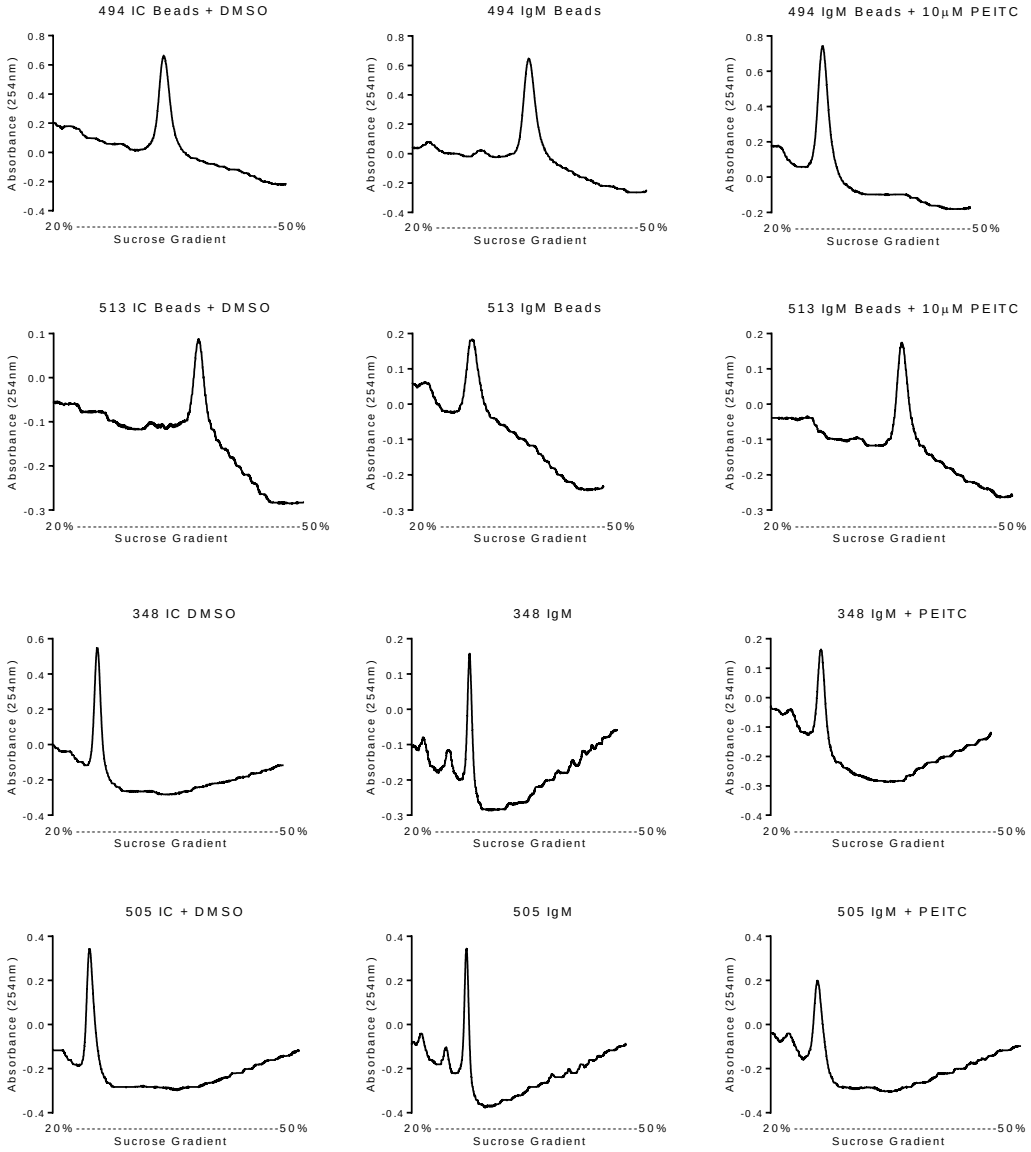

Figure S9-12: Effect of PEITC on sIgM Stimulated Polysome Profiles

CLL samples were recovered and incubated with anti-IgM beads or isotype control beads (IC) for 24 hours. In the final five hours cells were additionally treated with 10µM PEITC or equivalent DMSO before polysome cell lysates were collected and profiled.

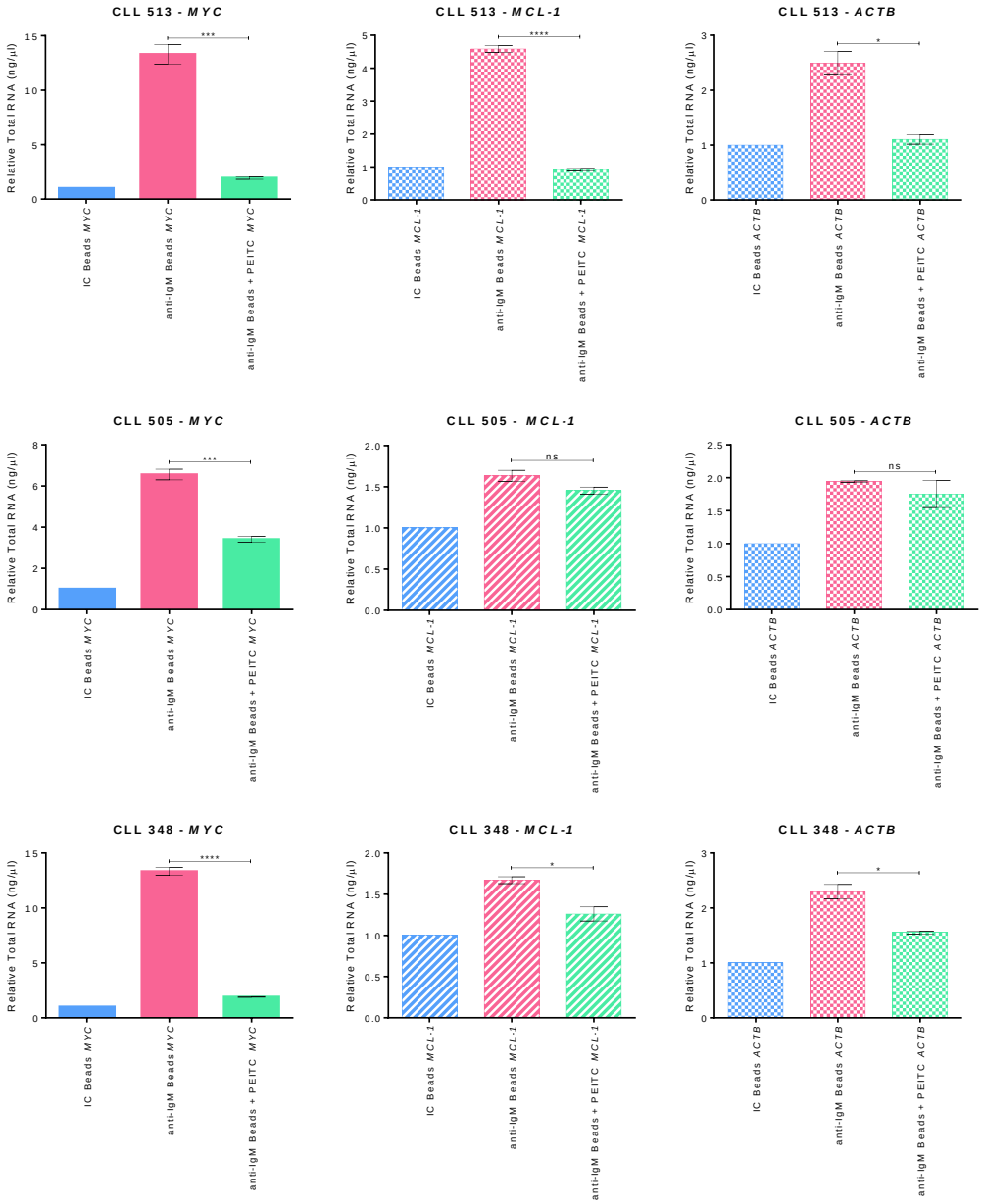

Figure S9-13: Abundance of Total *MYC*, *MCL-1* and *ACTB* Following sIgM Stimulation and Treatment with PEITC

CLL samples were incubated with anti-IgM beads or isotype control (IC) beads for a total of 24 hours and during the final five hours 10µM PEITC was added, prior to polysome profiling. Following polysome profiling qPCR analysis was undertaken to investigate the abundance of *MYC*, *MCL-1* and *ACTB* mRNA levels in the whole profile. Bars represent the average total mRNA relative to isotype control (IC) beads. Error bars indicate the standard deviation and significantly different data is indicated, * = p≤ 0.05, ** = p≤ 0.01, *** = p≤ 0.005, **** = p≤ 0.001, t-test (n=2).

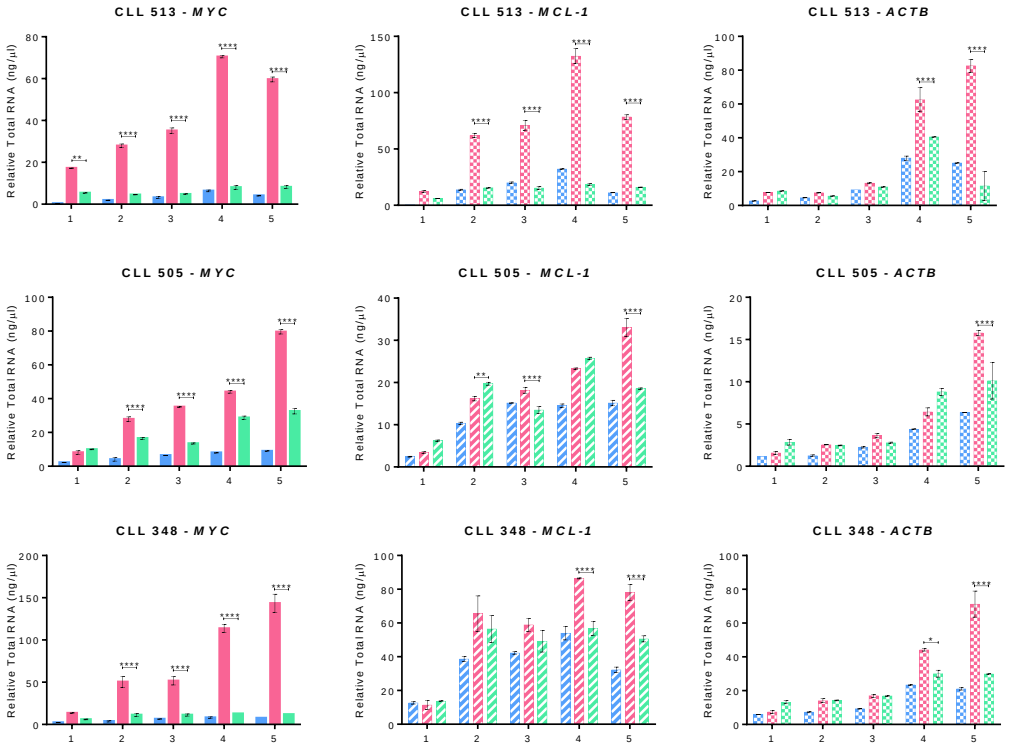

Figure S9-14: Polysome Distribution of *MYC, MCL-1* and *ACTB* mRNA Following Treatment with PEITC

Following polysome profiling of CLL samples qPCR analysis was undertaken to investigate the abundance of *MYC, MCL-1* and *ACTB* mRNA levels in each fraction of the polysome profile. Bars represent the average mRNA in each fraction. Error bars indicate the standard deviation and significantly different data is indicated, ** = $p \leq 0.01$, **** = $p \leq 0.001$, Two-way ANOVA (n=2).

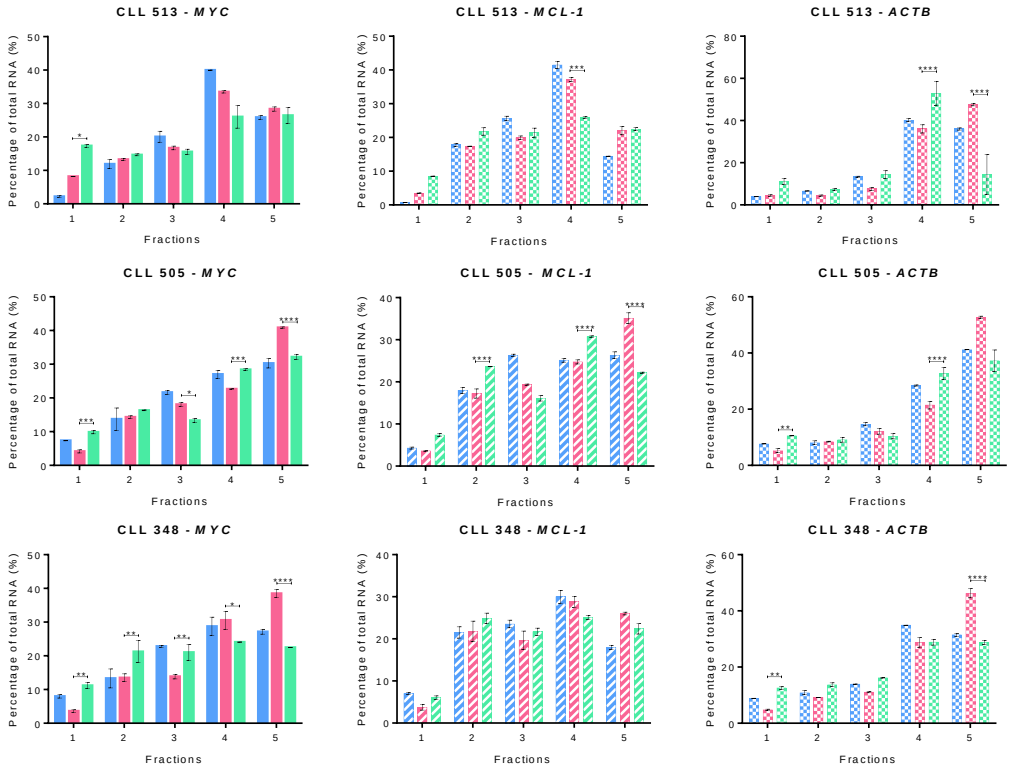

Figure S9-15: Percentage of *MYC*, *MCL-1* and *ACTB* mRNA Associated with Polysome Profile Fractions Following Treatment with PEITC

Following polysome profiling of CLL samples qPCR analysis was undertaken to investigate the abundance of *MYC*, *MCL-1* and *ACTB* mRNA levels in each fraction of the polysome profile. Bars represent the average percentage of mRNA in each fraction. Error bars indicate the standard deviation and significantly different data is indicated, * = p≤ 0.05, ** = p≤ 0.01, *** = p≤ 0.005, **** = p≤ 0.001, Two-way ANOVA (n=2).

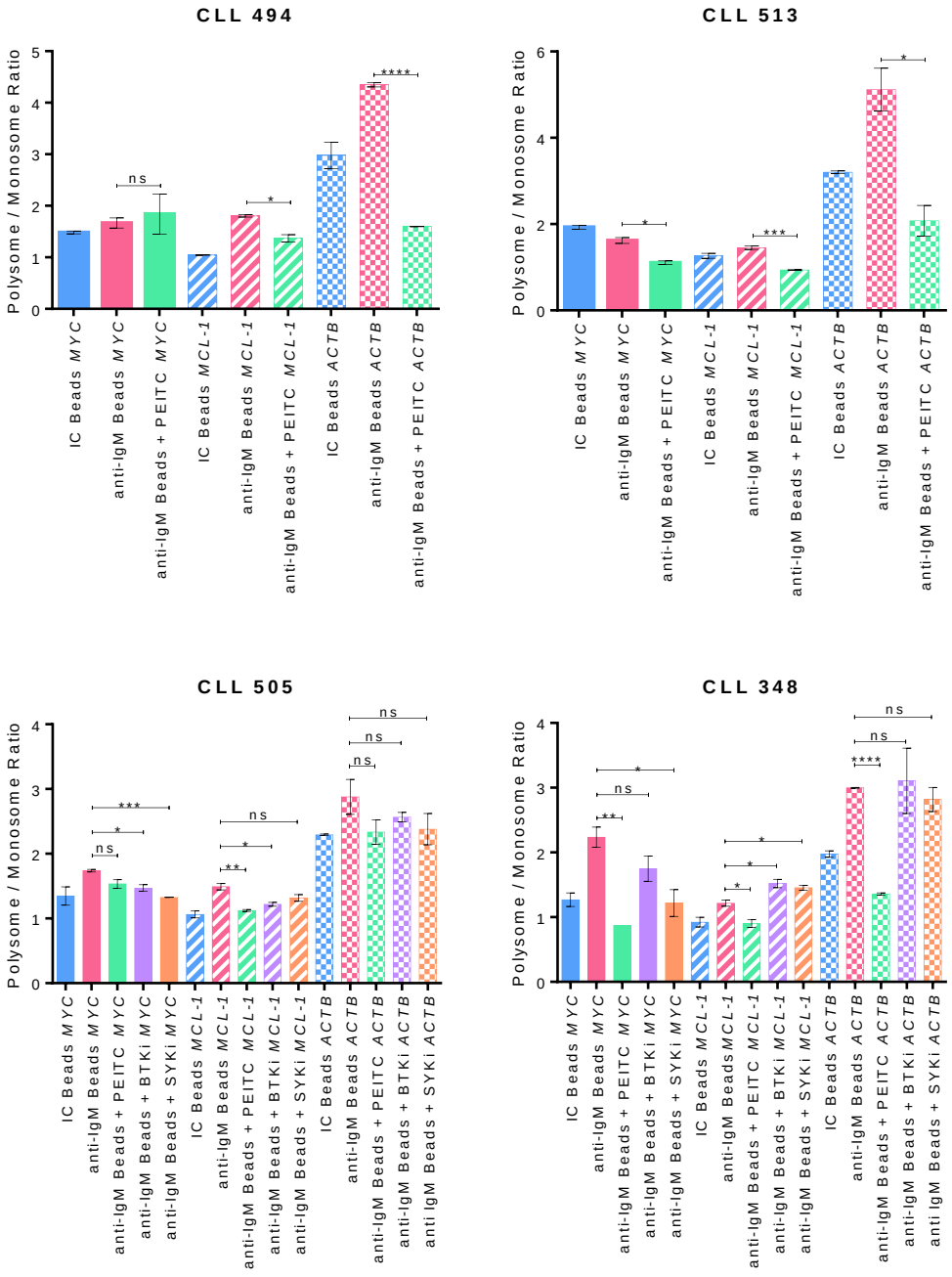

Figure S9-16: Polysome Association of *MYC, MCL-1* and *ACTB* mRNA Following Treatment with PEITC, BTKi or SYKi

Following polysome profiling of CLL samples qPCR analysis was undertaken to investigate the accumulation of *MYC, MCL-1* and *ACTB* mRNA levels in polysome fractions (fractions 3-5). Bars represent the average ratio of polysomally associated mRNA (fractions 3-5) with respect to sub-polysome associated mRNA (fractions 1 and 2). Error bars indicate the standard deviation and significantly different data is indicated, *** = $p \leq 0.005$, **** = $p \leq 0.001$, Two-way ANOVA (n=4).

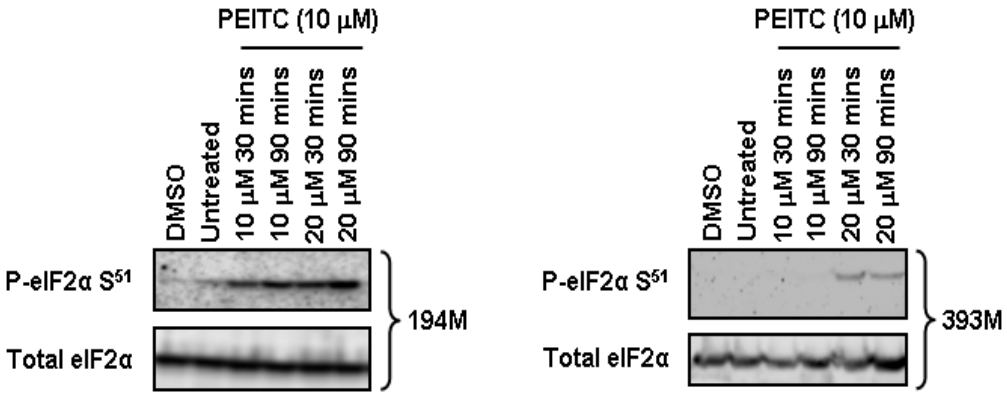

Figure S9-17: Phosphorylation Status of eIF2α Following PEITC treatment of CLL cells

CLL cells were treated with 10 or 20µM PEITC, equivalent DMSO or left untreated for the times indicated prior to western blotting. Western blotting was carried out to determine the phosphorylation status of eIF2α as well as the total levels of eIF2α. Representative western blot from two samples, carried out by Dr. Marina Sanchez Hidalgo.

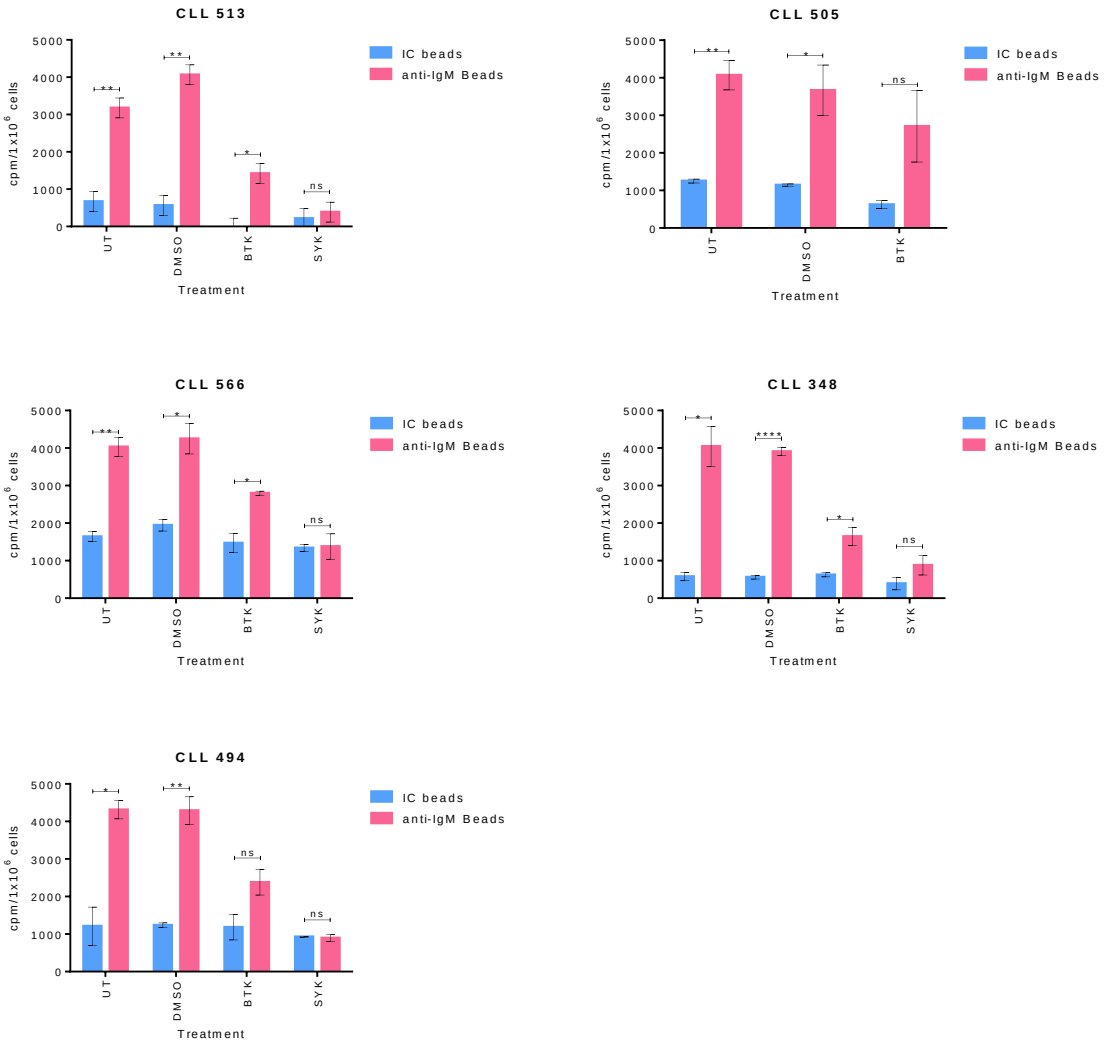

Figure S9-18: Effect of BTKi and SYKi on sIgM-Induced Translation

CLL cells were recovered from cryopreservation and incubated with either treated with 10µM Ibrutinib (BTKi), 10µM Tamatinib (SYKi) for one hour, equivalent DMSO or left untreated (UT) for 1 hour. Anti-IgM beads or isotype control beads (IC beads) where then added and cells were incubated for 24 hours prior to metabolic labelling. Bars represent the average incorporation, from duplicate experiments, with error bars representing the standard deviation from the mean. Significantly different data is indicated * = $p \leq 0.05$, ** = $p \leq 0.01$, **** = $p \leq 0.001$, paired t-test.

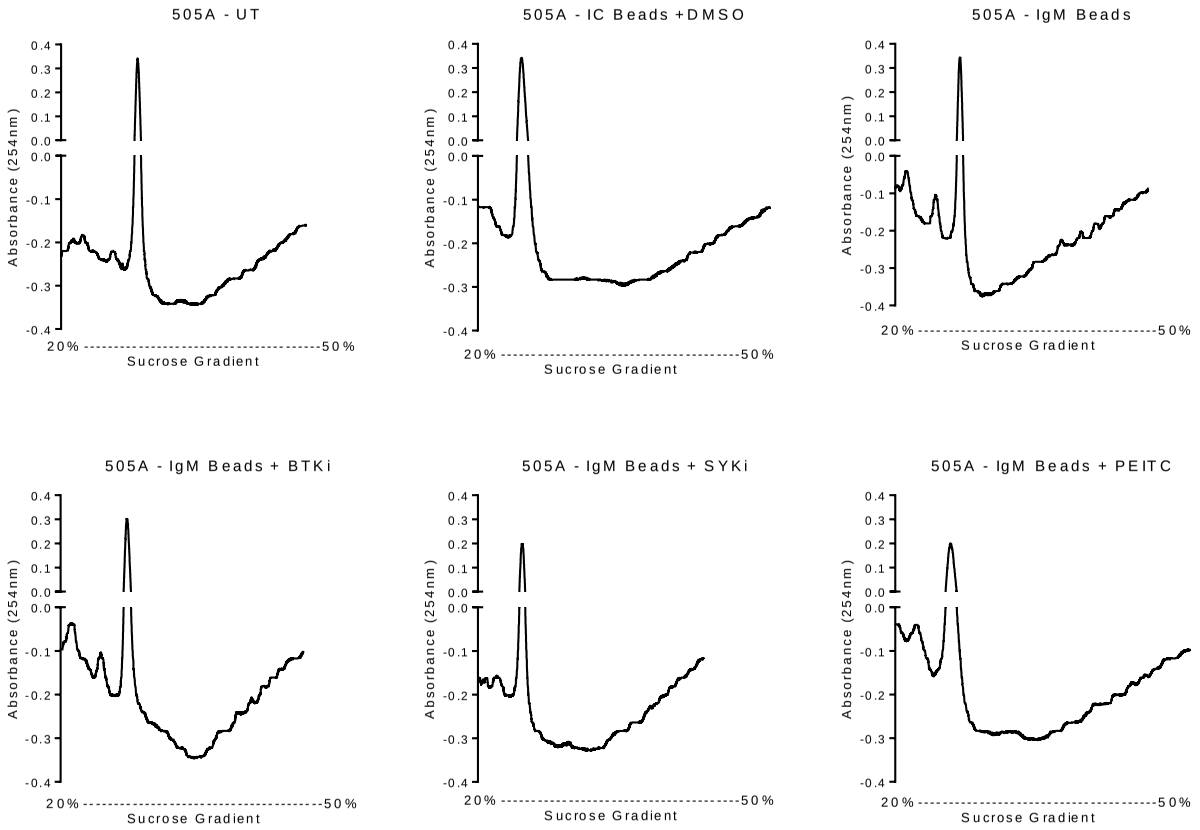

Figure S9-19: Polysome Profiling of CLL samples Stimulated with anti-IgM (1 of 2)

CLL samples were recovered were pre-treated with 10µM Ibrutinib (BTKi) or Tamatinib (SYKi) for one hour prior to the addition of anti-IgM beads or isotype control beads (IC) for 24 hours, cells were also treated with 10µM PEITC for the final five hours before polysome cell lysates were collected and profiled.

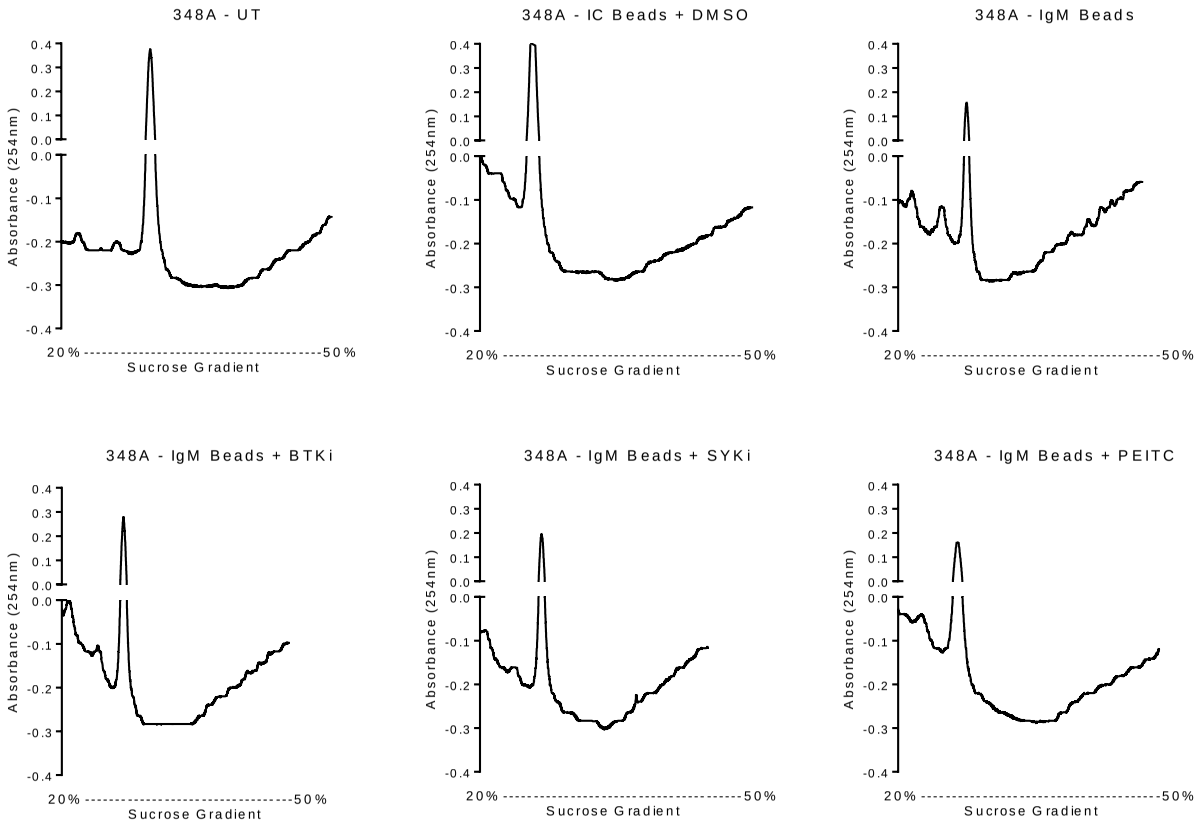

Figure S9-20: Polysome Profiling of CLL samples Stimulated with anti-IgM (2 of 2)

CLL samples were recovered were pre-treated with 10µM Ibrutinib (BTKi) or Tamatinib (SYKi) for one hour prior to the addition of anti-IgM beads or isotype control beads (IC) for 24 hours, cells were also treated with 10µM PEITC for the final five hours before polysome cell lysates were collected and profiled.

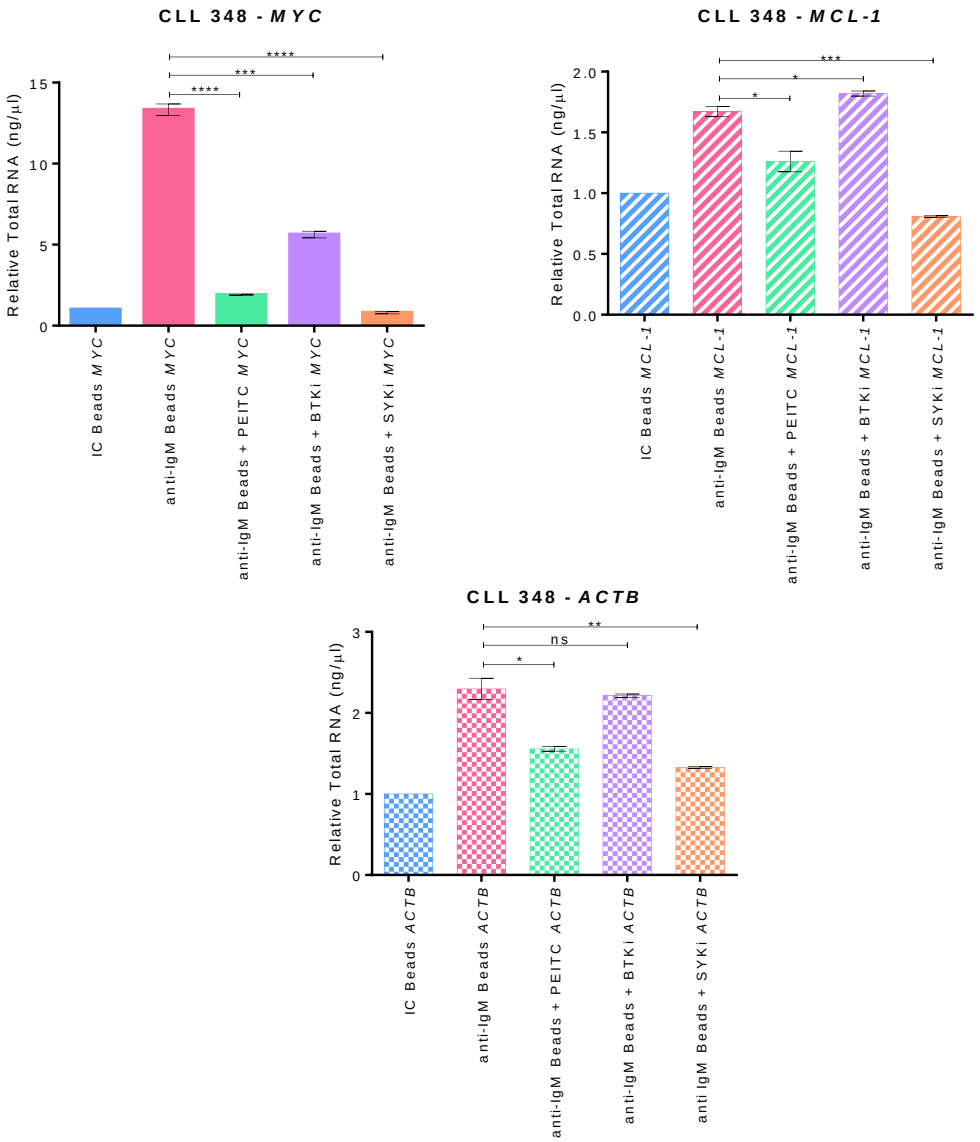

Figure S9-21: Abundance of *MYC, MCL-1* and *ACTB* mRNA Following Inhibition of BTK or SYK and Treatment with anti-IgM Beads

CLL sample 348 was treated with 10µM ibrutinib (BTKi) or 10µM Tamatinib (SYKi) for one hour prior to incubation with anti-IgM beads or isotype control (IC) beads for a total of 24 hours and during the final five hours 10µM PEITC was added, prior to polysome profiling. Following polysome profiling, qPCR analysis was undertaken to investigate the abundance of *MYC, MCL-1* and *ACTB* mRNA levels in the whole profile. Bars represent the average total mRNA relative to isotype control (IC) beads. Error bars indicate the standard deviation and significantly different data is indicated, * = $p \leq 0.05$, ** = $p \leq 0.01$, *** = $p \leq 0.005$, **** = $p \leq 0.001$ t-test (n=2).

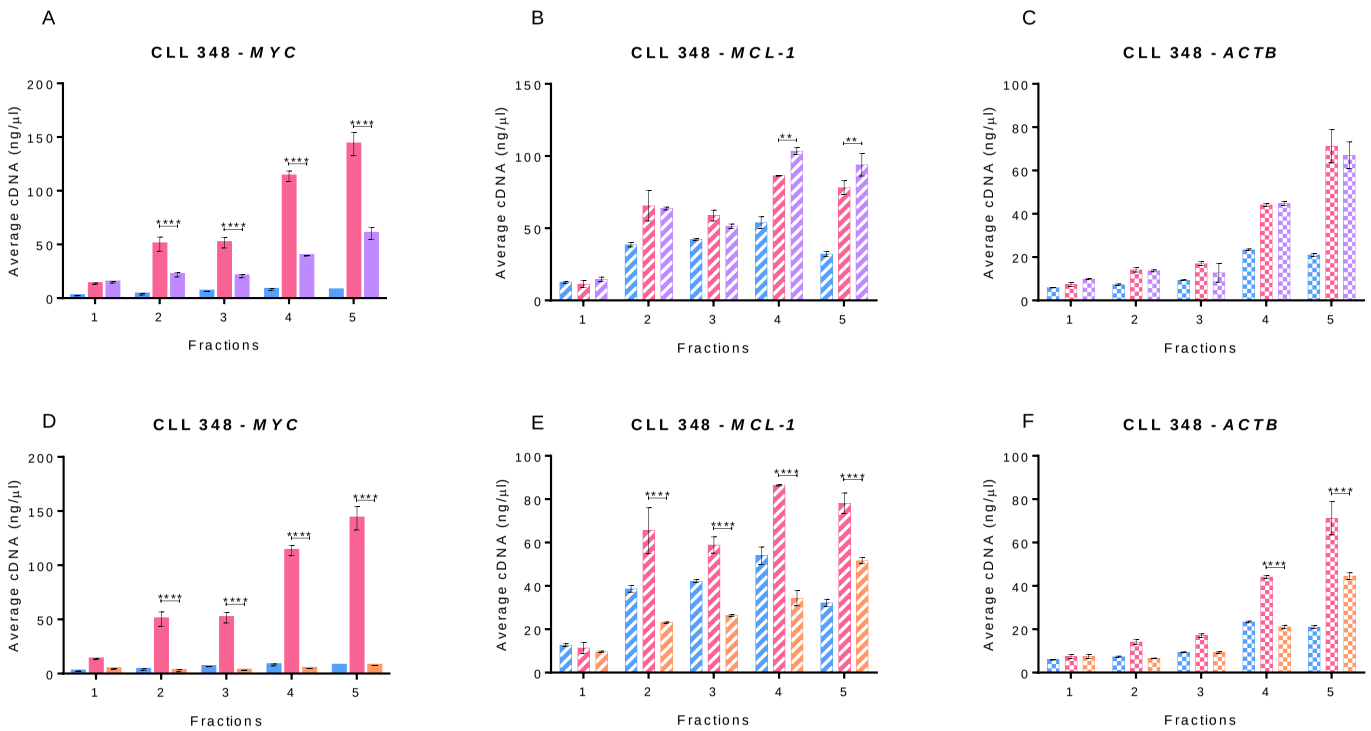

Figure S9-22: Abundance of *MYC, MCL-1 and ACTB* mRNA Following Inhibition of BTK or SYK in Combination with sIgM Stimulation

Following polysome profiling of CLL sample 348 qPCR analysis was undertaken to investigate the abundance of *MYC, MCL-1* and *ACTB* mRNA levels in each fraction of the polysome profile. Bars represent the average mRNA in each fraction following treatment with isotype control beads and DMSO (blue bars), treatment with anti-IgM beads (pink bars), treatment with anti-IgM beads in combination with 10µM Ibrutinib (purple bars – A to C) or treatment with anti-IgM beads in combination with 10µM Tamatinib (orange bars – D to E). Error bars indicate the standard deviation and significantly different data is indicated, **** = $p \leq 0.001$, Two-way ANOVA (n=2).

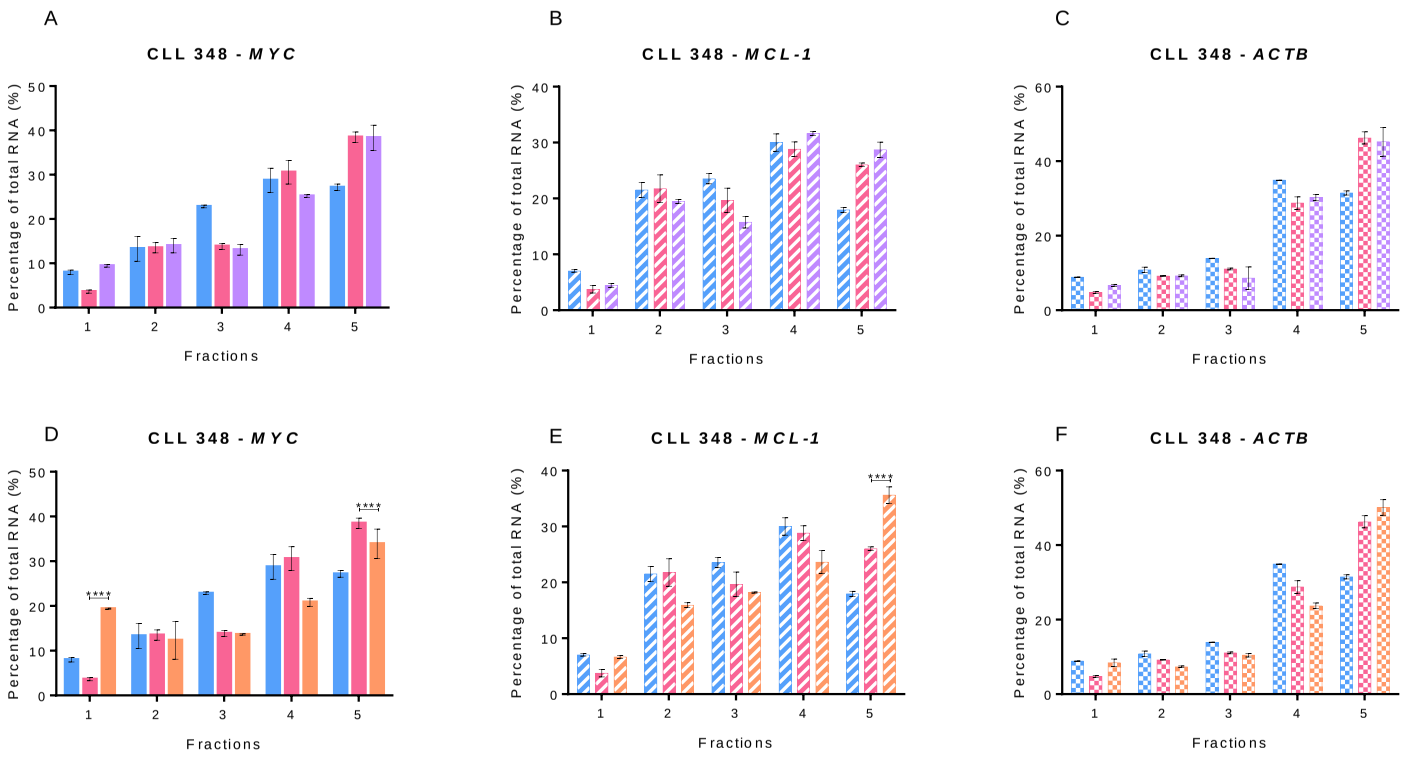

Figure S9-23: Percentage of *MYC*, *MCL-1* and *ACTB* mRNA Associated with Polysome Fractions Following Inhibition of BTK and SYK

Following polysome profiling of CLL sample 348 qPCR analysis was undertaken to investigate the abundance of *MYC*, *MCL-1* and *ACTB* mRNA levels in each fraction of the polysome profile. Bars represent the average percentage of mRNA in each fraction following treatment with isotype control beads and DMSO (blue bars), treatment with anti-IgM beads (pink bars), treatment with anti-IgM beads in combination with 10µM Ibrutinib (purple bars), or treatment with anti-IgM beads in combination with 10µM Tamatinib (orange bars). Error bars indicate the standard deviation and significantly different data is indicated, * = $p \leq 0.05$, ** = $p \leq 0.01$, **** = $p \leq 0.001$, Two-way ANOVA

Appendix